

UC Berkeley
SEMM Reports Series

Title

Slender Prestressed Concrete Columns

Permalink

<https://escholarship.org/uc/item/8b74p65r>

Author

Aroni, Samuel

Publication Date

1967-05-01

REPORT NO.
67-10

STRUCTURES AND MATERIALS RESEARCH
DEPARTMENT OF CIVIL ENGINEERING

SLENDER PRESTRESSED CONCRETE COLUMNS

BY
SAMUEL ARONI

MAY, 1967

STRUCTURAL ENGINEERING AND STRUCTURAL MECHANICS
COLLEGE OF ENGINEERING
UNIVERSITY OF CALIFORNIA
BERKELEY CALIFORNIA

Structures and Materials Research
Department of Civil Engineering
Division of Structural Engineering
and Structural Mechanics

SLENDER PRESTRESSED CONCRETE COLUMNS

by

Samuel Aroni

Associate Professor of Engineering
San Francisco State College

Submitted in partial satisfaction of the
requirements for the degree of DOCTOR OF
PHILOSOPHY in Engineering in the Graduate
Division of the University of California,
Berkeley

Reproduction of this report was supported
in part by the Prestressed Concrete Institute

Berkeley, California
May 1967

Copyright by SAMUEL ARONI 1966

TABLE OF CONTENTS

	<u>Page</u>
Abstract	vi
Acknowledgements	vii
List of Tables	viii
List of Figures	ix
List of Symbols	xii
Chapter 1. INTRODUCTION	1
1.1 General	1
1.2 Objective and Scope of This Investigation	9
(a) Experimental.	10
(b) Theoretical	11
Chapter 2. REVIEW OF LITERATURE ON PRESTRESSED CONCRETE COLUMNS	13
2.1 Breckenridge (1953).	13
2.2 Ozell and Jernigan (1956)	16
2.3 Zia (1957)	19
2.4 Lin and Itaya (1957)	20
2.5 H.R. Brown (1960), Hall (1961, 1962), Brown and Hall (1965, 1966)	22
2.6 Bakhoun, Samaan, Aboul Eid, Antar and Esmat (1962)	24
2.7 Moreadith (1964), Zia and Moreadith (1966)	24
2.8 K. J. Brown (1965)	26
2.9 Kabaila and Hall (1966)	29
2.10 Conclusions	30

Chapter 3. EXPERIMENTAL WORK	32
3.1 Introduction	32
3.2 Column Details	32
3.3 Materials	35
(a) Concrete	35
(b) Steel	38
3.4 Manufacture of Test Specimens	39
1. Columns	39
(a) Prestress	39
(b) Formwork	42
(c) Casting	43
(d) End Anchorage	43
(e) Curing	47
2. Cylinders and Cubes	47
3.5 Testing Methods	48
1. Columns	48
(a) Testing Frame	48
(b) Strain Measurements	52
(c) Deflection Measurements	54
(d) Testing Procedure	55
2. Cylinders and Cubes	56
3. Steel Wire Specimens	60

3.6	Test Results	62
1.	Columns	62
	(a) Initial Conditions	62
	(b) Test Results	70
2.	Cylinders and Cubes	73
3.	Steel Wire Specimens	73
Chapter 4.	THEORETICAL ANALYSIS	76
4.1	Criteria of Instability	76
4.2	General Assumptions	85
4.3	Analytic Procedure	91
1.	Initial Conditions	91
	(a) Eccentric Prestress	91
	(b) Axial Prestress	95
2.	Equilibrium at a Section	95
3.	Method of Solution	100
4.	Lower and Upper Bounds	105
4.4	Computer Program	108
1.	Input	108
2.	Main Control	112
3.	Initial Conditions	113
4.	Solution of Equilibrium Equations	114
5.	Material Failure	115
6.	Upper Bound	115

7. Functions FORS and DEFORS	116
8. Output.	117
9. Computer Times	117
 Chapter 5. COMPARISON OF EXPERIMENTAL RESULTS WITH THEORY	 119
5.1 Maximum Critical Load	120
5.2 Effect of Variables on P_{cr}	124
1. Prestress	124
2. Eccentricity	126
3. Slenderness	128
5.3 Material Failure Load	128
5.4 Maximum Compressive Strain at P_{cr}	132
5.5 Load Deformation Curves	132
1. Load-Central Deflection Curves	132
2. Load-Central Strain Curves	135
3. Deflected Shape Curves	135
 Chapter 6. ANALYSIS OF VARIABLES	 137
6.1 Effect of Concrete Tensile Strength	137
6.2 Effect of Initial Curvature	139
6.3 Effect of Concrete Compressive Strength	140
6.4 Effect of Area of Steel	147
 Chapter 7. SUMMARY AND CONCLUSIONS	 153

References	156
Appendix A. Experimental and Theoretical Curves	161
Appendix B. Properties of Concrete Stress Block	189
Appendix C. Newton's Method of Tangents	192
Appendix D. Equations of Equilibrium at a Section	194
Appendix E. Geometric Relations for Large Rotations	200
Appendix F. Upper Bound Method of Solution	204
Appendix G. Computer Program	210

SLENDER PRESTRESSED CONCRETE COLUMNS

Abstract

Samuel Aroni

August 1966

This thesis deals with slender prestressed concrete columns under eccentric loading. The work includes both experimental tests and analytical developments and investigation of the behavior of the columns through the full range of loading.

Tests on thirty-six slender eccentrically loaded, hinged, axially prestressed concrete columns are reported. The variables investigated were eccentricity, slenderness and prestress, each at three levels. The testing was performed in a special frame, with application of axial shortening and measurement of the resultant load. This enabled measurements to be made past the maximum buckling load, up to material failure.

The theoretical analysis was based on the cotangency criterion, and used a finite element approach and numerical techniques suitable for computer application. A computer program was developed to perform all the calculations. Good agreement was obtained between experimental and theoretical loads and deformations both before and in the post-buckling regions. The computer program proved to be a versatile tool for further theoretical analyses of the effects of tensile and compressive concrete strength, effect of initial curvature and of area of steel.

ACKNOWLEDGEMENTS

The experimental work described in the thesis was performed at the Structural Laboratory, Civil Engineering Department, University of Melbourne, Australia, which was under the direction of Professor A.J. Francis. Dr. K.G. Moody provided initial advice and Mr. Charles Tonta was of invaluable assistance in the execution of the experimental program. The author is most grateful for their help.

The reduction of the experimental data, the development and execution of the theoretical work and computer program, and the final production of the thesis, were all done at the University of California in Berkeley. The author would like to thank most sincerely the following persons and organizations for their contributions and for the help they have provided:

Professor B. Bresler, who as the Chairman of the thesis Committee, contributed in such a large part to the development of this study.

Professor T. Y. Lin for his advice and encouragement.

Professor A. S. Levens for his participation in the Committee in charge.

Professor M. Polivka for his help.

The Computer Center of the University of California, whose facilities were used to carry out all the computations, for generous support.

Mr. A. Klash and Mr. L. Knapp, who did all the drafting work.

Mrs. M. French for her excellent typing.

And finally, to my wife Malca for her continued support, encouragement and acceptance of many hardships, and to my daughters Ruth and Miriam for their silent support and help.

LIST OF TABLES

	<u>Page</u>
Table 1. Concrete Mix Details	35
Table 2. Material Gradings	38
Table 3. Details of Prestressing	42
Table 4. Experimental Data	63
Table 5. Average Strains During Release and Curing	66
Table 6. Average Maximum Compressive Strains at Mid-Height of Columns, Under P_{cr}	71
Table 7. Computer Input	108
Table 8. Computer Times	118
Table 9. Comparison of P_{cr} Loads	121
Table 10. Analysis of Variance of P_{cr} Ratios	123
Table 11. P_{cr} Loads for Column 40a, with Average Strains and Deflections	124
Table 12. Comparison of P_f Loads	130
Table 13. Comparison of Maximum Compressive Strains at P_{cr}	133
Table 14. Effect of Concrete Tensile Strength	138
Table 15. Effect of Concrete Tensile Strength - Average Load Ratios	139
Table 16. Effect of Concrete Compressive Strength	146
Table 17. Effect of Concrete Compressive Strength - Average Load Ratios	147

LIST OF FIGURES

	<u>Page</u>
Fig. 1	Details of Column 33
Fig. 2	Details of Loading Head 34
Fig. 3	Group of Columns 36
Fig. 4	Group of Columns 37
Fig. 5	Prestressing Bed 40
Fig. 6	Prestressing Procedure 41
Fig. 7	Loading Heads 45
Fig. 8	Adapted Bolt Clippers 45
Fig. 9	Preparations for End Anchorage 46
Fig. 10	Testing Frame 49
Fig. 11	End Details of Column in Testing Frame 51
Fig. 12	Concrete Strain Measurements 53
Fig. 13	Column C ₁ 20c1 Under Test 57
Fig. 14	Column A ₁ 30a3 Under Test 58
Fig. 15	Column D ₂ 40b3 Under Test 59
Fig. 16	Instrumentation for Cylinder Stress-Strain Measurements . 61
Fig. 17	Experimental Average Initial Central Deflections 69
Fig. 18	Concrete Stress-Strain Curves 74
Fig. 19	Steel Stress-Strain Curve 75
Fig. 20	Eccentrically Loaded Column 78
Fig. 21	Cotangency Criteria of Instability 81 ,82
Fig. 22	Theoretical Concrete Stress-Strain Curve 87

Fig. 23	Initial Conditions: Eccentric Prestress	92
Fig. 24	Initial Conditions: Axial Prestress	96
Fig. 25	Strain and Stress Conditions - Case 3	98
Fig. 26	Method of Solution	101
Fig. 27	Variation of P_{cr} with Finite Element Length	107
Fig. 28	Variation of 75% P_{cr} with Finite Element Length	109
Fig. 29	Histogram of P_{cr} Load Ratios	122
Fig. 30	Effect of Prestress on P_{cr}	125
Fig. 31	Effect of Eccentricity on P_{cr}	127
Fig. 32	Effect of Slenderness on P_{cr}	129
Fig. 33	Histogram of P_f Load Ratios	131
Fig. 34	Histogram of Strain Ratios (at P_{cr})	134
Fig. 35	Effect of Prestress on Load-Central Deflection Curves	136
Fig. 36	Effect of Initial Curvature ($f_{cp}/f'_c = 0.1$)	141
Fig. 37	Effect of Initial Curvature ($f_{cp}/f'_c = 0.3$)	142
Fig. 38	Effect of Initial Curvature ($f_{cp}/f'_c = 0.5$)	143
Fig. 39	Effect of Initial Curvature ($l/d = 30$)	144
Fig. 40	Effect of Area of Steel ($f_{cp}/f'_c = 0.1$)	149
Fig. 41	Effect of Area of Steel ($f_{cp}/f'_c = 0.3$)	150
Fig. 42	Effect of Area of Steel ($f_{cp}/f'_c = 0.5$)	151
Fig. 43	Effect of Prestress Ratio (Column 20a)	152
Figs. A1-A9	Load-Central Deflection	162-170
Figs. A10-A18	Load-Central Strains	171-179

Figs. A19-A27	Column Deflected Shape	180-188
Fig. B1	Properties of Concrete Stress Block	190
Fig. D1	Strain Distributions - Seven Cases	195
Fig. E1	Geometry of Large Rotations	201
Fig. F1	Upper Bound Iteration Procedure	207

LIST OF SYMBOLS

The symbols used in this thesis are generally defined when they are introduced. The most frequently used symbols are listed below. Note that concrete compressive strains and stresses are taken as positive.

- A_c = concrete area, bxd
- A_s = area of prestressing steel (two wires)
- a = height of finite element, see Fig. 26
- b = width of column cross-section
- C = concrete resultant force
- d = total depth of column cross-section
- d' = distance between steel wires, see Fig. 1
- d'' = cover to steel wires, see Fig. 1
- d_c = depth of concrete compressive stress block
- d_i = distance from tangent at mid-height to nodal point i , see Fig. 26
- E_c = initial concrete modulus of elasticity in compression
- E_s = steel modulus of elasticity
- E_t = concrete modulus of elasticity in tension
- e = eccentricity of load
- e_{cr} = critical eccentricity
- F = criterion function in upper bound solution, see Eqn. (F3)
- F_{s2}, F_{s3} = resultant steel forces
- f_c = concrete compressive stress
- f_{cp} = average concrete prestress

- f'_c = concrete cylinder strength
 f''_c = maximum concrete compressive stress in flexure
 f_s = steel stress
 f_t = concrete ultimate tensile stress
 i_m = initial central deflection
 $K_1 = k/d_c$
 k = distance from compression face to position of C, see Fig. B1
 ℓ = length of column
 ℓ' = initial column length, including prestress and creep effects
 ℓ_{cr} = critical column length
 M_A = applied moment
 M_R = moment of resistance
 n = number of nodal points, per half of column length
 P = eccentric column load
 P_{cr} = maximum, critical, buckling load
 P_f = material failure load
 p = ratio of steel to concrete areas
 r = radius of curvature
 r_i = radius of curvature of i -th finite element
 $S1-S4$ = increments in $\theta_n - (\Delta\epsilon)_n$ plane, see Fig. F1
 S_i = vertical movement of i -th element, see App. E
 V_i = length of i -th element, see App. E
 y_i = load eccentricity at i -th nodal point
 y_m = load eccentricity at column mid-height

α = concrete compressive stress factor, see Fig. 22

β = concrete compressive strain factor, see Fig. 22

γ = factor determining slope of concrete compressive strain-stress curve, past maximum stress, see Fig. 22

Δl = length of finite element

$\Delta l'$ = initial length of finite element, see App. E

$\Delta \delta_m$ = increments of central deflection

$$\Delta \epsilon = \epsilon_4 - \epsilon_1$$

$$\Delta \epsilon_c = (\epsilon_{c3} - \epsilon_{c2}) \frac{d'}{d}$$

$$\Delta \epsilon_d = \Delta \epsilon + \Delta \epsilon_c$$

$\Delta \epsilon_j$ = value of central $\Delta \epsilon$, at j-th columnwise iteration

δ = column deflection

δ_m = central deflection

ϵ_1 = concrete strain at tension face

ϵ_2, ϵ_3 = concrete strains at level of steel wires

ϵ_4 = concrete strain at compression face

ϵ_{14} = concrete strain at mid-depth, from release to testing

ϵ_{23} = concrete strain at compression face, from release to testing

ϵ_c = concrete compressive strain

ϵ_{pr} = prestress strain applied to the steel

$\epsilon_{c2}, \epsilon_{c3}$ = concrete creep strains, from release to testing, at level of steel

ϵ_o = concrete compressive strain at maximum stress

ϵ_s = steel strain

$\epsilon_{s2}, \epsilon_{s3}$ = steel strains of the two rows of wires

ϵ_t = maximum concrete tensile strain

ϵ_u = concrete compressive ultimate strain

θ_i = rotation at i-th nodal point

Chapter 1. INTRODUCTION

1.1 General

There seems little need to emphasize the importance of the engineering member subjected to compression. While our understanding of the load-carrying capacity of compression members, and the associated phenomenon of instability, has only been developing in the last 200 years, we do have columns built almost 5000 years ago still standing in Egypt.

It is of interest to review the outlook of the ancients towards the design of such members. Thus Vitruvius, an architect during the reign of the Roman Emperor Augustus or possibly Titus has the following to say about the Greek colonists in Asia Minor: (1)*

"There they began to erect fanes, and constitute temples to the immortal gods. First they erected the temple of Apollo Panionios, in the manner they had seen it in Achaia; which manner they called Doric, because they had seen it first used in the Dorian cities. In this temple they were desirous of using columns; but being ignorant of their symmetry, and of the proportions necessary to enable them to sustain the weight, and give them an handsome appearance, they measured the human foot of a man to be the sixth part of its height, they gave that proportion to their columns, making the thickness of the shaft at the base equal to the sixth part of the height, including the capital. Thus the Doric column, having the proportion, firmness and beauty of the human body, first began to be used in buildings.

"Afterwards, to construct the temple of Diana, they sought a new order from the same traces, copying the gracefulness of women, and making the thickness of the columns an eighth part of their height, in order to give them a taller appearance. Thus arose the invention of these two different orders; one of a masculine appearance, naked and unadorned; the other imitating the slenderness and fine proportion of women. But posterity, improving in ingenuity and judgement, and delighting in more graceful proportions, fixed the height of Doric columns at seven times their diameter; and of the Ionic at eight and a half. This latter order was called Ionic, because it was first used by Ion.

*Superscript numbers refer to the list of References.

"The Third which is called Corinthian, is in imitation of the delicacy of virgins; for in that tender age, the limbs are formed more slender and are more graceful in attire."

The above "design" method, trial and error based on the imitation of nature, continued well into recent times. The foundation stone of column theory was laid by Euler⁽²⁾ in 1759. Van den Broek⁽³⁾ (1947) gives an interesting commentary, as well as a translation of part of Euler's classic paper. Young⁽⁴⁾ (1807) was the first to give the analysis for eccentrically loaded and initially curved columns. However, during most of the 19th century little use was made in engineering practice of these theoretical developments. Without a proper understanding of all the variables influencing instability and a clear division between material and instability failures, there was little apparent agreement between experiments and theory. Many empirical relationships, for various materials, were developed during the period.⁽⁵⁾

Euler's theory for the bifurcation load of a slender axially loaded column was extended by Considère⁽⁶⁾ in 1889, to a non-linear inelastic material. Considère suggested the use of a reduced modulus of elasticity, somewhere between the elastic and the tangent modulus, and conducted some column tests in support of the theory. Independently, during the same year, Engesser⁽⁷⁾ proposed the tangent modulus as the proper one for use in Euler's equation. Later, however, apparently influenced by Jasinski's criticism, Engesser (1895) changed to a reduced modulus, which was a function of not only the material properties but the shape of the cross-section as well. Explicit expressions for this reduced modulus, namely the "double

modulus," were derived by Kármán⁽⁸⁾ in 1910. The controversy between the tangent modulus and the double modulus continued for another generation, with experimental results favouring the tangent modulus load, which is lower than the double modulus one. In 1946, Shanley^(9,10) explained this "column paradox" and reconciled the two theories. Simple in retrospect,⁽¹¹⁾ the above controversy highlights the subtleties and misconceptions that have arisen in column theory throughout its historical development.

A most significant contribution to the determination of the buckling load of an eccentrically loaded column was Kármán's⁽⁸⁾ paper in 1910. This was a general non-linear theory based on the actual stress-strain relationship of the column material. The deflected shape of the column, which is of critical importance in column instability, was determined by numerical integration of angle changes along the column length, using moment-curvature relationships, for increasing load increments. This procedure was very laborious but free of any assumptions regarding the column deflected shape. For hinged rectangular steel columns, Chwalla⁽¹²⁾ (1934) showed good agreement between Kármán's theory and tests. Because of the labor involved in the numerical integration, simplified deflected shapes have been suggested. Thus, the use of a part of a cosine curve as the deflected shape was proposed by Westergaard and Osgood⁽¹³⁾ (1928) and employed by many investigators since. With the development of the aircraft industry and various other uses of slender structural elements much experimental and theoretical work has accumulated and is well summarized in the

literature⁽¹⁴⁾ and recent textbooks, e.g., Bleich⁽¹⁵⁾ and Timoshenko and Gere.⁽¹⁶⁾

In the field of reinforced concrete columns, the progress was much slower. Additional problems existed related to material properties, cracking, the action of longitudinal and lateral reinforcement, spiral and tied, and types of failure. The A.C.I. column investigation⁽¹⁷⁾ (1930-1933), with over 500 tests, of axially-loaded short (length to least dimension ratio of $l/d = 7.5$) reinforced concrete columns provided a reliable basis for the design of such elements.

Over 1,000 tests of eccentrically loaded short ($l/d = 7.5$ to 10) reinforced concrete columns have been reported in the literature. About one half of these tests were made prior to 1920. The more important recent investigations were by Thomas⁽¹⁸⁾ (1938), Richart⁽¹⁹⁾ (1947), Andersen⁽²⁰⁾ (1941, tested 70 columns) and Hognestad⁽²¹⁾ (1951). Hognestad tested 120 columns ($l/d = 7.5$) and obtained good agreement with the proposed theory, based on an assumed non-linear stress-strain diagram, for both tensile and compressive failures. Following the A.S.C.E.-A.C.I. Joint Committee Report⁽²²⁾ (1955), most reinforced concrete column Codes in English-speaking countries are based on the above work.

In the case of buildings and other structures of normal proportions, the problem of buckling of reinforced concrete columns due to slenderness is not significant. However, with modern developments the tendency is towards more slender proportions. All this explains why so relatively little work

has been done on this problem, until recent years. One of the earliest investigations was performed by Baumann⁽²³⁾ (1934). He tested a total of 43 long columns ($l/d = 12.0$ to 40.7) including axially and eccentrically loaded columns and some with end restraints. The use of experimentally determined material properties and Karman's analysis gave good agreement between tests and theory. In a significant contribution, Broms and Viest^(24,25) (1958) presented theoretical analyses for both hinged and restrained long reinforced concrete columns. Their theory for axially loaded columns was based on the tangent modulus. For eccentrically loaded columns they used an assumed cosine deflected shape and Hognestad's⁽²¹⁾ stress-strain curve, and extended its applicability to columns with either equal or unequal end eccentricities. The basic buckling criterion (the "cotangency criterion") was based on the cotangency, at the point of neutral equilibrium, of the curves of applied and resisting moments versus deflection. This criterion will be discussed in greater detail later. Broms and Viest showed good agreement of the theory with test data from six independent previous investigations, covering a total of 48 axially and 79 eccentrically loaded columns and 6 columns with end restraints. The experimental investigations were by Baumann⁽²³⁾ (1934), Thomas⁽²⁶⁾ (1939), Hanson and Rosenström⁽²⁷⁾ (1947), Ramboll⁽²⁸⁾ (1951), Ernst, Hromadik and Riveland⁽²⁹⁾ (1953) and Gehler and Hütter⁽³⁰⁾ (1954).

More recent work has inevitably turned towards the computer for the laborious computational part of the analysis. Thus, Pfrang and Siess⁽³¹⁾ (1961) presented an analytic study of the long restrained reinforced concrete

column under eccentric load. Hognestad's stress-strain curve was again used but no assumption made of the deflected shape. This was determined by numerical integration in an iterative solution, using a computer program.

Chang and Ferguson⁽³²⁾ (1963) also used a computer program to determine, by numerical integration, the deflected shape of long slender concrete columns. Six columns were tested to verify the results obtained from the numerical method, in particular the moment-curvature relation. Reasonable agreement was found between theory and experiment. Their critical column load was based on the maximum resisting moment of the column section rather than on the cotangency criterion which leads to a larger critical load at a smaller moment. In the paper this difference is obscured and no reasons given for it. The point was brought into focus by Holley and Mauch's⁽³³⁾ discussion of the paper and Chang and Ferguson's arguments, in defence, do not seem to justify changing the cotangency criterion which is based on fundamental concepts.

The long restrained reinforced concrete column as part of a rectangular frame was investigated by Breen and Ferguson⁽³⁴⁾ (1964) and by Breen⁽³⁵⁾ (1965). They used computer programs to develop the moment-curvature-load relations and an iterative procedure, including numerical integration for the determination of deflected shape, to solve the non-linear indeterminate problem. The analysis was repeated with increasing load and the program determined the instability load by its failure to attain an equilibrium position at that load. Test results were presented which showed

reasonable agreement with theory.

The development of prestressed concrete, with the more efficient use of materials, resulted in slender structural elements. The advantages of long prestressed concrete piles and the speed and economy of using precast elements, including columns, brought the need of investigating their buckling behavior. The number of reported theoretical and experimental investigations is much smaller, and of more recent origin, than for reinforced concrete columns. A more detailed review of literature is given later and only a number of general comments will be made here.

Prestressing a structural element the main aim of which is to carry applied compressive load might seem an anomaly. It has been shown, however, that prestressing does not reduce the load carrying capacity of axially loaded columns and might even have a beneficial effect. It is for eccentrically loaded columns in particular that prestressing can be of great advantage. Such elements, exhibiting a combination of beam and column action, deflect from the very beginning of loading and prestressing can improve their flexibility characteristics and allow them to reach a higher buckling load. It is obvious, however, that excessive prestressing will lead to a premature material failure before the buckling load of the column can be reached. How much prestress to apply to a particular column to get a maximum load carrying capacity becomes one of the questions that research must answer.

The theoretical and experimental problems of prestressed concrete columns are similar to reinforced concrete but a number of additional complications exist. The testing of eccentrically loaded columns involves the application of a moment at the column ends. In pretensioned columns the lack of prestress along the end development lengths can result in local end failures unless special precautions are taken. In the actual structure, the end moments come from the beams, the column can be prestressed monolithically with the beams and no end trouble need arise. In the laboratory specimen the problem is to find a way of preventing end failures without disturbing the prestress in the rest of the column.

To observe the behavior of the column (deflections, strains and loads) near and at the buckling load, the manner of testing is very important. Most of the reported tests on columns, reinforced and prestressed, have been conducted in hydraulic testing machines. Under these circumstances, buckling occurs suddenly, it is almost impossible to determine accurately the deflected shape at buckling and the post-buckling behavior can not be investigated. Also, two distinct types of failures can occur, namely material and instability failure. When testing in a hydraulic testing machine, "each type of failure is immediately followed by the other so that it is difficult to say with certainty in the laboratory which has been the primary cause of failure."⁽³⁶⁾ These difficulties can be overcome if testing is performed in a screw-jack testing frame, where an axial shortening of the column is applied and the resultant load measured.

The theoretical prediction of the buckling load of a long column obviously necessitates the calculation of deflections and therefore the knowledge of the concrete stress-strain relationship. For reinforced concrete a body of knowledge has accumulated and such relationships can be assumed with reasonable accuracy and confidence. In prestressed concrete an additional variable is introduced. Here, between the time of release and testing, the concrete is subjected to creep under the prestress and the effect of this history on its stress-strain curve at testing is still a subject for future research.

Finally, the use of digital computers in the analytical development has reduced the number of simplifying assumptions to be made. A deflected shape need not be assumed and other factors could be considered, such as the strength of concrete in tension, realistic material properties, initial curvature and others. For the most efficient use of the computer, the theory should be "computer oriented" with maximum benefit derived from suitable numerical methods.

1.2 Objective and Scope of This Investigation

It was the objective of this investigation to determine the behavior of slender prestressed concrete columns under eccentric load through the full range of loading from zero to material failure and including a possible critical buckling load. The work includes both experimental tests and analytical developments and considers the influence of a number of variables on the behavior and buckling loads of the columns.

(a) Experimental

A total of 36 long eccentrically loaded, hinged, axially prestressed concrete columns have been tested. The columns were of model size, having a cross-section of 2 in. x 3 in. and pretensioned by four high tensile steel wires of 0.198 in. diameter. The columns were 3 ft. - 4 in., 5 ft. and 6 ft. - 8 in. long. The prestress was released at 14 days and the columns tested at an age of 28 to 30 days. The testing was performed in a specially designed frame, with the strain applied through a screw-jack and the resultant load measured by a load cell. Measurements were thus taken past the buckling load, if it occurred first, up to material failure. The deflected shape was determined by dial readings at seven points along the column length and strains on the concrete surface were measured around the mid-height section. The following variables were investigated.

1. Eccentricity

Eccentricity to least dimension ratios: $\frac{e}{d} = \frac{1}{8}, \frac{3}{4}$ and 2.

2. Slenderness

Length to least dimension ratios: $\frac{l}{d} = 20, 30$ and 40.

3. Prestress

Prestress to concrete strength ratios: $\frac{f_{cp}}{f_c} = 0.1, 0.3$ and 0.5.

In addition to the 27 columns representing all the possible combinations of the above three variables, 9 duplicates were tested. To determine the properties of the column materials, 36 concrete cylinders, 12 concrete cubes and 12 tensile steel tests were performed. The concrete

stress-strain relationship in compression was obtained on 12 of the 36 cylinders.

(b) Theoretical

For the theoretical analysis, a computer program was written, which gives, for each particular column, the full load-deflection curve, the buckling load, based on the cotangency criterion, and load-strain relations.

The analysis is based on a finite element approach and uses iteration and suitable numerical methods. The deflected shape of the column is established by assuming constant curvature within each of the short finite elements. The two equations of statics are written at one particular point in each of the finite elements. These simultaneous nonlinear equations, involving the details of cross-section and assumed non-linear material properties, are solved by successive approximations using Newton's method of tangents. Iteration along the column length is used to satisfy the boundary conditions. The resultant solution satisfies geometric compatibility but statics are satisfied only at selected points along the column lengths. This introduces an approximation, for which, by a suitable selection of these points, upper and lower bounds are obtained. The analysis includes considerations of the initial shape of the column, the contribution of the concrete in tension and a certain freedom in the selection of the material stress-strain curves. The overall method is to develop the load-central deflection curve by calculating the loads for increasing values of central deflections. The maximum load represents the critical buckling value.

Comparison of experimental and theoretical critical loads showed good agreement. Computer programs were also written and used for the automatic plotting of load-deflection, load-strains and deflected column shape of both experimental and theoretical values for each of the columns tested. Good agreement was observed throughout the loading history.

Using the developed computer program further analysis of the effect of variables on the critical load was performed. The variables investigated were:

- (1) effect of neglecting the tensile concrete contribution
- (2) effect of initial curvature
- (3) effect of concrete compressive strength
- (4) effect of area of steel.

Chapter 2. REVIEW OF LITERATURE ON PRESTRESSED CONCRETE COLUMNS

2.1 Breckenridge⁽³⁷⁾ (1953)

Breckenridge's study was one of the first reported experimental investigations of prestressed concrete columns. At that time, a literature survey revealed little information on the subject. There were, however, interesting pioneering uses of prestressed columns. Three similar arch bridges near Caracas in Venezuela,⁽³⁸⁾ designed by Freyssinet, used prestressed columns of deep I - section of a maximum slenderness of 116 (equivalent $\frac{l}{d} = 33.5$ for a rectangular column.) Other examples were an office building in Belgium⁽³⁹⁾ and three buildings in England^(40,41,42) (slenderness of up to $\frac{l}{d} = 37$). The advantages of these columns are discussed in the references mentioned.

Breckenridge tested 10 model size columns of five different types of rectangular cross-sections (from 3 in. x 3 in. down to 1-5/8 in. x 2 in.). The column slenderness varied between $\frac{l}{d} = 24.4$ to 44.9, with the actual lengths being 5 ft. - 10 in. to 6 ft. - 1 in. All but one of the columns were prestressed by post-tensioning using a single, central, axial 1/4 in. dia. high strength prestressing wire not bonded to the concrete.

The columns were tested under an axial load in a hydraulic testing machine. The columns had hinged end conditions supplied by ball joint arrangements. A special "eccentricity adjuster" was used at both column ends to ensure an axial application of the load. The "buckling criterion" was taken as the point at which an increase in load caused a decrease in strain on one side of the column, as measured by SR-4 electrical resistance strain

gages attached to the concrete surface. With this non-destructive buckling criterion, a total of 68 axial load tests were performed on the 10 columns. During this testing the prestress was varied with the f_{cp}'/f_c' ratio ranging from 0 to 0.2. One of the columns, in addition to 14 axial tests, was also tested three times under an eccentric load, with the eccentricities of $\frac{e}{d} = \frac{1}{16}$, $\frac{1}{8}$ and $\frac{1}{6}$. The eccentric tests used a prestress of about $f_{cp}'/f_c' = 0.2$ and the load was increased until the strain on the tensile face of the concrete was reduced to zero.

A theoretical analysis was presented investigating the effect of axial prestressing on the load that a slender column can carry. The analysis was for a column with a single concentrically placed prestressing unit which is not bonded but in contact with the concrete throughout its length. Breckenridge assumed a linear elastic material and considered the forces that the prestressing wire applies to the concrete. In addition to the axial forces at the ends, which tend to buckle the column, as soon as the column starts to bend, i.e., deflect from its straight shape, there will be lateral forces acting along the column length, with the prestressing wire resisting the bending. It was shown that the sum of the moments at any point along the column due to the forces transferred from the prestressing wire to the concrete is equal to zero. Thus, the conclusion was reached that the "prestressing such as described (no matter how great, just as long as it does not exceed the difference between the critical load and the ultimate compressive strength of the concrete) will

have absolutely no effect on the critical superimposed load which the column will carry." Some other methods of prestressing were considered, all leading to the same conclusion. Experimentally, no effect of prestress on the axial buckling load was observed. The axial test results were compared with Euler's formula, using a reduced modulus of elasticity, obtained by dividing the average stress at buckling by the average concrete strain. Though this modulus is higher than either the tangent modulus or the 80% secant modulus, as determined from concrete cylinder tests, nevertheless, the experimental loads were higher than the theoretical values. There was a high variability in the test results and even the average ratios of experimental to theoretical loads for the five column types varied between 0.72 and 2.18. This variability and higher test results are probably due to accidental eccentricities, some friction at the ball joints and the repeated testing of specimens.

For the few eccentric tests no real buckling analysis was presented. In the range of testing, i.e., within the "buckling criterion" used, good agreement was obtained between stresses measured on the concrete surface and those calculated from the secant formula.

In conclusion, repeated testing does not seem to be justified for a material like concrete, with its non-linear inelastic stress-strain relationship, if a proper definition of buckling is to be used, which is needed as the "cornerstone" of any theoretical analysis.

2.2 Ozell and Jernigan⁽⁴³⁾ (1956)

The objectives of this investigation were to study:

1. The relation between slenderness and ultimate strength of prestressed concrete columns.
2. The establishing of an optimum value of "p", the ratio of prestressing steel area (A_s) to net concrete area (A_c).
3. The effect of lateral ties on the ultimate strength and the general behavior of the columns.
4. The comparative ultimate strength of prestressed and reinforced columns of approximately the same cross section and properties.

The experimental work consisted in the testing of 47 full-sized columns. All but one of the columns were axially loaded in a hydraulic testing machine, with a flat end at the bottom and a rounded end, through a spherical loading block, at the top. All columns were of square cross-section, 11 of 7-3/4 in. x 7-3/4 in. and 36 of 6 in. x 6 in. nominal sizes. The columns were made up of 16 groups, each with triplicate specimens, except one group which had two specimens. The range of variables investigated were:

(a) Slenderness ratios:

<u>l/d</u>	<u>Number of specimens</u>
10	5
15	3
20	18
30	15
32	6
	<hr/> 47

Actual column lengths varied between 6 ft. - 8 in. and 15 ft.

(b) The columns were pretensioned axially by means of Roebling seven-wire strands of sizes 5/16, 3/8 and 7/16 in. The percentage of prestressing steel (p) varied between 0.53 and 2.50%. This represented a variation of prestress to concrete strength ratio (f_{cp}'/f_c') of about 0.10 to 0.50. It should be noted that, since the prestress in the strands was kept constant at 140,000 p.s.i., the two variables of amount of steel and concrete prestress are combined here into one.

(c) There were 32 columns with lateral ties and 15 without.

(d) There were 41 prestressed columns and 6 reinforced. The reinforced concrete columns had slenderness ratios of 20 (3 columns) and 30 (3 columns) and a steel percentage of $p = 3.56\%$.

The following conclusions were drawn from the test results:

1. Based on the average values of the groups of columns, it was concluded that "the optimum p value for l/d ratios of 20 and 30 is about 1.25%, which corresponds to about 0.25 f_c' precompression" i.e., $f_{cp}'/f_c' = 0.25$. However, using the tabulated values of the replicas within each group, a statistical analysis shows that the differences with p are not significant for $l/d = 20$ and are just significant (at the 5% level) for $l/d = 30$.
2. Lateral ties were shown to have a beneficial effect. The columns without ties had much larger lateral deflections although the average ultimate load was almost the same for both series.

3. For the axial loading of this investigation, prestressed concrete columns with $l/d = 20$ had lower ultimate strengths than reinforced concrete columns, whereas those with $l/d = 30$ had almost the same strength.

An approximate empirical formula was suggested to predict the ultimate load of short prestressed pretensioned columns:

$$P_u = 0.77 f_c' (A_c - A_s) - A_s (k f_s) \quad (2.1)$$

where P_u = ultimate strength of column, lb.
 f_c' = ultimate strength of concrete, p.s.i.
 A_c = cross-sectional area of column, sq. in.
 A_s = cross-sectional area of steel strands, sq. in.
 k = reduction factor in strand stress due to column deflection, per cent (i.e., reduction factor for loss of prestress at ultimate load)
 f_s = working stress in strand, p.s.i.

This expression should be restricted to the ultimate axial load of a square, prestressed, pretensioned concrete column, with lateral ties, with p values between 1.2 and 2.0%, f_c' between 6,500 and 8,000 p.s.i and l/d ratio up to 20. For l/d of 30 a reduction factor of 0.90 was suggested. Within the stated range of variables, fair agreement was obtained between test results and Equation (2.1).

A theoretical study was also presented for axially loaded long columns. It was assumed that the columns had an initial curvature. Assuming also that the initial shape is sinusoidal and that the material is linearly elastic, the initial central deflection can be calculated using Southwell's⁽⁴⁴⁾ plot. This requires the knowledge of the load-deflection relationship. Using the experimental results a conservative value of the initial deflection was found to be $\ell/417$. An approximate expression was then used for the central deflection y under any given load. This involved the calculated initial central deflection and the Euler buckling load of the column. The extreme concrete fiber stress was written as the sum of the axial and the bending stresses, which involve the central deflection y . By substituting the value of f'_c for the maximum extreme concrete fiber stress, the required relationship between slenderness (which comes from the Euler buckling load) and the ultimate load of the column was obtained. This procedure was shown to give a lower bound to the experimental test results. It should be noted, however, that the above procedure is mostly empirical. The calculated initial deflection is a fictitious one, being based on a linearly elastic material. It also requires the test results for its determination. Moreover, the ultimate load is not based here on instability but on a material failure, considered to be reached when the extreme fiber stress becomes equal to f'_c .

2.3 Zia⁽⁴⁵⁾ (1957)

Zia presented a theoretical analysis of the ultimate strength of slender hinged prestressed concrete columns. He assumed an elasto-plastic

compressive stress-strain curve for the concrete, as first proposed by Jensen. The deflected shape of the column was assumed to be sinusoidal. The criterion used for the ultimate load was not one of instability but based on material failure, i.e., the load at which the maximum strain in the column reaches the value of the concrete crushing strain. The theoretical results were presented by means of appropriate curves and a favorable comparison was obtained with the experimental results of Ozell and Jernigan. On the influence of prestressing on the ultimate load, Zia felt that "too little prestressing sacrifices the flexural resistance of the column and too much prestressing penalizes its axial load carrying capacity."

2.4 Lin and Itaya⁽⁴⁶⁾ (1957)

Lin and Itaya reported on one full size column, tested in a hydraulic testing machine as a demonstration for delegates to the World Conference on Prestressed Concrete in San Francisco. The 16 in. octagonal shape column was 25 ft. long, axially pretensioned with thirteen 3/8 in. dia. 7-wire strands. The column was tested under an eccentric load and had the following details

$$\text{prestress: } f_{cp}'/f_c' = 0.12$$

$$\text{load eccentricity: } e/d = 0.25$$

$$\text{slenderness: } l/d = 18-3/4$$

Before cracking, the column was assumed to behave elastically and the secant formula was used to calculate mid-height deflections. Beyond cracking, plastic analysis was applied with elasto-plastic stress-strain curves assumed for both steel and concrete. It was assumed that concrete could take tension for stresses below the modulus of rupture and that its ultimate compressive strain was 0.0031. Two methods of analysis were presented. In method I the deflected shape of the column was obtained by numerical integration using a derived moment-curvature relation, while method II was an approximate solution, assuming the deflected shape to be part of a cosine wave, similar to Broms and Viest.⁽²⁴⁾ Using both methods, load-deflection and load-strain curves were obtained. In this case both methods indicated an instability failure. The buckling load was given by the maximum of the load-deflection curve, which is the proper cotangency criterion. The ultimate loads obtained by various means were as follows.

	<u>Ult. load Kips</u>	<u>% of test load</u>
Experimental	390	100
Analytical, method I	357	92
Analytical, method II	351	90
Elastic theory (assuming un-cracked sections)	333	85

The relatively high experimental value was attributed to the possibility of higher strength of concrete in the column (as against the strength of 6x12 in. cylinders which was used in the analysis) or due to errors in the assumed stress-strain relationships.

Lin and Itaya concluded that "needless to mention, much more experimental data and analyses are necessary for the solution of this problem of eccentrically loaded prestressed concrete columns."

2.5 H. R. Brown⁽⁴⁷⁾ (1960), Hall^(36,48) (1961, 1962), Brown and Hall^(49,50) (1965, 1966).

Brown's thesis⁽⁴⁷⁾ and the subsequent four papers^(36,48,49,50) describe tests on 30 prestressed concrete columns. The columns were 3 in. x 2 in. in cross-section, 66 in long ($\ell/d = 33$) and axially pretensioned with four 0.2 in. dia. high tensile steel wires. The cross-sectional details of these columns are the same as of the columns tested in the present investigation. The variables investigated were

prestress: f_{cp}'/f_c' of 0, 0.15, 0.31, 0.47 and 0.62
and load eccentricity: e/d of 0, $\frac{1}{20}$, $\frac{1}{8}$, $\frac{1}{4}$, $\frac{3}{4}$ and 2. Testing was performed in a hydraulic testing machine, so that deflections and strains at buckling could be determined only approximately.

An initial difficulty was encountered in columns with large eccentricities. These columns exhibited premature end failures and this was attributed to lack of prestress in the finite bond development length at both column ends. Collars and serrated-wedge grips did not solve the problem, which was finally overcome by an additional post-tensioning operation after the release of the initial pretensioning. In this laborious operation, each wire was post-tensioned individually and anchored at each end with a barrel grip. For the sake of uniformity, this operation was

performed on all columns, regardless of eccentricity. In the opinion of the writer, the post-tensioning probably destroyed the bond over a significant portion of the column length and introduced inaccuracies in the column prestress, particularly for large prestress values.

Brown⁽⁴⁷⁾ presented an approximate analytical solution based on Hognestad's⁽²¹⁾ stress-strain curve for concrete, the proper cotangency criterion and a modified cosine deflected shape at buckling. He assumed the actual radius of curvature at column mid-height, under the buckling load, to be only 0.72 times the value calculated from the cosine curve. The value of 0.72 was obtained from the experimental results by extrapolating to the conditions at buckling. A comparison of experimental buckling loads with the theoretical values showed reasonable agreement for prestress values (f_{cp}/f'_c) up to about 0.30. For higher prestress the disagreement was very significant, the experimental loads increased with the prestress while the theoretical values decreased. This discrepancy was attributed to variation of basic concrete properties (stress-strain curve parameters) with prestress. While such a variation might well exist, the writer believes that the observed discrepancy is, in this case, due to the post-tensioning experimental procedure.

Hall⁽³⁶⁾ presented a suggested analytic method which uses a deflected shape determined by numerical integration and assumes that the curvature can be represented by the second derivative of the deflection. However, no theoretical results were given.

2.6 Bakhoun, Samaan, Aboul Eid, Antar and Esmat⁽⁵¹⁾ (1962)

A very brief report is presented of test results on six eccentrically loaded columns (tested by Antar). All columns were 15x20 cm. in cross-section, $l/d = 30$, $e/d = 2.5$ and varying amount of steel, both tensioned 5 mm. wires and untensioned 1/2 in. and 3/8 in. dia. steel. From the arrangement of the steel it would appear that the columns were eccentrically prestressed but no details are given.

The authors claim that "The failure of long columns eccentrically loaded is sometimes referred to as eccentric buckling. However, the ultimate load is usually reached long before any condition of elastic instability is approached. We have merely to consider the effect of the additional moment due to deflection at failure." The writer strongly disagrees with these statements; the presence of instability in most cases, though not linearly elastic instability, is amply demonstrated by tests described later in this thesis.

Comparison between test results and ultimate loads computed on the basis of the above approach, using a rectangular compressive stress distribution in the concrete and a simplified analytic method, shows satisfactory agreement. Here, this agreement is probably due to the high eccentricity ratio and possibly high prestress.

2.7 Moreadith⁽⁵²⁾ (1964), Zia and Moreadith⁽⁵³⁾ (1966)

This work dealt with an analytical investigation of load carrying capacity of rectangular prestressed concrete columns. No testing was in-

volved and the primary purpose of the investigation was to determine the effects of various parameters on the column strength. These included concrete strength, steel ratio (with the steel always prestressed to the same value), slenderness ratio and eccentricity of load.

The analysis of axially loaded columns made use of the generalized Euler equation with the tangent modulus of elasticity.

The analysis of eccentrically loaded columns assumed a Hognestad⁽²¹⁾ type of concrete stress-strain curve, neglecting tension and with the maximum compressive stress equal to the cylinder strength, and an elasto-plastic stress-strain curve for the steel. Small deflections were assumed and the curvature taken equal to the second derivative of deflection. The method of analysis was similar to that of Chang and Ferguson,⁽³²⁾ however, a proper cotangency criterion was used. This took the form of

$$d\delta/dy_m = 0$$

where y_m = midheight deflection of column.

The procedure was to determine the maximum, critical, length for a column of given cross-section under a given load and end eccentricity. This was achieved by varying the midheight column deflection. Numerical integration was used to obtain the deflected shape of the column. Thus, the method is most suitable for the construction of curves relating the critical load to various parameters rather than the investigation of the behavior of a given column both before and after buckling. A limitation of the analysis is the assumption that the steel is always stressed to the same value (an

effective steel stress of 140,000 p.s.i. was used, after all losses.) A change of prestress (f_{cp}/f_c') thus requires a change in the steel percentage and the two parameters, steel prestress and steel area, are not separated.

Some of the conclusions reached were:

1. For short columns with low strength concrete ($f_c' = 4,000$ p.s.i.), heavy prestress is detrimental to column strength.
2. The greatest advantage of prestressing lies with the slender columns under large eccentric load (maximum e/d considered was 0.50).
3. Simple design procedures were suggested⁽⁵³⁾ for short ($l/d \leq 10$) and intermediate ($10 \leq l/d \leq 30$) columns.
4. It was considered⁽⁵²⁾ that "the results of available experimental investigations of prestressed concrete columns are too limited to offer comparisons with the theoretical results of this work. There is a definite need for more carefully conducted experimental programs to substantiate the results of this investigation."

2.8 K. J. Brown⁽⁵⁴⁾ (1965)

Brown reported the testing of 65 pin-ended prestressed concrete columns (13 axially loaded and 52 eccentrically loaded). The columns had a rectangular cross-section of 3-1/2 in. x 4 in. and were reinforced with 4 x 1/4 in. dia. mild steel rods, one deformed Macalloy high tensile prestressing bar (1/2 in. or 5/8 in. dia.) and lateral ties. Other details were:

1. slenderness: ℓ/d of 5, 15, 22 and 29
(actual lengths 12, 50, 75 and 100 inches)
2. concrete quality: $f'_c = 4,800$ p.s.i. (average).
3. prestress: axial: f_{cp}/f'_c approx. 0.25 to 0.30, eccentric:
bar eccentricities of $d/7$ and $2d/7$.
4. load eccentricities: e/d of $1/7$, $2/7$ and $3/7$.

The longest columns were tested in a special test rig with the load applied by turnbuckle. All other columns were tested in a hydraulic machine.

The analytical calculation of the ultimate column load used two main assumptions:

- (a) that the critical concrete compressive strain at failure was 0.00180, due to both prestress and load.
- (b) that the total deflection due to prestress and loading at mid-height under critical conditions was given by $\ell^2 a/15$ where ℓ = length of column, $a = 0.00180/c$ and c = depth of neutral axis from extreme compression fibres.

The first above assumption was based on the experimental critical compressive strains, which had an average of 0.00180 (range 0.00120 to 0.00280, standard deviation 0.00025). In addition a parabolic stress-strain curve was assumed for the concrete, with a maximum stress of $0.85 f'_c$ at the maximum 0.00180 strain. The prestressing steel was assumed to

be a linearly elastic material. With all these assumptions, the problem reduces to the solution of the two equations of equilibrium at mid-height and the compatibility equation (based on Bernoulli's hypothesis). A cubic equation results for the depth of the neutral axis (c) and this is solved graphically by successive approximations.

Comparison of experimental and theoretical ultimate loads showed close agreement. The average ratios of $P_{exp.}/P_{th.}$ were 1.00 and 1.06, with standard deviations of 0.04 and 0.08, for the axially and eccentrically loaded columns respectively. Brown also applied his analytical method to 162 test columns reported in ten previous investigations. These were mostly short reinforced concrete columns, both axially and eccentrically loaded. For all the 227 test columns the average ratio of test to calculated ultimate load was 1.01 with a standard deviation of 0.09. However, it should be emphasized that this analytical method is basically empirical, it does not include an instability criterion, could not be extended to columns with end restraints and could not predict the column behavior either before or after the maximum, critical load.

Among the conclusions reached from Brown's experimental work were the following:

1. With axial prestress, an increase in ultimate load was obtained when the load eccentricity was high enough ($e/d = 3/7$).
2. Eccentric prestress is beneficial for columns of higher slenderness and load eccentricity. An increase in eccentric prestress resulted

in a reduced ultimate strength for the lower load eccentricities up to $e/d = 1/7$, hardly altered ultimate strength when $e/d = 2/7$ and resulted in greater ultimate load carrying capacity when e/d was equal to $3/7$.

2.9 Kabaila and Hall⁽⁵⁵⁾ (1966)

This paper presents an analytical solution of the instability of unrestrained prestressed concrete columns with end eccentricities. The cotangency instability criterion is used, curvature is taken equal to the second derivative of deflection and the column deflected shape is determined using arithmetic integration with central difference expressions. A continuous stress-strain curve is adopted for the concrete, including some contribution in tension. Kabaila and Hall considered it unnecessary to adopt a critical concrete compressive strain as a criterion of material failure. Instead they used the maximum moment that can be developed at the critical mid-height section, which represents a condition of local instability. It should be emphasized, however, that when a column is subjected to loads less than the critical load, in the unstable post-buckling region, the maximum moment of the section will not suffice to determine the point of material failure.

The analytical results were compared with Brown's^(36,47,48,49,50) tests (see Section 2.5 above). To explain the observed increases in critical loads with increase in prestress, the secant modulus of elasticity and the cylinder strength, which are used in the concrete stress-strain curve, were

assumed to increase with prestress, according to expressions suggested by Brettle^(56,57). Nevertheless, analytical values compared well with experimental results for values of prestress only up to $0.30 f_c'$, i.e., in about the same prestress range as Brown's⁽³⁶⁾ original approximate analysis. Kabaila and Hall concluded that "the divergence of the experimental results for higher values of prestress throws doubt on the range of validity of the two latter [Brettle's] equations, indicating that further research is necessary in this field." It is the writer's opinion that the divergence is mainly due to Brown's post-tensioning experimental procedure.

2.10 Conclusions

The nine investigations described above probably represent the bulk of the published work on hinged prestressed concrete columns, axially and eccentrically loaded, in the thirteen years since Breckenridge's study in 1953. They contain a total of 159 tests on prestressed columns, as well as theoretical methods, though some do not use proper instability criteria.^(37,43,45,51,54) Nevertheless one must agree with Itaya's⁽⁵⁸⁾ (1965) conclusion that "additional research, both theoretical and experimental, is urged to determine the effects of many variables on these columns."

There does not seem to be an analytical method, predicting the behavior of columns over the full loading range including post-buckling, which has been substantiated by tests over a wide range of variables. Some questions have been raised in the range of high prestress and the manner of testing of almost all the columns reported does not provide data on the

post-buckling behavior, which becomes important when the column is part of an indeterminate frame. Analytical methods could be developed which are particularly suitable for computer use and which could be extended to restrained columns. It is hoped that the present investigation will contribute to some extent towards the solution of the above mentioned problems.

Chapter 3. EXPERIMENTAL WORK

3.1 Introduction

This chapter describes the experimental work of the present investigation, which consists of 36 prestressed concrete columns and material control tests.

The variables investigated were eccentricity, slenderness and prestress. The scope of the experimental work has been discussed in Section 1.2. The total number of columns tested for each variable were

eccentricity: $\frac{e}{d} = \frac{1}{8}, \frac{3}{4}$ and 2 - 10, 17 and 9 columns respectively

slenderness: $\frac{l}{d} = 20, 30$ and 40 - 12 columns each

prestress: $\frac{f_{cp}}{f_c} = 0.1, 0.3$ and 0.5 - 12 columns each.

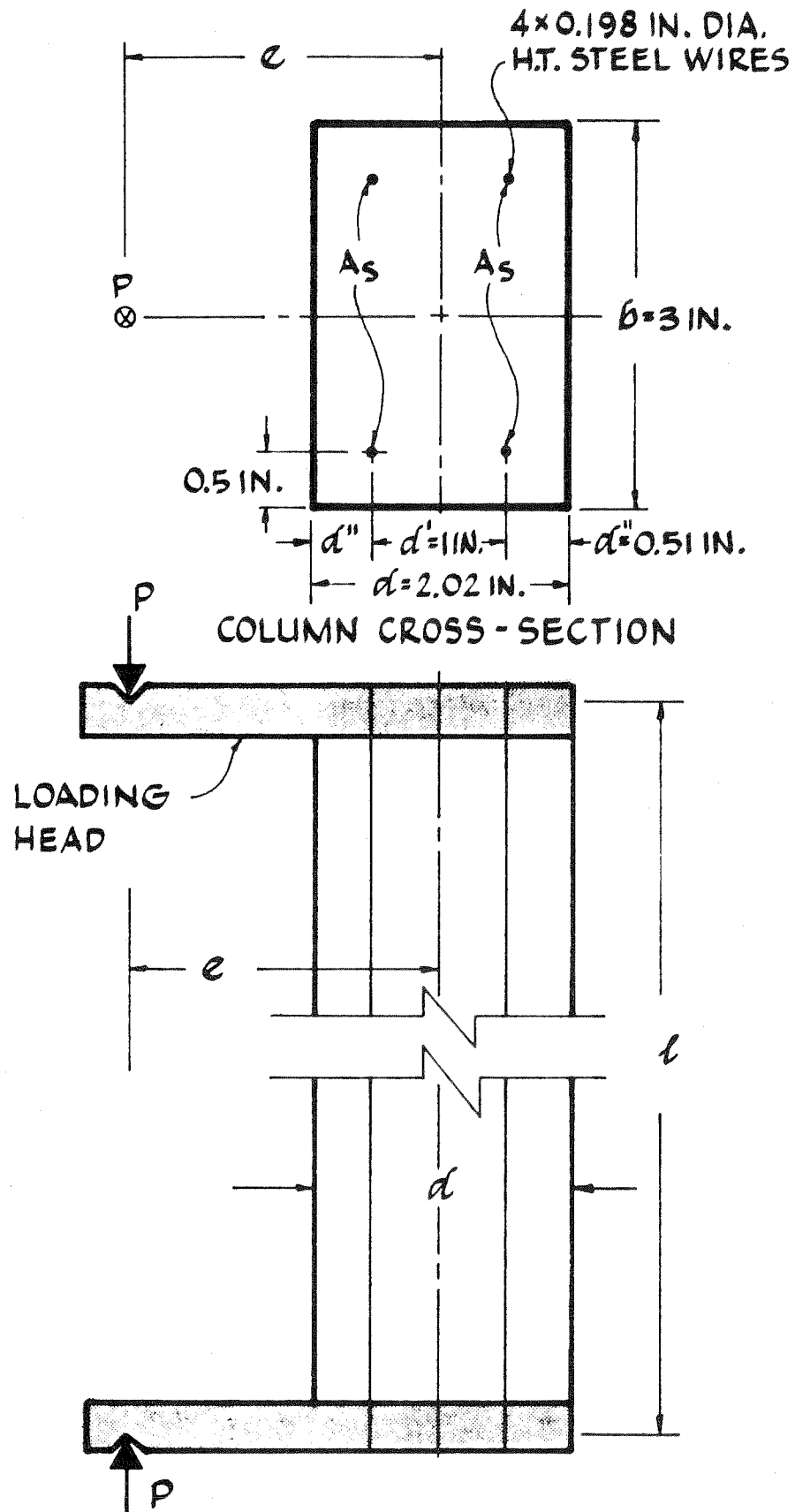
3.2 Column Details

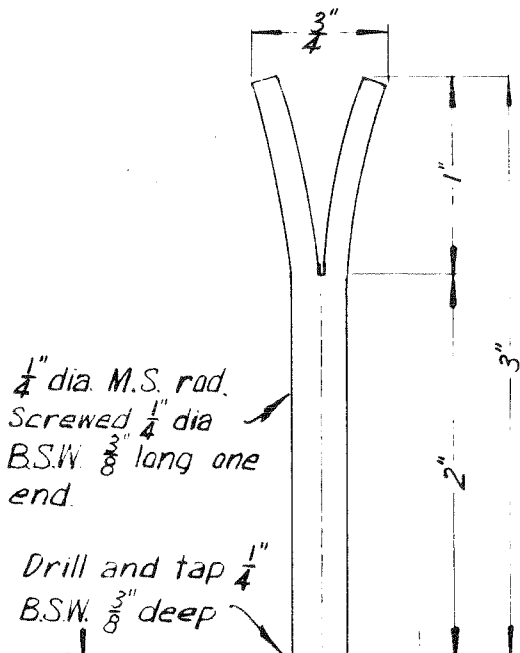
The details of the column cross-section are shown in Fig. 1. The average measured dimensions were $b = 3$ in. and $d = 2.02$ in., with maximum deviations of ± 0.02 in. The prestressing steel consisted of four high tensile steel wires of 0.198 in. diameter, with $A_s =$ area of two wires = 0.0616 sq. in. The items varied were

eccentricity: $e = 1/4$ in., 1-1/2 in. or 4 in.

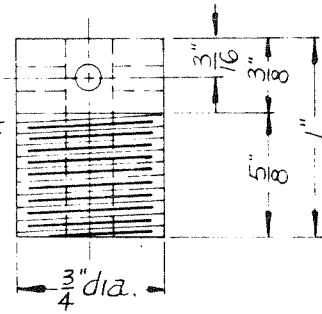
length: $l = 40, 60$ or 80 in.

prestress: f_{cp} = concrete axial prestress
= nominal 500, 1,500 or 2,500 p.s.i.

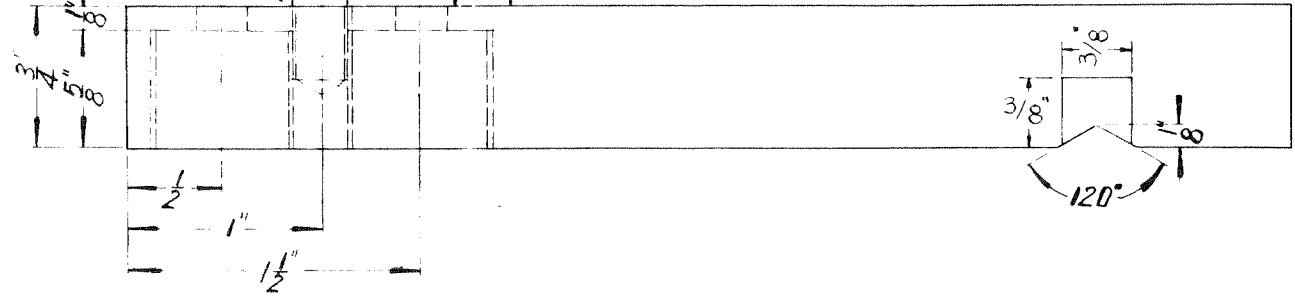




Screw 3/4" A.N.F.
5/8" LONG

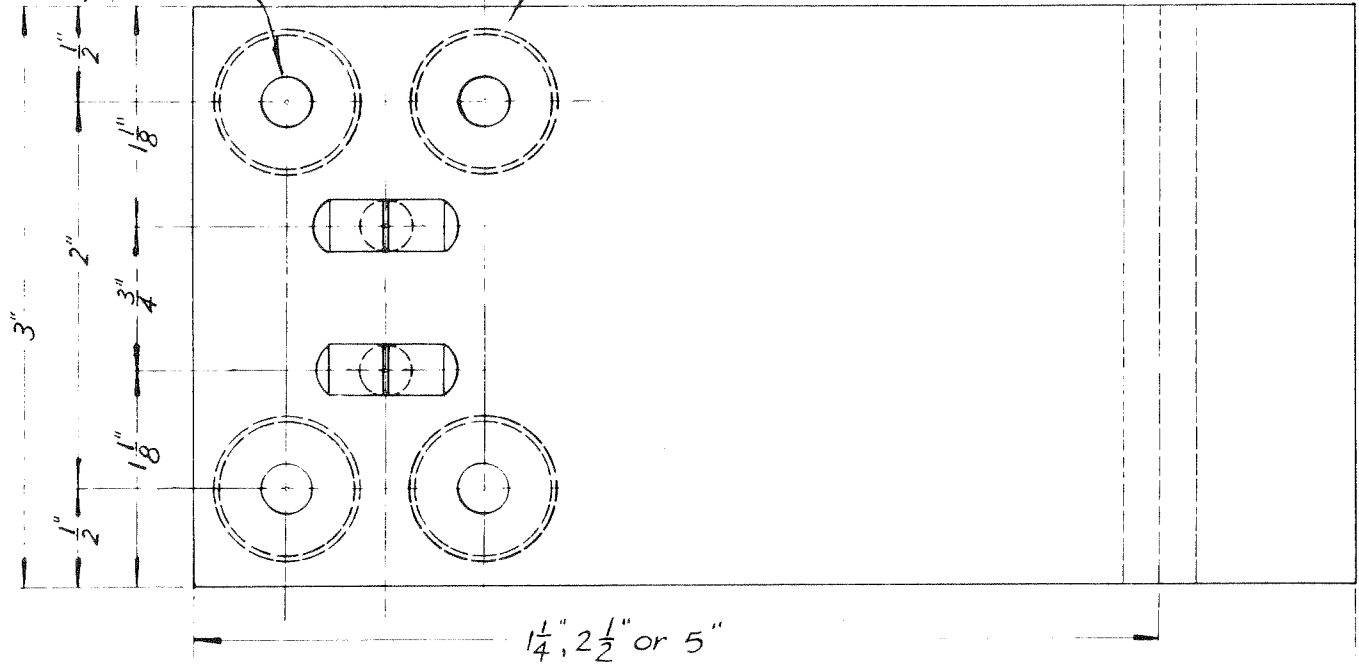


INSERT



11/16" drill and tap
3/4" A.N.F. 5/8" deep,
4 holes.

Drill 1/4", 4 holes



The load was applied by means of loading heads at each column end. The loading head details are shown in Fig. 2. Three sizes are involved, depending on eccentricity, and a photograph of the loading heads is shown in Fig. 7. The loading heads were made of alloy tool steel (Balfour steel "Kite N.S.S.3" hardened to Rockwell C45; composition 1% C, 0.3% Si and 2% Mn) and the Knife-edges (3/8 x 3/8 in. inserts) of 1% Carbon Tool Steel (hardened to Rockwell C55). The screwed inserts, the use of which will be explained later, were of mild steel, case hardened.

A group of six columns, ready for testing, including all three lengths, eccentricities and prestresses, is shown in Figs. 3 and 4.

3.3 Materials

(a) Concrete

The nominal design strength of the concrete mix was 5,000 p.s.i. The proportions, by weight, of the mix materials are shown in Table 1. The mix had a slump of 1/2-1 in.

Table 1. Concrete Mix Details

<u>Material</u>	<u>Proportions by Weight, Dry Condition</u>
Coarse Aggregate	2.7
Sand	1.8
Cement	1
Water	0.45
	<hr/> 5.95

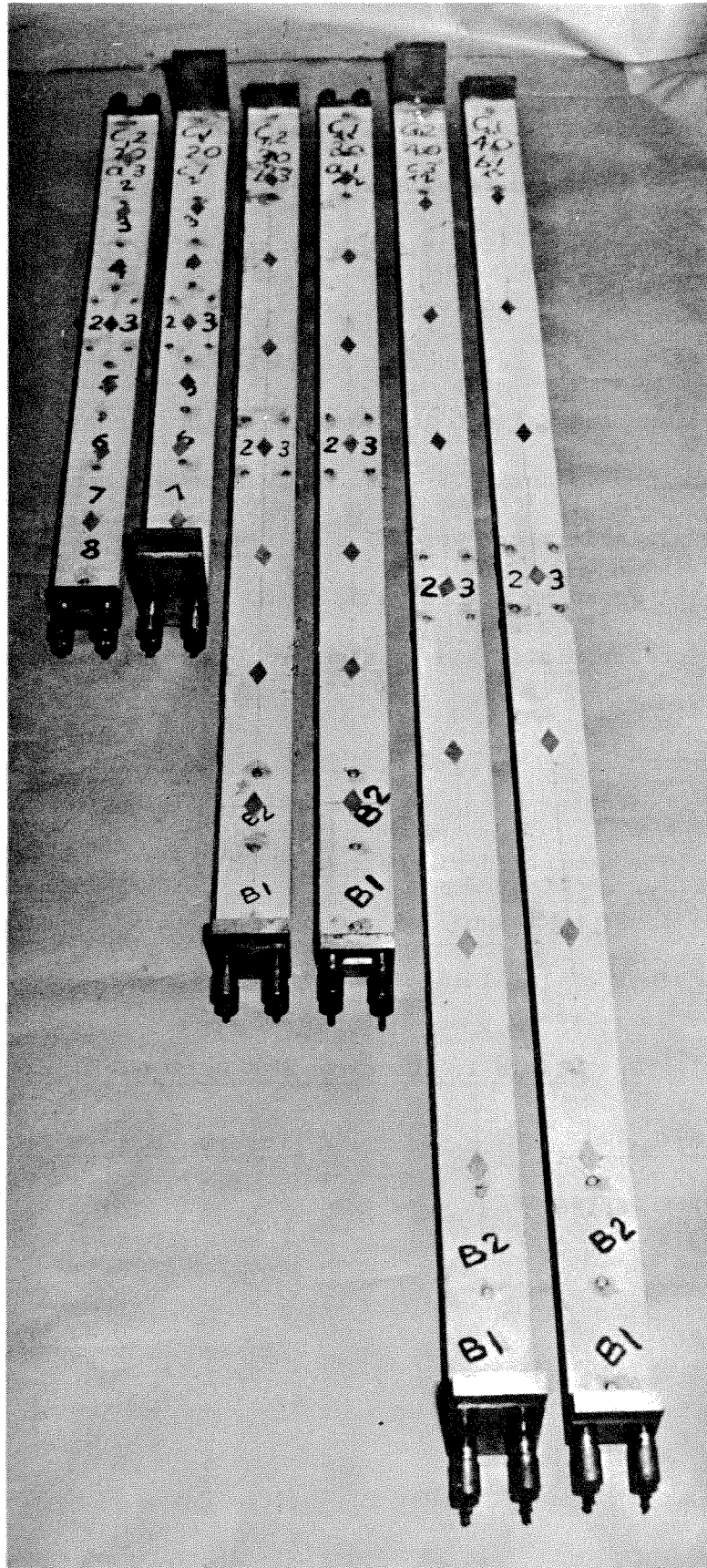


FIG. 3 GROUP OF COLUMNS

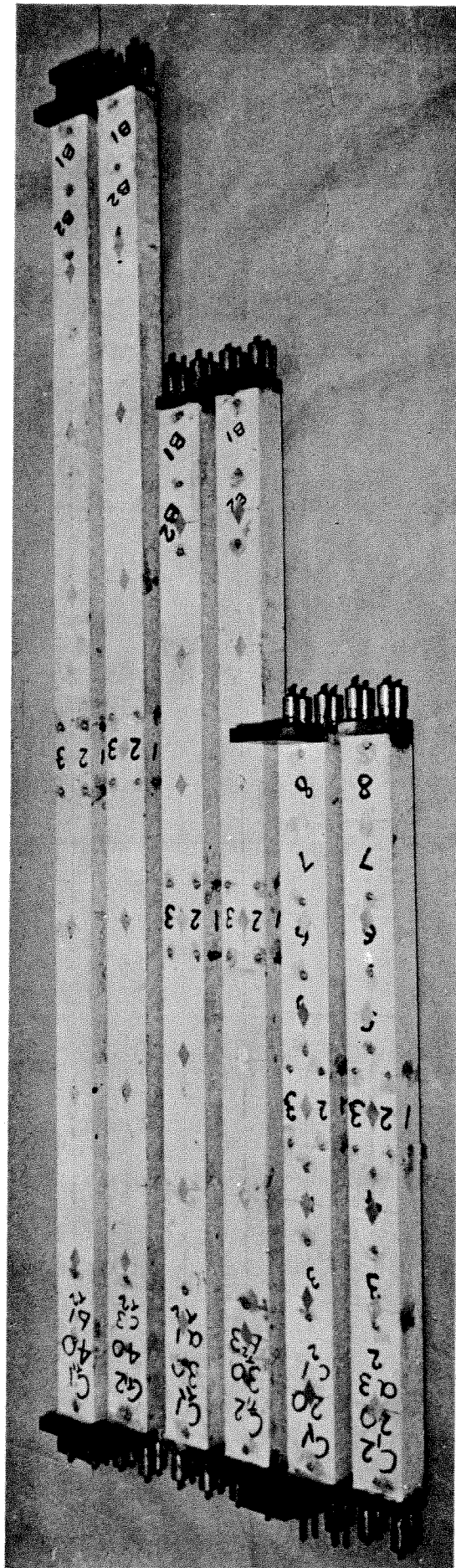


FIG. 4 GROUP OF COLUMNS

The coarse aggregate was a rounded river gravel, of 3/8 in. maximum size. The material gradings are given in Table 2.

Table 2. Material Gradings

Sieve Size	Sand Cumulative Percentage Retained	Coarse Aggregate Percentage Retained
3/4 in.	0	0
3/8 in.	0	35
3/16 in.	3	94
No. 7	13	99
No. 14	29	
No. 25	51	
No. 52	75	
No. 100	93	
No. 200	98	

No admixtures were used.

(b) Steel

The prestressing wires were of high tensile steel, 0.198 in. diameter and 0.0308 sq. in. in cross-section. The average ultimate strength of the wire, as determined from twelve tests in a 10 ton capacity Amsler testing machine, was 3.45 tons (250,900 psi) with a coefficient of variation of 0.66%. The stress-strain relation of the prestressing steel will be discussed later.

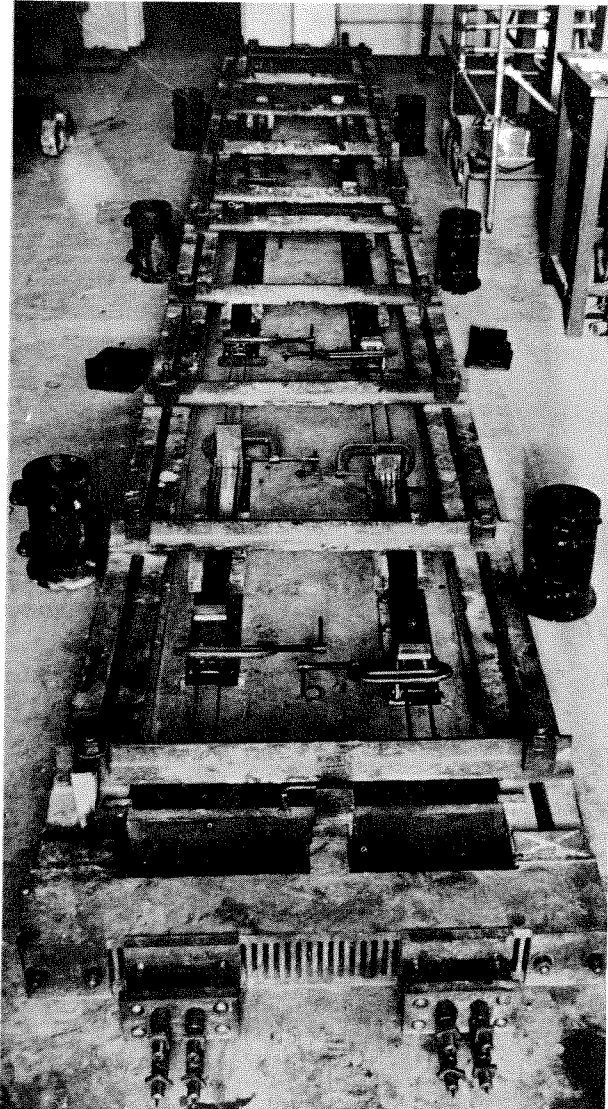
3.4 Manufacture of Test Specimens

1. Columns

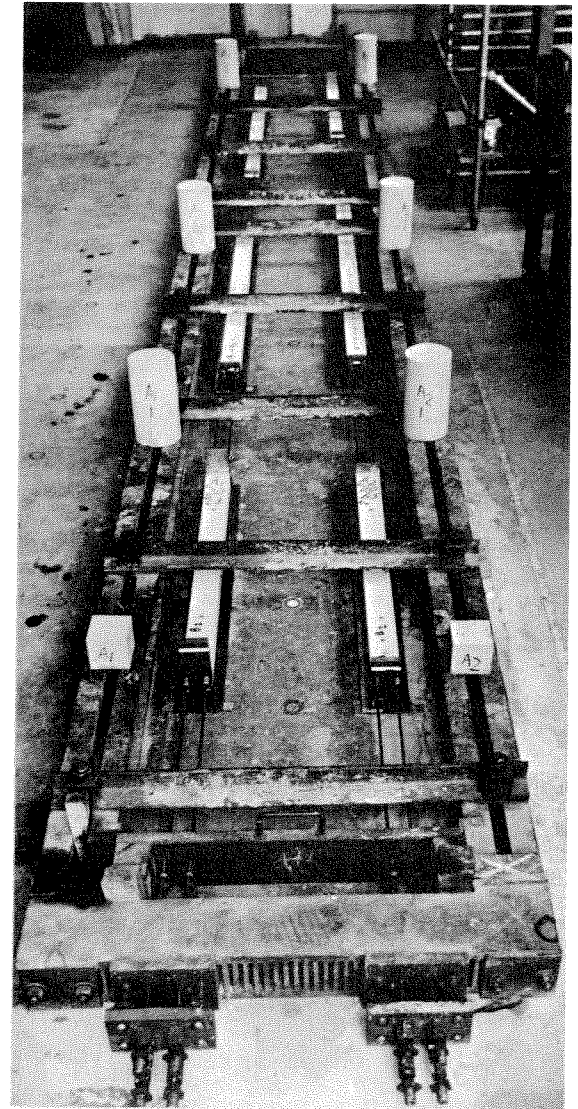
(a) Prestress

The prestressing bed used had overall dimensions of 29 ft. x 3 ft. 6 in. This allowed six columns to be made at the same time, with three columns sharing the same prestress, as shown in Fig. 5. The prestressing bed was bolted down to a structural floor.

Each wire was stressed individually with a Gifford-Udall prestressing jack of 13,000 lb. capacity. Fig. 6 shows the prestressing procedure. The wires were anchored with suitable barrels and split cone wedges. Provision was made for independent adjustment of each wire and for the joint release of the four wires of each row of columns. The required prestress was achieved by measuring the total elongation over a wire length of 27 ft. - 4 in. A depth micrometer, reading to 0.001 in., was used for the measurement (see Fig. 6). Suitable allowance was made for the sag in the wire, as determined from initial tests on wires with electrical resistance strain gages. Table 3 gives the details of steel stresses and total elongations for the three prestress values. The steel strains and stresses are based on an assumed value of 20% losses to time of testing.



(a)



(b)

FIG.5 PRESTRESSING BED
(a) FORMS READY FOR CASTING
(b) AFTER CASTING AND STRIPPING OF SIDE FORMS

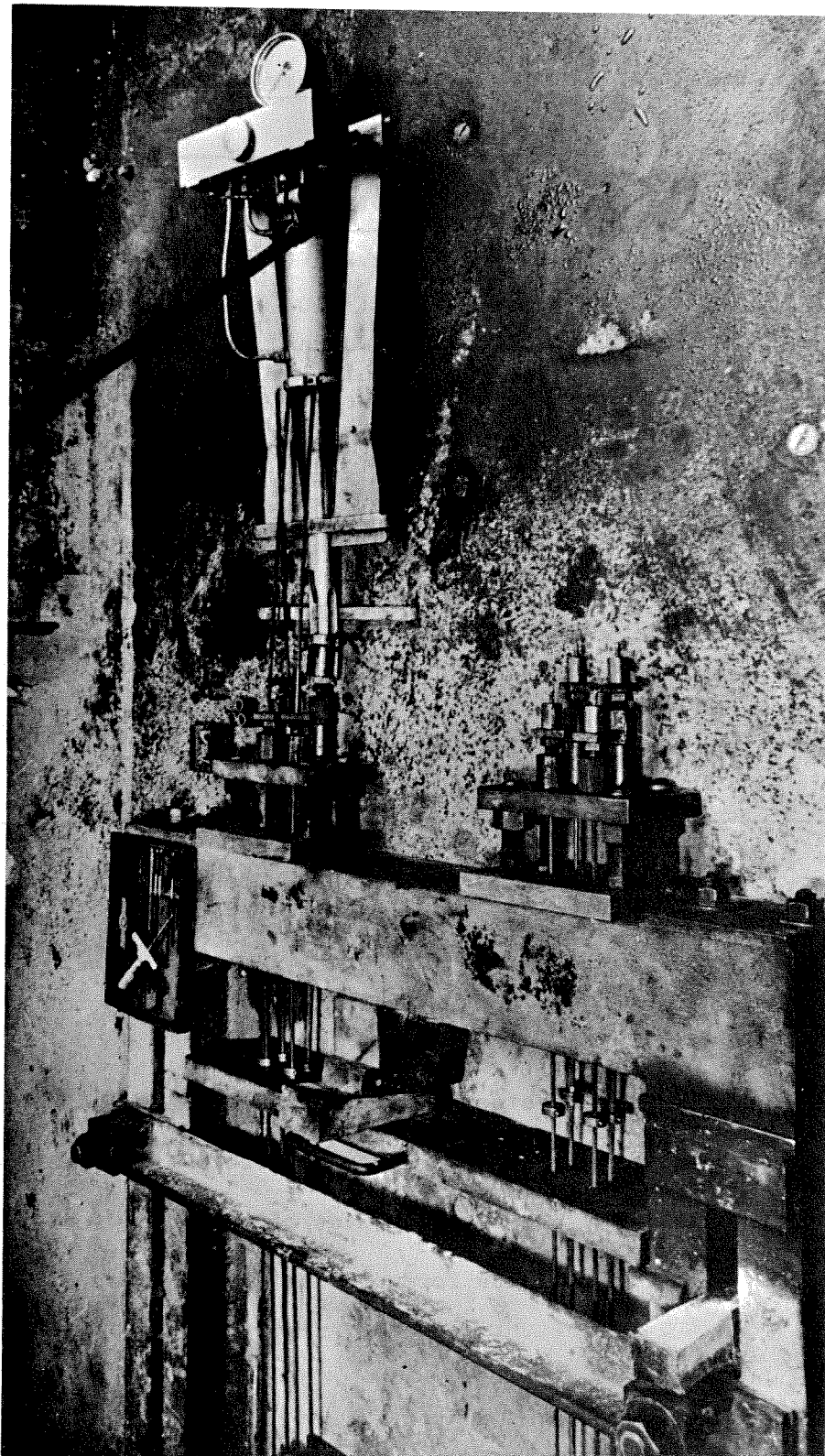


FIG. 6 PRESTRESSING PROCEDURE

Table 3. Details of Prestressing

Nominal Prestress Ratio (f_{cp}/f'_c)	Nominal ^(a) Concrete Prestress (f_{cp}) psi	Steel Prestress Values ^(b)		Total Elongation ^(c) in.
		Strain (ϵ_{pr}) ($\times 10^{-4}$)	Stress psi	
0.1	500	10.37	30,440	0.340
0.3	1500	31.12	91,315	1.021
0.5	2500	52.15	152,190	1.710

(a) Based on design value $f'_c = 5,000$ psi.

(b) Before assumed 20% losses.

(c) For 27 ft. - 4 in. length of wire.

The wires were stressed the day before and adjusted at the time of casting. The prestress was released at 14 days after casting.

(b) Formwork

Specially made steel formwork was used for the casting of the columns (see Fig. 5). The formwork had removable sides, bolted to the base at frequent intervals. The base was made of a channel section welded to a steel plate. The depth of the formwork was the required column width of 2 in.

(c) Casting

The concrete was mixed in a 1-1/2 cu. ft. capacity "Cumflow" mixer, each batch containing 250 lb. of weighed materials. The mixer was first buttered with 1/3 of batch quantities. Before water was added, the materials were mixed dry, and the total mixing time was 4 minutes. The casting of a group of six columns involved two concrete batches. Out of each batch the three columns of a prestress line were cast, as well as three 6x12 in. cylinders and one 6 in. cube. The three columns, cast from the same batch and sharing the same prestress, were one each of the three lengths and usually one each of the three eccentricities.

Before placing the concrete, the forms were lightly oiled and the wires cleaned with Carbon Tetrachloride. The concrete was thoroughly compacted in the forms using a pencil vibrator, and finished to a smooth surface. The horizontal position of the forms was such that the top surface represented the compression side in the subsequent testing.

(d) End Anchorage

The aim of the additional end anchorage was to achieve full prestress at the very ends of the columns, by preventing, at release, the wire slip in the usual bond development length. This was done using inserts screwed into the loading heads (see Figs. 2 and 7) and barrels fixed to the wires, which could bear against the inserts.

Each barrel was attached to the wire with two split cone wedges. The wedges had to be driven in with a force equal to or greater than the

maximum subsequent load in the wire. This required the development of special tools and procedures. Bolt clippers ("Record" brand No. 604, overall length about 42 in.) with a large mechanical advantage (over 80 to 1) were adapted by suitable machining of the jaws. High tensile pieces were designed, with a round end, to maintain an applied axial load on the wedges with the closing of the jaws. Split, high tensile steel, washers were used to follow the wedges, if necessary, into the barrels. The adapted bolt clippers, with a barrel and wedges, end pieces and split washers are shown in the photograph of Fig. 8. To check the force applied by the bolt clippers to the wedges, tests were performed using a short piece of mild steel bar with an electric resistance strain gage and these indicated a load above 2.5 tons.

Fig. 9 shows the procedure followed before the casting of the columns. With the inserts screwed most of the way into the loading head, and the loading head moved away along the formwork base, a barrel was attached to each of the four wires. When the loading head was back in position, a gap remained between the inserts and the loading head, with a washer between them (Fig. 9 (b)). The side forms were then attached and the concrete placed as described above. Just before the release of prestress, at the age of 14 days, the inserts were screwed out to be in firm contact with the barrels, through the washers. To facilitate free rotation of the inserts they were initially protected with an anti-seize, anti-frictional, compound (Molybond GA50). Care was taken to avoid the application of additional prestress by the movement of the inserts against the barrels.

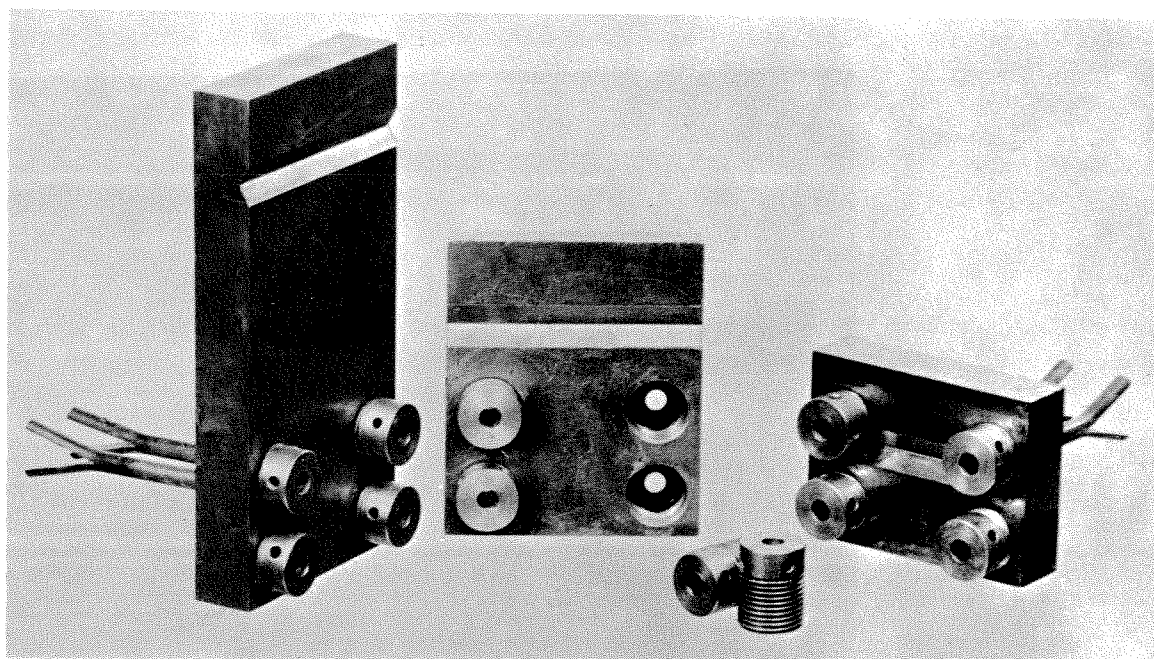


FIG. 7 LOADING HEADS

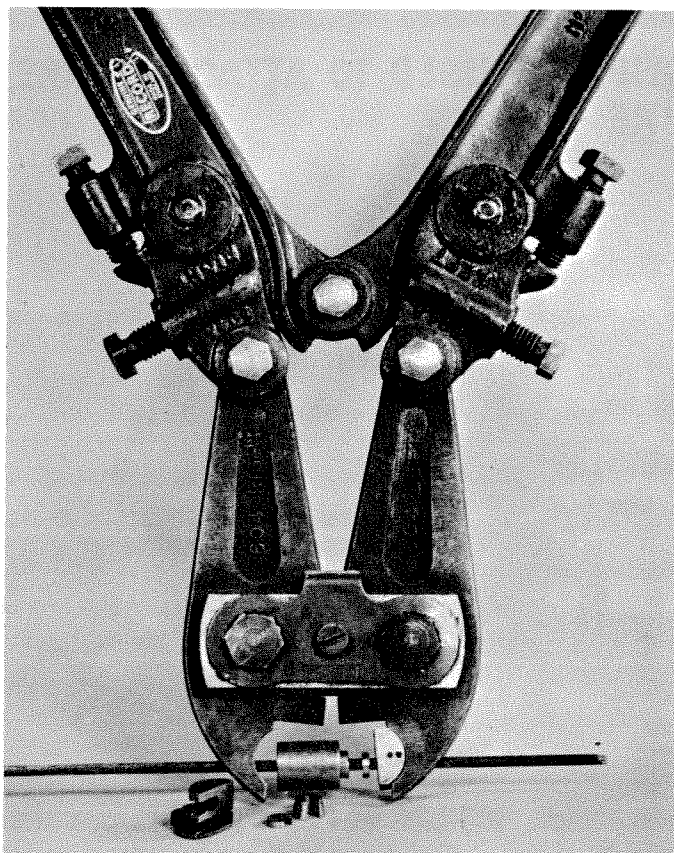
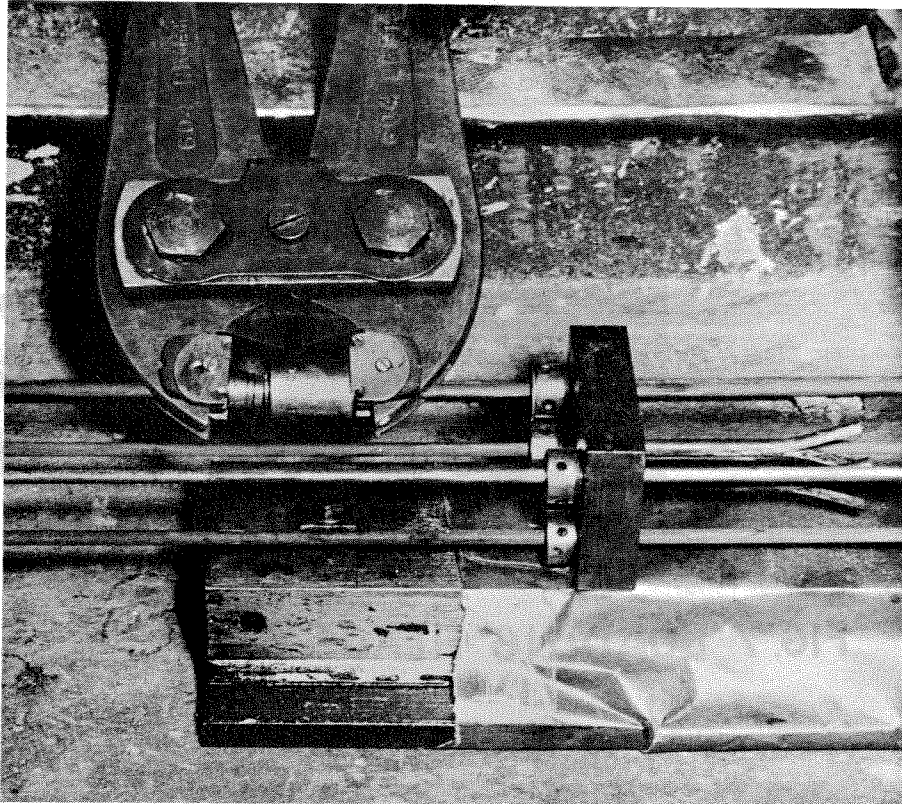
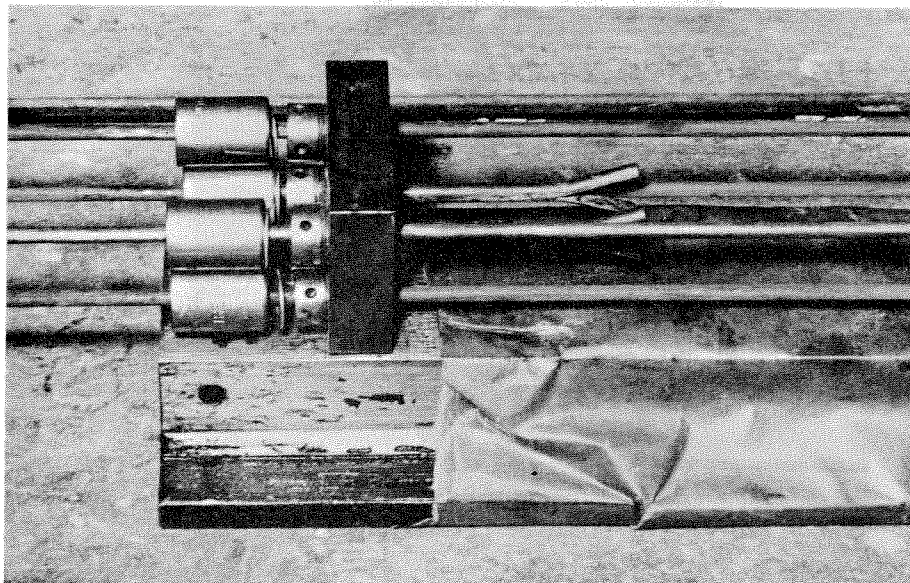


FIG. 8 ADAPTED BOLT CLIPPERS



(a) BOLT CLIPPERS USED TO ATTACH BARREL TO WIRE



(b) BARRELS AND LOADING HEAD IN PLACE FOR CASTING

FIG. 9 PREPARATIONS FOR END ANCHORAGE

When the wires were now released, the end anchorage prevented slip and the full prestress was developed over the whole column length.

(e) Curing

Subsequent to casting the columns were cured under wet burlap for 3 days. On the 3rd day the formwork sides were removed and the columns left in the prestressing bed, under atmospheric conditions, until release of prestress at 14 days. From 14 days until 27 days the columns were cured under water, at 70^o F. During this period the steel loading heads, the end barrels and any strain measuring points attached to the columns were protected with multi-purpose heavy grease. The columns were removed from water on the 27th day and kept at 70^o F during the attachment of additional strain and deflection points until testing at an age of 28 to 30 days.

2. Cylinders and Cubes

Three 6x12 in. cylinders and one 6 in. cube were made from each batch of concrete (each three columns cast). Steel forms were used (see Fig. 5 (a)) and the cylinders were compacted in three layers. The same curing timetable was used as for the columns. The cube was tested at 14 days, to determine the concrete strength before the release of prestress. The cylinders were tested at the same age as the columns (one each at 28, 29 and 30 days).

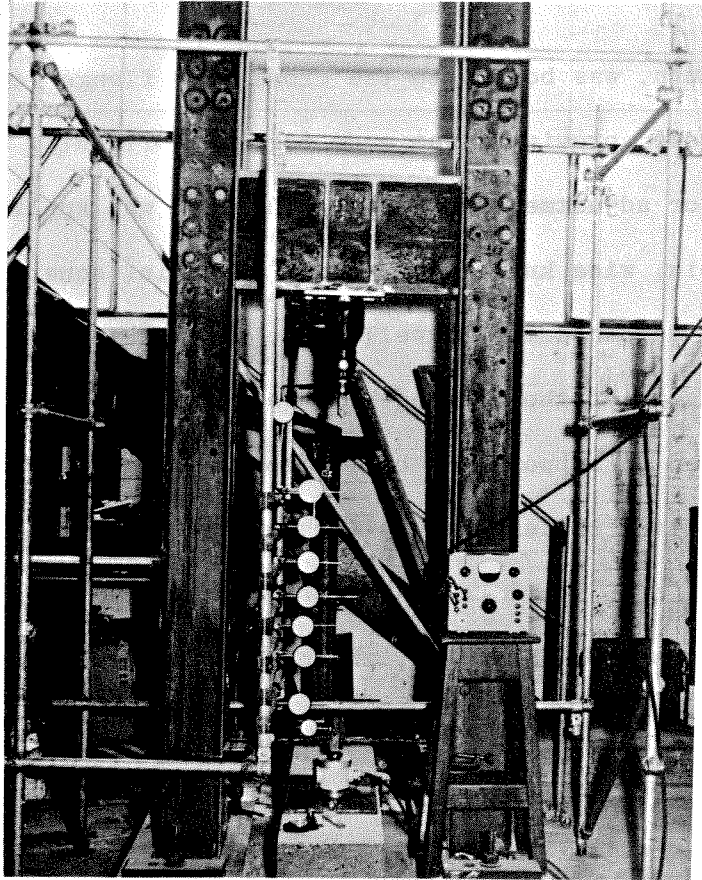
3.5 Testing Methods

1. Columns

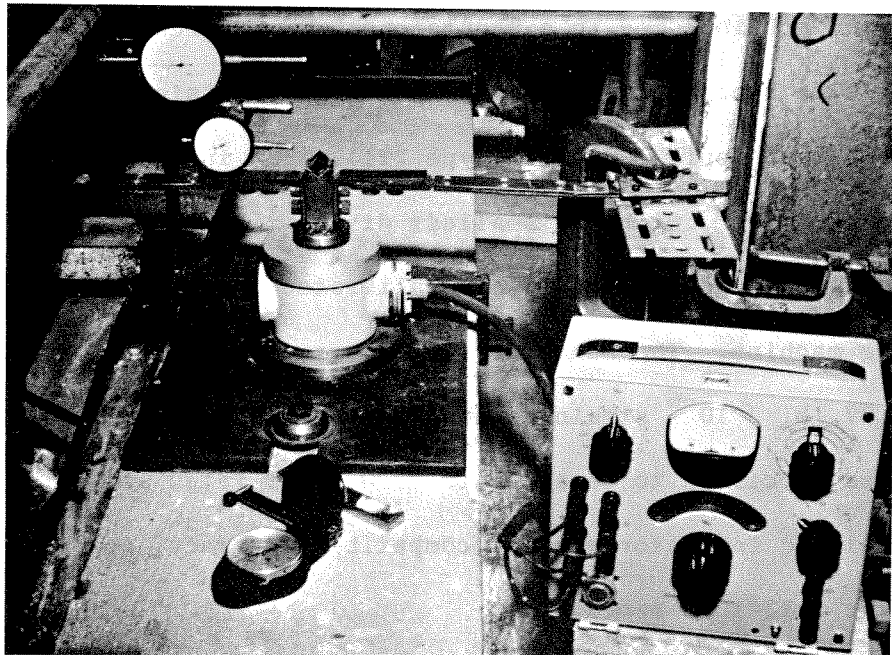
The 36 columns were made and tested in six groups of 6 columns each. The testing was performed over a period of 4 months. Each group of six columns contained two of each lengths, usually two of each eccentricity and two prestress values (one for each batch of three columns), which were randomized over the testing period. Each column was denoted by a label, for e.g., C₁ 20 c1, where C₁ stands for the first batch of group C, 20 denotes the slenderness ratio ($\frac{l}{d}$), c signifies the highest of the three eccentricities (denoted a, b and c in increasing order) and 1 stands for the nominal prestress ratio $f_{cp}/f'_c = 0.1$. The chronological order in which the groups were made and tested was B, C, A, D, E and F.

(a) Testing Frame

A special testing frame was developed for the column specimens. Photographs of the frame are shown in Fig. 10. It consisted of two 13 ft. - 10 in. high legs, each made up of two 8 in. x 3 in. channels, with a stiffened 15 in. x 6 in. I-beam placed as a cross-beam between them. The clear distance between the legs was 2 ft. - 3-3/4 in. The cross-beam was attached by six 3/4 in. bolts to each leg and it was possible to adjust its height to suit the column specimen being tested. Each leg was welded, at its lower end, to two horizontal channels which were bolted to a structural floor. A 20 ton capacity, 5 in. travel, screw jack was attached to the lower flange of the cross-beam. The jack was held by four screws to a 1/2 in. thick



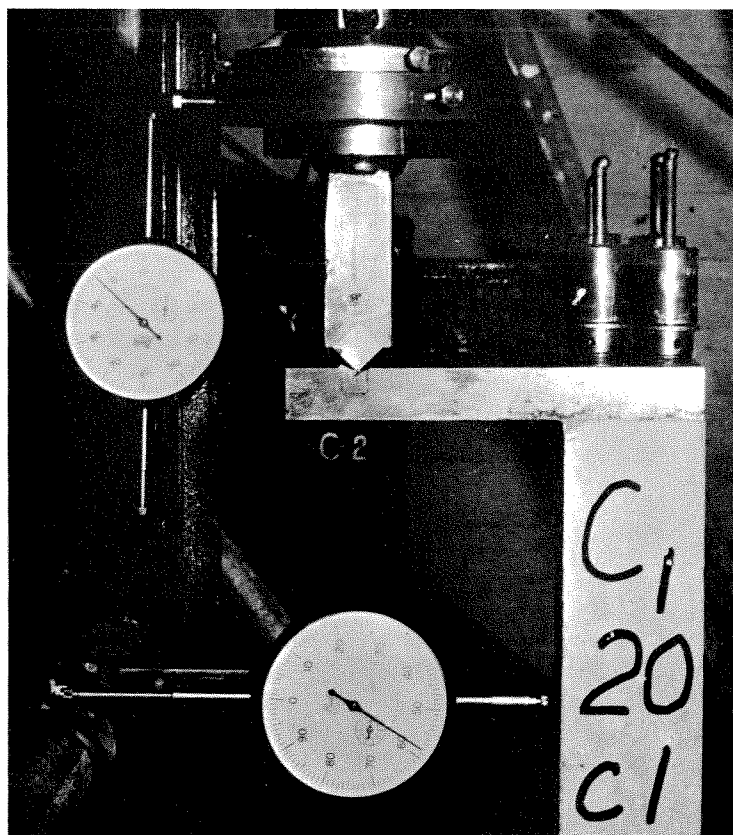
(a) OVERALL VIEW



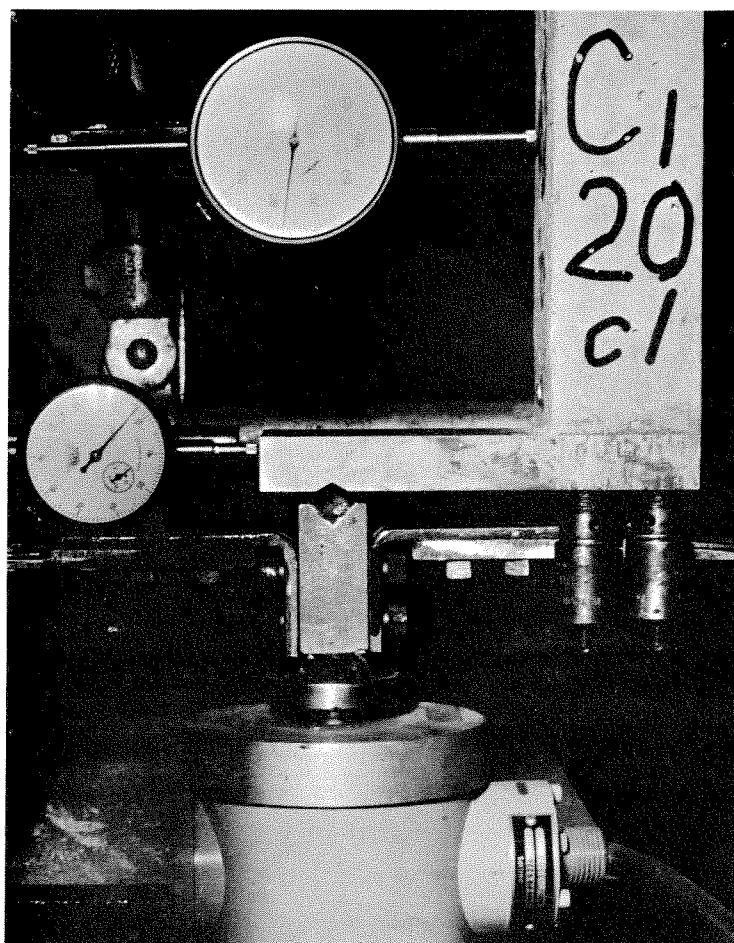
(b) LOAD MEASURING LOWER END
FIG.10 TESTING FRAME

plate which, in turn, was bolted to the cross-beam flange (two 1/2 in. bolts). With the bolts loose, provision was made for the horizontal movement of the plate and jack, for adjustment purposes. The load was applied by the screw jack through a 1 in. wide knife-edge (using a 1/2 in. square high speed tool steel insert hardened to Rockwell C50), which was placed centrally in the 3 in. wide insert of the loading head (see Fig. 11 (a)). A similar knife-edge was used to support the bottom loading head (see Figs. 10 and 11 (b)). The bottom knife-edge was located on top of a load cell, by means of a 3/4 in. dia. steel ball. To prevent lateral movement of the knife-edge special straps were used, which were designed to contribute no restraint in the vertical direction. The average maximum observed lateral movement was 0.021 in.

The load cell (Philips PR9226) had a rated capacity of 10 tons. The heart of the load cell was a chrome-nickel steel pressure billet fitted with four strain gages in a Wheatstone bridge circuit. The bridge output was read on a portable transistorized high precision strain indicator (Huggenberger Tepic Indicator Type IT1). The indicator could be read to a strain of 10^{-6} , with the smallest division being 10^{-5} . Before testing, the load cell and indicator were calibrated in a 10 ton Amster hydraulic testing machine. The behavior was linear over the full range with a factor of 11.07 lb. / 10^{-6} strain reading (gage factor setting of 2.0). The load cell was specified to be accurate to 0.1% of rated load i.e., + 11 lb. Thus, the cell and indicator were of compatible accuracy, approximately + 10 lb. over the full load range.



(a) TOP END, SCREW JACK KNIFE EDGE



(b) BOTTOM END, LOAD CELL KNIFE EDGE

FIG. 11 END DETAILS OF COLUMN IN TESTING FRAME

(b) Strain Measurements

Various strain measurements were taken on the surface of the concrete. This was done using a Huggenberger Tensotast instrument over a gage length of 100 mm. (about 4 in.). The change of length was read on a graduated dial with the smallest division of 0.001 mm., representing a strain of 10^{-6} . The gage points consisted of 1/16 in. dia. steel balls sunk into small disks (1/4 in. dia. and 1/16 in. thick) which were glued to the concrete surface. A standard bar was used to allow for temperature changes. The various strain measurements, on each of the columns tested can be classified as follows:

(i) Strains at column mid-height:

Six strain gages were read around the mid-height of the column. Their position is shown in Fig. 12 and they can also be seen in the photographs of Figs. 3 and 4. Gages 1, 2, 3 and 4 were attached to the concrete at the age of 7 days, before the release of prestress. Thus, strain readings were determined at the tightening of end anchorages, at release of prestress and at the end of the curing period. At 27 days, on the removal from water curing, strain gages 5 and 6 were added to the tensile face of the column. All six gages were read during loading up to failure.

(ii) Strains at column ends:

Gages B_1 , B_2 , T_1 and T_2 were attached to the concrete at the age of 7 days (see Fig. 12). They were used to determine the effectiveness of the end anchorage and were not read during the load testing.

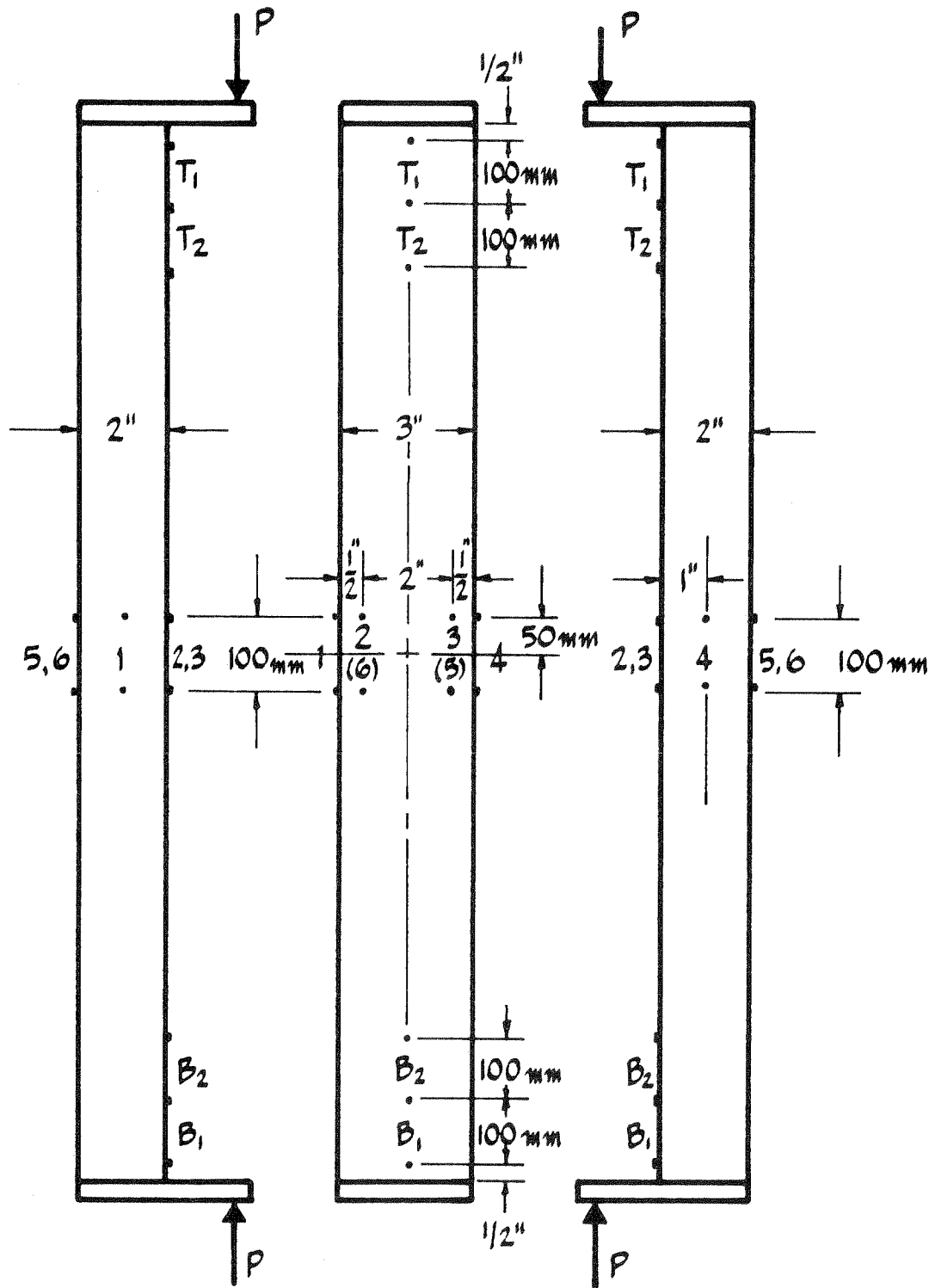


FIG. 12 CONCRETE STRAIN MEASUREMENTS (NOT TO SCALE)

(iii) Strains along column length:

Eight columns were instrumented with strain gages on the compression face along the centre line over the full column length. The eight columns included all combinations of length and prestress except column 30a. Columns C₁20c1 and C₂20a3 can be seen in Figs. 3 and 4. The purpose of these gages was to determine the strain variation along the length at release of prestress and at the end of the curing period. These gages were not read during load testing.

(c) Deflection Measurements

After removal from water curing and before testing, the initial deflected shape of the columns was determined by measuring, to an accuracy of 1/64 in., from a thin wire stretched between the column ends.

To determine the deflected shape during loading, an independent scaffolding was erected to which dial gages were attached (see Fig. 10 (a)). The dial gages were read to 0.001 in. and had 2-1/4 in. travel. Machined extension arms enabled the dial gages to be moved horizontally to follow the deflected column, if necessary. The column deflection was measured at seven points spaced at $l/8$ intervals along the column length. Small aluminum disks were glued to the concrete the day before testing to provide a smooth bearing surface for the dial gages.

In addition to the above 7 dial gages, one gage each determined the vertical movement of the screw jack (see Fig. 11 (a)) and checked the stability of the lower knife-edge by measuring the horizontal movement (see Fig. 11 (b)).

(d) Testing Procedure

The following procedure was followed in the column testing:

1. Using a plumb-bob, the knife-edges were checked to be in the same vertical line and adjusted if necessary by horizontal movement of the screw jack.
2. The column was inserted in the proper position between the knife-edges under a very small load, 10-20 lb., the dial gages set in position and all zero readings taken.
3. An axial shortening was applied to the column by the screw jack and the load read on the strain indicator. There was an initial increase in load followed by relaxation and load drop. A condition of equilibrium was assumed to exist when the rate of load drop was less than 10 lb. per 30 seconds. At that stage all readings of strain, deflection and load were taken. Also the cracking on the tensile side was observed with a small magnifying glass.
4. Additional increments of axial shortening were applied and the above procedure repeated until material failure occurred.

At the beginning of loading equal load increments were aimed at and later equal maximum deflection increments. A total of 10 to 15 increments was desired. The above equilibrium criteria was followed at all loads and the total time of testing, per column, varied from 1 hr. 40 min. to 6 hr. 10 min., with an average of 3 hr. 10 min. Thus, a group of six columns

was tested over three days, with two columns tested each day.

The above testing procedure has a very significant feature. If an instability critical load is reached, before material failure, this simply represents a maximum load. With continued applications of axial shortening, the equilibrium loads decrease and the column is in a state of unstable equilibrium. However, due to the physical boundary conditions provided in the testing frame, the column does not actually buckle but remains "stable", enabling all readings to be taken and the post-critical range to be determined. Finally, a stage was reached when material failure occurred, with the concrete crushing in compression. If the material failure occurred before a drop of load, this represented a primary material failure and not instability.

Figs. 13, 14 and 15 show three columns, of different lengths and eccentricities, at four stages of loading. Note that column C₁20c1 failed by primary material failure and the other two by instability. Note also the significant straightening out on unloading after failure.

2. Cylinders and Cubes

The twelve 6 in. cubes were tested in compression in a 200-ton capacity Dennison hydraulic testing machine. The tests, at 14 days, were made to determine the strength of the concrete before release of prestress.

Twenty-four 6 x 12 in. cylinders, out of the total of thirty-six, were also tested in the 200-ton machine, at a constant rate within the standard range of 20 to 50 psi per second. The remaining twelve cylinders

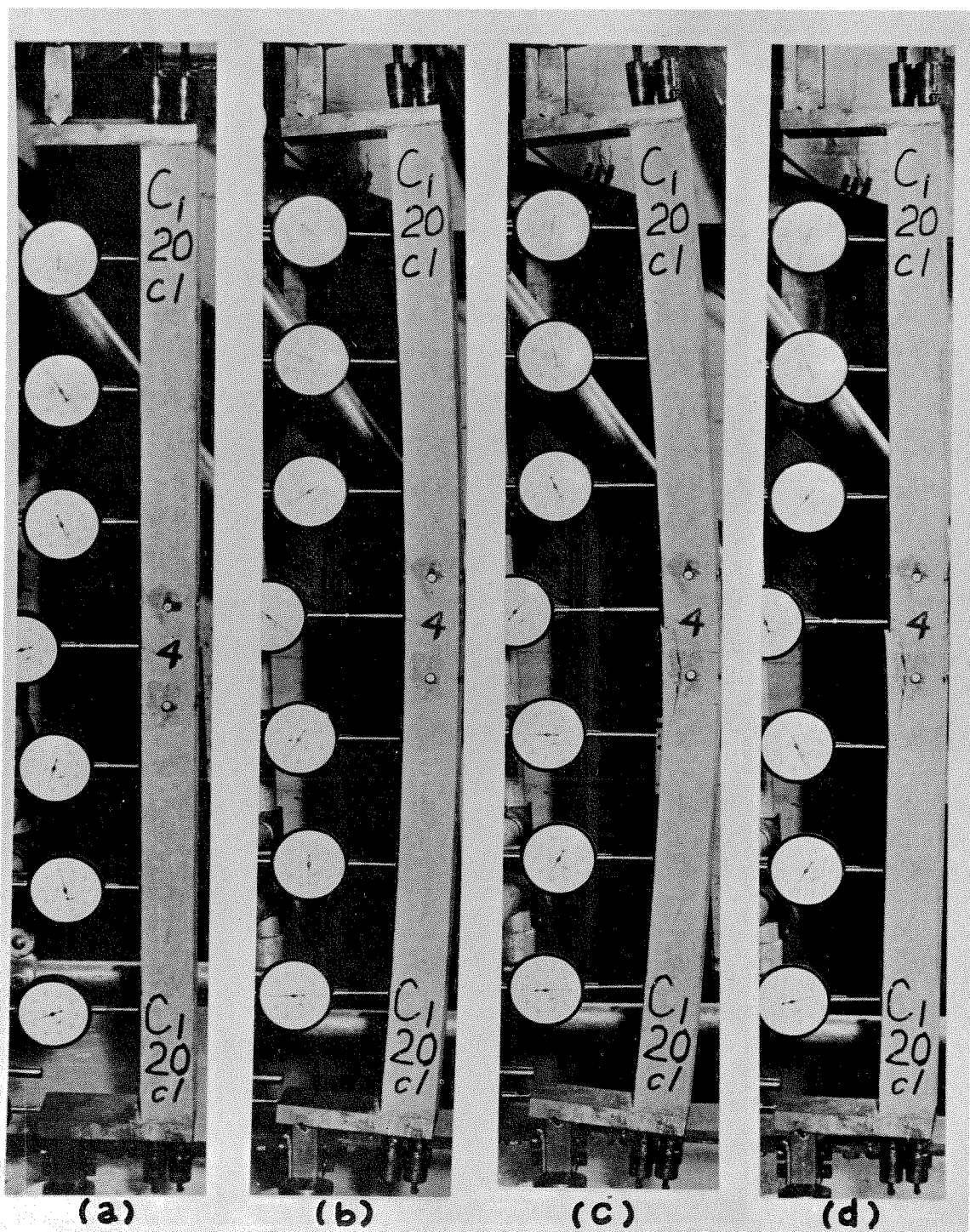


FIG. 13 COLUMN C₁ 20 c₁ UNDER TEST

(a) INITIAL LOAD $P = 20$ lb.

(b) $P = 2,410$ lb.

(c) MATERIAL FAILURE AT MAXIMUM $P = 2,690$ lb.

(d) AFTER UNLOADING $P = 80$ lb.

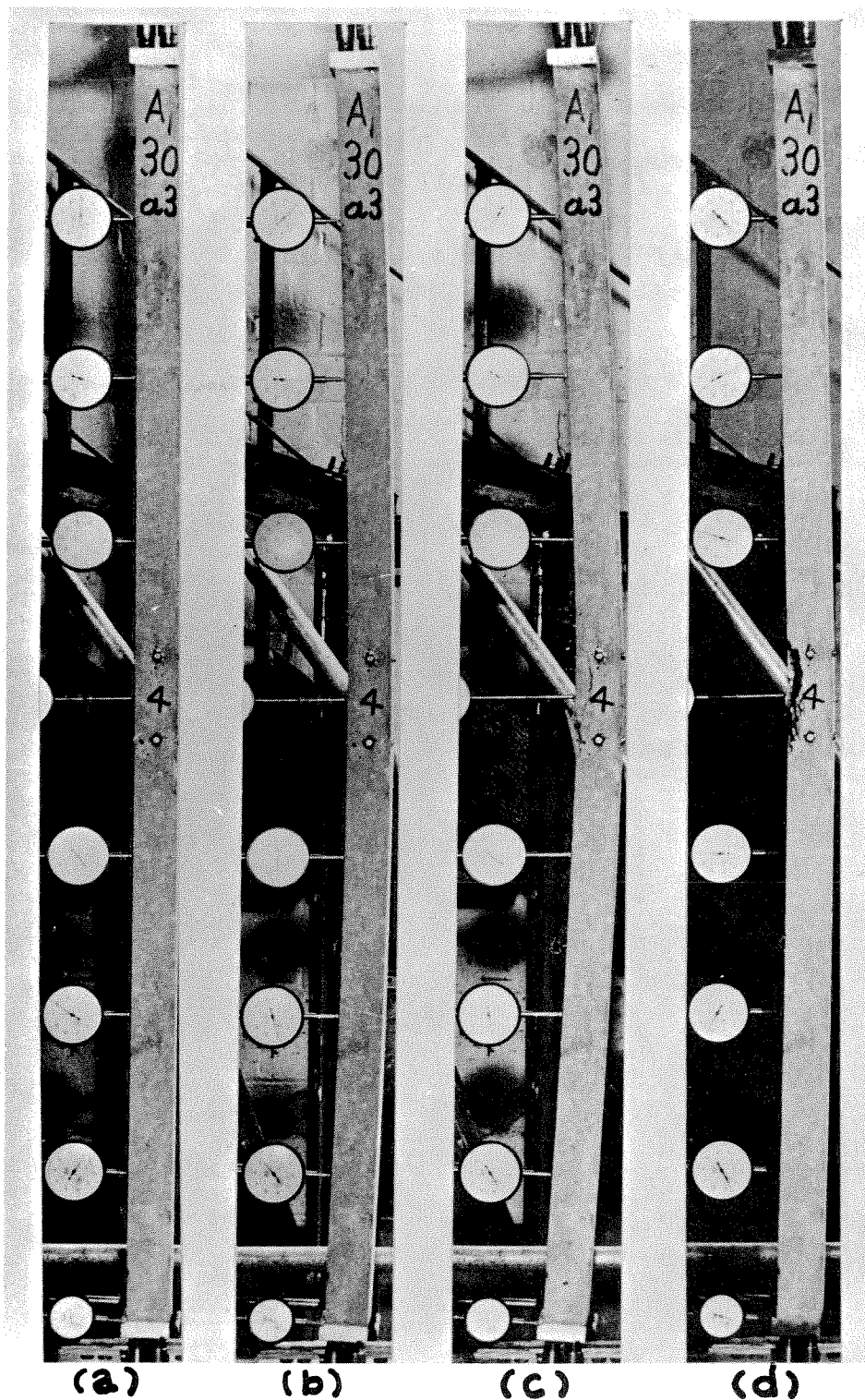


FIG. 14 COLUMN A₁30a₃ UNDER TEST

(a) INITIAL LOAD $P=10$ lb.

(b) CLOSE TO MAXIMUM CRITICAL $P=10,430$ lb.

(c) MATERIAL FAILURE AT $P=8,900$ lb.

(d) AFTER UNLOADING $P=20$ lb.

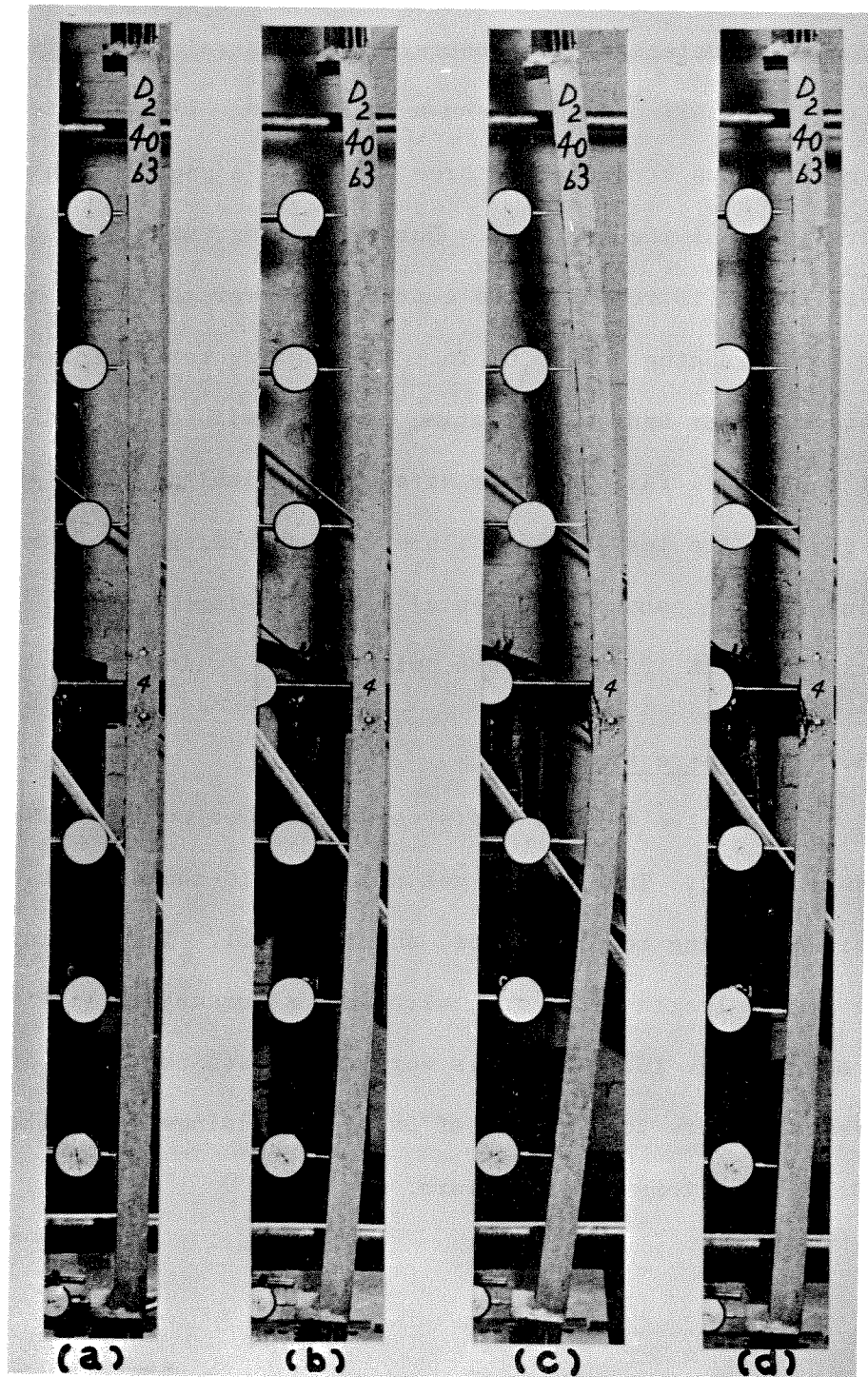


FIG. 15 COLUMN D₂40b3 UNDER TEST

(a) INITIAL LOAD $P=201b$.

(b) CLOSE TO MAXIMUM CRITICAL $P=2,930b$.

(c) MATERIAL FAILURE AT $P=2,700b$.

(d) AFTER UNLOADING $P=201b$.

were used to determine the concrete stress-strain curve in axial compression. The instrumentation used is shown in Fig. 16. It consisted of two steel rings attached to the concrete by three screws at a gage length of 6 in. over the central part of the cylinder. During testing, with the vertical straps shown in Fig. 16 removed, the contraction over the 6 in. was measured by two dial gages reading to 0.0001 in. The testing was performed in a 100-ton capacity Amster hydraulic testing machine, with dial readings taken every 2 to 4 tons until failure. The strain was calculated from the average of the two gages. The testing to failure took an average of 20 minutes. All cylinders were capped with dental plaster before testing. The ages at testing were 28, 29 or 30 days, with twelve cylinders tested at each age.

3. Steel wire specimens

Twelve tensile tests were performed on the 0.198 in. dia. prestressing wire. The testing was done in a 10-ton capacity Amsler machine (minimum reading to 0.005 tons, about 10 lb.). The strain was determined over a gage length of 20 in., with an instrument similar in principle to the one in Fig. 16. Two dials were read, each to 0.0001 in. which corresponds here to a strain of 5×10^{-5} . Readings were taken at intervals of 0.1 to 0.3 tons up to failure.

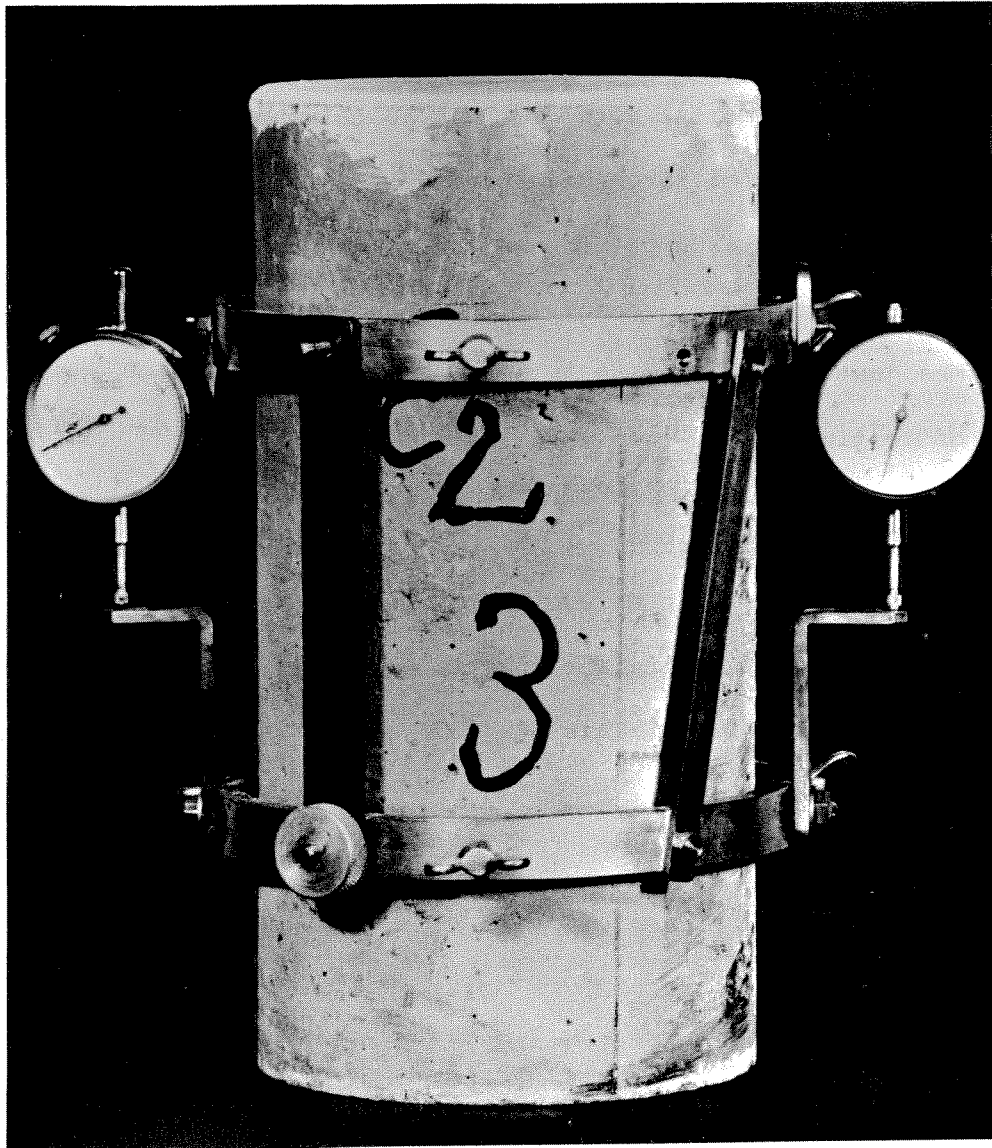


FIG.16 INSTRUMENTATION FOR CYLINDER
STRESS-STRAIN MEASUREMENTS

3.6 Test Results

1. Columns

The experimental data, for all 36 columns, are listed in Table 4. The table is composed of three main parts. The first part (column details) tabulates the label of each column and the values of the three variables investigated, namely length, eccentricity and nominal prestress. The state of the columns just before testing is given under "initial conditions" and the results of testing under "test results".

(a) Initial conditions

The first strain determinations were made during the end anchorage operation of moving the inserts out in firm contact with the barrels fixed to the wires. This was done at 14 days, just before the release of prestress.

Table 4. Experimental Data

Notes

*1 Column label (eg. A₁20c3):

A₁ denotes the first batch of group A

20 denotes the l/d value

"c" denotes the eccentricity: "a" stands for $e/d = \frac{1}{8}$

"b" stands for $e/d = \frac{3}{4}$

"c" stands for $e/d = 2$

"3" denotes the nominal prestress:

"1" stands for nominal $f_{cp}/f'_c = 0.1$

"3" " " " " 0.3

"5" " " " " 0.5

*2 Average compressive strain of gages 1 and 4 (see Fig. 12) from before release to beginning of testing.

*3 Average compressive strain of gages 2 and 3 (see Fig. 12) from before release to beginning of testing.

*4 Average concrete prestress, calculated from strains ϵ_{pr} (Table 3) and ϵ_{14} and a steel modulus of elasticity of 29.34×10^6 psi.

*5 Based on experimental average $f'_c = 5585$ psi.

*6 From time of beginning of loading to material failure.

*7 Last readings before material failure.

- *8 Average strain of gages 2 and 3 (see Fig. 12) from beginning of loading.
- *9 Deflection at mid-height from beginning of loading, excluding initial deflection.
- *10 Columns with duplicates.
- *11 Cracking occurred after the maximum critical load.

The effect of this operation, as measured on strain gages 1,2,3,4, B_1, B_2 , T_1 and T_2 , was negligible.

Table 5 gives the average strains, for the different gages, due to release of prestress and during the water curing period. The individual strains for each column (ϵ_{14} and ϵ_{23}), from before release to beginning of testing, are listed in Table 4.

Table 5. Average Strains During Release and Curing^{*1}

Condition and Gages	Average Strains ($\times 10^{-4}$)		
	Nominal Prestress (f_{cp}/f'_c)		
	0.1	0.3	0.5
<u>(a) Due to Release of Prestress</u>			
Average of gages B_1 and T_1	1.99	6.03	10.18
" " B_2 and T_2	2.30	6.97	11.35
" " 1 and 4	1.98	5.72	9.63
" " 2 and 3	2.13	6.79	11.11
Overall Averages	2.10	6.38	10.57
<u>(b) During Water Curing (from after release to beginning of testing)</u>			
Average of gages B_1 and T_1	-0.55	2.10	5.23
" " B_2 and T_2	-0.39	2.63	5.99
" " 1 and 4	-0.19	1.99	4.49
" " 2 and 3	-0.27	3.28	6.60
Overall Averages	-0.35	2.50	5.58

Table 5 (Con't)

(c) <u>Total (from before release to beginning of testing)</u>			
Average of gages B ₁ and T ₁	1.44	8.13	15.41
" " B ₂ and T ₂	1.91	9.60	17.34
ε ₁₄ (av. of 1 and 4)	1.79	7.71	14.12
ε ₂₃ (av. of 2 and 3)	1.86	10.07	17.71
Overall Averages	1.75	8.88	16.15

*1 Compressive strains taken positive.

It can be seen from Table 5 that, on release of prestress, the very end gages B₁ and T₁ had somewhat lower strains than either gages B₂ and T₂ or the central 2 and 3. This is probably due to a small slip still occurring at the column ends. Also, at the column mid-height, gages 2 and 3 (on the top surface) had higher compressive strains than gages 1 and 4 (at column mid-depth). The difference between these gages, which increased during curing, is consistent with the observed initial deflected shape of the columns with gages 2 and 3 being on the compression side. This difference increased with the column prestress.

During the period of water curing, the strain changes are probably due to two main effects. These are the creep under the prestress and the expansion due to water intake. The columns with the lowest prestress (0.1) can be seen to have an increase in strain, with the expansion predominating.

The strain readings taken along the full length of eight columns showed little variation, except at the end gages B₁ and T₁, from the mid-height

readings of gages 2 and 3. This was for both the curing period and the total initial period from before release to beginning of testing.

The measured initial central deflections are listed in Table 4. Their averages are also shown in Fig. 17, and are seen to increase with both prestress and column length. The maximum average deflection was 0.43 in., representing 0.54% of the column length (for $\frac{\ell}{d} = 40$ and maximum prestress.)

Due to the presence of initial curvatures the columns were in a state of eccentric prestress. The average steel strain was

$$\epsilon_s = \epsilon_{pr} - \epsilon_{14} \quad (3.1)$$

and stress

$$f_s = E_s \epsilon_s \quad (3.2)$$

where,

ϵ_{pr} = steel prestress strain (Table 3), tensile.

ϵ_{14} = average (gages 1 and 4) concrete compressive strain from before release to testing (Table 4).

E_s = steel modulus of elasticity, over the initial range (29.34×10^6 psi)

The average actual concrete prestress values can be calculated from

$$f_{cp} = \frac{f_s A_s}{A_c} = \frac{E_s (\epsilon_{pr} - \epsilon_{14}) A_s}{bd} \quad (3.3)$$

where,

A_s = the total area of steel (4×0.0308 sq. in.)

A_c = area of concrete ($b \times d = 6$ sq. in.)

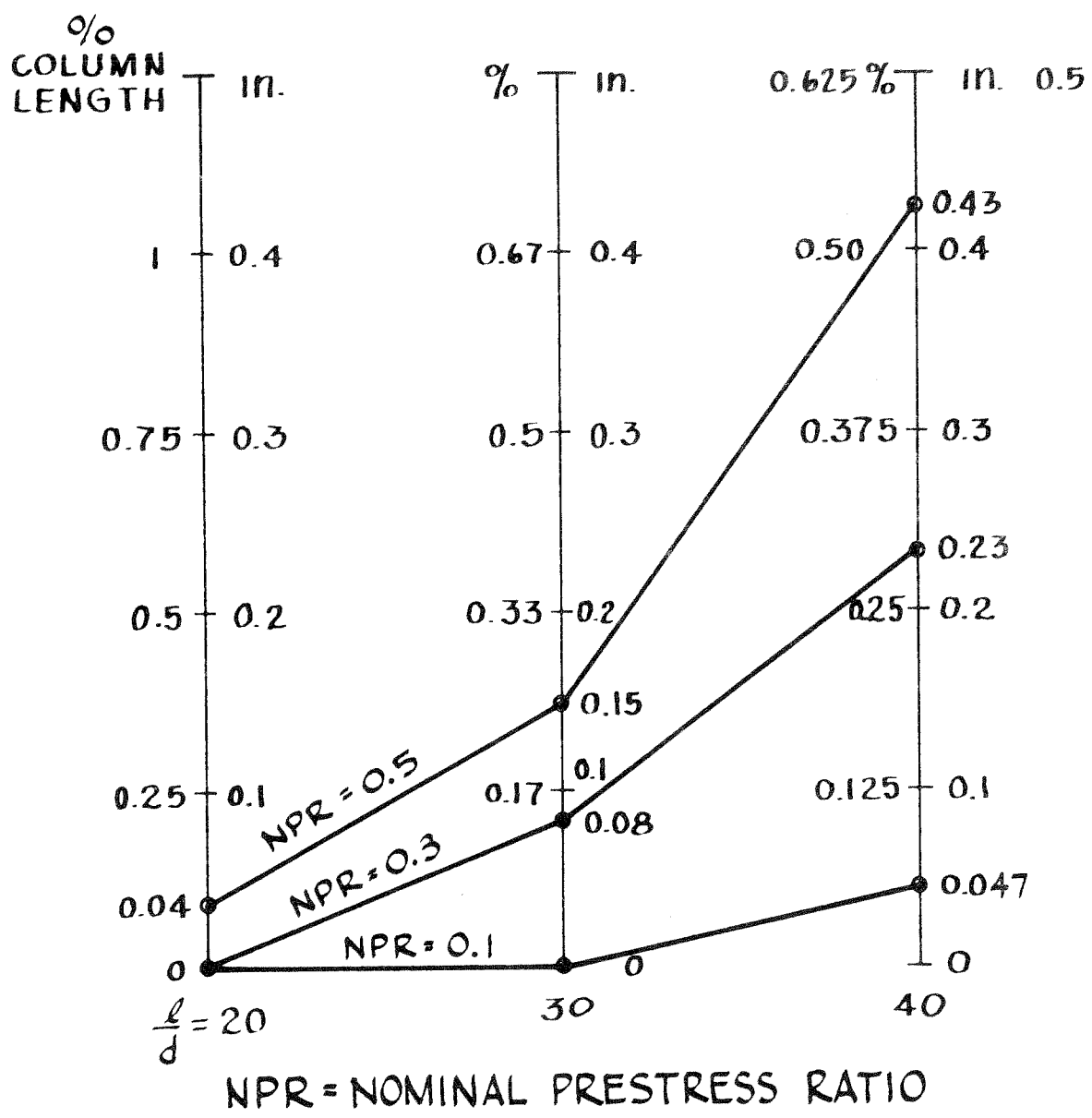


FIG. 17 EXPERIMENTAL AVERAGE INITIAL CENTRAL DEFLECTIONS

and are given in Table 4. For the two higher prestress ratios, the values are somewhat lower than the nominal prestress, the losses having been underestimated. The listed prestress ratios (f_{cp}'/f_c') were calculated using the average concrete strength of $f_c' = 5,585$ psi. The average values of the actual prestress ratios were 0.092, 0.252 and 0.410, as compared with the nominal 0.1, 0.3 and 0.5.

(b) Test Results

In addition to the data listed in Table 4, Appendix A presents experimental results of load-central deflection and load-central strains for the full range of loading up to material failure. The column deflected shapes are also plotted both at initial conditions and the maximum critical loads.

The cracking loads listed in Table 4 represent loads at which the first crack was observed anywhere on the tensile side of the column. The magnitude of the cracking load, relative to the maximum load of a column, depends on length, eccentricity and column prestress. Not one of the 10 columns of the smallest eccentricity "a" ($e/d = 1/8$) cracked before the maximum load was reached. Columns B₁20a1 and E₁20a5 exhibited material failure without having previously cracked.

The load P_{cr} represents the maximum load that each column was able to carry; it is the load at which stable equilibrium of the column ceased to exist.

The failure load P_f occurred with a concrete material compression failure over an average length of 3 to 4 inches at the column mid-height. For five columns ($B_1 20a1$, $B_2 30c3$, $C_1 20c1$, $E_1 20a5$ and $E_2 30c1$) the material failure load was also their maximum load.

The measured axial movements of the screw jack, at P_{cr} and P_f , are also listed in Table 4. These values include the effect of rotation of the loading leads and thus are larger than the actual column shortenings (see Fig. 11 (a)).

The observed average (gages 2 and 3) maximum compressive strains at column mid-height, under the critical load P_{cr} , had an average value of 30.15×10^{-4} and a standard deviation of 12.18×10^{-4} . A statistical analysis of variance showed significant differences with eccentricity, slenderness and prestress. The average values for each of these variables are shown in Table 6. The compressive strains at P_{cr} are seen to decrease with larger slenderness and prestress and smaller eccentricity. The largest variation is with eccentricity.

Table 6. Average Maximum Compressive Strains at
Mid-Height of Columns, Under P_{cr}

Variable	Number of Columns	Average Strain ($\times 10^{-4}$)	Ratio
(a) <u>Eccentricity:</u>			
a - $e/d = 1/8$	10	17.80	1.00
b - $e/d = 3/4$	17	31.95	1.79
c - $e/d = 2$	9	40.55	2.28

Table 6 (Con't)

(b) <u>Slenderness:</u>				
	$\ell/d = 20$	12	37.0	1.55
	$\ell/d = 30$	12	29.65	1.25
	$\ell/d = 40$	12	23.80	1.00
(c) <u>Prestress</u>				
1 -	Nominal $f_{cp}/f'_c = 0.1$	12	35.45	1.36
3 -	Nominal $f_{cp}/f'_c = 0.3$	12	29.00	1.12
5 -	Nominal $f_{cp}/f'_c = 0.5$	12	26.00	1.00

*From beginning of loading only.

The tabulated values of the average maximum compressive strains at column mid-height, due to the failure load P_f , represent last readings taken before the actual material failure. Thus they could be significantly lower than the actual failure strains. To a much smaller extent this also applies to the central deflections under P_f . To estimate the total concrete compressive strains at material failure, the initial strains ϵ_{23} were added to the strains due to P_f . The average value of the total strains was 52.95×10^{-4} with a standard deviation of 8.57×10^{-4} . A statistical analysis of variance showed the total strains not to be significantly affected by eccentricity, slenderness or prestress.

A comparison of the test results for the nine pairs of duplicate columns showed good agreement. Thus, the critical loads P_{cr} differed by an average of 6.4%, with a range of 0.3% to 14.6%.

2. Cylinders and Cubes

The average strength of the twelve 6 in. cubes, at 14 days, was 4,290 psi with a coefficient of variation (C.V.) of 10.6%.

The concrete stress-strain curves obtained from twelve 6x12 in. cylinders, tested in a 100-ton machine, are shown in Fig. 18. The average strength of these cylinders was 5,085 psi with a C.V. of 7.2%. The other twenty-four cylinders, tested in a 200-ton machine, had an average strength of 5,835 psi with a C.V. of 5.6%. The difference in strength between the two groups was probably due to the different rates of testing. The overall average strength of the thirty-six cylinders was 5,585 psi with a C.V. of 9.8%.

3. Steel wire specimens

The ultimate strength of the twelve specimens was 250,900 psi with a C.V. of 0.66% (range of 254,200 to 247,300 psi). The permanent elongation, over a gage length of 20 in., had an average value of 3%.

The best fit stress-strain relationship was obtained by linear regression over four ranges from zero to ultimate. The resulting stress-strain curve is shown in Fig. 19. The maximum range of observed strains, for a given stress, varied less than $\pm 5\%$ from the regression lines.

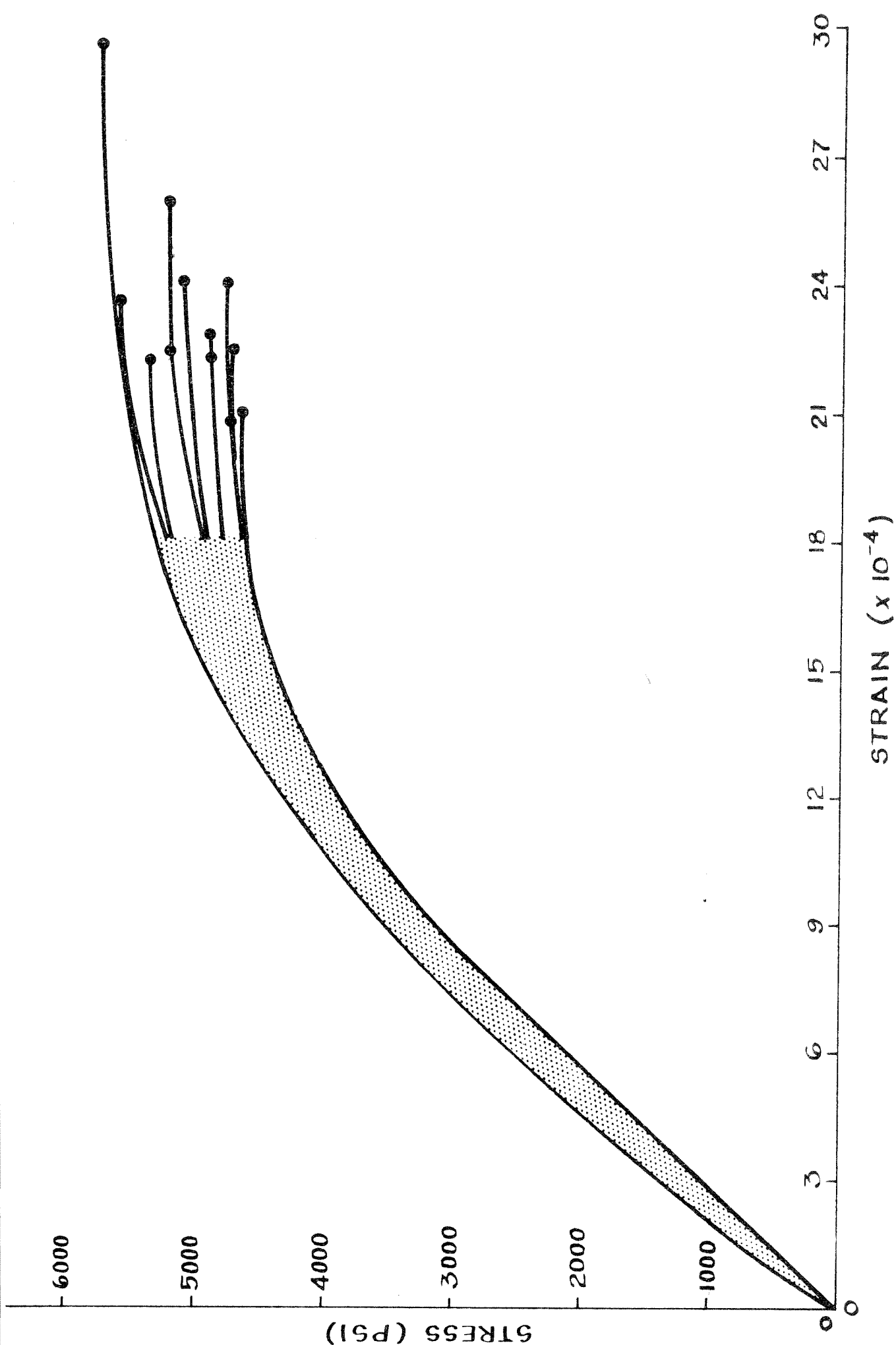


FIG. 18 CONCRETE STRESS - STRAIN CURVES

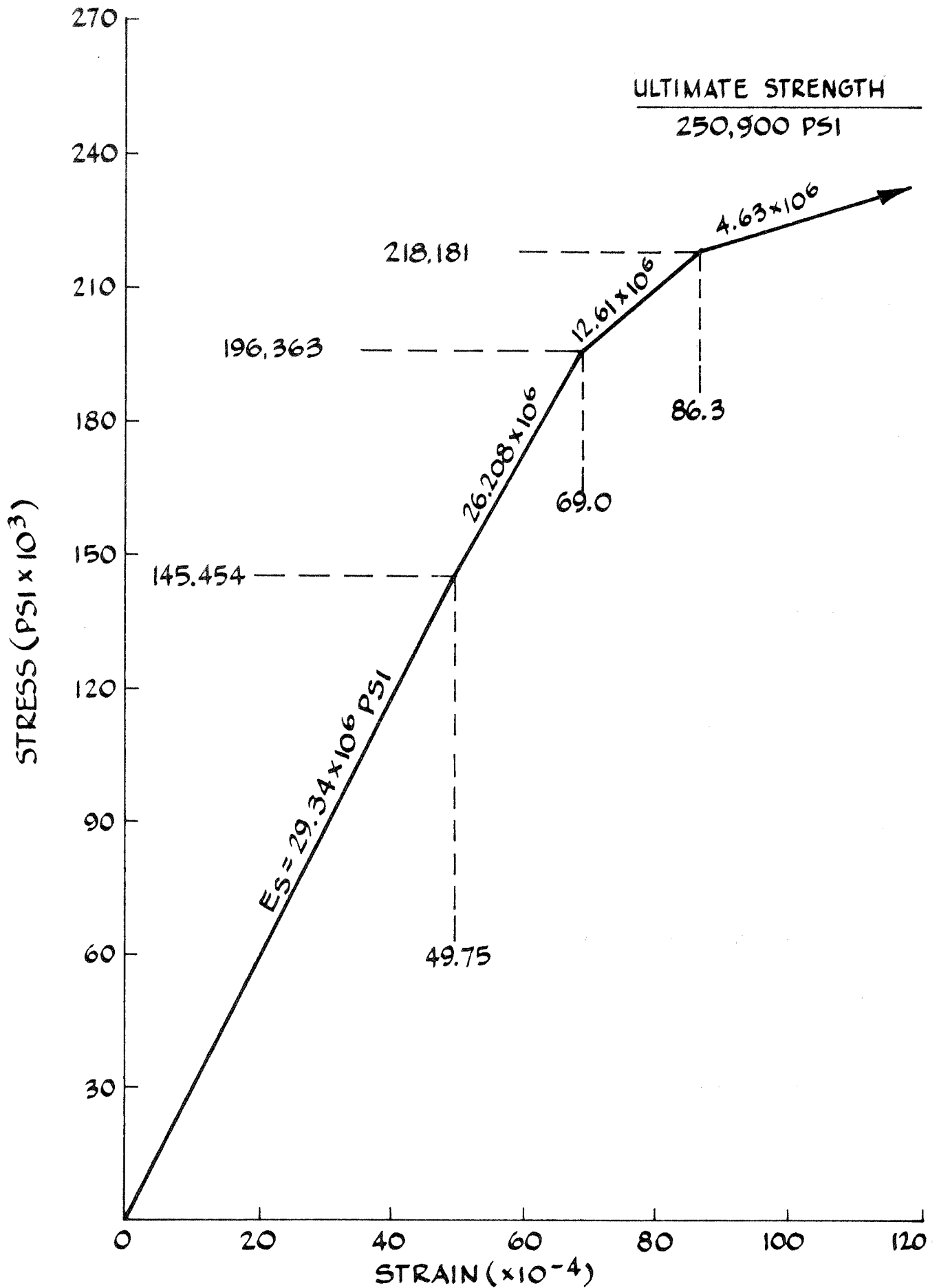


FIG. 19 STEEL STRESS - STRAIN CURVE

Chapter 4. THEORETICAL ANALYSIS

The theoretical analysis of eccentrically loaded prestressed concrete columns is developed and presented in this chapter.

4.1 Criteria of Instability

Eccentrically loaded columns deflect laterally from the very first application of load. Thus, unlike in the axially loaded case, their instability is not a question of bifurcation, i.e., neutral equilibrium at which two positions of equilibrium are possible, straight and slightly deflected. Instability here can be related to the equilibrium between the applied moment (M_A) and the moment of resistance (M_R) at some critical section, at which the deflection due to the load is δ . Equilibrium, of all types, requires

$$M_A = M_R \quad (4.1)$$

Depending on the relative increases of the two moments under an infinitesimal increase in deflection, we can distinguish the three types of equilibrium:

$$(i) \text{ Stable equilibrium, at which } \frac{\partial M_R}{\partial \delta} > \frac{\partial M_A}{\partial \delta} \quad (4.2)$$

$$(ii) \text{ Unstable equilibrium, at which } \frac{\partial M_R}{\partial \delta} < \frac{\partial M_A}{\partial \delta} \quad (4.3)$$

and

$$(iii) \text{ Neutral equilibrium, at which } \frac{\partial M_R}{\partial \delta} = \frac{\partial M_A}{\partial \delta} \quad (4.4)$$

The critical section is the one of maximum moment and the effects of the rest of the column and its boundary conditions are reflected in the deflection δ .

Consider now an eccentrically loaded pin-ended column, with equal end eccentricities e (Fig. 20). The critical, maximum moment, section "m" is at column mid-height. The column is assumed to have an initial curved shape.

At section m, the applied moment is given by

$$M_A = P(e + i_m + \delta_m) = Py_m \quad (4.5)$$

Also, from the details of the column cross-section, material stress-strain relations and some assumption about strain distribution (say Bernoulli's assumption) the moment-load-curvature relation at section m can be established

$$M_R = f_1 \left(\frac{1}{r_m}, P \right) \quad (4.6)$$

where

r_m = radius of curvature at section m.

From geometry, for a given column, there is a relationship between central deflection and curvature

$$\delta_m = f_2 \left(\frac{1}{r_m} \right) \quad (4.7)$$

For non-linear material properties, there are a number of procedures which might be used to establish the deflected shape of the column, and thus determine Equation (4.7). The following have been used:

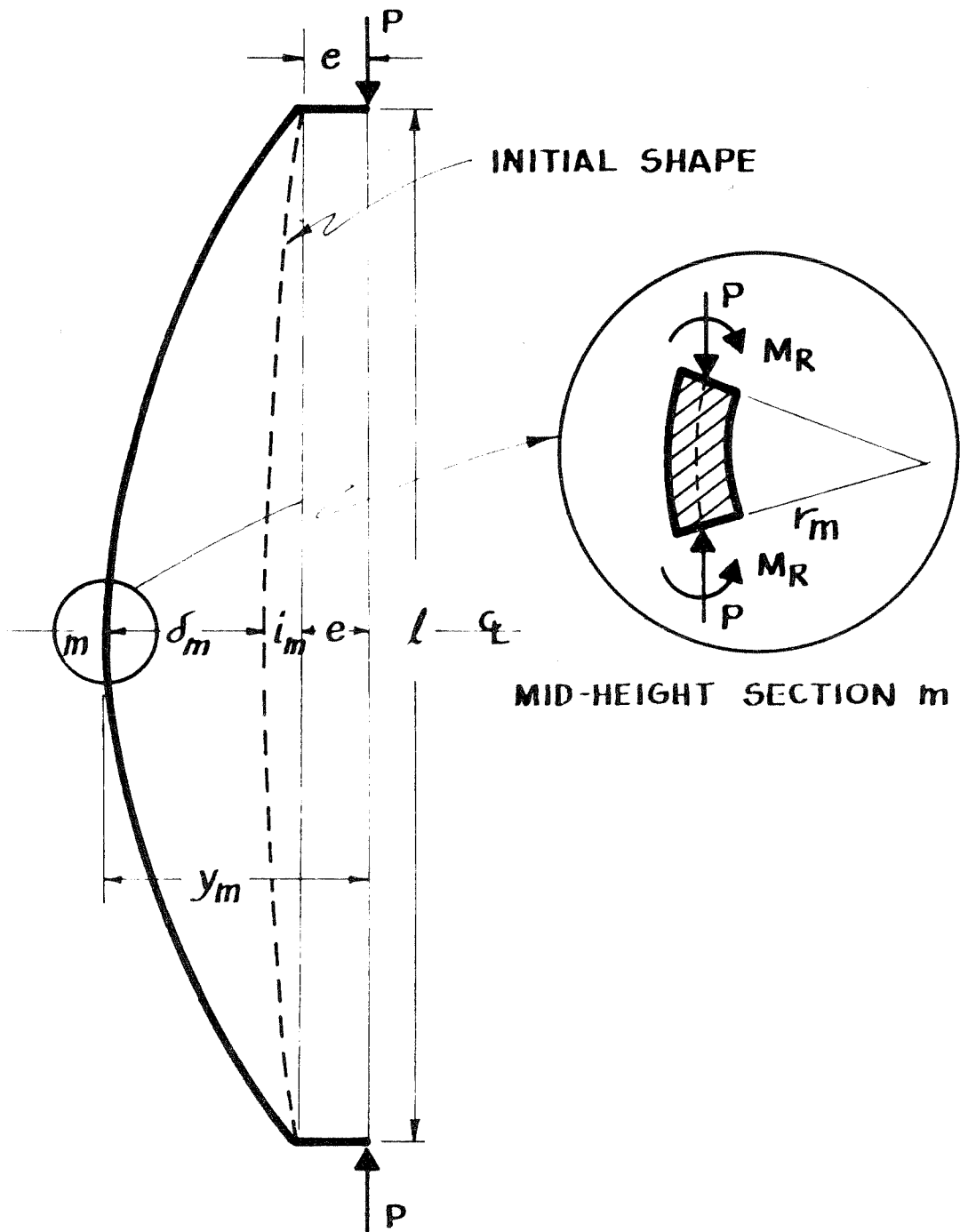


FIG. 20 ECCENTRICALLY
LOADED COLUMN

- (i) step-by-step numerical integration of angle changes along the column length, using the moment-load-curvature relation (4.6).
- (ii) an assumed deflected shape, usually part of a cosine wave.
- or (iii) finite elements, the use of which is developed in this investigation.

Now, combining (4.6) and (4.7), we can write

$$M_R = f_3(\delta_m, P) \quad (4.8)$$

The critical load P_{cr} , at which (4.4) is satisfied, can next be found by obtaining $\partial M_A / \partial \delta_m = P$ and $\partial M_R / \partial \delta_m$, from (4.5) and (4.8) respectively, and substituting into (4.4). For any other load P , a comparison of the partial derivatives will indicate the type of equilibrium.

The procedure described above is, however, not the most convenient one. The instability condition (4.4) can be expressed in equivalent mathematical forms, which are more useful for analytic procedures. Four such expressions will be developed, all of which are referred to as "cotangency criteria" of instability.

- (a) Consider a given column under a changing load.

Fig. 21(a) shows moment-deflection curves, for various load magnitudes. The applied moment (M_A) curves, from Equation (4.5), are straight lines from point O' , which is the origin of y_m . The slope of each line is equal to the appropriate load P . The moment of resistance (M_R) curves, for the various loads, are a plot of Equation (4.8) and are

shown dashed. We know from (4.1) that any point of intersection of the two moment curves, for the same load, represents a possible condition of equilibrium.

Consider a low load magnitude P_1 . The point of equilibrium, point 1, is a state of stable equilibrium since condition (4.2) is satisfied, i.e., the slope of the tangent to the M_R curve is larger than the slope of the straight line M_A curve. No other point of intersection exists between the two moment curves, for load P_1 , since the M_R curve is terminated by material failure. Consider next an increase in load to P_2 . The two possible conditions of equilibrium are points 2 and 4. A comparison of tangent slopes indicates that point 2 represents stable equilibrium and point 4 unstable equilibrium, under the same load P_2 . The point of unstable equilibrium (pt. 4) occurs at a much higher deflection value. If we further increase the load, the difference in the deflections at which stable and unstable equilibrium occurs becomes smaller. A load P_3 is finally reached at which the M_A curve is tangential to the M_R curve, point 3. Thus, point 3 satisfies (4.4) and it represents a condition of neutral equilibrium. The equality of tangent slopes leads to the name of "cotangency criteria." The critical load, P_{cr} , is equal to P_3 and the point of instability is represented by

$$\frac{dM}{dy_m} = P_{cr} \quad (4.9)$$

A load higher than $P_3 = P_{cr}$, say P_4 , can not find a position of equilibrium since there is no intersection between the two moment curves. To seek points of equilibrium for deflections higher than the deflection at

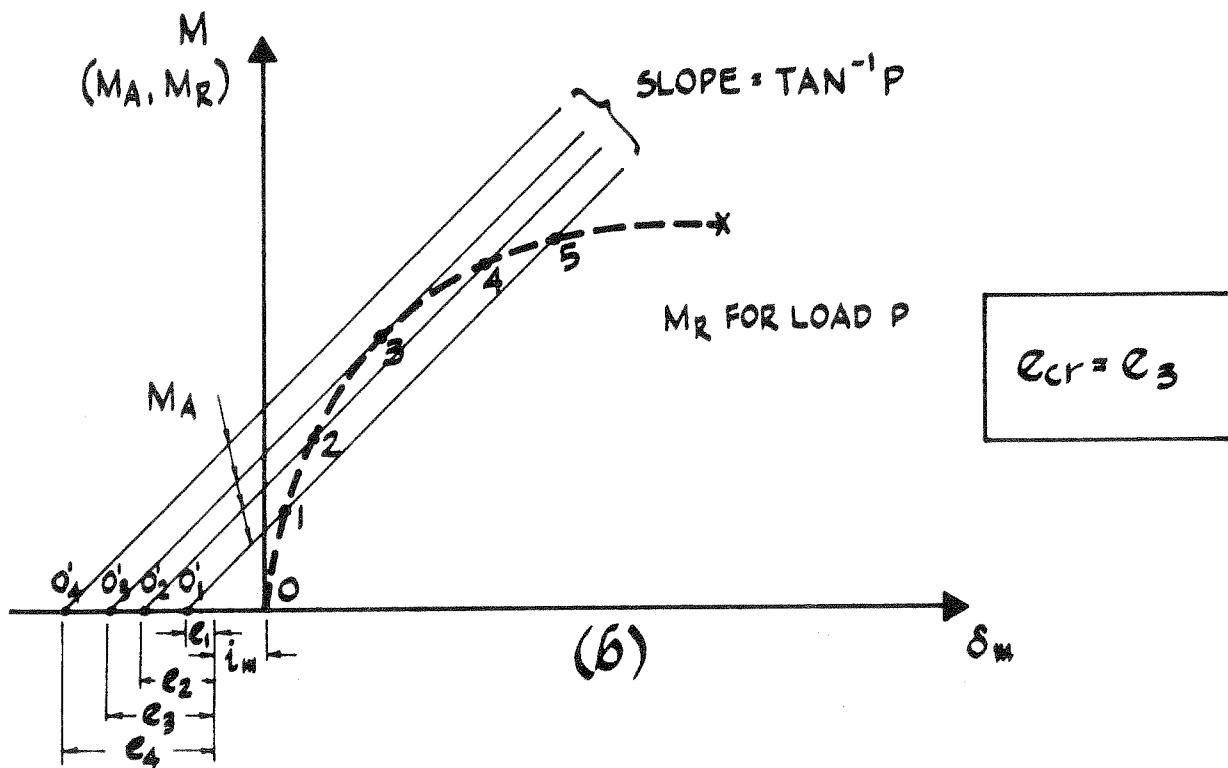
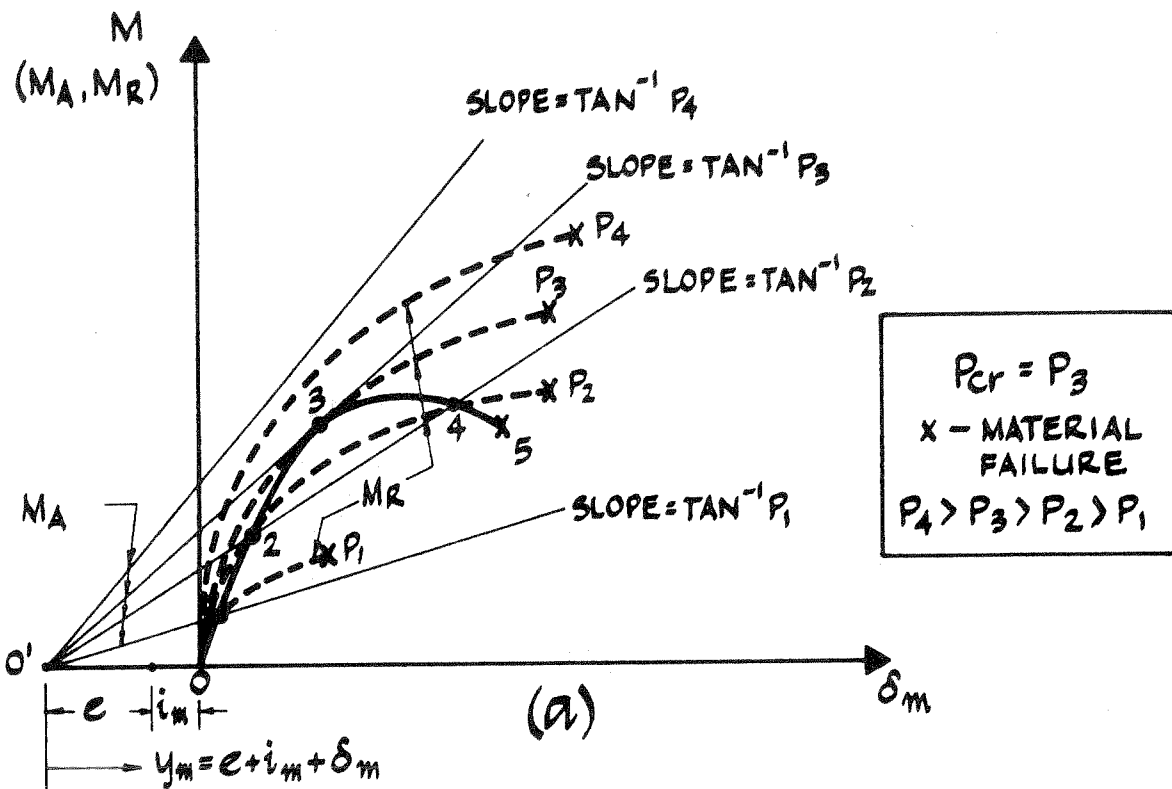


FIG. 21. COTANGENCY CRITERIA

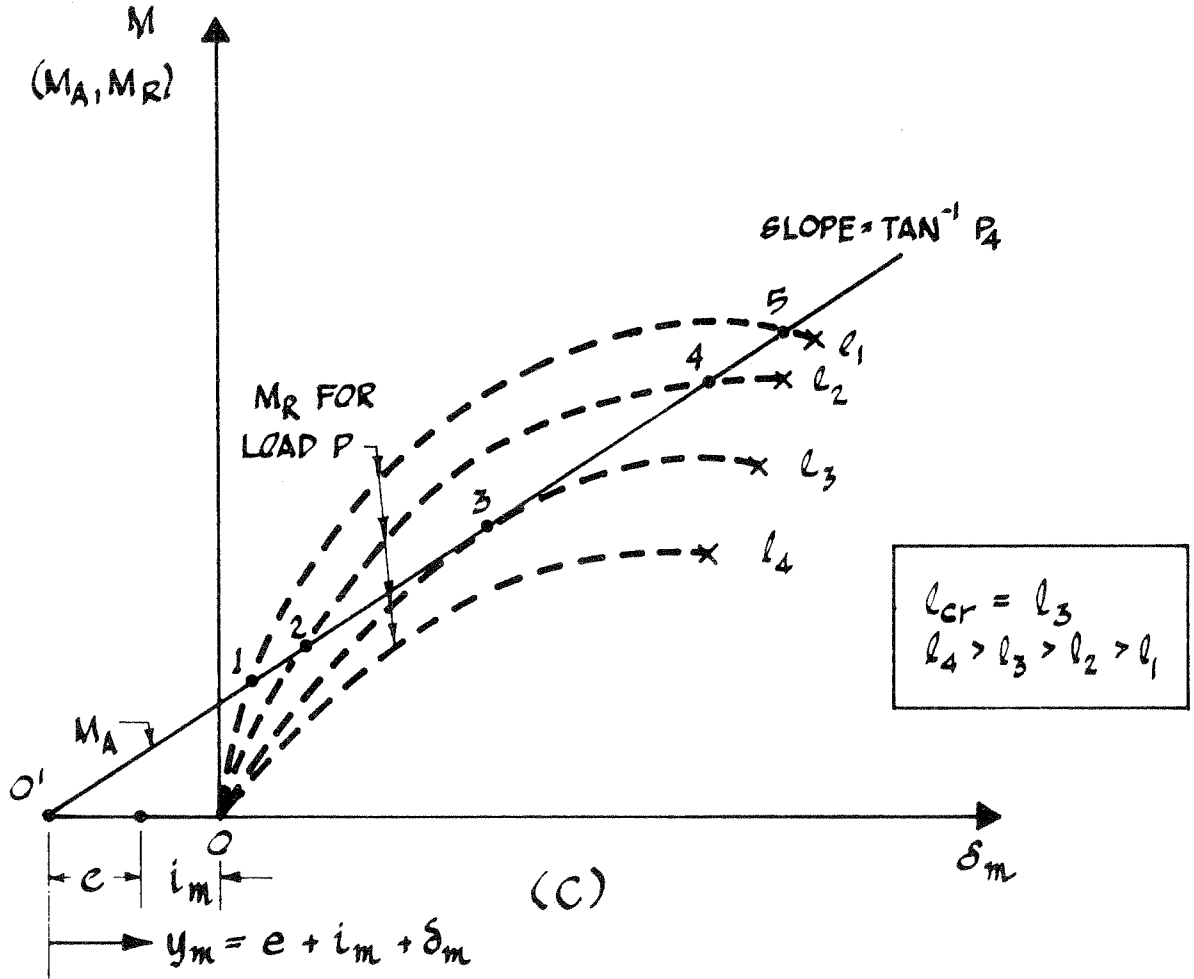


FIG. 21 (CTD.) COTANGENCY CRITERIA OF INSTABILITY

P_{cr} we have to decrease the magnitude of the load. This leads to conditions of unstable equilibrium, such as point 4, under lower loads ($P_2 < P_{cr} = P_3$).

Thus, the critical load is a maximum and

$$\frac{dP}{dy_m} = 0 \quad (4.10)$$

The line 0-1-2-3-4-5, joining all the points of equilibrium, represents the moment-deflection relation for the particular column. Over the segment 0-3 we have stable equilibrium, point 3 represents the critical state of neutral equilibrium and the segment 3-5 describes unstable equilibrium. Note that the critical condition occurs at a moment below the maximum and that point 5 represents material failure. The case illustrated is one of primary instability. A column in which point 5 occurs before point 3, i.e., before a decrease of load occurs, will fail by primary material failure.

(b) Consider next a column under a given load but varying eccentricity.

The aim is to find the eccentricity for which the given load P is the critical load. The $M_R - \delta_m$ curve, for load P , is shown in Fig. 21(b). The M_A curves are straight lines of equal slope, the change in eccentricity being equivalent to a shift of the O' origin. For a low eccentricity, e_1 , the two points of equilibrium 1 and 5 represent stable and unstable states respectively. As the eccentricity increases to e_2 , we still have the same two states at points 2 and 4, now closer to each other. Further increase of the eccentricity to a particular value e_3 results in a state of neutral

equilibrium at the point of equal tangents, point 3. Any larger eccentricity, say e_4 , has no points of equilibrium. To proceed in the unstable segment, past point 3, the eccentricity has to be reduced from its maximum critical value $e_{cr} = e_3$. Thus the point of instability is represented by

$$\frac{de}{dy_m} = 0 \quad (4.11)$$

- (c) Consider finally a column under a given load and eccentricity but of varying length.

The aim is to find the column length for which the given load P , under a given eccentricity e , is the critical load. Fig. 21(c) shows $M_R - \delta_m$ curves for load P but different column lengths. The column length is a parameter in the central deflection-curvature relation (4.7), which is used in the derivation of Equation (4.8). Since load and eccentricity are here prescribed, there is a unique applied moment curve, as shown. For increasing δ_m , points on this straight line M_A curve represent conditions of equilibrium under varying length. Thus, point 1 is stable equilibrium for the length l_1 . Increasing δ_m , point 2 also represents stable equilibrium, but for a longer length l_2 . Further increases of column length lead to a length l_3 for which the moment curves are cotangent at point 3. Therefore this represents a point of neutral equilibrium and the critical length $l_{cr} = l_3$. In other words, the given load P is the critical load for a column of length l_3 . No position of equilibrium is possible for a longer column length, say l_4 . Further increases in δ_m are possible, leading to

unstable equilibrium with decreasing column lengths, for e.g., points 4 and 5 with l_2 and l_1 respectively. The point of instability, point 3, is thus represented by a maximum length and

$$\frac{d\ell}{dy_m} = 0 \quad (4.12)$$

In summary, Equations (4.9), (4.10), (4.11) and (4.12) represent different forms of the "cotangency criteria" of instability. Equation (4.9) was wrongly stated by Broms and Viest,⁽²⁴⁾ with the moment derivative equated to zero, and wrongly used by Chang and Ferguson.⁽³²⁾ The maximum load criteria, expressed by Equation (4.10), is used later in this investigation. Equation (4.11) was used by Broms and Viest^(24,25) and (4.12) by Moreadith.^(52,53)

4.2 General Assumptions

The following general assumptions have been made in the analysis of slender, hinged, axially prestressed concrete columns loaded with equal end eccentricities:

1. The column cross-section was restricted to a rectangular shape with two layers of prestressing steel placed symmetrically about the centreline (see Fig. 1).
2. Both concrete and steel were assumed to be non-linearly elastic homogeneous materials.

The steel stress-strain curve used was as shown in Fig. 19, which is a close idealization of the test data. Any other steel stress-strain curve can be easily substituted in the analysis.

The theoretical concrete stress-strain curve is shown in Fig. 22. It is supposed to be applicable for short-term testing and to include any creep during testing but not during the period from release to testing. In compression, the curve is based on Hognestad's⁽²¹⁾ assumption and is made up of a parabola and straight line. The initial tangent modulus of elasticity is

$$E_c = (1.8 \times 10^6 + 391 f_c') \text{ psi} \quad (4.13)$$

and the parabola has the equation

$$f_c = \frac{\alpha}{\beta} \epsilon_c E_c \left(1 - \frac{\epsilon_c}{2\epsilon_o}\right) \quad (4.14)$$

where f_c = concrete compressive stress, psi

ϵ_c = concrete compressive strain

α = stress scale factor

β = strain scale factor

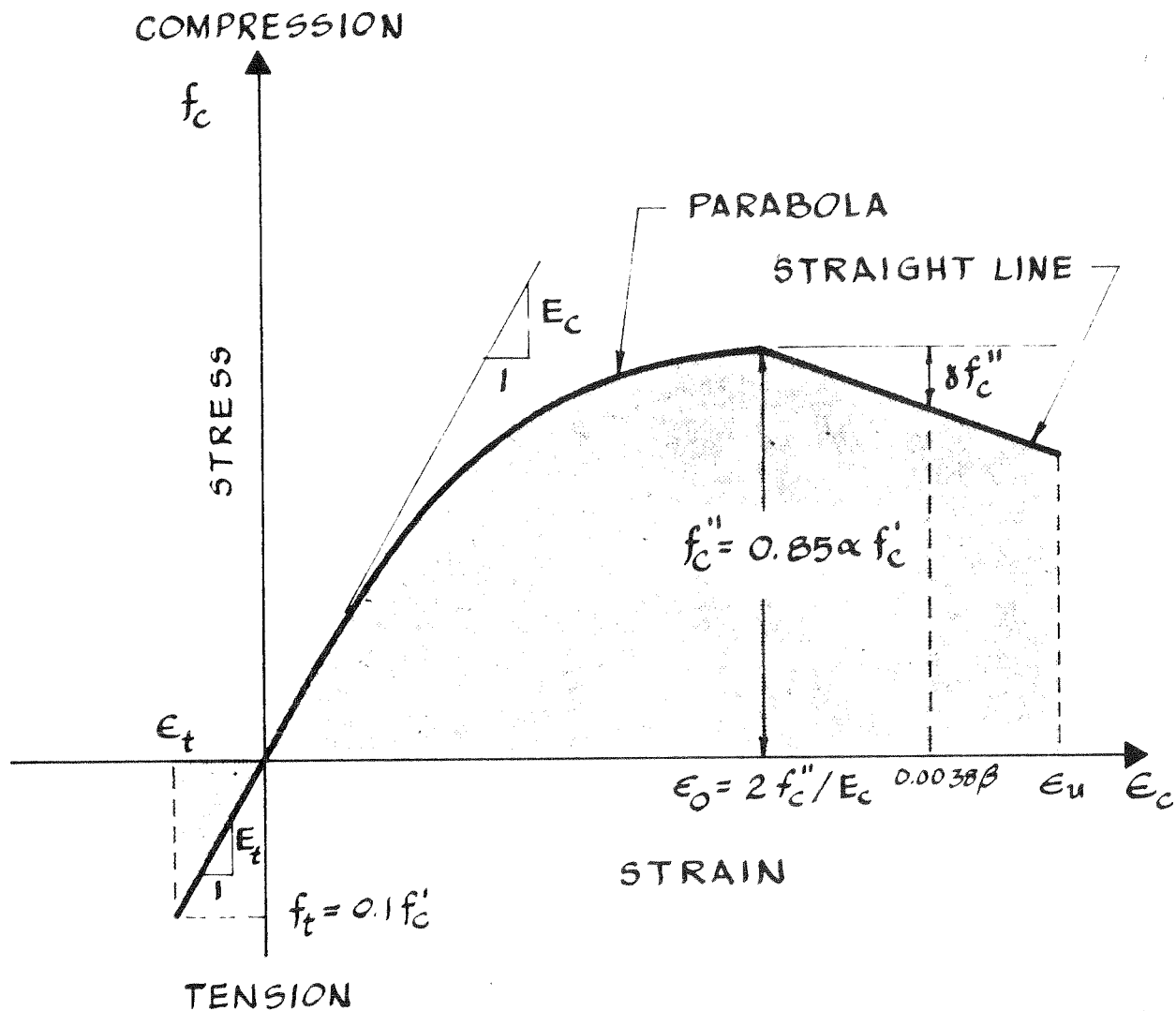
ϵ_o = strain at maximum stress.

The maximum stress, at which the tangent to the parabola is horizontal, is

$$f_c'' = 0.85 \alpha f_c' \quad (4.15)$$

at a strain of

$$\epsilon_o = \frac{2 f_c''}{E_c} \quad (4.16)$$



INITIAL MODULUS: $E_c = (1.8 \times 10^6 + 391 f_c') \text{ PSI}$

EQUATIONS

$$\text{PARABOLA: } f_c = \frac{\alpha}{\beta} \epsilon_c E_c \left(1 - \frac{\epsilon_c}{2 \epsilon_0}\right)$$

$$\text{STRAIGHT LINE: } f_c = f_c'' \left(1 - \delta \frac{\epsilon_c - \epsilon_0}{0.0038 \beta - \epsilon_0}\right)$$

FIG. 22 THEORETICAL CONCRETE
STRESS - STRAIN CURVE

The equation of the descending straight line is

$$f_c = f_c'' \left(1 - \gamma \frac{\epsilon_c - \epsilon_0}{0.0038 \beta - \epsilon_0} \right) \quad (4.17)$$

and material failure was assumed to occur at a strain ϵ_u . A straight line relation was assumed for the concrete in tension, with a modulus of elasticity E_t and a modulus of rupture $f_t = 0.1 f_c'$.

The curve described above actually represents a family of curves and requires seven parameters, namely α , β , γ , ϵ_u , f_c' , E_t and f_t , for its full specification. In his original work, Hognestad⁽²¹⁾ neglected the contribution in tension and used a compressive stress-strain curve, for any f_c' , described by the following values

$$\alpha = 1.0$$

$$\beta = 1.0$$

$$\gamma = 0.150$$

(4.18)

and $\epsilon_u = 0.0038$.

3. Full bond was assumed to exist between the steel and the concrete, from the time of release.
4. Allowance is made for the loss of prestress, due to creep, shrinkage and expansion, from the time of release to testing.
5. The column can have an assumed initial shape. With few changes any shape can be used in the analysis, but the shape actually assumed was based on the experimental data.

A number of possible reasons were investigated to explain the observed initial deflections of the columns (see Table 4 and Fig. 17), all of whom had the top face, as placed, on the concave compression side of the initial shape. The wires were accurately stressed and located and experimental errors in these items could not, on their own, explain the observations. The conclusion was reached that the most probable single reason is the variation of concrete properties with the two inch depth of section, as placed, the concrete at the bottom being better compacted and stronger. This would create an effective prestress eccentricity and the type of initial shape observed. Also, it follows that the initial moments and curvatures are essentially uniform over the column length. Thus, the initial shape was assumed to be circular.

The circular initial shape is confirmed indirectly in two ways. First, the strain readings taken along the full length of the top face of eight columns showed little variation. Secondly, using the measured strains, from release to testing, the assumed constant initial radius of curvature r for each column can be calculated from

$$\frac{1}{r} = \frac{\epsilon_{23} - \epsilon_{14}}{d/2} \quad (4.19)$$

Since the deflections are much smaller than the radius, the maximum central initial deflection is given by

$$i_m = \frac{l^2}{8r} = \frac{l^2 (\epsilon_{23} - \epsilon_{14})}{4d} \quad (4.20)$$

This calculated deflection, based on a circular shape and measured central initial strains, can now be compared with the observed initial central deflection. The average ratio of calculated (from 4.20) to observed initial central deflections was 0.98. Figs. A19 to A27 show both the observed initial deflected shapes and the assumed circular curves. Good agreement exists between the two.

6. Bernoulli's assumption is made, namely plane sections are assumed to remain plane on bending.
7. The column is assumed to be divided into a relatively large number of finite elements, each of constant curvature, i.e., circular shape. Certain additional assumptions were made, the details of which are given later, which restrict the analysis to small rotations and neglect the effect of axial strain on the deflected shape of the column. In essence, the slopes were assumed to be small enough for $\sin \theta = \theta$ and $\cos \theta = 1$ to be used. For the maximum observed slopes of about 10 degrees, this introduces an error of about 1-1/2%. The limitation introduced by this assumption can, if required, be removed from the analysis with relative ease.
8. Shear deformations are neglected.

4.3 Analytic Procedure

1. Initial Conditions

Two initial condition cases can be distinguished, namely

- (a) Eccentric prestress, when there are initial curvatures and deflections, and the strains ϵ_{14} and ϵ_{23} are different, and
- (b) Axial prestress, when $\epsilon_{14} = \epsilon_{23}$ and the column is initially straight with zero deflections.

We shall consider each case separately.

(a) Eccentric prestress

Fig. 23 shows the distribution, at column mid-height, of strains and stresses under initial conditions of eccentric prestress.

Note the different lines of zero concrete and steel strains and the positive sign convention for concrete compressive and steel tensile strains. Line AB is drawn from the initial strain values ϵ_{14} and ϵ_{23} . These strains, and the prestress ϵ_{pr} , determine the steel strains along the two rows of prestressing steel. Thus

$$\begin{aligned}\epsilon_{s2} &= \epsilon_{pr} - \epsilon_{14} + (\epsilon_{23} - \epsilon_{14}) \frac{d'}{d} \\ \epsilon_{s3} &= \epsilon_{pr} - \epsilon_{14} - (\epsilon_{23} - \epsilon_{14}) \frac{d'}{d}\end{aligned}\tag{4.21}$$

The steel forces (each representing the force in two bars) can be obtained from the steel stress-strain curve

$$F_{s2} = f(\epsilon_{s2}) \text{ and } F_{s3} = f(\epsilon_{s3})\tag{4.22}$$

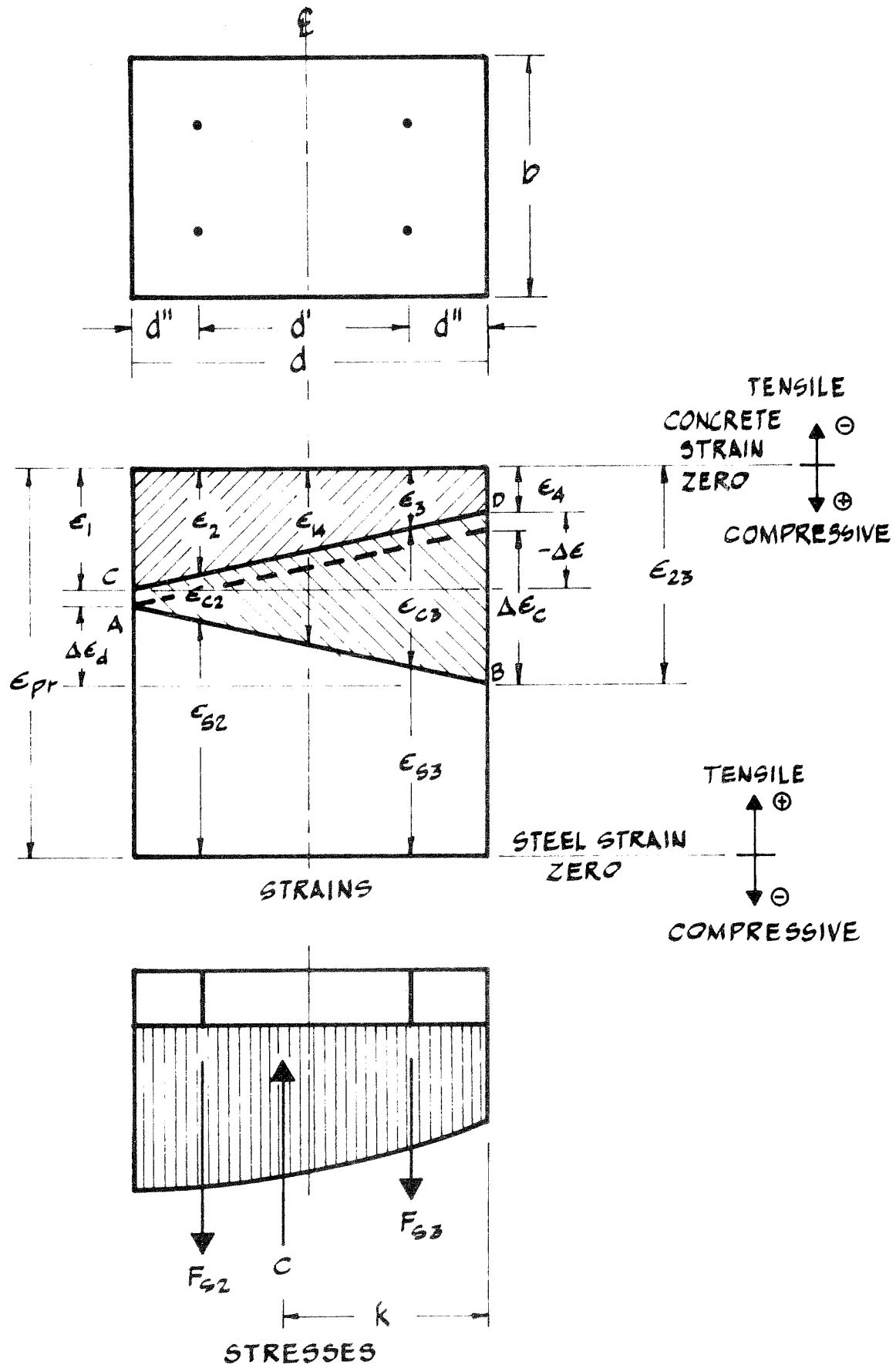


FIG. 23 INITIAL CONDITIONS: ECCENTRIC PRESTRESS

The first equation, of force equilibrium, to be satisfied is

$$F_{s2} + F_{s3} = C \quad (4.23)$$

where C is the resultant of the concrete stress block. It is assumed that the concrete compression extends over the full area of the cross-section (bxd), neglecting the small steel area. The strains, which are related to the concrete stresses through the stress-strain curve, are given by the line CD. The position of this line is unknown and it is the aim of the analysis to obtain the values of ϵ_1 and ϵ_4 . An expression for C, in terms of ϵ_1 and ϵ_4 , is given by Equation (B6). Integration and substitution into (4.23) give

$$(\epsilon_4 + \epsilon_1) \frac{bd\alpha E_c}{2\beta} + \frac{\alpha bd E_c^2}{10.2 \beta^2 f'_c} \left[\frac{(\epsilon_1^3 - \epsilon_4^3)}{(\epsilon_4 - \epsilon_1)} \right] - (F_{s2} + F_{s3}) = 0 \quad (4.24)$$

where all symbols have been previously defined and the unknowns are ϵ_4 and ϵ_1 .

The second equation, representing moment equilibrium, is

$$F_{s2} (d' + d'') + F_{s3} d'' = Ck = (F_{s2} + F_{s3}) k \quad (4.25)$$

The lever arm k is given by (B8). Integration and substitution into (4.25) give

$$\frac{\epsilon_4}{(\epsilon_4 - \epsilon_1)} - \frac{F_{s2}(d' + d'') + F_{s3} d''}{(F_{s2} + F_{s3}) d} - \frac{1}{(\epsilon_4 - \epsilon_1)^2} \left[\frac{bd\alpha E_c}{3\beta(F_{s2} + F_{s3})} (\epsilon_4^3 - \epsilon_1^3) + \frac{bd \alpha E_c^2}{13.6 \beta^2 f'_c (F_{s2} + F_{s3})} (\epsilon_1^4 - \epsilon_4^4) \right] = 0 \quad (4.26)$$

Equations (4.24) and (4.26) can now be solved by successive approximations, for ϵ_1 and ϵ_4 , using Newton's method of tangents (see Appendix C).

Strains ϵ_{c2} and ϵ_{c3} can next be obtained from

$$\begin{aligned}\epsilon_{c2} &= \epsilon_{pr} - \epsilon_{s2} - \epsilon_4 + \frac{d' + d''}{d} \Delta\epsilon \\ \epsilon_{c3} &= \epsilon_{pr} - \epsilon_{s3} - \epsilon_4 + \frac{d''}{d} \Delta\epsilon\end{aligned}\quad (4.27)$$

where

$$\Delta\epsilon = \epsilon_4 - \epsilon_1.$$

The above strains, representing the difference between lines AB and CD, are considered to be due to all the dimensional changes, creep, shrinkage, etc., from the time of release to testing. The contribution to curvature of these strains is measured by

$$\Delta\epsilon_c = (\epsilon_{c3} - \epsilon_{c2}) \frac{d'}{d} \quad (4.28)$$

and is assumed to remain constant during testing. The curvature at the section, which is used to calculate deflections, is given by

$$\frac{1}{r} = \frac{\Delta\epsilon_d}{d} \quad (4.29)$$

where

$$\Delta\epsilon_d = \Delta\epsilon + \Delta\epsilon_c$$

With the assumption of initial circular shape, the conditions at all other sections are the same as that described above for the mid-height.

With application of load, the "stress" strains ϵ_1 and ϵ_4 , and the "stress curvature" $\Delta\epsilon$, will change. To obtain the "deflection curvature" $\Delta\epsilon_d$, we have to add the constant "creep curvature" $\Delta\epsilon_c$, as shown above.

(b) Axial Prestress

This is a simplified case of the eccentric condition, with $\epsilon_{14} = \epsilon_{23}$. The strains and stresses are shown in Fig. 24. Equations (4.21) and (4.22) can still be used to determine the steel strains and forces. Since $\epsilon_4 = \epsilon_1$, we only have one unknown here. The condition of equilibrium of forces, Equation (4.23), with C obtained from

$$C = bd f_c$$

leads to a quadratic equation in ϵ_4 , the smallest root of which is

$$\epsilon_4 = \frac{6.8 \beta^2 f'_c}{bd \alpha E_c^2} \left[\frac{bd \alpha E_c}{\beta} - \sqrt{\left(\frac{bd \alpha E_c}{\beta} \right)^2 - (F_{s2} + F_{s3}) \frac{4 bd \alpha E_c^2}{3.4 \beta^2 f'_c}} \right] \quad (4.30)$$

Here, we have no initial curvature or deflections and no "creep curvature" to be added to calculate deflections due to load. However, the equal creep strains ϵ_{c2} and ϵ_{c3} still have to be considered in calculating the steel strains and stresses during loading.

2. Equilibrium at a Section

We shall consider now the stress and strain distributions at any cross-section of the column, under an eccentric load P. Our aim is to

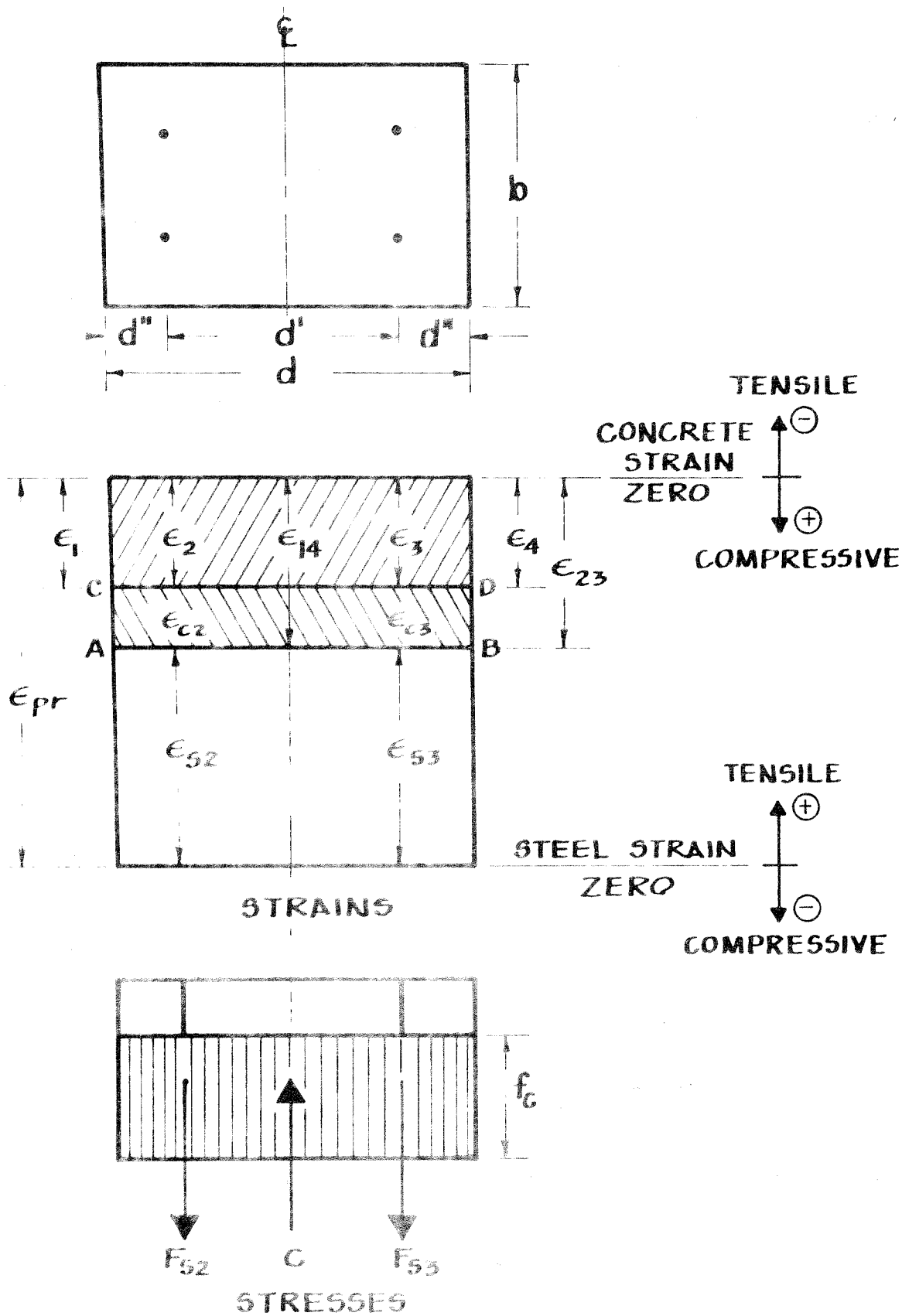


FIG. 24 INITIAL CONDITIONS:
AXIAL PRESTRESS

develop the two equations of equilibrium at the section.

Due to the discontinuities in the assumed concrete stress-strain curve (Fig. 22), in both tension and compression, a strain distribution can be classified as one of the seven cases shown in Fig. D1. Each case will lead to somewhat different equations of equilibrium.

The strain and stress conditions for case 3 are shown in detail in Fig. 25. Here, the minimum strain at the section, the tensile negative strain ϵ_1 , is taken to be larger than the modulus of rupture strain ϵ_t . The section is not yet cracked and the compression zone is over a depth

$$d_c = d \frac{\epsilon_4}{\Delta\epsilon} \quad (4.31)$$

The resultant concrete tensile force is

$$T = -b(d-d_c) \frac{E_t \epsilon_1}{2} \quad (4.32)$$

since ϵ_1 is negative.

The two equations of equilibrium are

$$P + F_{s2} + F_{s3} + T = C \quad (4.33)$$

and

$$F_{s2}(d'+d'') + F_{s3}d'' + T(d - \frac{d-d_c}{3}) = CkP(y - \frac{d}{2}) \quad (4.34)$$

Using (4.31) and (4.32), substituting C and k from (B2) and (B4), integrating and eliminating ϵ_1 with $\epsilon_1 = \epsilon_4 - \Delta\epsilon$, we finally get

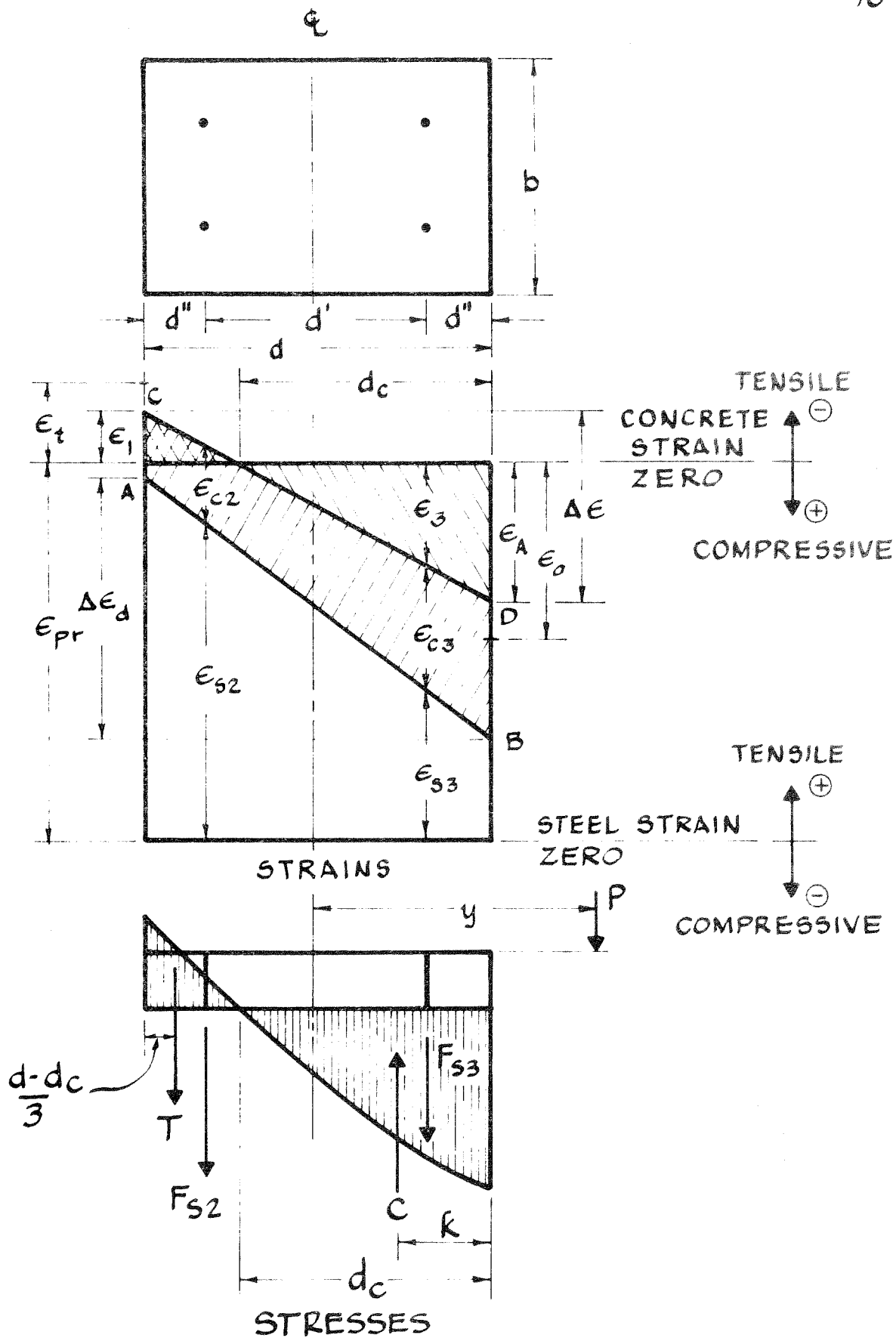


FIG. 25 STRAIN AND STRESS CONDITIONS - CASE 3

$$P + F_{s2} + F_{s3} - \frac{bd \alpha E_c}{2\beta} \frac{\epsilon_4^2}{\Delta\epsilon} \left(1 - \frac{E_c \epsilon_4}{5.1 \beta f_c} \right) + \frac{bd E_t}{2\Delta\epsilon} (\epsilon_4 - \Delta\epsilon)^2 = 0 \quad (4.35)$$

and

$$F_{s2}(d' + d'') + F_{s3} d'' - P \left(y - \frac{d}{2} \right) + \frac{bd^2 E_t}{6\Delta\epsilon} (\epsilon_4 - \Delta\epsilon)^2 \left(2 + \frac{\epsilon_4}{\Delta\epsilon} \right) - \frac{bd^2 \alpha E_c}{2\beta} \frac{\epsilon_4^3}{\Delta\epsilon^2} \left(1 - \frac{E_c \epsilon_4}{5.1 \beta f_c} \right) \left(1 - \frac{6.8 \beta f_c - 1.5 E_c \epsilon_4}{10.2 \beta f_c - 2 E_c \epsilon_4} \right) = 0 \quad (4.36)$$

The forces F_{s2} and F_{s3} depend on ϵ_4 , $\Delta\epsilon$, the known strains ϵ_{c2} , ϵ_{c3} , ϵ_{pr} and the known steel stress-strain curve. Thus, the two nonlinear equations of equilibrium (4.35) and (4.36) are in terms of four variables, namely P , y , ϵ_4 and $\Delta\epsilon$, and can be written symbolically as

$$f_1(P, \epsilon_4, \Delta\epsilon) = 0 \quad (4.37)$$

and

$$f_2(P, y, \epsilon_4, \Delta\epsilon) = 0$$

Given any two parameters, Equations (4.37) can be solved simultaneously, using Newton's method of tangents (App. C), for the remaining two unknowns.

Appendix D gives the details of the equilibrium equations (4.37) for all seven strain distribution cases.

After the solution of the equilibrium equations, the curvature at the section can be determined from (4.29), using the obtained $\Delta\epsilon$ and the constant "creep curvature" $\Delta\epsilon_c$, known from the solution of the initial conditions.

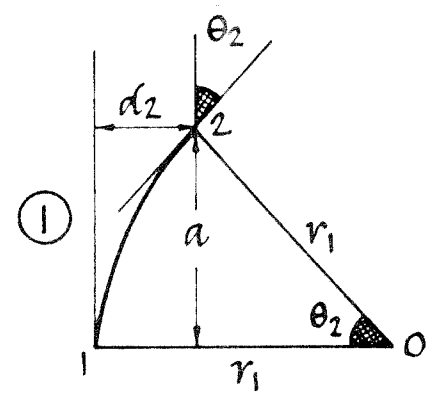
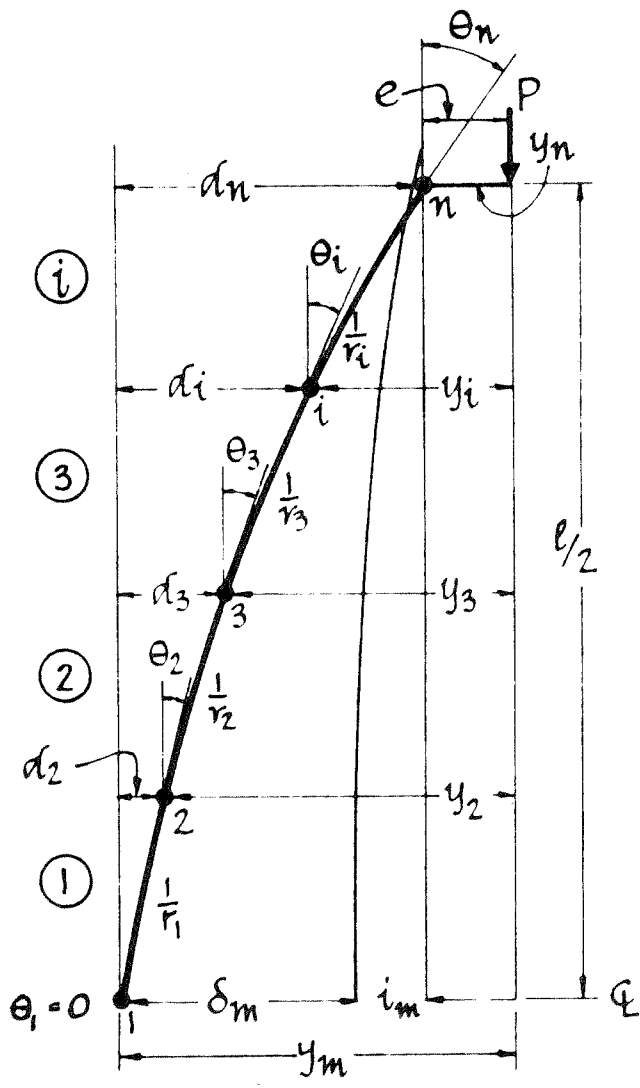
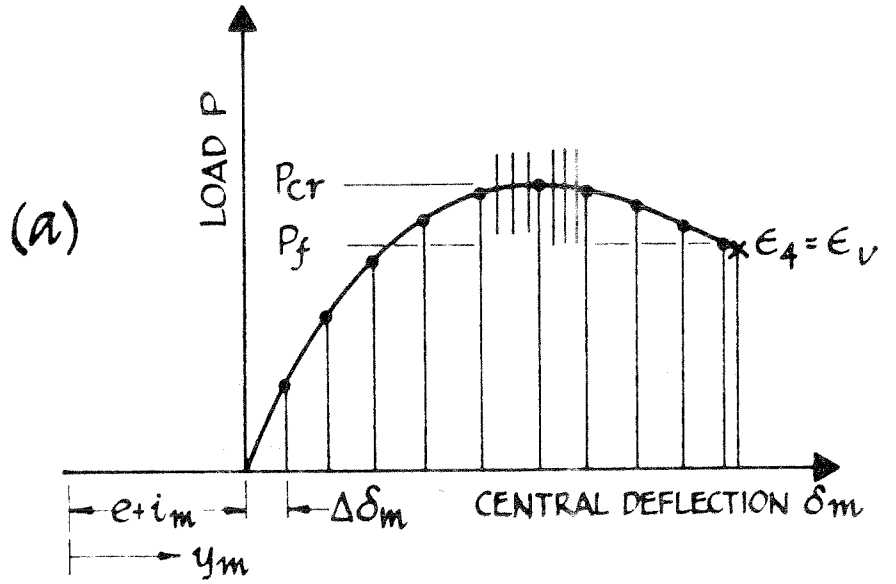
3. Method of Solution

The aim of the analysis is to construct the $P-\delta_m$ (load-central deflection) curve, as shown in Fig. 26(a). From the cotangency criteria (4.10), the maximum load represents the required critical value P_{cr} . The analysis is performed by considering small increments $\Delta\delta_m$ of the central deflection and obtaining the load corresponding to the prescribed deflection. To increase the accuracy in the region of the critical maximum load, $\Delta\delta_m$ is divided into any desired number of smaller increments. The increments of deflection are continued in the post-critical region until material failure occurs, represented by the maximum strain at mid-height ϵ_4 reaching the failure strain ϵ_u .

To calculate the load P corresponding to a given central deflection δ_m , the column is divided into a number of finite elements. Due to symmetry about the mid-height, we need only consider one half of the column, which is shown in Fig. 26(b). The finite elements are connected at nodal points, numbered 1 to n , and are assumed to be of constant curvature, i.e., circular shape. Two adjacent elements have a common tangent at a nodal point. The total number of elements, for one half of column length, is $(n-1)$, each of length

$$\Delta\ell = \frac{\ell/2}{n-1} \quad (4.38)$$

The axial shortening of the column, due to P , is neglected. Thus, the finite elements are assumed to remain of constant length $\Delta\ell$ during loading and bending.



ELEMENT ① OF CIRCULAR SHAPE, ARC LENGTH Δl

FIG 26 METHOD OF SOLUTION

The calculations start at the central nodal point 1, with a known total deflection y_m . The two equations of equilibrium at the point, Equations (4.37), still contain three unknowns, namely P , ϵ_4 and $\Delta\epsilon$. To find the value of $\Delta\epsilon$, columnwise iterations will be performed until the boundary condition is satisfied at the top of the column. The first assumed value of $\Delta\epsilon$ is based on a sine curve deflected shape

$$\Delta\epsilon = \frac{(\delta_m + i_m) d\pi^2}{\ell^2} - \Delta\epsilon_c \quad (4.39)$$

The two equations of equilibrium can now be solved at point 1 by Newton's method, for the unknown P and ϵ_4 . Using initial assumed values of P and ϵ_4 , appropriate equations of equilibrium are selected, out of the seven cases.

The position of nodal point 2 can now be determined (see Fig. 26(c)). The tangent at point 1 is known to be vertical and finite element 1 is assumed to be of the above constant curvature $\Delta\epsilon$, i.e., circular arc of radius r_1 , from (4.29), and length $\Delta\ell$. Thus, the change of slope over the finite element length is

$$\theta_2 = \frac{\Delta\ell}{r_1} \quad (4.40)$$

and the horizontal deviation of point 2 from the vertical tangent is given by

$$d_2 = r_1 (1 - \cos \theta_2) \quad (4.41)$$

Using only the first two terms of the series expansion for $\cos \theta_2$, and substituting (4.40) we get

$$d_2 = \frac{\Delta\ell^2}{2r_1} \quad (4.42)$$

The total deflection at point 2, y_2 , can now be calculated from

$$y_2 = y_m - d_2 \quad (4.43)$$

and the appropriate two equations of equilibrium solved for the "stress curvature" $\Delta\epsilon$ and the maximum strain ϵ_4 , at point 2, with the load P kept constant at the value previously determined at nodal point 1. Thus, we have the constant radius, r_2 , of element 2 and the slope at point 3 becomes

$$\theta_3 = \theta_2 + \frac{\Delta l}{r_2} \quad (4.44)$$

The horizontal deviation of point 3 is given by

$$d_3 = d_2 + \Delta l \theta_2 + \frac{\Delta l^2}{2r_2} \quad (4.45)$$

In the above expression, the second term represents the contribution of the slope at point 2 and the third term the contribution due to the curvature of element 2, similar to d_2 in Fig. 26(c) as given by (4.42). Equation (4.45) contains the assumption of small rotations, i.e., the assumption that $\sin \theta = \theta$ and $\cos \theta = 1$.

Next, we can again solve the appropriate two equations of equilibrium, this time at nodal point 3, for the unknowns $\Delta\epsilon$ and ϵ_4 .

Similarly, we proceed to higher nodal points, using the general recurrence relations

$$d_i = d_{i-1} + \Delta l \theta_{i-1} + \frac{\Delta l^2}{2r_{i-1}} \quad (4.46)$$

and

$$\theta_i = \theta_{i-1} + \frac{\Delta l}{r_{i-1}} \quad (4.47)$$

Finally, the total deflection y_n , at the top nodal point n , is determined

$$y_n = y_m - d_n \quad (4.48)$$

and the required boundary condition

$$y_n = e \quad (4.49)$$

can be checked. If this is satisfied, within a very small prescribed tolerance, the value of P , which was determined at nodal point 1 and used at all other points, represents the required load for the particular central deflection δ_m and a point has been determined on the load-central deflection curve (Fig. 26 (a)). If (4.49) is not satisfied, the assumed value of $\Delta\epsilon$, at central nodal point 1, is changed and the whole procedure repeated again.

The value of $\Delta\epsilon$ for the j -th columnwise iteration, $\Delta\epsilon_j$, is calculated from

$$\Delta\epsilon_j = \Delta\epsilon_{j-1} + (y_n - e)_{j-1} \frac{\Delta\epsilon_{j-2} - \Delta\epsilon_{j-1}}{(y_n - e)_{j-1} - (y_n - e)_{j-2}} \quad (4.50)$$

where

$$(y_n - e)_{j-1} = \text{error in top boundary condition, after the } (j-1)\text{th iteration, which used } \Delta\epsilon_{j-1}.$$

It is considered that the effects of assuming small rotations and neglecting the axial shortening are very small. It is relatively easy to remove these assumptions, if desired, and the correct expressions are presented in Appendix E.

To determine the material failure load P_f , the strain ϵ_4 is checked after the solution of each load-central deflection point. When ϵ_4 exceeds the ultimate strain ϵ_u , an iteration is performed on the central deflection δ_m , to find the value at which $\epsilon_4 = \epsilon_u$. The value of δ_m for the i -th iteration, is given by

$$\delta_{m_i} = \delta_{m_{i-1}} + (\delta_{m_{i-2}} - \delta_{m_{i-1}}) \frac{\epsilon_u - (\epsilon_4)_{i-1}}{(\epsilon_4)_{i-2} - (\epsilon_4)_{i-1}} \quad (4.51)$$

where

$\delta_{m_{i-1}}$ = the central deflection on the $(i-1)$ th iteration, which resulted in a maximum strain $(\epsilon_4)_{i-1}$, when the boundary conditions were satisfied.

The number of calculations involved, in the method of solution described above, is too large for manual operations. Thus, a computer program was developed and will be described later.

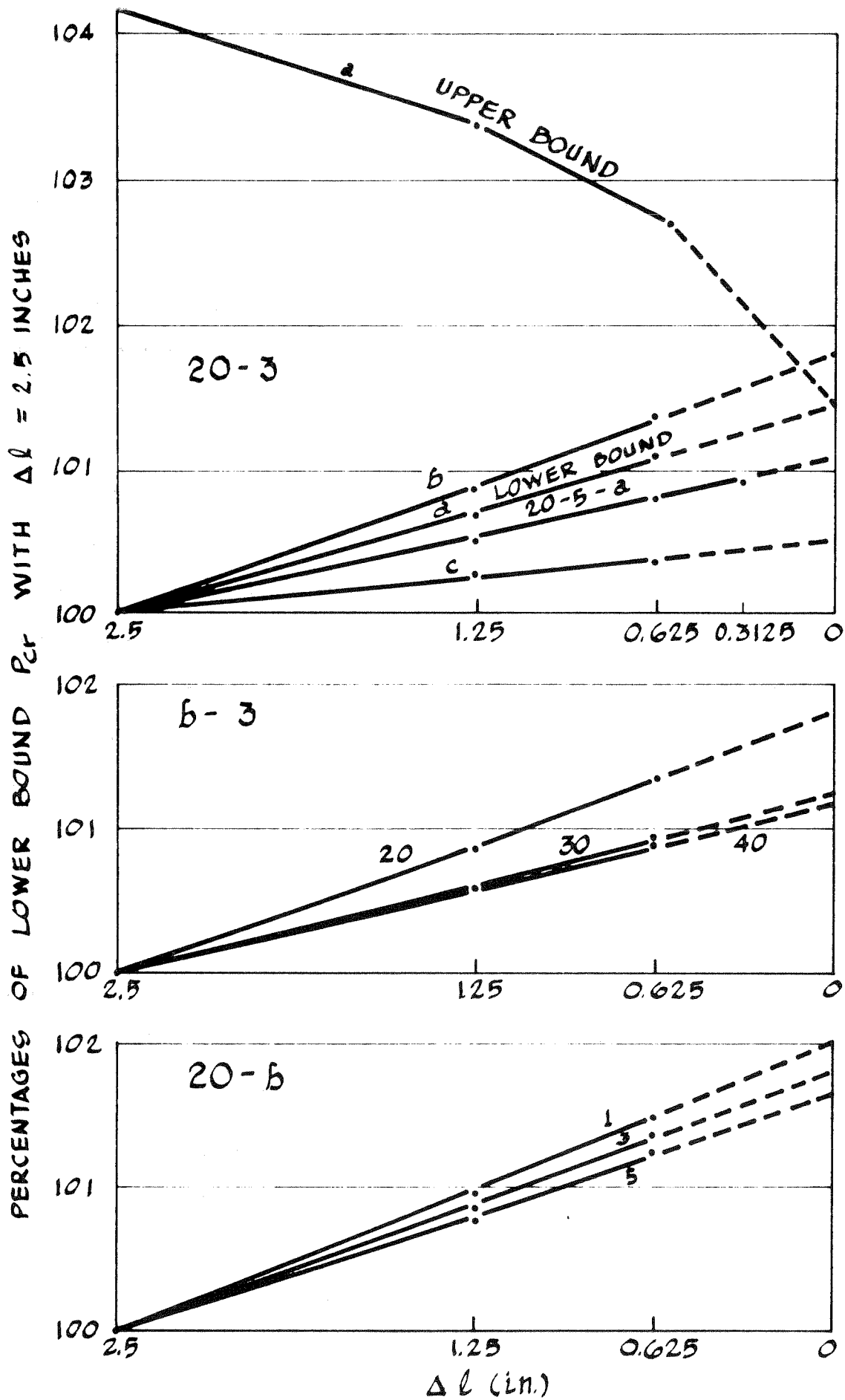
4. Lower and Upper Bounds

The assumption of finite elements, described above, obviously introduces an approximation into the calculated loads. Let us examine the nature of this approximation.

The assumed deflected shape of the column has continuous slopes and satisfies the boundary conditions. However, the two equations of equilibrium were only satisfied at the lower nodal point of each finite element. Within each element this is the point of maximum moment and,

therefore, maximum curvature, at least at or before the maximum load is reached. Thus, the constant curvature assumed within each element is a maximum of the actual curvatures and the column is assumed to be more flexible than it actually is. This results in a load, which is lower than the correct load. If we increase the number of elements, i.e., decrease the element length $\Delta\ell$, the load should increase and tend to the correct load as $\Delta\ell$ tends to zero. Though no mathematically rigorous argument can be presented, in this nonlinear problem, the calculations performed substantiate the above expectation. Fig. 27 presents results of computer calculations of eight columns of different length, eccentricity and prestress. The columns had the same details as the experimental specimens and the meaning of the labels is as described in Table 4. The maximum load P_{cr} , calculated with $\Delta\ell = 2.5$ in., is taken as the basis for comparison (100%) for each column. The loads for all columns are seen to increase linearly with the decrease of element length, to $\Delta\ell = 1.25, 0.625$ and 0.3125 in. for one column. No large difference is seen between the various parameters and extrapolations to zero element length indicate that the results with $\Delta\ell = 2.5$ in. represent a lower bound by a maximum of 2%.

The arguments presented above suggest a way of obtaining upper bound loads. This would result if, within each finite element, the assumed constant curvature would be the minimum in the element, giving a column of higher stiffness. A suitable method of analysis was developed, which satisfies the equations of equilibrium at the top nodal point of each element,



LENGTH OF FINITE ELEMENTS
FIG. 27 VARIATION OF P_{cr} WITH FINITE ELEMENT LENGTH

the point of minimum moment and curvature. A description of the method is given in Appendix F. The procedure is more involved than the lower bound solution and requires much longer computer times. The upper bound results, for column 20a3, are shown in Fig. 27. The loads are seen to decrease with the decrease of Δl , but the lower bound solution is closer to the correct value, for any given Δl .

The same behavior, of both upper and lower bounds, can be seen in Fig. 28, for loads representing 75% of the maximum load, in the stable equilibrium region. However, the differences from the correct value are smaller here than for the maximum load, shown in Fig. 27. This is probably due to the more uniform curvature distribution at lower loads and moments.

4.4 Computer Program

A computer program was written to perform the analysis described above. The listing of the program is presented in Appendix G. Some aspects of the computer program will be discussed in this section.

1. Input

The input, for each column analyzed, consists of 36 items presented on thirteen cards. The variables on each card are listed in Table 7.

Table 7. Computer Input

Card Number	Variables
1	Column label
2	NF1, NF2, NF3, NF4, NF5, FAC1, FAC2, E5, E6, E7
3	b, d, d', d'', A_s , f'_c , α
4	β , ϵ_{pr} , ϵ_{23} , ϵ_{14}

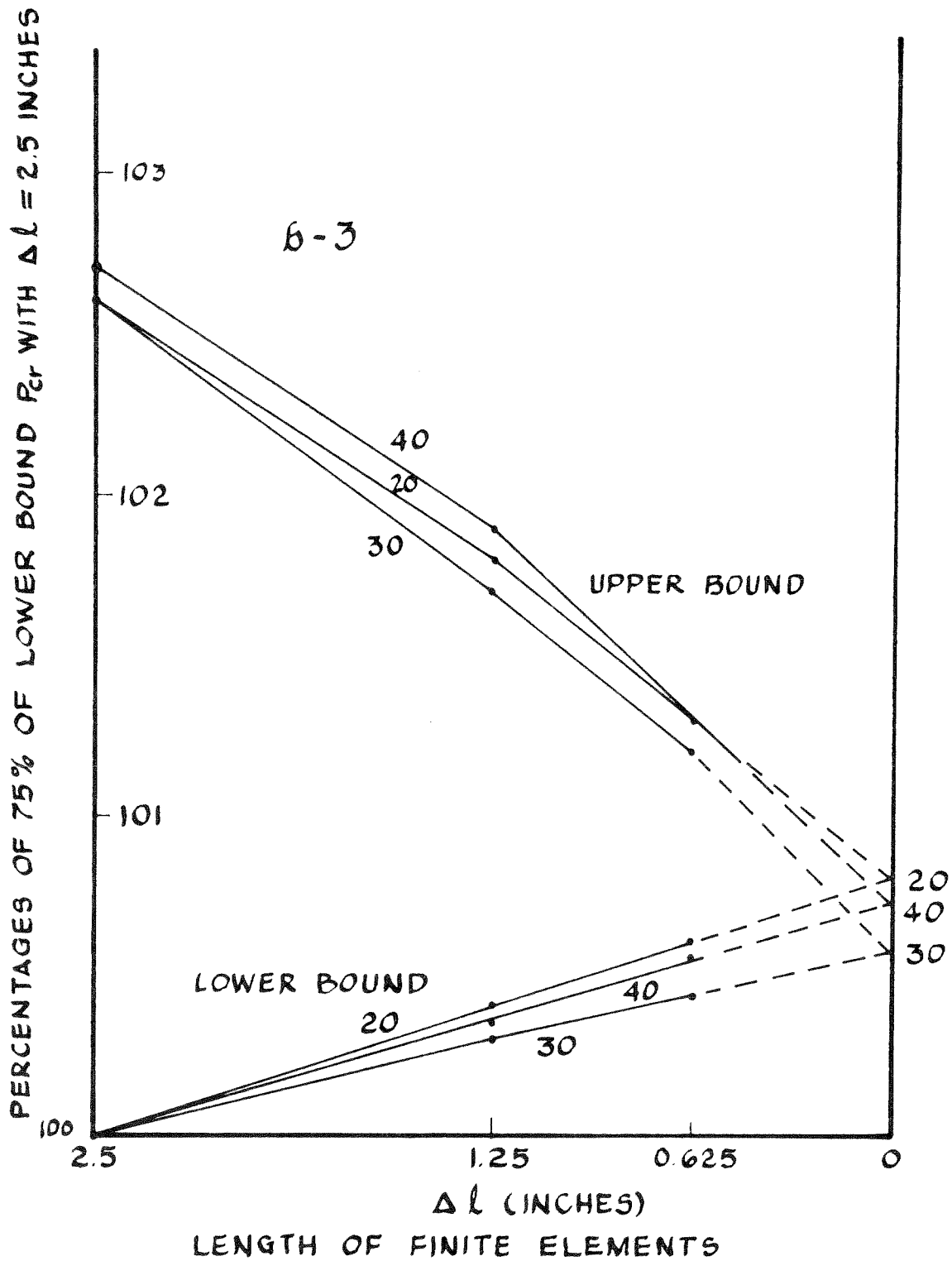


FIG. 28 VARIATION OF 75% P_{cr} WITH FINITE ELEMENT LENGTH

Table 7 (Con't)

Card Number	Variables
5	$\Delta l, E1, E2, E3, \epsilon_u, E_t$
6	n
7	l
8	e
9	f_t
10	$\Delta \delta_m$
11	DINC
12	E4
13	γ

The input variables can be classified in four categories and have the following meaning.

(a) Column details

"Column label" (e.g., A₁20c3) has been explained in Table 4.

b, d, d', d'', l and e have been defined in Fig. 1.

A_s = cross-sectional area of two steel wires.

(b) Material

$f'_c, \alpha, \beta, \gamma, f_t, \epsilon_u$ and E_t have been defined in Fig. 22.

(c) Program

NF1 = 1 or 0, is a flag which determines if the analysis results should be punched on cards, for graph plotting purposes, in addition to the printed output. When NF1=1, the punched cards are obtained.

NF2 = 1 or 0, is a flag which determines if the upper bound load analysis should be performed. When NF1=1, the upper bound load is calculated.

NF3 = 1 or 0, is a flag which determines if the "diagnostic output" should be printed. For cases when convergence difficulties occur, and it is desirable to know the intermediate iteration values NF = 1 will cause all this data to be printed out.

NF4 = 1 or 0, is a flag which determines if the calculation of the lower bound solution should proceed after convergence difficulties are encountered in the upper bound calculations. NF4 = 0 terminates the calculations, if the upper bound solution does not converge.

NF5 = 1 or 0, is a flag which determines the "diagnostic output" for the upper bound calculations only. NF5 = 1 will print out all the intermediate values of the upper bound iterations.

FAC1 = factor determining the $(\Delta\epsilon)_n$ mesh size in upper bound solution (see Equation (F4)).

FAC2 = factor determining the θ_n mesh size in upper bound solution (see Equation (F5)).

E1 = allowable error in ϵ_4 and $\Delta\epsilon$, in the iterative solution of the equations of equilibrium.

E2 = allowable error in P, in the iterative solution of the equations of equilibrium.

E3 = allowable error in the deflection boundary condition, Equations (4.49) and (F2).

E4 = allowable error in $\epsilon_4 = \epsilon_u$, at the point of material failure.

E5 = allowable error in the slope boundary condition, equation (F1).

E6 = magnification factor for θ_1 , in the criterion function F, equation (F3).

E7 = factor used in the initial upper bound load assumption.

n = the total number of nodal points in half the column length.

Number of finite elements is (n-1).

Δl = finite element length, equation (4.38)

$\Delta \delta_m$ = increment of central deflection

DINC = factor determining the reduced increments of central deflection in the region of maximum critical load. Reduced increment = $\Delta \delta_m / \text{DINC}$.

(d) Prestress and initial conditions

ϵ_{pr} = initial strain applied to the prestressing steel

ϵ_{23} = concrete strain, from release to testing, on the concrete compressive face at column mid-height.

ϵ_{14} = concrete strain, from release to testing, at the section mid-depth, at column mid-height.

2. Main Control

This portion of the program contains most of the lower bound solution. It controls the calculation of the initial conditions, the columnwise iteration and the iterative solution of the equations of equilibrium.

A limit of 50 iterations was set for the columnwise procedure to satisfy the top boundary condition. If no convergence is obtained after 50 iterations a diagnostic statement is printed out. The average number of columnwise iterations was about two. No difficulties were encountered with columnwise convergence that could not be overcome by a change of finite element length or deflection increment.

A number of flags are used to control the calculations close to the maximum critical load. When the load first decreases, the values are reset to the previous deflection and the calculations continued with a reduced deflection increment. If the load continues to decrease, a backward reduced deflection increment is taken. Reduced deflection increments are used until a maximum load is established.

3. Initial Conditions

The two cases of initial conditions have been described in Section 4.3.1. We have

- (a) Case A. This is eccentric prestress, requiring iteration of equations (4.24) and (4.26) for the initial strains ϵ_1 and ϵ_4 , using Newton's method. The arbitrary initial values assumed for iteration are

$$\epsilon_4 = 0.3 \epsilon_{23}$$

and

$$\epsilon_1 = 0.75 (2 \epsilon_{14} - \epsilon_{23}) \tag{4.52}$$

- (b) Case B. This is axial prestress, requiring no iteration. The strains are calculated from equation (4.30).

4. Solution of Equilibrium Equations

The equilibrium equations (4.37) are solved by Newton's method of tangents. There are two types of operations.

- (a) Case A. Here equations (4.37) are solved for the unknowns P and ϵ_4 .

This is required only at the column mid-height, nodal point 1. At the beginning of the column analysis, for the first increment $\Delta\delta_m$, the following initial values are assumed for iteration

$$P = \frac{\pi^2 E_c b d^3 \Delta\delta_m}{12\ell^2 (\Delta\delta_m + e)} \quad (4.53)$$

and

$$\epsilon_4 = (\epsilon_4)_{\text{int.}} + \frac{\Delta\epsilon}{2} + \frac{P}{bdE_c} \quad (4.54)$$

where

$(\epsilon_4)_{\text{int.}}$ = ϵ_4 value obtained from the solution of the initial conditions.

$\Delta\epsilon$ = assumed initial value for columnwise iteration, calculated from equation (4.39).

Equation (4.53) is an adaptation of an approximate expression and (4.54) assumes that the load P is carried by the concrete only. The initial values of P and ϵ_4 , used for iteration at all other deflection increments, are taken

equal to the values of the solution at the previous deflection.

- (b) Case B. In this case, equilibrium equations (4.37) are solved for the unknowns ϵ_4 and $\Delta\epsilon$. The initial values for iteration are taken equal to the respective magnitudes obtained in the solution of the previous, lower, finite element.

In both cases, A and B above, there is first a selection of the appropriate equations of equilibrium. The seven sets of equations (4.37) are listed, together with the required partial derivatives. The iterations are performed to the accuracy specified in the input, E1 for ϵ_4 and $\Delta\epsilon$ and E2 for P. A limit of 500 iterations was set and, if no convergence is obtained, a diagnostic statement is printed out and the calculations for the particular column terminated. Convergence difficulties, which occurred in some cases, were overcome by reduced finite element lengths.

5. Material Failure

The material failure condition, at which $\epsilon_4 = \epsilon_u$, is obtained by iteration on the central deflection δ_m , as described in Section 4.3.3 above. A specified total of five iterations are performed, which in most cases result in the prescribed accuracy of E4.

6. Upper Bound

The upper bound calculations are programmed according to the method of solution described in Appendix F. The initial values for iteration of equilibrium equations are taken equal to the lower bound solution at a

neighbouring nodal point or the solution at the nodal point in question, obtained during the previous columnwise iteration.

To satisfy the boundary conditions, errors of E5 and E3 are allowed in equations (F1) and (F2) respectively, during the first 10 columnwise iterations. After the first 10 iterations, the accuracy requirements are relaxed somewhat by specifying an allowable error on the combined boundary condition $F = 0$ (see equation (F3)) of $E8 = (E6 \times E5)^2 + E3^2$. A limit of 20 sets of columnwise iterations was set (each set made up of seven points, as shown in Fig. F1), after which, if no convergence was obtained, a diagnostic statement is printed out.

The convergence of the upper bound solution is more difficult than the lower bound and a judicious selection is necessary of the factors involved. An example of the numerical values used is (for column C₂20a3 with $\Delta\epsilon = 2.5$ in.)

FAC1=1.010		FAC2=1.001
E5=0.0005	E6=2.5	E7=1.06

7. Functions FORS and DEFORS

These are the functions listed in the two last pages of Appendix G.

Function FORS calculates the steel force F_s , used in the equilibrium equations, for given steel strain ϵ_s . The required partial derivative of the steel force, for given steel strain, with respect to the strain, is calculated by function DEFORS. The steel material properties, as shown in Fig.

19, are used only in the above two functions. Thus, for a different steel stress-strain curve, the only changes that need be made are in these two functions.

8. Output

The printed output lists the input data and the analysis results in the form of load, mid-height strains (on the tensile, mid-depth, and compressive faces) and deflections at nodal points. The strains and deflections listed are those due to load only.

The results are also available, on punched cards, if the input flag NF1=1. Full diagnostic printed outputs can also be obtained, if required.

The computer time, in minutes, used for the calculation of each column, is also printed out.

9. Computer Times

The average time, per column, for the analysis of the thirty-six experimental columns, with $\Delta l = 2.5$ in., was 0.165 min. (range 0.06 - 0.68 min.). The upper bound solutions required much longer computer times. Table 8 shows, as an example, the values for column C₂20a3.

Table 8. Computer Times(Column C₂20a3)

Δl (in)	Lower bound (minutes)	Upper bound (minutes)
2.5	0.28	1.14
1.25	0.38	1.30
0.625	0.66	8.52

Chapter 5. COMPARISON OF EXPERIMENTAL RESULTS WITH THEORY

The thirty-six columns tested experimentally were analyzed, using the theory and computer program described earlier. The columns were analyzed for the lower bound solution only, using individual values of length, eccentricity, nominal prestress strain ϵ_{pr} (Table 3), and initial strains ϵ_{14} and ϵ_{23} (Table 4). Deflection increments $\Delta\delta_m$, shown in Table 9, were selected to give a reasonable number of points for each column and also to ensure convergence. In addition, the following input values were used for all the columns.

(a) Column details

$$b = 3.0 \text{ in.} \qquad d = 2.02 \text{ in.}$$

$$d' = 1.0 \text{ in.} \qquad d'' = 0.51 \text{ in.}$$

$$A_s = 0.0616 \text{ sq. in. (area of two wires)}$$

These were the average dimensions, as shown in Fig. 1

(b) Material

$$f'_c = 5,585 \text{ psi} \qquad f_t = 558.5 \text{ psi}$$

$$E_t = 4.2 \times 10^6 \text{ psi} \qquad \epsilon_u = 0.0060$$

$$\alpha = 1.176 \qquad \beta = 1.0 \qquad \gamma = 0.050$$

The above cylinder strength f'_c represents the overall average of the thirty-six cylinders tested. The modulus of elasticity in tension, E_t , was calculated to be equal to the compressive modulus E_c , obtained from Equation (4.13). A number of different compressive stress-strain curves were tried, from the family of curves of Fig. 22, and the one giving best agreement for the maximum

loads had the parameters listed above. The value of $\alpha = 1.176$ represents a maximum compressive stress of $f_c'' = f_c'$ and this is regarded appropriate for horizontally placed members. The value of maximum strain ϵ_u was selected in view of the experimental strain measurements at material failure load P_f .

(c) Program

$$E1 = 0.5 \times 10^{-7}$$

$$E2 = 1 \text{ lb.}$$

$$E3 = 0.001 \text{ in.}$$

$$E4 = 0.00005$$

$$\text{DINC} = 4$$

and $\Delta \ell = 2.5 \text{ in.}$

5.1 Maximum Critical Load

The values of the theoretical maximum critical loads P_{cr} are given in Table 9, which also lists the deflection increments $\Delta \delta_m$ used in the analysis, the experimental critical loads and the ratio of experimental to theoretical loads. Three of the five columns, that reached a maximum load with material failure, are predicted by the theory to do so. The theory predicts primary material failure in four other columns, which, however, reached an experimental maximum before observed failure. In all these four cases the observed failure load was 90 lb. or less from the maximum load.

A histogram of the load ratios is shown in Fig. 29. The average ratio was 1.018 (range: 0.821-1.123) with a standard deviation of 0.065. The agreement of the maximum critical loads is considered to be very good. The average ratio is consistent with the theoretical load being a lower bound, of about 2% below the limiting $\Delta \ell = 0$ value. The standard deviation

Table 9. Comparison of P_{cr} Loads

Column ^{*1}	Experimental P_{cr} (lb)	Theoretical Analysis		Ratio $(P_{cr})_{exp.} / (P_{cr})_{th}$
		$\Delta\delta_m$ (in)	P_{cr} (lb)	
A ₁ 20c3	2,650	0.060	2,581 ^{*3}	1.027
A ₁ 30a3	10,430	0.020	10,123	1.030
A ₁ 40b3 ^{*2}	3,100	0.200	3,042	1.019
A ₂ 20b5 ^{*2}	5,130	0.040	5,301	0.968
A ₂ 30c5 ^{*2}	1,980	0.120	2,093	0.946
A ₂ 40a5	5,930 ^{*3}	0.120	5,545	1.069
B ₁ 20a1 ^{*2}	18,820 ^{*3}	0.004	17,123	1.099
B ₁ 30b1 ^{*2}	3,890	0.160	3,465	1.123
B ₁ 40c1 ^{*2}	1,630	0.320	1,529	1.066
B ₂ 20b3 ^{*2}	4,870 ^{*3}	0.060	5,281 ^{*3}	0.922
B ₂ 30c3	1,960 ^{*3}	0.120	2,063 ^{*3}	0.950
B ₂ 40a3	5,970 ^{*3}	0.120	6,237 ^{*3}	0.957
C ₁ 20c1	2,690 ^{*3}	0.060	2,572 ^{*3}	1.046
C ₁ 30a1 ^{*2}	11,660	0.020	11,022	1.058
C ₁ 40b1 ^{*2}	2,670	0.200	2,499	1.068
C ₂ 20a3 ^{*2}	12,790	0.010	15,570	0.821
C ₂ 30b3 ^{*2}	3,950	0.120	3,936	1.004
C ₂ 40c3	1,610	0.280	1,654 ^{*3}	0.973
D ₁ 20c5 ^{*2}	2,810	0.040	2,521 ^{*3}	1.115
D ₁ 30b5 ^{*2}	4,510	0.120	4,113	1.097
D ₁ 40a5 ^{*2}	5,910	0.160	6,098	0.969
D ₂ 20b3 ^{*2}	5,580	0.040	5,281	1.057
D ₂ 30b3 ^{*2}	4,250	0.160	3,960	1.073
D ₂ 40b3 ^{*2}	2,930 ^{*3}	0.280	2,937	0.998
E ₁ 20a5 ^{*2}	13,100 ^{*3}	0.020	13,592	0.964
E ₁ 30b5 ^{*2}	4,330	0.120	4,084	1.060
E ₁ 40c5 ^{*2}	1,880	0.200	1,774 ^{*3}	1.060
E ₂ 20b1 ^{*2}	5,090 ^{*3}	0.060	5,062 ^{*3}	1.006
E ₂ 30c1	2,010 ^{*3}	0.120	1,993 ^{*3}	1.009
E ₂ 40a1 ^{*2}	6,700	0.040	7,519 ^{*3}	0.891
F ₁ 20b1 ^{*2}	5,570	0.060	5,071 ^{*3}	1.098
F ₁ 30b1 ^{*2}	3,700	0.160	3,446	1.074
F ₁ 40b1 ^{*2}	2,500	0.240	2,492	1.003
F ₂ 20b5 ^{*2}	5,310	0.040	5,288	1.004
F ₂ 30a5	9,620	0.060	9,331	1.031
F ₂ 40b5	3,010	0.200	2,989	1.007

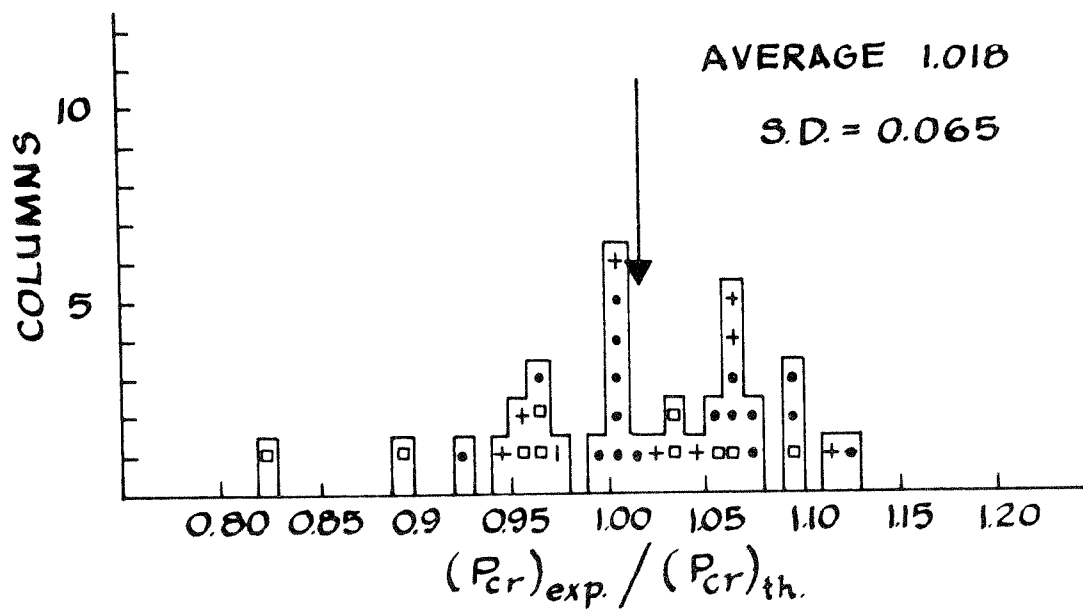
*1 For details see Table 4

*2 Columns with duplicates

*3 Material failure

SYMBOLS

□	ECCENTRICITY	a	(10 COLUMNS)
•	"	b	(17 COLUMNS)
+	"	c	(9 COLUMNS)

FIG. 29 HISTOGRAM OF P_{cr} LOAD RATIOS

compares favourably with those of other investigations. Thus, Hognestad⁽²¹⁾ had a standard deviation of 0.058 for 120 short, eccentrically loaded, reinforced concrete columns and Broms and Viest⁽²⁴⁾ calculated a value of 0.129 for 79 long, eccentrically loaded, columns from six different investigations. The points in Fig. 29 are distinguished with respect to eccentricity. It can be noted that, as could be expected, the lowest eccentricity "a" has the largest variability.

The above load ratios were analyzed statistically to determine if they are significantly different with respect to any of the variables involved. The analysis of variance results are shown in Table 10. The ratios are seen not to be significantly different, and it can thus be claimed that the theory is not biased with respect to the variables investigated.

Table 10. Analysis of Variance of P_{cr} Ratios

Variable	Degrees of Freedom	Sum of Squares	Mean Square	F	Significant F(5% level)
Groups	5	0.0146	0.0029	0.75	2.62
Slenderness	2	0.0070	0.0035	0.89	3.40
Eccentricity	2	0.0130	0.0065	1.67	3.40
Prestress	2	0.0216	0.0108	2.77	3.40
Error	24	0.0937	0.0039		
Total	35	0.1499			

5.2 Effect of Variables on P_{cr}

1. Prestress

Fig. 30 shows the variation of P_{cr} with prestress ratio, in a dimensionless form, for the nine combinations of slenderness and eccentricity. Note the reduced scale for the 20a columns. The values of prestress ratios, for each column, are those presented in Table 4. Experimental and theoretical points, or averages of duplicates, when available, are connected by straight lines. The theoretical points do not lie on smooth curves since each is calculated with its particular, experimentally observed, initial conditions (values of ϵ_{14} , ϵ_{23} and ϵ_{pr}). The values of zero prestress were obtained assuming an initially straight shape. To illustrate the point, the theoretical curve for column 40a was recalculated, using a smooth variation of ϵ_{14} and initial deflection i_m , based on the average values of all the columns. The data used for this curve are given in Table 11.

Table 11. P_{cr} Loads for Column 40a, with Average
Strains and Deflections

Prestress Ratio f_{cp}/f'_c	Initial Deflection i_m (in.)	Strain ϵ_{14} ($\times 10^{-4}$)	Strain ϵ_{23} ($\times 10^{-4}$)	Strain ϵ_{pr} ($\times 10^{-4}$)	Theoretical P_{cr} (lb)	P_{cr}/bdf'_c
0	0	0	0	0	6,684	0.197
0.03	0.011	0.58	0.72	3.37	6,917	0.204
0.06	0.026	1.17	1.5	6.74	7,026	0.207
0.092	0.047	2.0	2.59	10.37	7,037	0.208
0.125	0.078	2.9	3.88	14.5	6,959	0.205
0.150	0.106	3.9	5.24	17.8	6,846	0.202
0.175	0.138	4.8	6.54	21.0	6,715	0.198
0.252	0.234	7.65	10.6	31.12	6,346	0.187
0.410	0.428	13.1	18.5	52.15	5,527	0.163

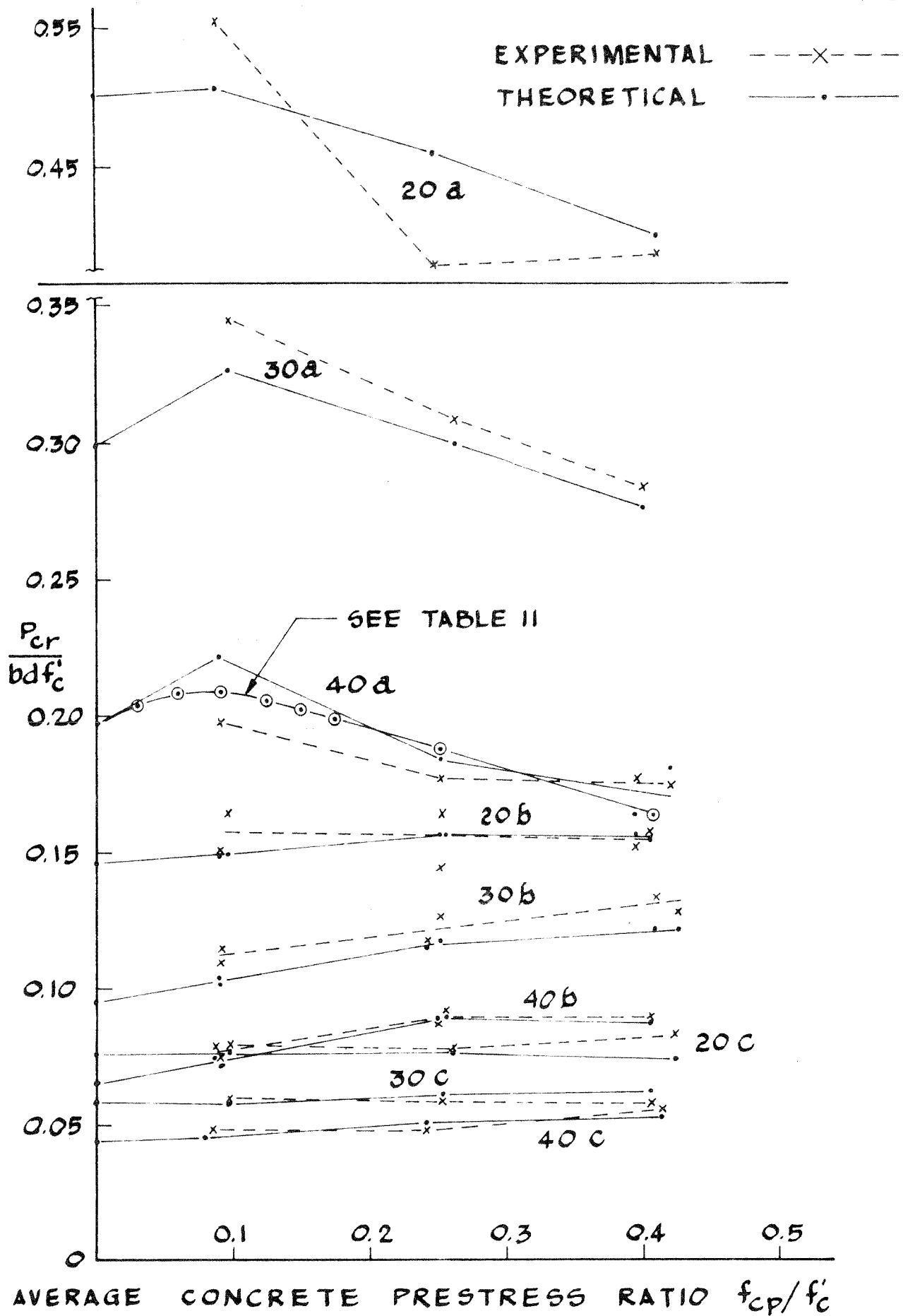


FIG 30 EFFECT OF PRESTRESS ON P_{cr}

The agreement between the experimental and theoretical lines is generally good, with the exception of column 20a3, which had the lowest relative experimental P_{cr} . For columns of smallest eccentricity "a", increase of prestress beyond a ratio of about 0.1 decreases significantly the value of P_{cr} . However, prestress is beneficial over a small range of f_{cp}/f'_c , up to about 0.1. It seems reasonable to conclude that columns with some eccentricity will have some prestress, no matter how small, which will give a P_{cr} higher than that for zero prestress. The relative increase due to prestress, for eccentricity "a", is smallest for the shortest column 20. Columns of medium eccentricity "b", acting as beam-columns, show an increase of P_{cr} with prestress, with a maximum in the region of $f_{cp}/f'_c = 0.3$ to 0.35. Again, the least relative benefit of prestress is for columns of $l/d = 20$. Finally, for the largest eccentricity "c", prestress is seen to have no effect on columns of slenderness 20. For the longer columns, P_{cr} keeps increasing with prestress, the increase being larger for the higher slenderness.

2. Eccentricity

The effect of eccentricity on P_{cr} is illustrated in Fig. 31, for a nominal prestress ratio of 0.1. The critical load decreases sharply with increase of eccentricity. This decrease is larger, the shorter the column. Good agreement exists between experimental and theoretical values, with the theoretical loads being on the lower side. The loads plotted for the medium "b" eccentricity are averages of duplicate columns.

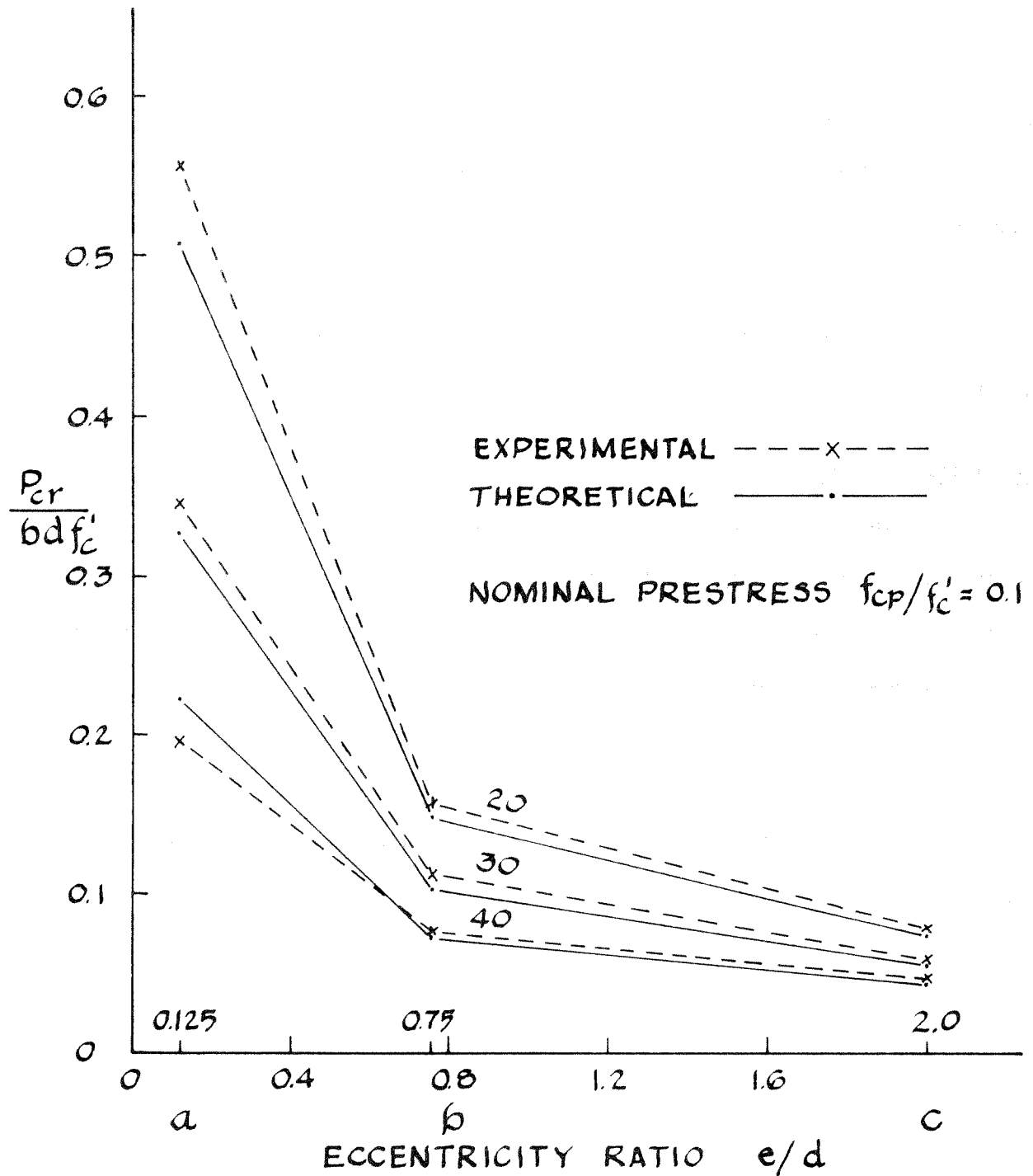


FIG. 31 EFFECT OF ECCENTRICITY ON P_{cr}

Similar relations exist at the higher prestress values, the curves for the three slenderness ratios being somewhat closer to each other.

3. Slenderness

Fig. 32 shows the variation of critical load with slenderness, for a nominal prestress ratio of 0.1. P_{cr} is seen to decrease almost linearly with increase in column length, the rate of decrease being largest for the smallest eccentricity. As in Fig. 31, the values for eccentricity "b" represent averages of duplicate columns.

The relations for the higher prestress values are similar to Fig. 32.

5.3 Material Failure Load

Table 12 presents experimental and theoretical values of the material failure loads P_f and their ratios. A histogram of the load ratios is shown in Fig. 33. The average ratio was 1.071 (range: 0.795-1.557) with a standard deviation of 0.129.

The high average ratio, due to low theoretical values, is probably caused by the assumed value of the maximum concrete strain ϵ_u , $\epsilon_u = 0.0060$. Since, in most columns, the load is already decreasing before material failure is reached, a lower ϵ_u will result in higher theoretical loads.

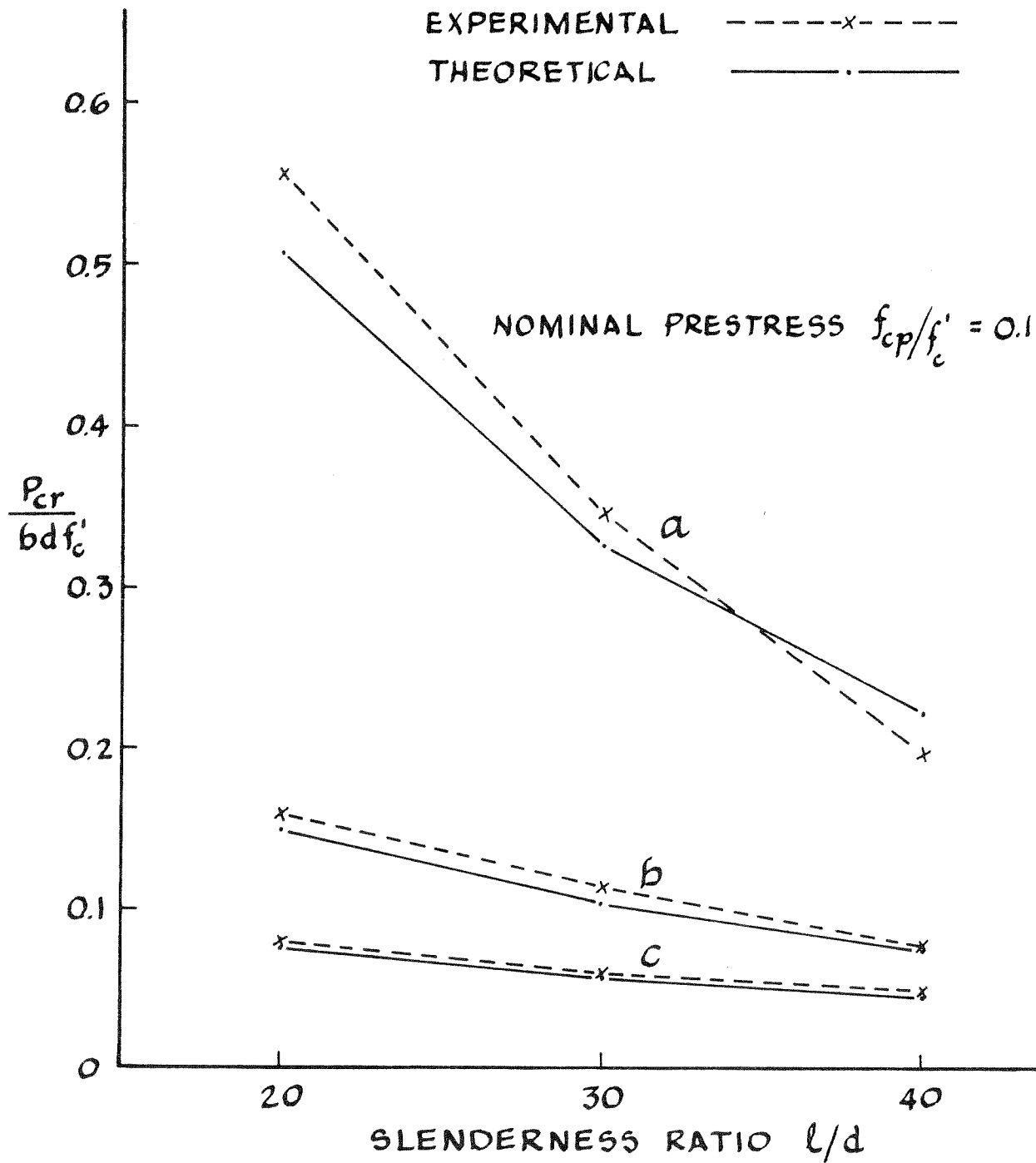


FIG. 32 EFFECT OF SLENDERNESS ON P_{cr}

Table 12. Comparison of P_f Loads

Column ^{*1}	Experimental P_f (lb)	Theoretical P_f (lb)	$(P_f)_{exp.}/(P_f)_{th}$
A ₁ 20c3	2,630	2,581	1.019
A ₁ 30a3	8,840	6,558	1.348
A ₁ 40b3 ^{*2}	2,830	2,523	1.122
A ₁ 20b5 ^{*2}	4,900	5,244	0.934
A ₂ 30c5	1,950	2,090	0.933
A ₂ 40a5 ^{*2}	4,730	3,911	1.209
B ₂ 20a1	18,820	12,084	1.557
B ₁ 30b1 ^{*2}	3,820	3,330	1.147
B ₁ 40c1	1,610	1,525	1.056
B ₁ 20b3 ^{*2}	4,800	5,244	0.915
B ₂ 30c3	1,960	2,063	0.950
B ₂ 40a3	4,000	3,632	1.101
C ₂ 20c1	2,690	2,572	1.046
C ₁ 30a1	7,570	6,121	1.237
C ₁ 40b1 ^{*2}	2,580	2,252	1.146
C ₁ 20a3	10,770	12,805	0.841
C ₂ 30b3 ^{*2}	3,440	3,595	0.957
C ₂ 40c3	1,570	1,616	0.972
D ₂ 20c5 ^{*2}	2,780	2,521	1.103
D ₁ 30b5 ^{*2}	4,350	3,756	1.158
D ₁ 40a5 ^{*2}	4,590	4,165	1.102
D ₁ 20b3 ^{*2}	5,200	5,244	0.992
D ₂ 30b3 ^{*2}	4,000	3,610	1.108
D ₂ 40b3 ^{*2}	2,600	2,476	1.050
E ₂ 20a5 ^{*2}	13,100	12,309	1.064
E ₁ 30b5	4,090	3,746	1.092
E ₁ 40c5 ^{*2}	1,840	1,696	1.085
E ₁ 20b1 ^{*2}	5,000	5,062	0.988
E ₂ 30c1	2,010	1,993	1.009
E ₂ 40a1 ^{*2}	3,240	4,073	0.795
F ₂ 20b1 ^{*2}	5,550	5,071	1.094
F ₁ 30b1 ^{*2}	3,610	3,316	1,089
F ₁ 40b1 ^{*2}	2,360	2,248	1.050
F ₁ 20b5 ^{*2}	5,180	5,234	0.990
F ₂ 30a5	8,500	6,989	1.216
F ₂ 40b5	2,780	2,589	1.074

^{*1} For details see Table 4

^{*2} Columns with duplicates

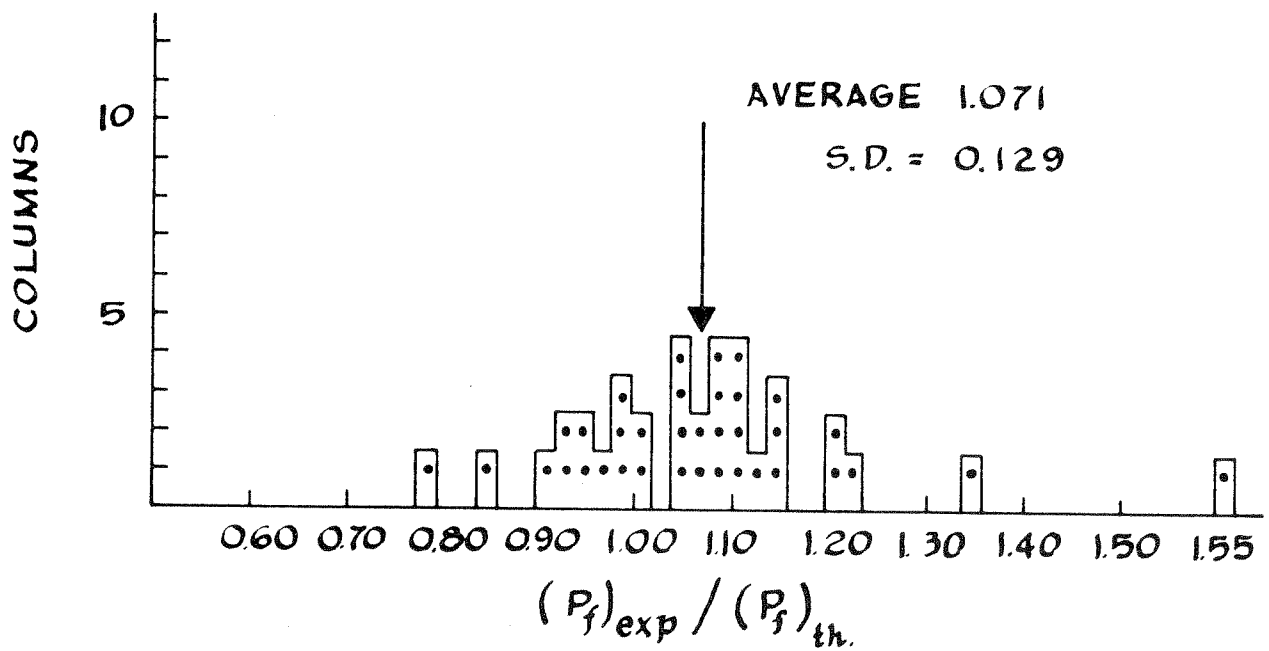


FIG. 33 HISTOGRAM OF P_f LOAD RATIOS

5.4 Maximum Compressive Strain at P_{cr}

The maximum compressive strains at column mid-height, under the critical load, experimental and theoretical, and their ratios, are given in Table 13. The experimental strains represent the average readings of gages 2 and 3 (see Fig. 12). All the strains are due to load only and exclude initial strains, caused by prestress and creep. A histogram of the strain ratios is shown in Fig. 34. The average ratio was 0.963 (range: 0.584-1.340) with a standard deviation of 0.189.

The comparison of strains is only fair. An analysis of variance revealed that the strain ratios are not significantly different, at 5% level, with respect to the parameters involved in the study. Local strains might be expected to show a larger experimental variation than load measurements.

5.5 Load Deformation Curves

There are three types of curves, containing comparisons between experimental and theoretical results, drawn by means of the computer and presented in Appendix A.

1. Load-Central Deflection Curves

Figs. A1-A9 show experimental and theoretical load-central deflection curves. The deflections plotted exclude initial deflections and are due to the load only.

The general agreement is good, extending over the full range of loading and including the post-critical region. In most cases the theoretical curve, based on the lower bound solution, is below the experimental results.

Table 13. Comparison of Maximum Compressive Strains at P_{cr}

Column*1	Maximum Compressive Strain at P_{cr} ($\times 10^{-4}$)		Strain Ratio Exp./Th.
	Experimental	Theoretical	
A ₁ 20c3	41.9	56.84	0.737
A ₁ 30a3*2	19.75	18.19	1.086
A ₁ 40b3*2	20.0	18.92	1.057
A ₁ 20b5	29.15	37.41	0.779
A ₂ 30c5*2	26.75	45.82	0.584
A ₂ 40a5	17.75	17.88	0.993
B ₂ 20a1*2	19.9	22.22	0.896
B ₁ 30b1	40.65	32.19	1.263
B ₁ 40c1*2	50.95	50.70	1.005
B ₁ 20b3	37.7	42.72	0.882
B ₂ 30c3	41.15	57.11	0.721
B ₂ 40a3	11.5	13.73	0.838
C ₁ 20c1	49.75	58.81	0.829
C ₁ 30a1*2	17.05	13.73	1.242
C ₁ 40b1	24.7	23.94	1.032
C ₁ 20a3*2	20.0	24.83	0.805
C ₂ 30b3	20.45	24.63	0.830
C ₂ 40c3	40.0	32.70	1.223
D ₂ 20c5*2	35.65	54.43	0.655
D ₁ 30c5*2	25.6	24.95	1.026
D ₁ 40a5*2	16.75	17.26	0.970
D ₁ 20b3*2	47.0	42.81	1.098
D ₂ 30b3*2	27.75	24.17	1.148
D ₂ 40b3	20.8	19.25	1.081
E ₁ 20a5*2	26.7	27.89	0.957
E ₁ 30b5	27.25	24.27	1.123
E ₁ 40c5*2	30.9	27.36	1.129
E ₁ 20b1	49.35	58.91	0.838
E ₂ 30c1	47.8	58.84	0.812
E ₂ 40a1*2	11.2	9.13	1.227
F ₂ 20b1*2	48.2	58.83	0.819
F ₁ 30b1*2	44.5	33.22	1.340
F ₁ 40b1*2	21.4	24.45	0.875
F ₁ 20b5	38.6	37.08	1.041
F ₂ 30a5	17.25	20.61	0.837
F ₂ 40b5	19.7	21.86	0.901

*1 For details see Table 4

*2 Columns with duplicates

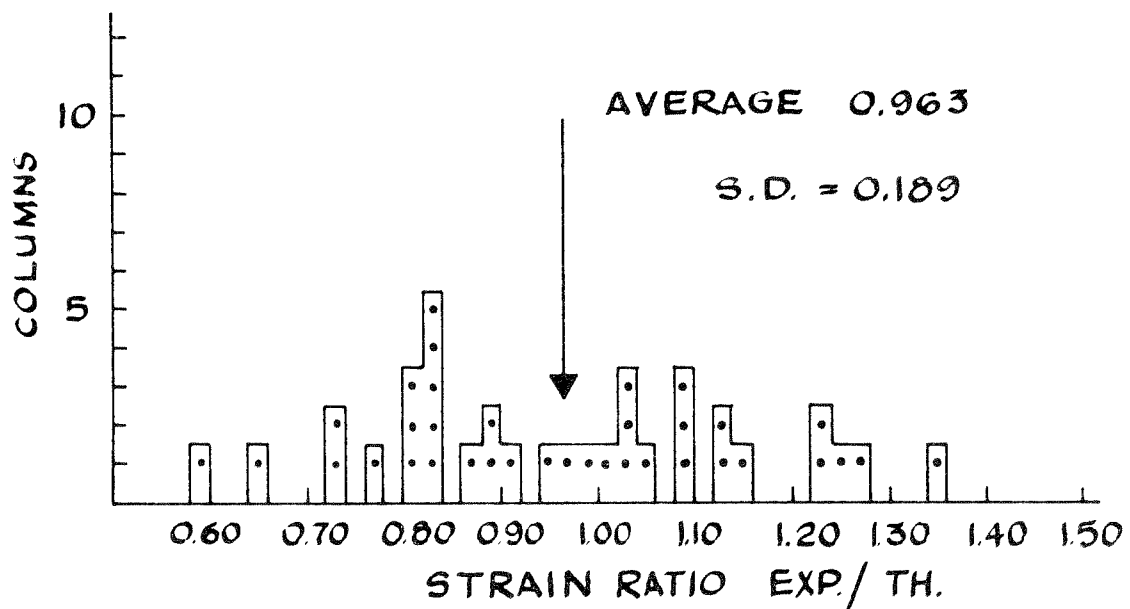


FIG. 34 HISTOGRAM OF STRAIN RATIOS (AT P_{cr})

This situation is sometimes reversed in the post-critical region. Most columns maintain a very high proportion of their maximum critical load, up to material failure. Columns of low eccentricity exhibit a more drastic reduction of load after the maximum is reached, at a much smaller deflection than that of ultimate load. This tendency increases with increase in slenderness. The effect of prestress, on columns of $l/d = 40$ and eccentricity "a", is shown in Fig. 35. It can be seen that, in addition to a decrease in maximum load, an increase in prestress has the effect of increasing the deflection at which the maximum load is reached. In the post-critical region the curves are very close to each other. The fractional drop in load, from the maximum, decreases with increase in prestress. The curves plotted in Fig. 35 are from theoretical results only. Note that they differ in their initial deflection.

2. Load-Central Strain Curves

These are shown in Figs. A10-A18. The curves exhibit, in general, very good agreement between experiment and theory, for tensile, compressive and mid-depth strains.

3. Deflected Shape Curves

Figs. A19-A27 show a distorted plot of experimental and theoretical deflected curves. While the agreement of initial shape is good, the curves at maximum load differ significantly, in some cases. The variability is not so much in the shape of the column as in the magnitude of deflections. It should be noted, however, that the comparisons are made not at the same load, but at the maximum load for each case, theoretical and experimental.

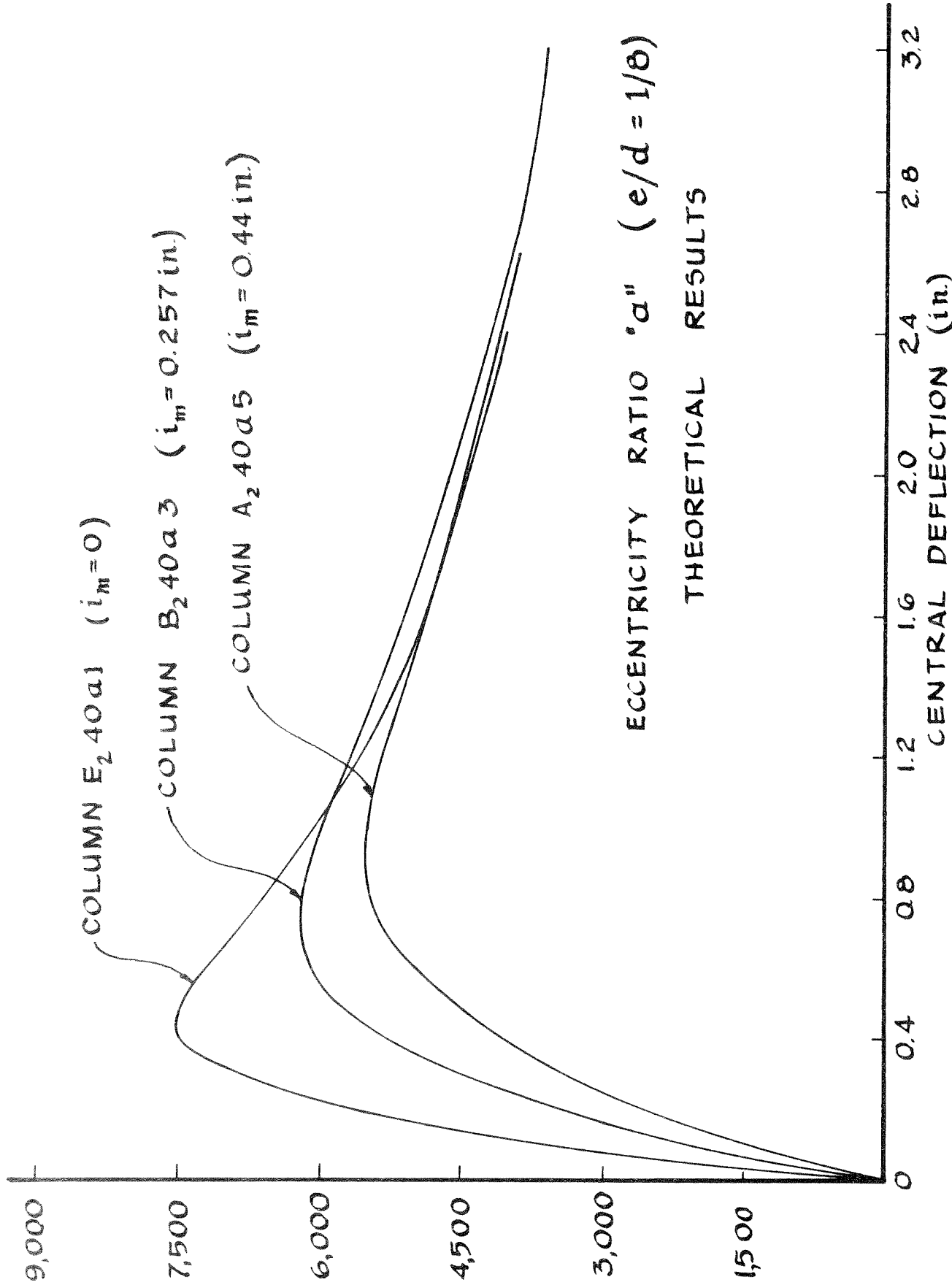


FIG. 35 EFFECT OF PRESTRESS ON LOAD-CENTRAL DEFLECTION CURVES

Chapter 6. ANALYSIS OF VARIABLES

In addition to the theoretical analysis of the columns described in Chapter 5, a total of 252 columns were analyzed, using the computer program, to investigate the effect of four types of variables. The variables investigated, and described in this chapter, are:

- (1) effect of concrete tensile strength
- (2) effect of initial curvature
- (3) effect of concrete compressive strength
- (4) effect of area of steel.

6.1 Effect of Concrete Tensile Strength

To investigate the effect of concrete tensile strength on the maximum critical load P_{cr} , the thirty-six columns, the analysis of which was presented in Chapter 5, were calculated again with $f_t=0$. It was considered interesting to investigate this aspect since most theoretical analyses, published in the past, neglect the concrete strength in tension.

Table 14 presents the results of the analysis, as well as the ratios of the maximum critical loads, with and without the contribution in tension.

The concrete tensile strength can be seen to have a negligible effect on P_{cr} . The average ratio of loads, in Table 14, is 1.004. However, the effect depends significantly on the values of the three parameters investigated. The average ratios for these parameters, neglecting the duplicates,

Table 14. Effect of Concrete Tensile Strength

Column ^{*1}	Theoretical Analysis		Ratio (P _{cr}) with/(P _{cr}) without
	P _{cr} with tension (lb)	P _{cr} without tension (lb)	
A ₁ 20c3	2,581 ^{*3}	2,581 ^{*3}	1.000
A ₁ 30a3	10,123	10,047	1.008
A ₁ 40b3 ^{*2}	3,042	3,029	1.004
A ₂ 20b5 ^{*2}	5,301	5,295	1.001
A ₂ 30c5 ^{*2}	2,093	2,092	1.000
A ₂ 40a5 ^{*2}	5,545	5,509	1.007
B ₁ 20a1 ^{*2}	17,123	17,019	1.006
B ₁ 30b1	3,465	3,464	1.000
B ₁ 40c1 ^{*2}	1,529	1,529	1.000
B ₂ 20b3	5,281	5,279	1.000
B ₂ 30c3	2,063 ^{*3}	2,062 ^{*3}	1.000
B ₂ 40a3	6,237 ^{*3}	6,165 ^{*3}	1.012
C ₁ 20c1	2,572 ^{*3}	2,572 ^{*3}	1.000
C ₁ 30a1 ^{*2}	11,022	10,841	1.017
C ₁ 40b1	2,499	2,497	1.001
C ₂ 20a3 ^{*2}	15,570	15,510	1.004
C ₂ 30b3	3,936	3,928	1.002
C ₂ 40c3	1,654 ^{*3}	1,653 ^{*3}	1.001
D ₁ 20c5 ^{*2}	2,521	2,520	1.000
D ₁ 30b5 ^{*2}	4,113	4,101	1.003
D ₁ 40a5 ^{*2}	6,098	6,058	1.007
D ₂ 20b3 ^{*2}	5,281	5,279	1.000
D ₂ 30b3 ^{*2}	3,960	3,952	1.002
D ₂ 40b3	2,937	2,926	1.004
E ₁ 20a5 ^{*2}	13,592	13,560	1.002
E ₁ 30b5	4,084	4,072	1.003
E ₁ 40c5 ^{*2}	1,774 ^{*3}	1,771 ^{*3}	1.002
E ₂ 20b1	5,062 ^{*3}	5,062 ^{*3}	1.000
E ₂ 30c1	1,993 ^{*3}	1,993 ^{*3}	1.000
E ₂ 40a1 ^{*2}	7,519 ^{*3}	7,262 ^{*3}	1.035
F ₁ 20b1 ^{*2}	5,071	5,071	1.000
F ₁ 30b1 ^{*2}	3,446	3,445	1.000
F ₁ 40b1 ^{*2}	2,492	2,489	1.001
F ₂ 20b5	5,288	5,282	1.001
F ₂ 30a5	9,331	9,286	1.005
F ₂ 40b5	2,989	2,978	1.004

*1 For details see Table 4

*2 Columns with duplicates

*3 Material failure

are shown in Table 15. The ratios, and effect of tension, increase with slenderness and decrease with eccentricity and prestress. Thus, the column with the maximum ratio of 1.035 is 40a1.

Table 15. Effect of Concrete Tensile Strength-Average Load Ratios

Slenderness l/d	Load Ratio ^{*1}	Eccentricity (e/d)	Load ^{*1} Ratio	Nominal Prestress f_{cp}/f'_c	Load ^{*1} Ratio
20	1.001	a(1/8)	1.011	0.1	1.007
30	1.004	b(3/4)	1.002	0.3	1.003
40	1.007	c(2)	1.000	0.5	1.003

*1 (P_{cr}) with tension / (P_{cr}) without tension

6.2 Effect of Initial Curvature

The effect of the column initial shape, curvature and deflection, on the maximum critical load P_{cr} , was investigated by the analysis of eighty-one columns. Each of the twenty-seven unique combinations of slenderness, eccentricity and prestress, at the three levels used in the experimental study, was analyzed with three values of initial central deflection, representing 0, 0.25% and 0.5% of the column length. An initial circular shape was assumed for the columns. The values used in the analysis were the same as in Chapter 5, except the initial central deflections. Also, the ϵ_{pr} strains used were the same as before (Table 3), average values of ϵ_{14} were used (Table 5, (c)) and the ϵ_{23} strains were calculated, for the required deflections, from Equation (4.20).

The results of the analyses are presented, in terms of load ratios of initially deflected to initially straight columns, in Figs. 36, 37 and 38 for nominal prestress ratios of 0.1, 0.3 and 0.5 respectively. It can be seen that the load ratios vary almost linearly with initial central deflection. The detrimental effect of initial curvature increases with longer columns, shorter eccentricities and smaller prestress. For the largest initial deflection considered, 0.5% of length, the maximum drop of load, for column 40a1, is 36%. It is interesting to note that for columns 20c1, 30c1, 20c3, 30c3 and 20c5, there is an increase in load with increase in initial deflection. All these columns reach their maximum load with material failure, governed by $\epsilon_4 = \epsilon_u$. With the assumptions made in the analysis, an increased initial deflection leads to a lower initial strain ϵ_4 , on the compressive face, and therefore to a higher load capacity, when material failure is governing the maximum load.

Some of the results are plotted again in Fig. 39, for the constant slenderness of $l/d = 30$. It can be seen that the largest influence is eccentricity. The effect of prestress also increases as the eccentricity becomes smaller.

6.3 Effect of Concrete Compressive Strength

Twenty-seven columns, representing unique combinations of the three variables of slenderness, eccentricity, and prestress, were analyzed with the same input data as in Chapter 5, except each with two different values of f'_c , namely 3,500 and 7,500 psi. The values of $f'_t = 0.1 f'_c$ were

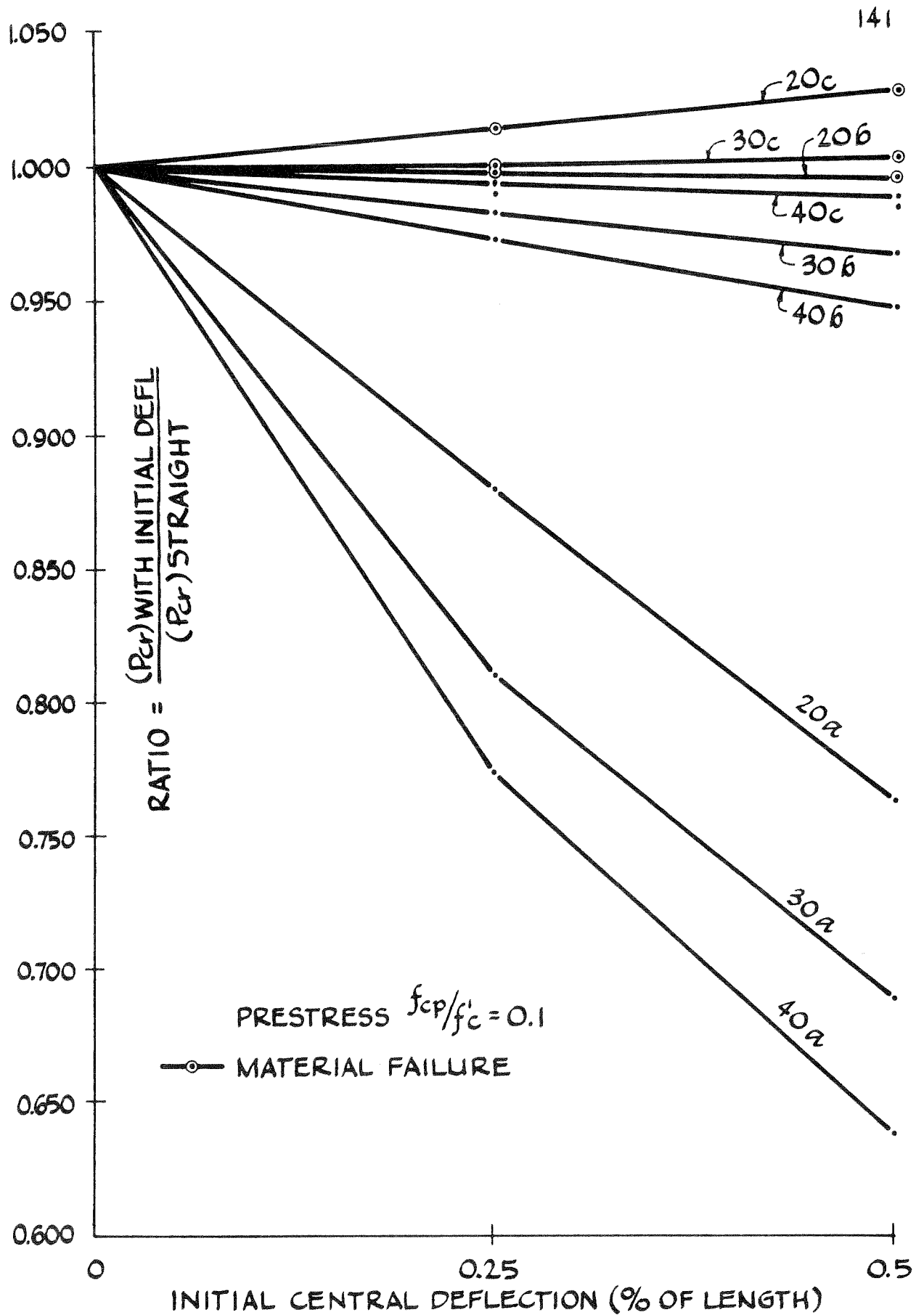


FIG. 36 EFFECT OF INITIAL CURVATURE
 $(f_{cp}/f'_c = 0.1)$

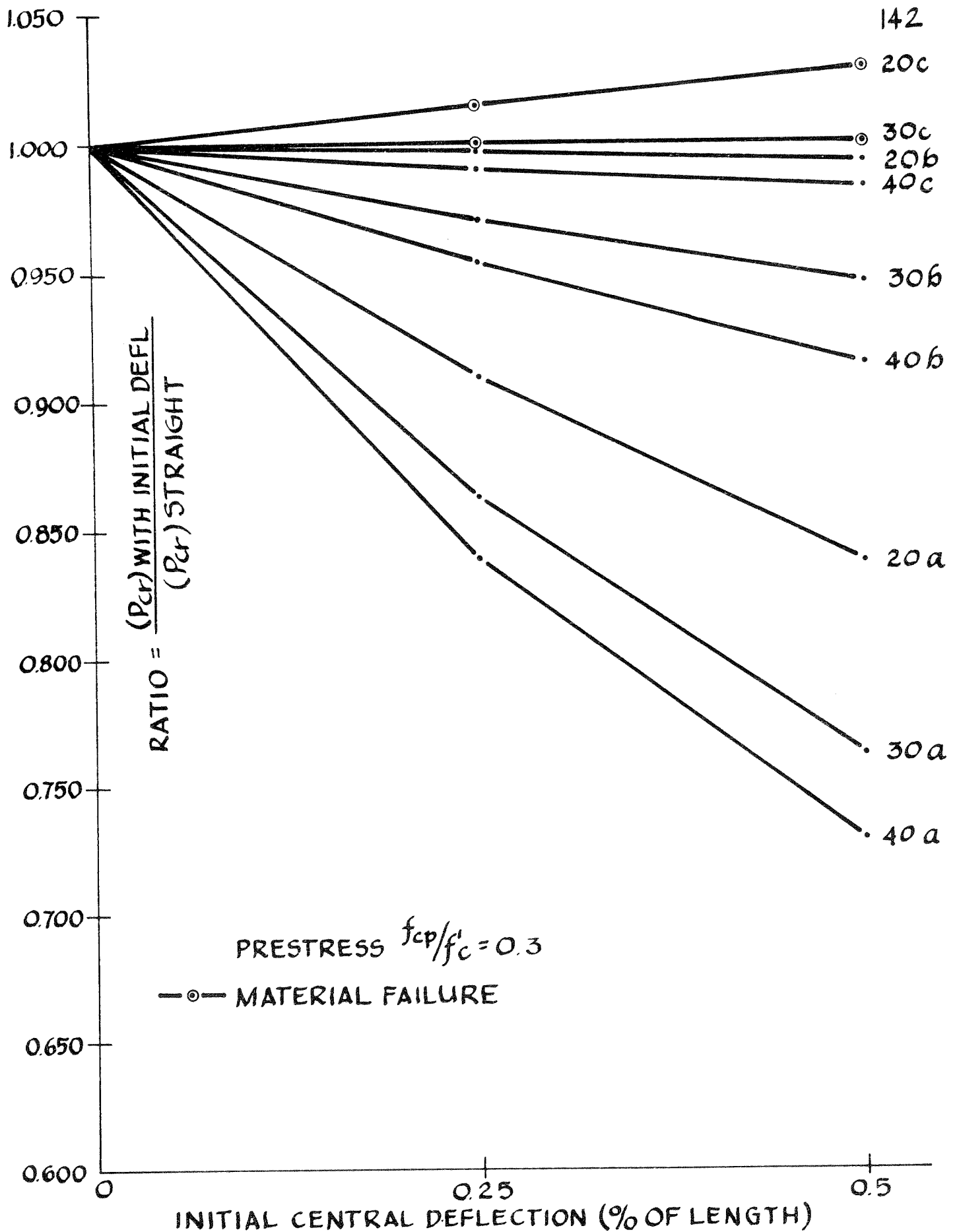


FIG. 37 EFFECT OF INITIAL CURVATURE
 ($f_{cp}/f'_c = 0.3$)

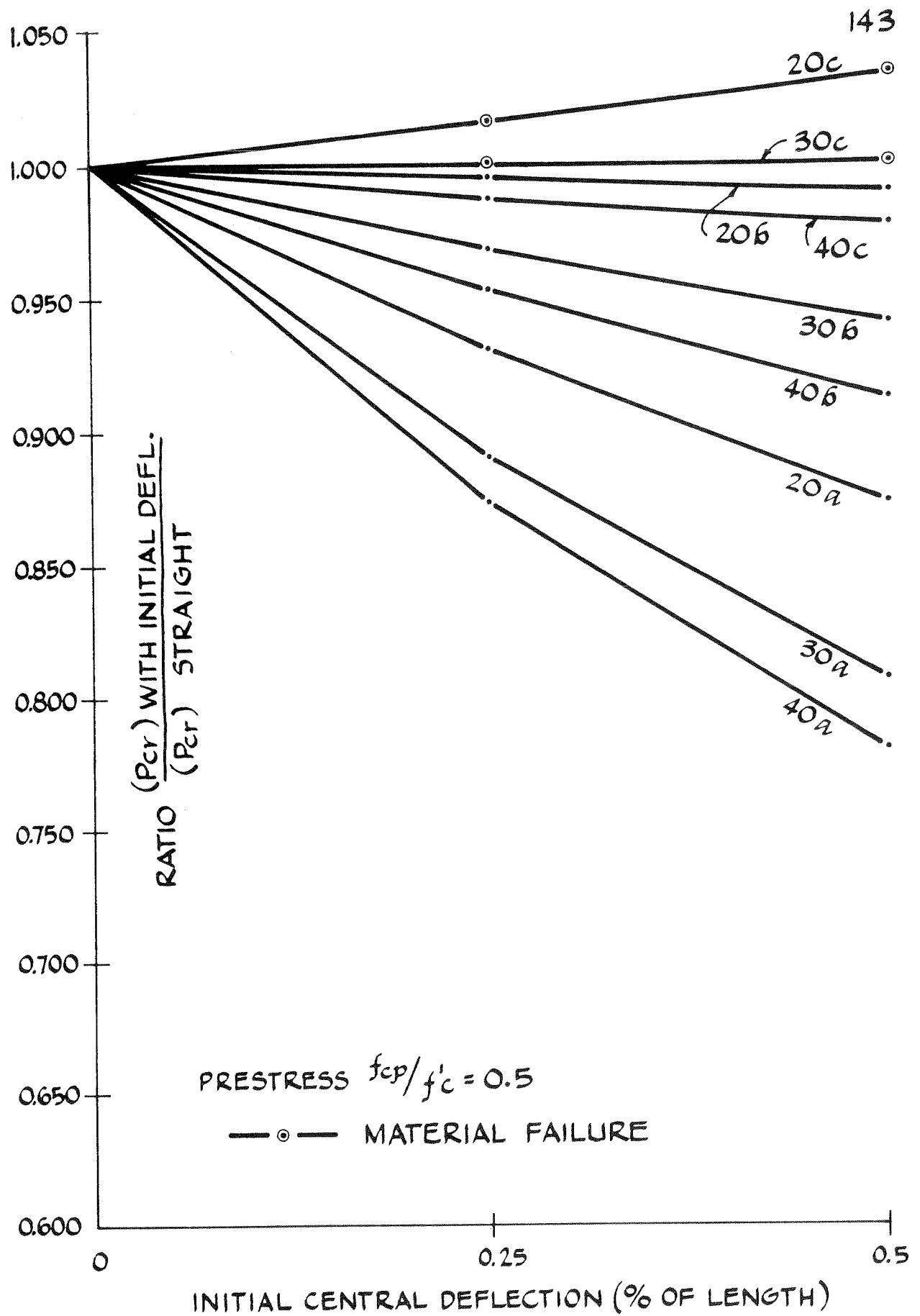


FIG. 38 EFFECT OF INITIAL CURVATURE
($f_{cp}/f'_c = 0.5$)

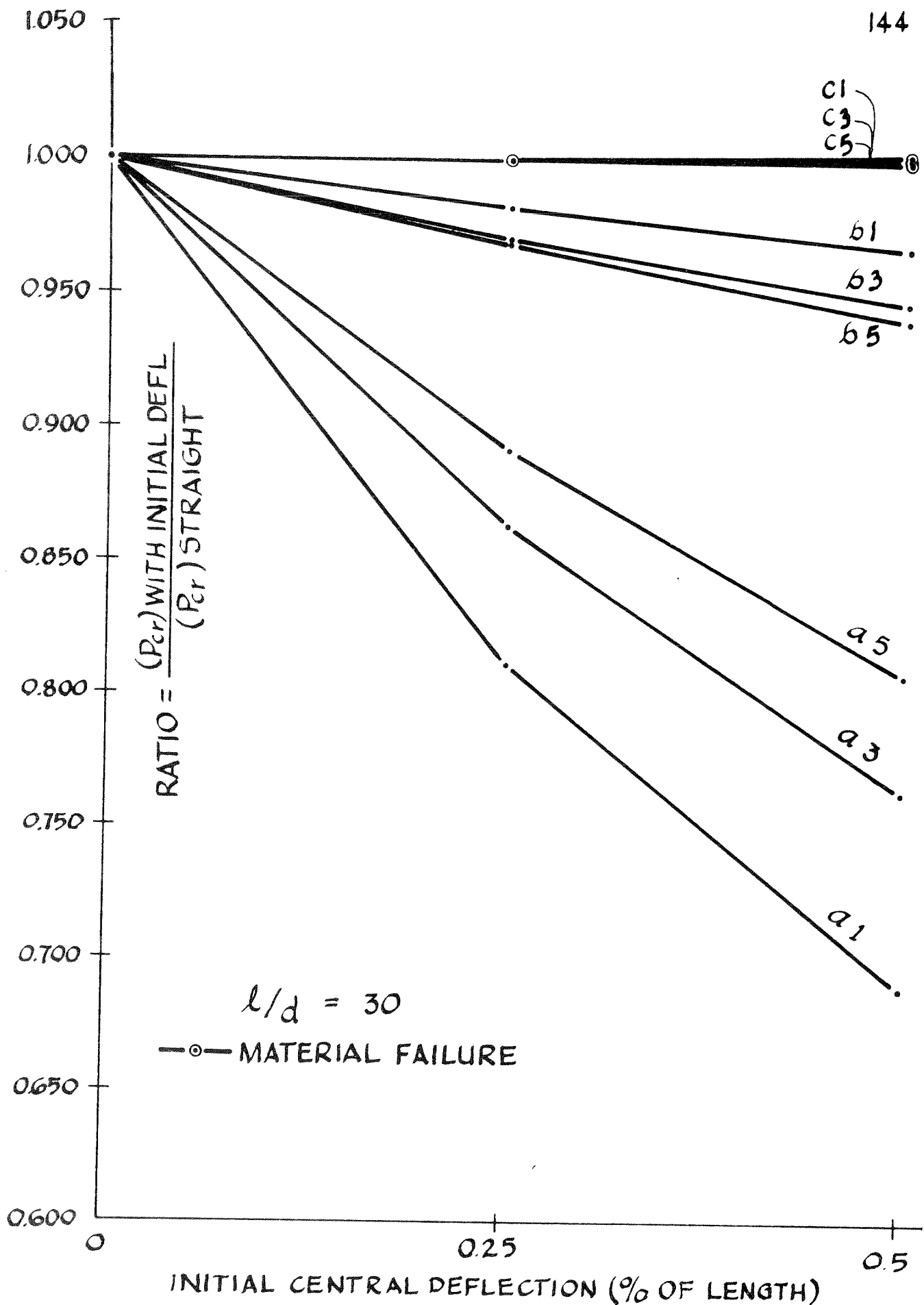


FIG.39 EFFECT OF INITIAL CURVATURE
($l/d = 30$)

changed accordingly. The prestress and initial strains ϵ_{pr} , ϵ_{14} , and ϵ_{23} were kept at the observed experimental values for each column. Since the experimental columns had an average $f'_c = 5,585$ psi, this assumption implies the same creep from release to testing, irrespective of f'_c , and might be in error.

The results of the analysis are presented in Table 16, where the P_{cr} loads are given for the three values of f'_c , and also the load ratios with respect to the load for the experimental $f'_c = 5,585$ psi. Increase in f'_c is seen to decrease the number of columns that reach their maximum at material failure. Thus, there are 10, 6, and 2 material failures with increasing compressive strength. The compressive strengths of 3,500 and 7,500 psi represent -37.3% and +34.3% of the experimental $f'_c = 5,585$ psi. The P_{cr} loads, however, were affected to a smaller degree, the overall average being -27% and +19.2% for the low and high strength respectively.

Table 17 shows the average load ratios for the three variables investigated. The effect of compressive strength is greatest for columns of low slenderness, low eccentricity and high prestress. Thus, column 20a5 (Table 16) exhibited changes in P_{cr} of -43.4% and +38.1 for the low and high strength concrete respectively. For this column, the P_{cr} load ratios are larger than the respective ratios of f'_c .

Table 16. Effect of Concrete Compressive Strength

Column ^{*1}	Theoretical P_{cr}			Load Ratios	
	$f'_c=3,500$ psi	$f'_c=5,585$ psi	$f'_c=7,500$ psi	$(P_{cr})_{3,500/}$	$(P_{cr})_{7,500/}$
				$(P_{cr})_{5,585}$	$(P_{cr})_{5,585}$
A _{20c3}	1,978 ^{*2}	2,581 ^{*2}	3,015 ^{*2}	0.766	1.168
A _{130a3}	6,830	10,123	12,473	0.675	1.232
A _{140b3}	2,375 ^{*2}	3,042	3,421	0.781	1.125
A _{120b5}	3,701 ^{*2}	5,301	6,528	0.698	1.231
A _{230c5}	1,526 ^{*2}	2,093	2,491	0.729	1.190
A _{240a5}	3,437	5,545	6,812	0.620	1.228
B _{220a1}	12,048	17,123	21,274	0.704	1.242
B _{130b1}	2,803	3,465	3,923	0.809	1.132
B _{140c1}	1,265 ^{*2}	1,529	1,720	0.827	1.125
B _{220b3}	3,999 ^{*2}	5,281 ^{*2}	6,258	0.757	1.185
B _{230c3}	1,621 ^{*2}	2,063 ^{*2}	2,378	0.786	1.153
B _{240a3}	4,577 ^{*2}	6,237 ^{*2}	7,414 ^{*2}	0.734	1.189
C _{220c1}	2,059 ^{*2}	2,572 ^{*2}	2,958 ^{*2}	0.801	1.150
C _{130a1}	8,299	11,022	13,299	0.753	1.207
C _{140b1}	2,105	2,499	2,758	0.842	1.104
C _{120a3}	9,900	15,570	20,128	0.636	1.293
C _{230b3}	2,996	3,936	4,513	0.761	1.147
C _{240c3}	1,301 ^{*2}	1,654 ^{*2}	1,881	0.787	1.137
D _{120c5}	1,762 ^{*2}	2,521 ^{*2}	3,029	0.699	1.202
D _{130b5}	2,690	4,113	4,979	0.654	1.211
E _{120a5}	7,697 ^{*2}	13,592	18,773	0.566	1.381
E _{140c5}	1,237 ^{*2}	1,774 ^{*2}	2,099	0.697	1.183
E _{120b1}	4,052 ^{*2}	5,062 ^{*2}	5,826	0.800	1.151
E _{230c1}	1,624 ^{*2}	1,993 ^{*2}	2,255	0.815	1.131
E _{240a1}	5,821	7,519	9,022	0.774	1.200
F _{230a5}	5,248	9,331	12,139	0.562	1.301
F _{240b5}	2,007	2,989	3,513	0.671	1.175

*1 For details see Table 4

*2 Material failure

Table 17. Effect of Concrete Compressive Strength-Average Load Ratios

Variable	Average Load Ratio ^{*1}	
	$f'_c=3,500$ psi	$f'_c=7,500$ psi
(a) <u>Slenderness</u> (ℓ/d)		
20	0.714	1.223
30	0.727	1.189
40	0.748	1.163
(b) <u>Eccentricity</u> (e/d)		
a (1/8)	0.669	1.253
b (3/4)	0.753	1.162
c (2)	0.767	1.160
(c) <u>Prestress</u> (f_{cp}/f'_c)		
0.1	0.792	1.160
0.3	0.743	1.181
0.5	0.655	1.234

$$*1 \frac{(P_{cr})_{f'_c}}{(P_{cr})_{5,585}}$$

6.4 Effect of Area of Steel

All the columns involved in the experimental work described earlier had the same steel area ($A_s/A_c = 2.05\%$). The prestress was varied by changing the stress in the steel wires. To investigate the effect of variation of steel area on the maximum load P_{cr} , eighty-one additional columns were analyzed. Each of the twenty-seven unique combinations of

slenderness, eccentricity, and prestress ratio, were used three times with varying steel stresses, and thus different steel areas. All columns were assumed initially straight and the remaining details of cross-section, material properties and program parameters were the same as in Chapter 5. The three steel stresses used, assumed after all losses before testing, were 50, 100, and 150 ksi, representing approximately 20, 40 and 60% of the ultimate steel stress of 250.9 ksi. The prestress ratios, 0.1, 0.3, and 0.5, were also assumed to exist at testing and the required steel areas calculated from Equation (3.3). The prestress strain ϵ_{pr} was calculated from the steel stress, concrete prestress and concrete stress-strain curve.

The results of the analysis are presented in Figs. 40, 41, and 42, for the prestress ratios of 0.1, 0.3, and 0.5, respectively. In all cases, for a given prestress ratio, an increase in the steel area results in a higher maximum P_{cr} . The change in maximum load increases for lower slenderness, lower eccentricity and higher prestress ratio. For the column 20a5, P_{cr} increased from 11,946 lb. with $A_s = 0.0564$ sq. in. (two wires) to 18,213 lb. with $A_s = 0.1692$ sq. in.

It is interesting to note that the relation of the maximum load P_{cr} and prestress ratio f_{cp}/f'_c depends on the steel stress. Fig. 43 shows the results of column 20a, obtained from Figs. 40, 41, and 42, for three steel stress values. Each point in Fig. 43 represents a different area of steel. The maximum load decreases with increase in prestress ratio, for high values of steel stress, and increases for the low stress. At a steel stress of about 75 ksi, P_{cr} is approximately 15,600 lb., irrespective of the prestress ratio.

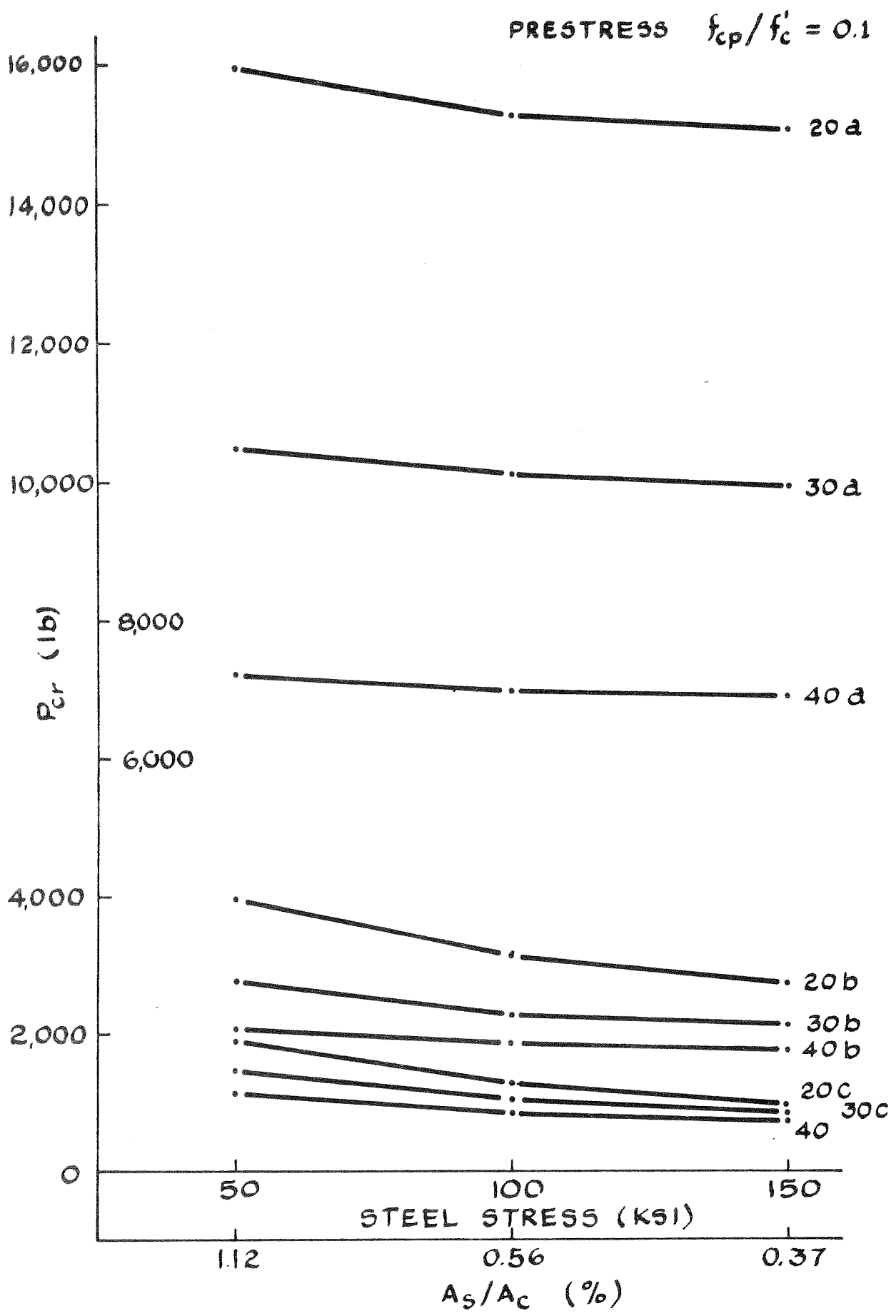


FIG. 40 EFFECT OF AREA OF STEEL

($f_{cp}/f'_c = 0.1$)

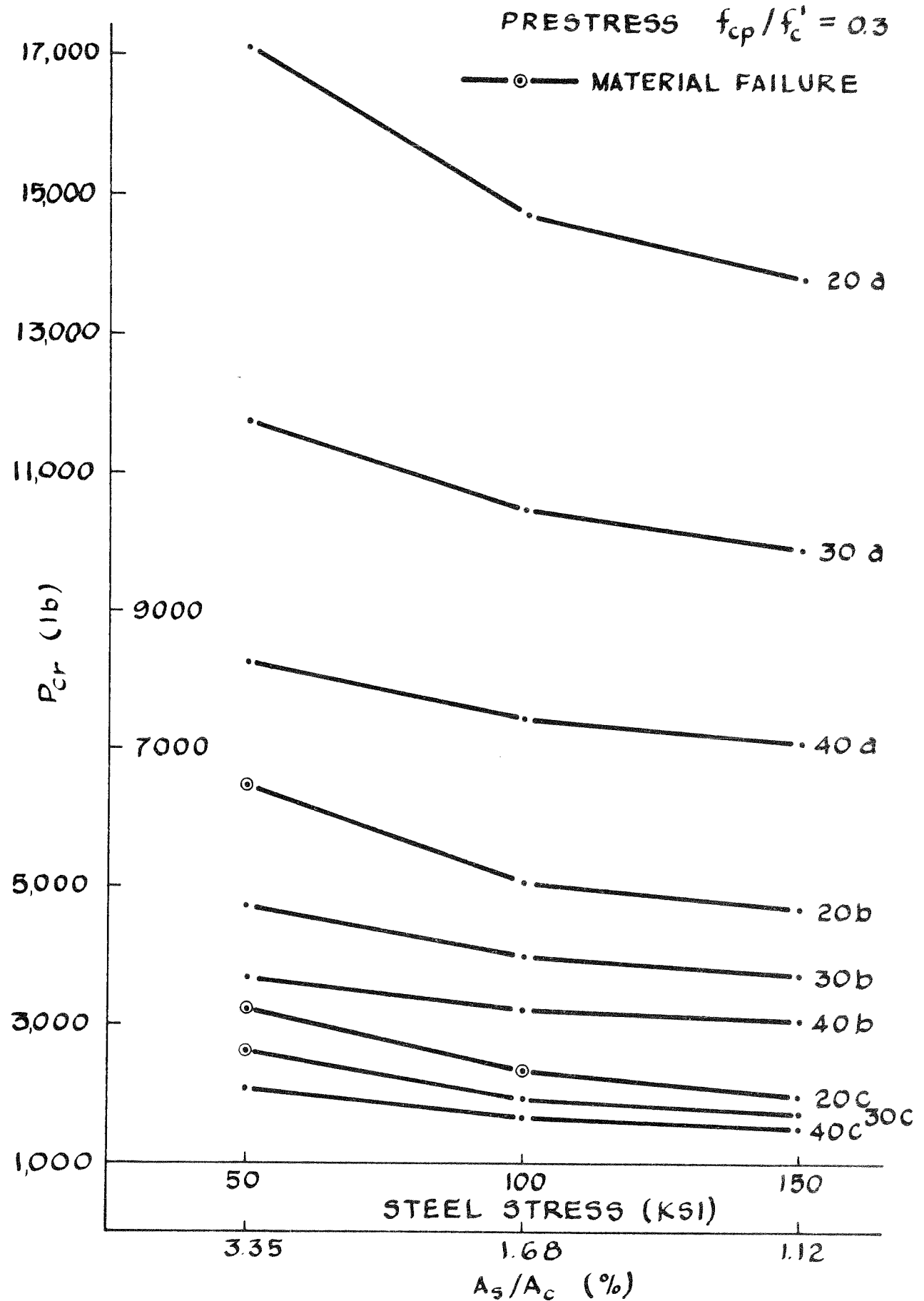


FIG. 41 EFFECT OF AREA OF STEEL
($f_{cp}/f'_c = 0.3$)

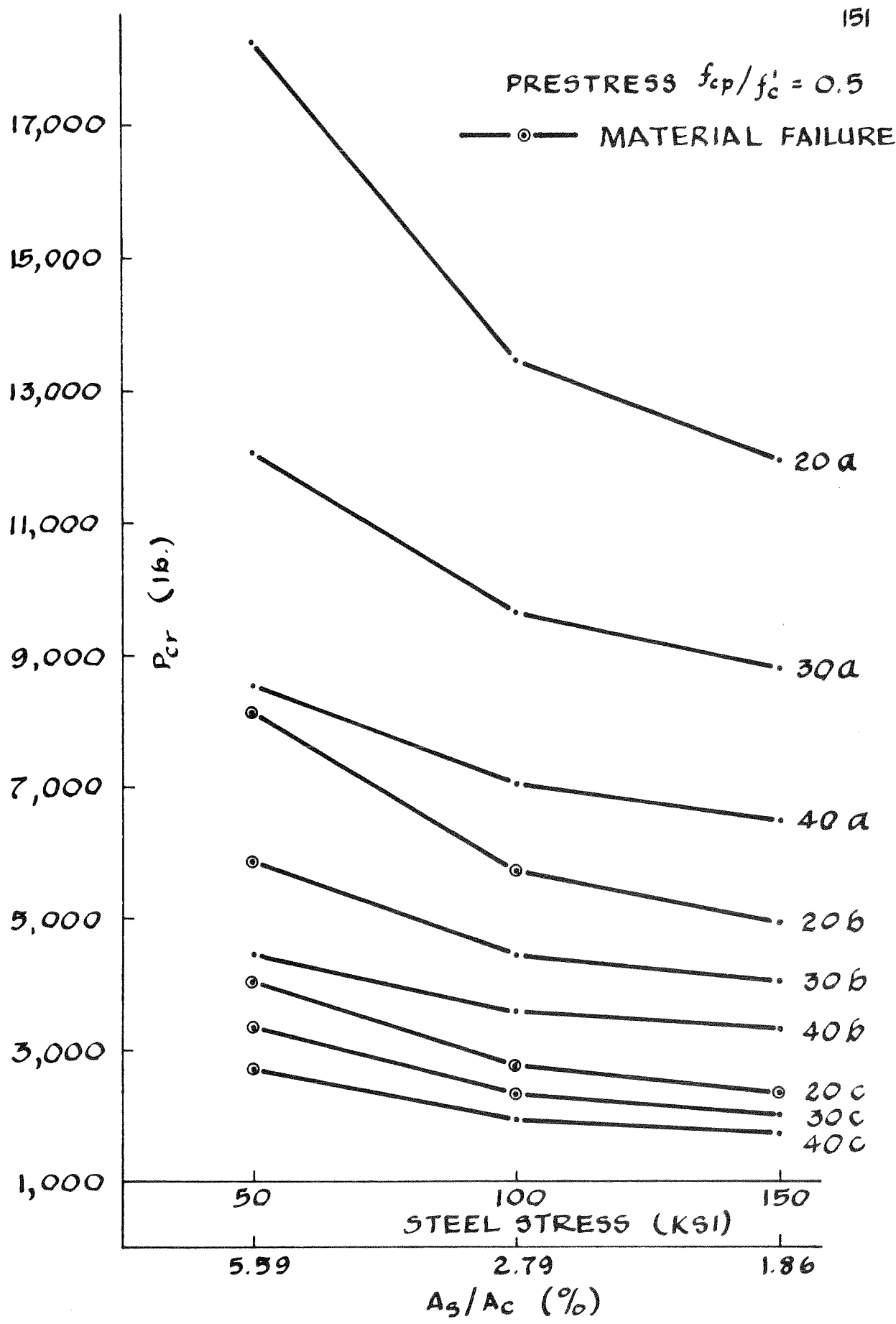


FIG. 42 EFFECT OF AREA OF STEEL
 ($f_{cp}/f'_c = 0.5$)

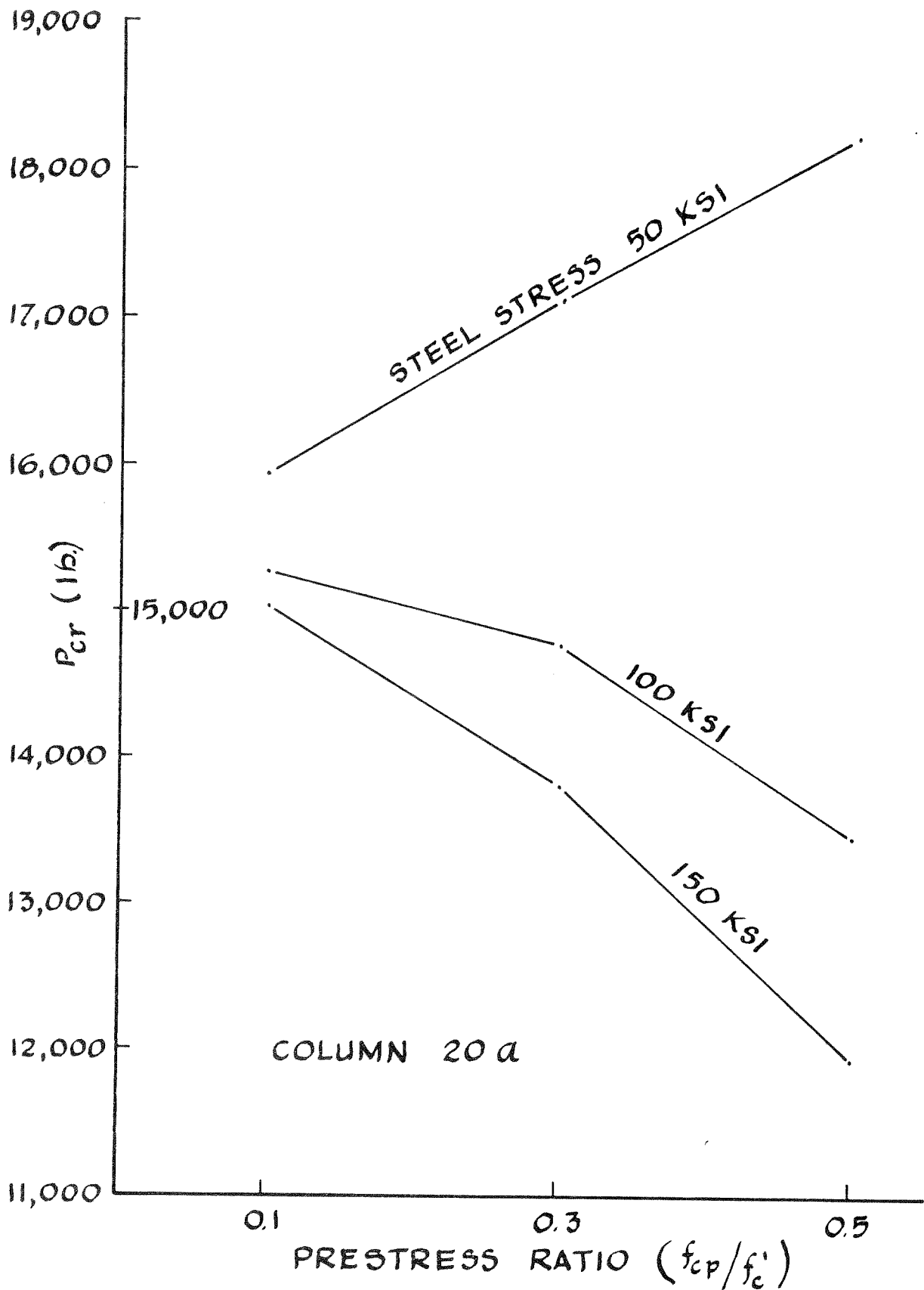


FIG. 43 EFFECT OF PRESTRESS RATIO
(COLUMN 20 a)

Chapter 7. SUMMARY AND CONCLUSIONS

1. An experimental investigation of the strength and behavior of eccentrically loaded, prestressed concrete columns, has been described. Thirty-six columns were tested and the variables of slenderness, eccentricity and prestress, each at three levels, were investigated. A technique of end anchorage was developed to ensure full prestress at the column ends. The testing was performed in a special frame which enabled the investigation of post-buckling behavior, by applying increments of axial shortening and measuring the resulting loads.

2. An analytical method was developed, based on the cotangency criterion and using finite elements and numerical computer techniques. The calculation of the loads under applied, increasing, deformations is shown to be a powerful technique to investigate the full range of loading, including post-buckling.

3. Good general agreement was shown between the experimental results and theory, over the full range of the variables investigated. The average ratio of maximum critical loads (P_{cr}), experimental/theoretical, was 1.018 with a standard deviation of 0.065. Material failure loads, which occurred mostly after the maximum critical loads, had an average ratio of 1.071 and standard deviation of 0.129. The maximum compressive strains at critical loads had an average ratio of 0.963 and standard deviation of 0.189. Statistical analyses of variance showed no significant bias with respect to any of the parameters investigated. Good agreement was also obtained between experimental and theoretical load deformation curves.

4. The effect of prestress on P_{cr} depends mainly on the eccentricity. For low eccentricities, ($e/d = 1/8$), a maximum P_{cr} was reached at low prestress ratios of about 0.1. For medium eccentricity ($e/d = 3/4$), a maximum P_{cr} was observed in the region of $f_{cp}/f'_c = 0.3$ to 0.35, the least benefit of prestressing being for shorter columns. For the largest eccentricity, $e/d = 2$, prestress had no effect on the shorter columns; $l/d = 20$, while the longer columns showed continued increase of P_{cr} with prestress. With increase in eccentricity and slenderness the critical loads decreased, the maximum effect being on shorter columns and columns with low eccentricity respectively.

5. The computer program, developed to perform the theoretical analysis, proved a versatile tool for the analysis of further variables.

(a) The concrete tensile strength was shown to have a negligible overall effect on P_{cr} , the maximum influence being on long columns with low eccentricity and prestress.

(b) Changes in initial curvature had significant effects on P_{cr} . The detrimental effect of increased initial deflections increases with increase in slenderness and decrease of eccentricity and prestress.

(c) Increasing the concrete compressive strength was shown to be more effective in increasing the P_{cr} loads for shorter columns with smaller eccentricities and higher prestress.

(d) In all cases, for a given prestress ratio, an increase in the steel area resulted in a higher P_{cr} . The change in P_{cr}

is greater for lower slenderness, lower eccentricity and higher prestress ratio. For some columns, the variation of P_{cr} with prestress ratio, with the same steel stress but varying steel areas, depends significantly on the level of the steel stress.

6. Future theoretical work should extend the analytical approach presented in this thesis to columns with end restraints, time dependent load and material characteristics, and eventually to the analysis of structures with prestressed beams and columns. The availability of the post-buckling behavior should be utilized for the analysis of the prestressed column as part of an indeterminate structure.

7. Future experimental work is required to determine in a more direct manner the stress-strain relation of concrete, under conditions similar to those in the test specimens, and particularly accounting for the previous history of creep under prestress from release to testing. Tests are also needed on eccentrically-prestressed columns, prestressed columns tested in double curvature, columns restrained elastically, and as parts of structural frames, in which the restraint is nonlinear.

REFERENCES

1. Shaw, F.S., 1955, "Elastic Instability," Notes of Extension Course Lectures delivered at the University of Melbourne.
2. Euler, L., 1759, "Sur la Force des Colonnes," Memoires de l'Academie Royale des Sciences et Belles Lettres de Berlin, Vol. 13, 1759, pp. 252-282 (submitted 1757).
3. Van den Broek, J.A., 1947, "Euler's Classic Paper 'On the Strength of Columns' ", American Journal of Physics, July-Aug. 1947, p. 309.
4. Young, T., 1807, "Course of Lectures on Natural Philosophy," Vol. 1, 1807.
5. Salmon, E.H., 1921, "Columns," London, 1921.
6. Considere A., 1889, "Résistance des pièces comprimées," Congrès International de Procédés de Construction, Exposition Univ. Int. de 1889, Vol. 3, Paris, 1889, p. 371.
7. Engesser, F., 1889, "Ueber die Knickfestigkeit gerader stäbe," Zeitschrift d. Arch.-u. Ing-Ver. Zu Hannover, Vol. 35, Hannover, 1889, p. 455.
8. Karman, T.V., 1910, "Untersuchungen über Knickfestigkeit," Mitteilungen über Forschungsarbeiten auf dem Gebiete des Ingenieurwesens, No. 81, Berlin, 1910.
9. Shanley, F.R., 1946, "The Column Paradox," Journal of the Aeronautical Sciences, Vol. 13, No. 5, December 1946, p. 678.
10. Shanley, F.R., 1947, "Inelastic Column Theory," Journal of the Aeronautical Sciences, Vol. 14, No. 5, May 1947, pp. 261-267. (Including discussion by T. von Karman).
11. Johnston, B.G., 1961, "Buckling Behavior Above the Tangent Modulus Load," Journal, Eng. Mech. Div., Proc. ASCE, Vol. 87, No. EM6, December 1961.
12. Chwalla, E., 1934, "Theorie des aussermittig gedrückten Stabes aus Baustahl," Der Stahlbau, Vol. 7, Berlin, 1934, No. 21, pp. 161-165, No. 22, pp. 173-176, No. 23, pp. 180-184.

13. Westergaard, H.M. and Osgood, W.R., 1928, "Strength of Steel Columns," Trans. of the American Society of Mechanical Engineers, Vol. 51, 1928, pp. 65-80.
14. Hoff, N.J., 1954, "Buckling and Stability," Journal, Royal Aeronautics Society, Vol. 58, Aero Reprint No. 123, January 1954.
15. Bleich, F., 1951, "Buckling Strength of Metal Structures," McGraw-Hill, New York, 1951.
16. Timoshenko, S.P., and Gere, J.M., 1961, "Theory of Elastic Stability," McGraw-Hill, New York, 1961.
17. Richard, F.E., 1933, "Reinforced Concrete Column Investigation, Tentative Final Report," Chairman's Report A.C.I. Committee 105, Journal Amer. Concr. Inst., Paper 29-12, February 1933.
18. Thomas, F.G., 1938, "Studies in R.C. VI - Strength and Deformation of Reinforced Concrete Columns under Combined Direct Stress and Bending," The Building Research Board (England) Technical Paper 23, 1938.
19. Richart, F.E., Druffin, J.O., Olsen, T.A., and Hectman, R.H., 1947, "The Effect of Eccentric Loading, Protective Shells, Slenderness Ratio and Other Variables on Reinforced Concrete Columns," Univ. of Illinois Eng. Expt. Station Bull. No. 368, 1947.
20. Andersen, P., 1941, "The Resistance to Combined Flexure and Compression of Square Concrete Sections," Univ. of Minnesota Eng. Exp. Station Technical Paper No. 29, 1941.
21. Hognestad, E., 1951, "A Study of Combined Bending and Axial Load in Reinforced Concrete Members," Univ. of Illinois Eng. Expt. Station Bull.No. 399, 1951.
22. A.S.C.E. - A.C.I. Joint Committee, 1955, "Report on Ultimate Strength Design," Proc. A.S.C.E. Paper 809, October 1955.
23. Baumann, O., 1934, "Die Knickung der Eisenbeton-Säulen," Eidg. Materialprüfungsanstalt an der E.T.H. in Zürich, Bericht, No. 89, Zürich, 1934.
24. Broms, B., and Viest, I.M., 1958, "Ultimate Strength Analysis of Long Hinged Reinforced Concrete Columns," Proc. A.S.C.E. Str. Div. ST 1, Vol. 84, Paper 1510, January 1958.

25. Viest, I.M., and Broms, B., 1958, "Ultimate Strength Analysis of Long Restrained Reinforced Concrete Columns," Proc. A.S.C.E. Str. Div., ST3, Vol. 84, Paper 1635, May 1958.
26. Thomas, F.G., 1939, "Studies in Reinforced Concrete VII - The Strength of Long Reinforced Concrete Columns in Short Period Tests to Destruction," D.S.I.R., Building Research Technical Paper No. 24, London, 1939.
27. Hanson, R., and Rosenström, S., 1947, "Tryckförsök med slanka betongpelare," Betong, Vol. 32, No. 3, Stockholm, 1947, pp. 247-262.
28. Ramboll, B.J., 1951, "Reinforced Concrete Columns," Teknisk Förlag, Copenhagen, 1951.
29. Ernst, G.C., Hromadik, J.J., and Riveland, A.R., 1953, "Inelastic Buckling of Plain and Reinforced Concrete Columns, Plates and Shells," Univ. of Nebraska Eng. Exp. Station Bulletin No. 3, Lincoln, 1953.
30. Gehler, W. and Hütter, A., 1954, "Knickversuche mit Stahebetonsäulen," Deutscher Ausschuss für Stahlbeton, No. 113, Berlin, 1954.
31. Pfrang, E.O., and Siess, C.P., 1961, "Analytical Study of the Behavior of Long Restrained Reinforced Concrete Columns Subjected to Eccentric Loads," Univ. of Illinois, Civil Eng. Studies, Structural Research Series No. 214, June 1961.
32. Chang, W.F. and Ferguson, P.M., 1963, "Long Hinged Reinforced Concrete Columns," Journal A.C.I., V. 60, Paper 60-1, January 1963.
33. Holley, M.J. Jr., and Mauch, S., 1963, Discussion of the Paper by Chang and Ferguson (Ref. 32), Jour. A.C.I., V. 60, September 1963.
34. Breen, J.E., and Ferguson, P.M., 1964, "The Restrained Long Concrete Column as a Part of a Rectangular Frame," Journal A.C.I., V. 61, No. 5, May 1964.
35. Breen, J.E., 1965, "Computer Use in Studies of Frames with Long Columns," Flexural Mechanics of Reinforced Concrete, A.S.C.E. - A.C.I., 1965, pp. 535-556.
36. Hall, A.S., 1961, "Buckling of Prestressed Columns," Symposium on Prestressed Concrete, Cement and Concrete Association of Australia, Sydney, August 1961.

37. Breckenridge, R.A., 1953, "A Study of the Characteristics of Prestressed Concrete Columns," Univ. of Southern California Eng. Center, Report 18-6, April 1953.
38. _____, 1952, "Spectacular Venezuelan Concrete Arch Bridge," Engineering News-Record, 149: 28-32, September 11, 1952, pp. 28-32.
39. Marcel, F., 1951, "Problem de Precontrainte de Pierre Naturelle," Int. Congress of Prestressed Concrete, Ghent, 1951, pp. B14-1-B14-14.
40. _____, 1949, "Prestressed Concrete Columns at Newport, Monmouthshire," Concrete and Coustructional Engineering, 44:289-92, September 1949.
41. Brewster, F.R., 1949, "Concrete Building Columns Prestressed," Engineering News-Record, 143:34-36, November 10, 1949, p. 34.
42. Williams, W.H., 1948, "B.O.A.C. Office Extension. Great West Road," The Builder, Vol. 175, 1948.
43. Ozell, A.M. and Jernigan A.M., 1956, "Some Studies on the Behavior of Prestressed Concrete Columns," Technical Progress Report No. 3, Florida Eng. and Industrial Exp. Station, Univ. of Florida, July 1956.
44. Southwell, R.V., 1932, "On the Analysis of Experimental Observations in Problems of Elastic Stability," Proc. Royal Society, London, v. 135, series A, p. 601, 1932.
45. Zia, P.Z-T., 1957, "Ultimate Strength of Slender Prestressed Concrete Columns," Technical Paper Series No. 131, Florida Eng. and Industrial Exp. Station, Univ. of Florida, July 1957.
46. Lin, T.Y. and Itaya, R., 1957, "A Prestressed Concrete Column under Eccentric Loading," Journal of Prestressed Concrete Institute, Vol. 2, No. 3, December 1957.
47. Brown, H.R., 1960, "The Strength of Long Prestressed Concrete Columns," M. Eng. Thesis, School of Civil Eng., Univ. of New South Wales, 1960.
48. Hall, A.S., 1962, "Prestressed Concrete Research in Australia," Federation Int. de la Précontrainte, 4th Congress, Rome 1962.
49. Brown, H.R. and Hall, A.S., 1965, "Tests on Slender Prestressed Concrete Columns," UNICIV Report No. R-12, Univ. of New South Wales, August 1965.

50. Brown, H.R. and Hall, A.S., 1966, "Tests on Slender Prestressed Concrete Columns," Symposium on Reinforced Concrete Columns, A.C.I. Special Publication, 1966.
51. Bakhoun, M., Samaan, S., Aboul Eid A, Antar A. and Esmat M., 1962, "Simple and Compound Bending of Prestressed Units," Fédération Int. de la Précontrainte, 4th Congress, Rome 1962.
52. Moreadith, F.L., 1964, "An Analytical Study of Ultimate Load Capacity of Long Hinged Prestressed Concrete Columns," Ph.D. Thesis, Dept. of Civil Eng., Univ. of North Carolina, Raleigh, 1964.
53. Zia, P., and Moreadith, F.L., 1966, "Ultimate Load Capacity of Prestressed Concrete Columns," Journal A.C.I., V. 63, July 1966.
54. Brown, K.J., 1965, "The Ultimate Load Carrying Capacity of P.C. Columns Under Direct and Eccentric Loading," Civil Engineering and Public Works Review, April, May and June 1965.
55. Kabaila, A.P., and Hall, A.S., 1966, "The Analysis of Instability of Unrestrained Prestressed Concrete Columns with End Eccentricities," Symposium on Reinforced Concrete Columns, A.C.I. Special Publication, 1966.
56. Brettle, H.J., 1958, "Increase in Concrete Modulus of Elasticity due to Prestress and its Effect on Beam Deflection," Constructional Review (Aust.), No. 8, Vol. 31, August 1958.
57. Brettle, H.J., 1960, "Effect of Variable Concrete Modulus of Elasticity on the Deflection of Prestressed Beams," Australian Journal of Science, Vol. 11, No. 1, March 1960.
58. Itaya, R., 1965, "Design and Uses of Prestressed Concrete Columns," Journal of Prestressed Concrete Institute, June 1965.
59. Solvadori, M.G., and Baron, M.L., 1961, "Numerical Methods in Engineering," Prentice-Hall, New York, p. 46.

APPENDIX AExperimental and Theoretical Curves

This appendix contains 27 graphs which present both experimental and theoretical results. All graphs have been drawn by computer plotting programs, each to a different scale in order to fill fully the available space. In every graph, x represents experimental results.

. represents theoretical results.

There are three types of figures:

(a) Figs. A1-A9 : Load-Central Deflection

The deflections plotted are due to load only, excluding initial deflections.

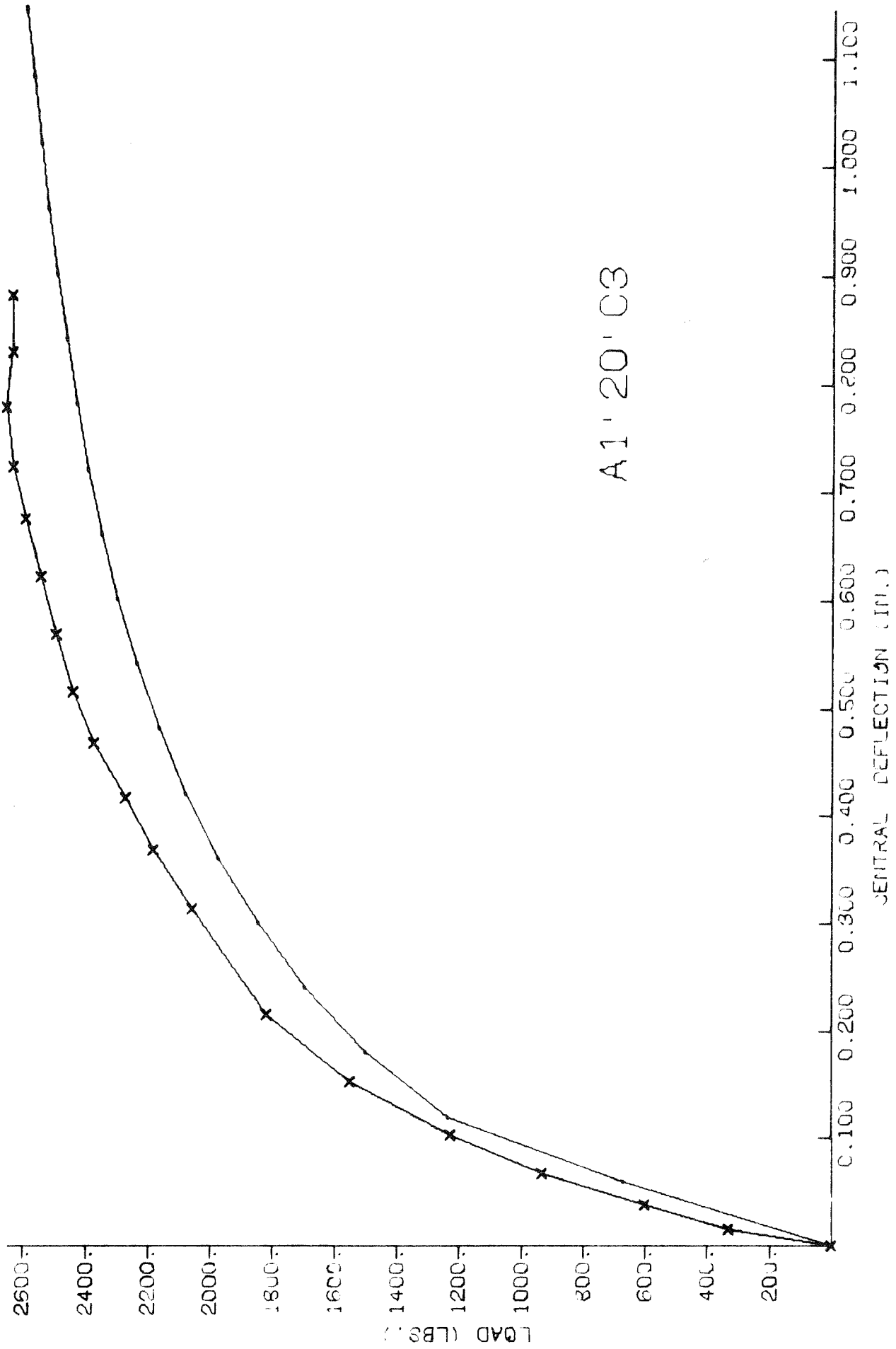
(b) Figs. A10-A18: Load-Central Strains

The compressive strains represent the average of gages 2 and 3, the tensile strains the average of gages 5 and 6 and the strains between them are the average of gages 1 and 4 (see Fig. 12). All strains plotted are due to load only, excluding initial conditions.

(c) Figs. A19-A27 : Column Deflected Shape

One-half of the column shape is plotted, to a distorted scale, at both initial conditions and the maximum critical load. The experimental and theoretical values of the critical loads are also given.

Note: The graphs presented in this appendix are a selection of 9 out of the 36 columns tested. Similar graphs for the remaining 27 columns can be found in the original thesis at the University of California Engineering Library, at Berkeley.



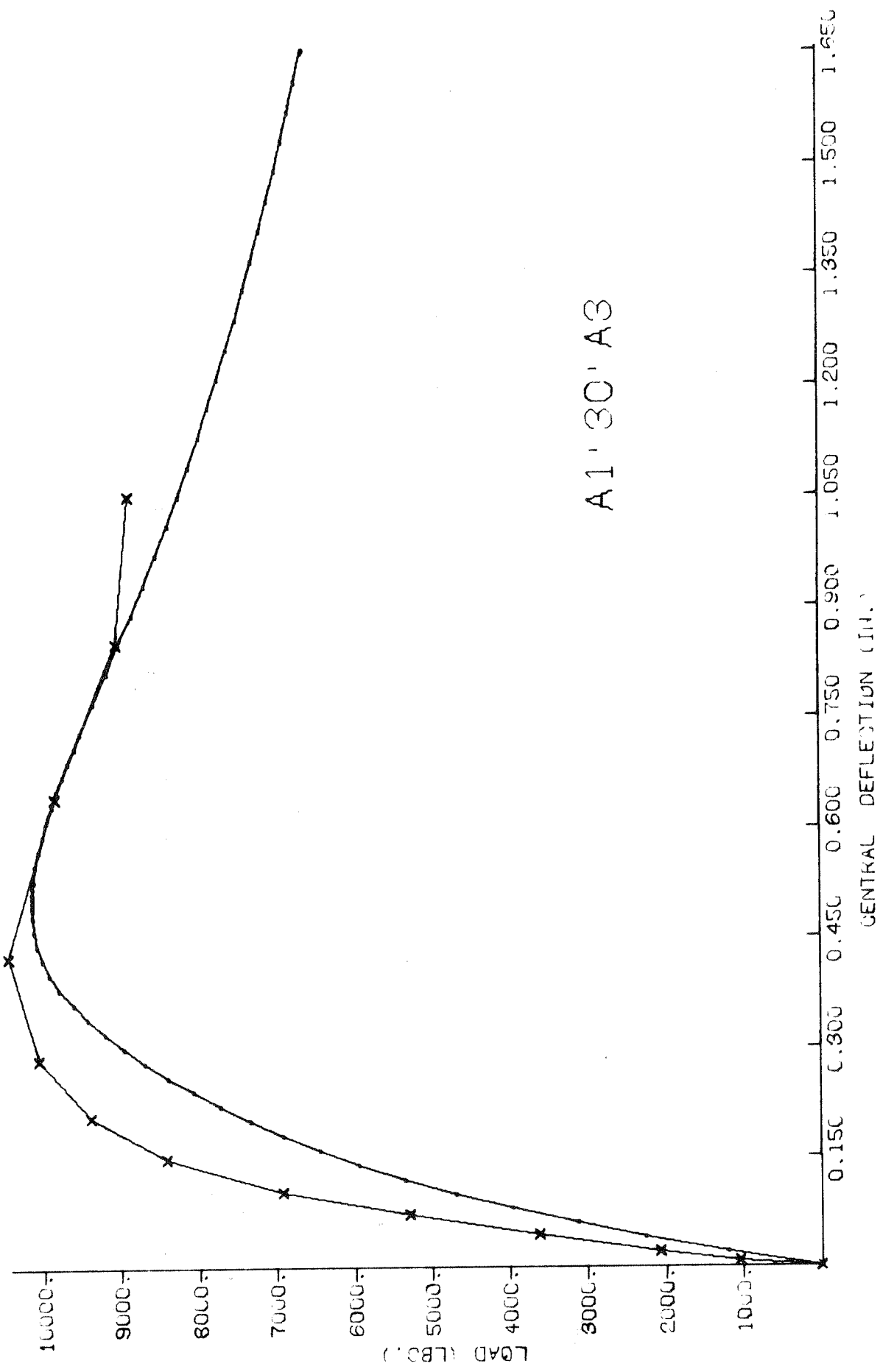
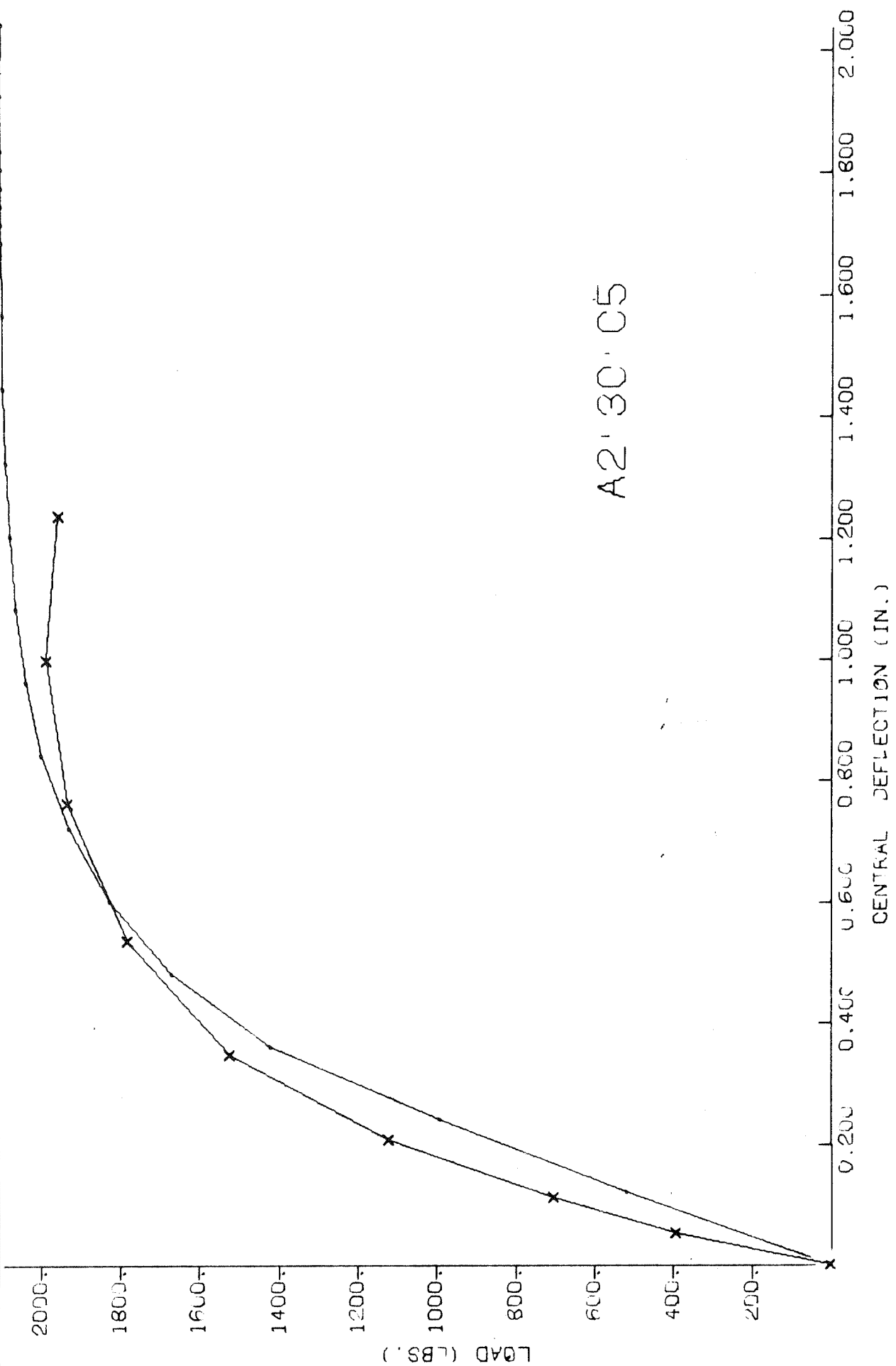


FIG.A2

A2' 30" C5



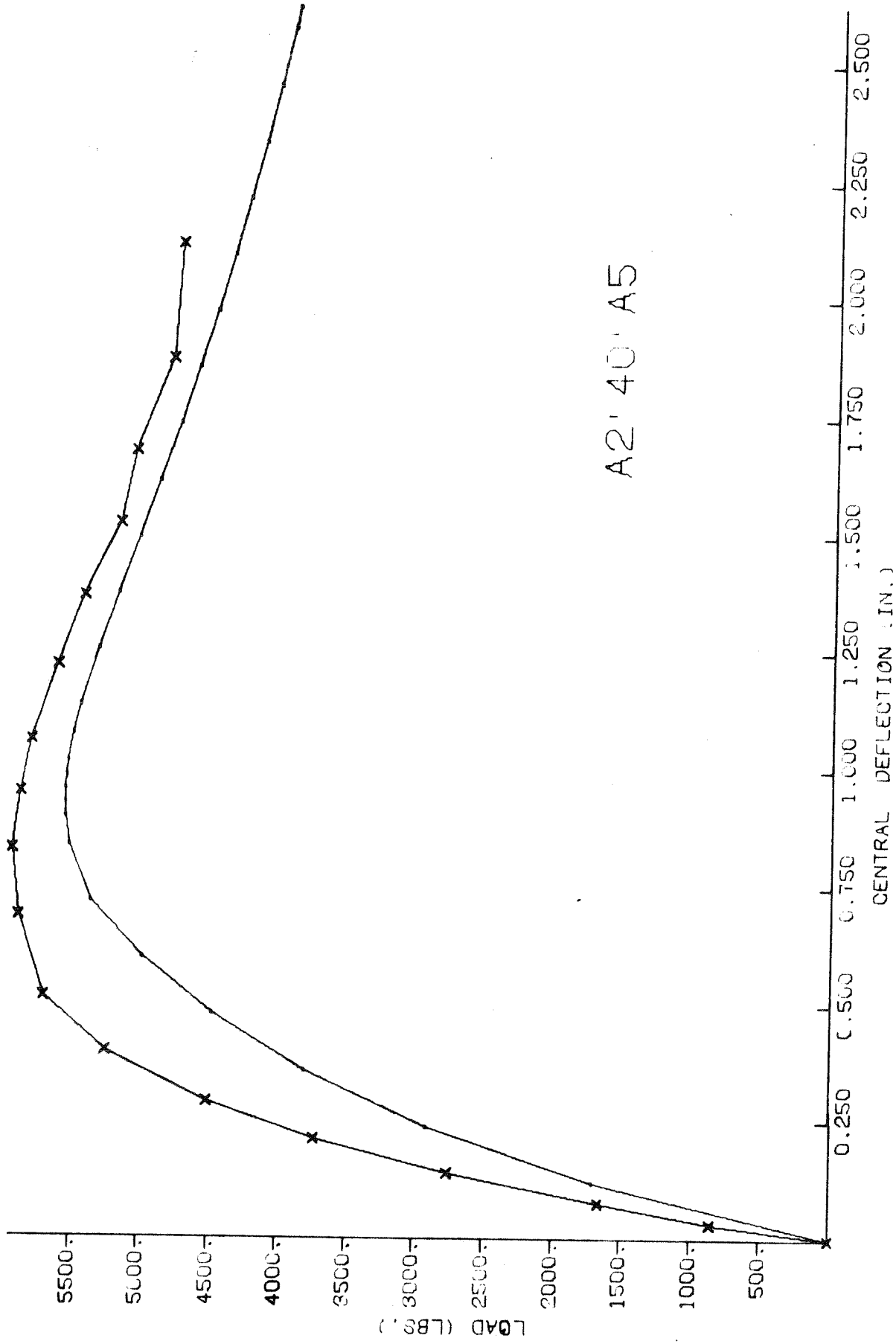


FIG A4

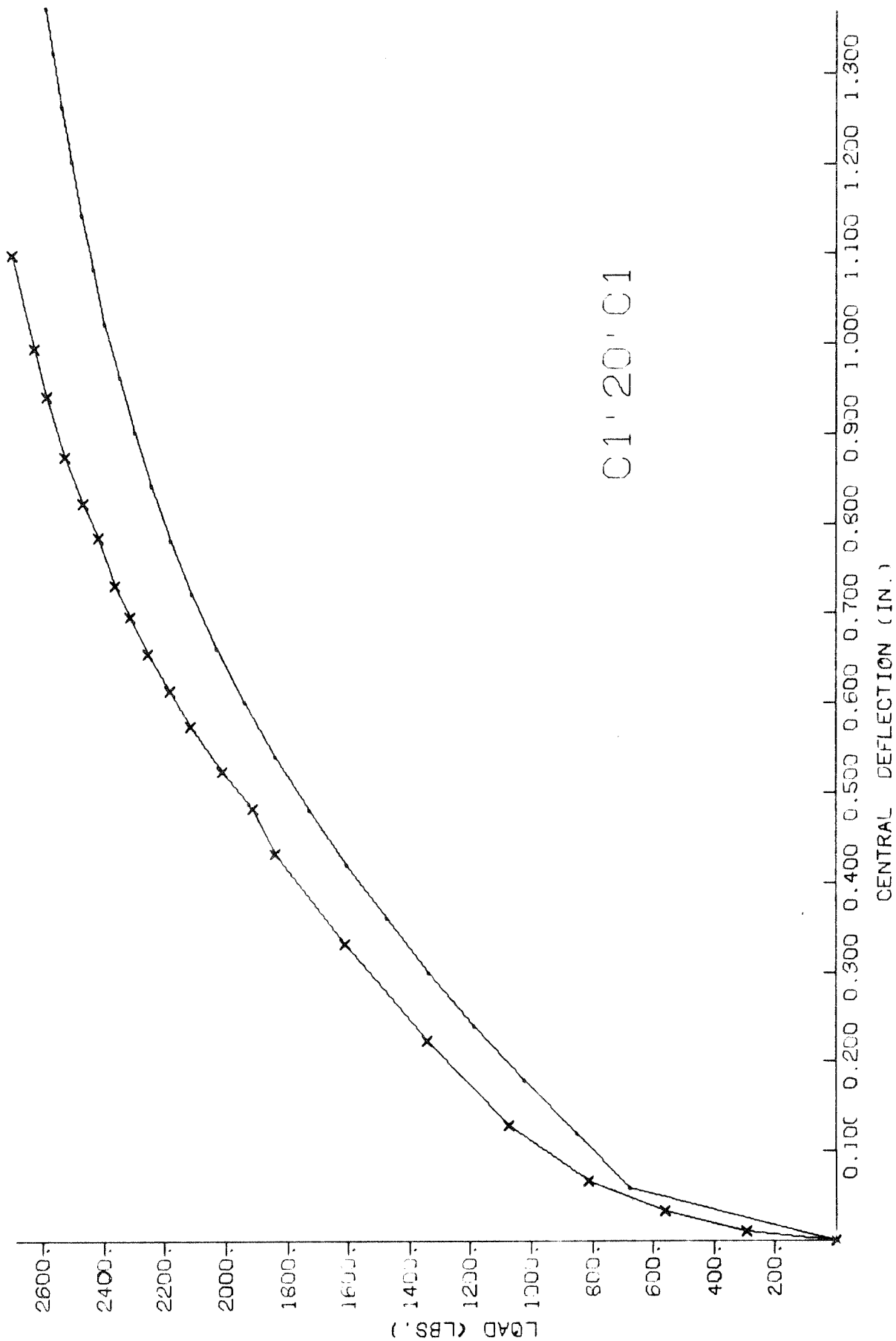


FIG A5

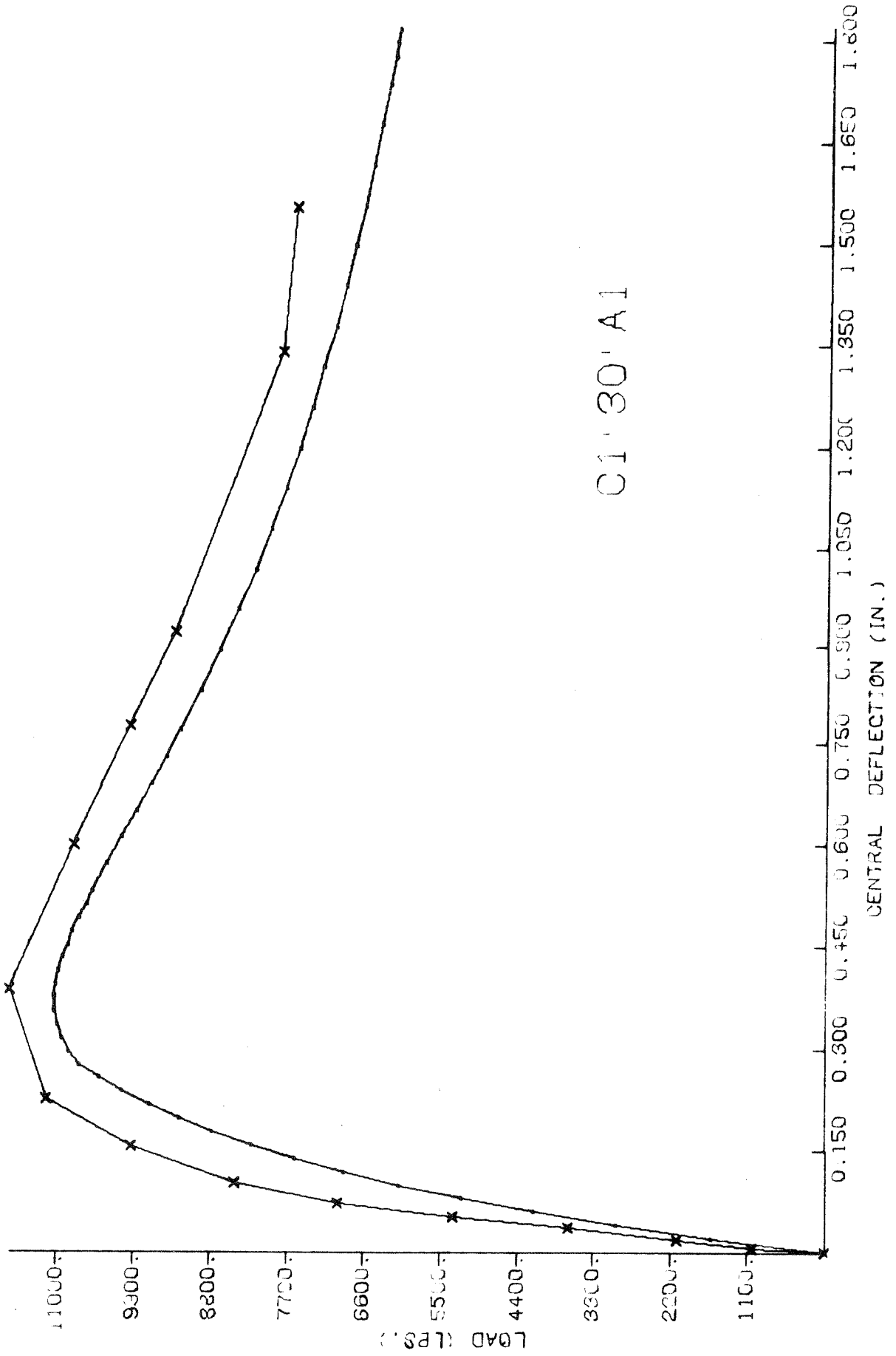


FIG A6

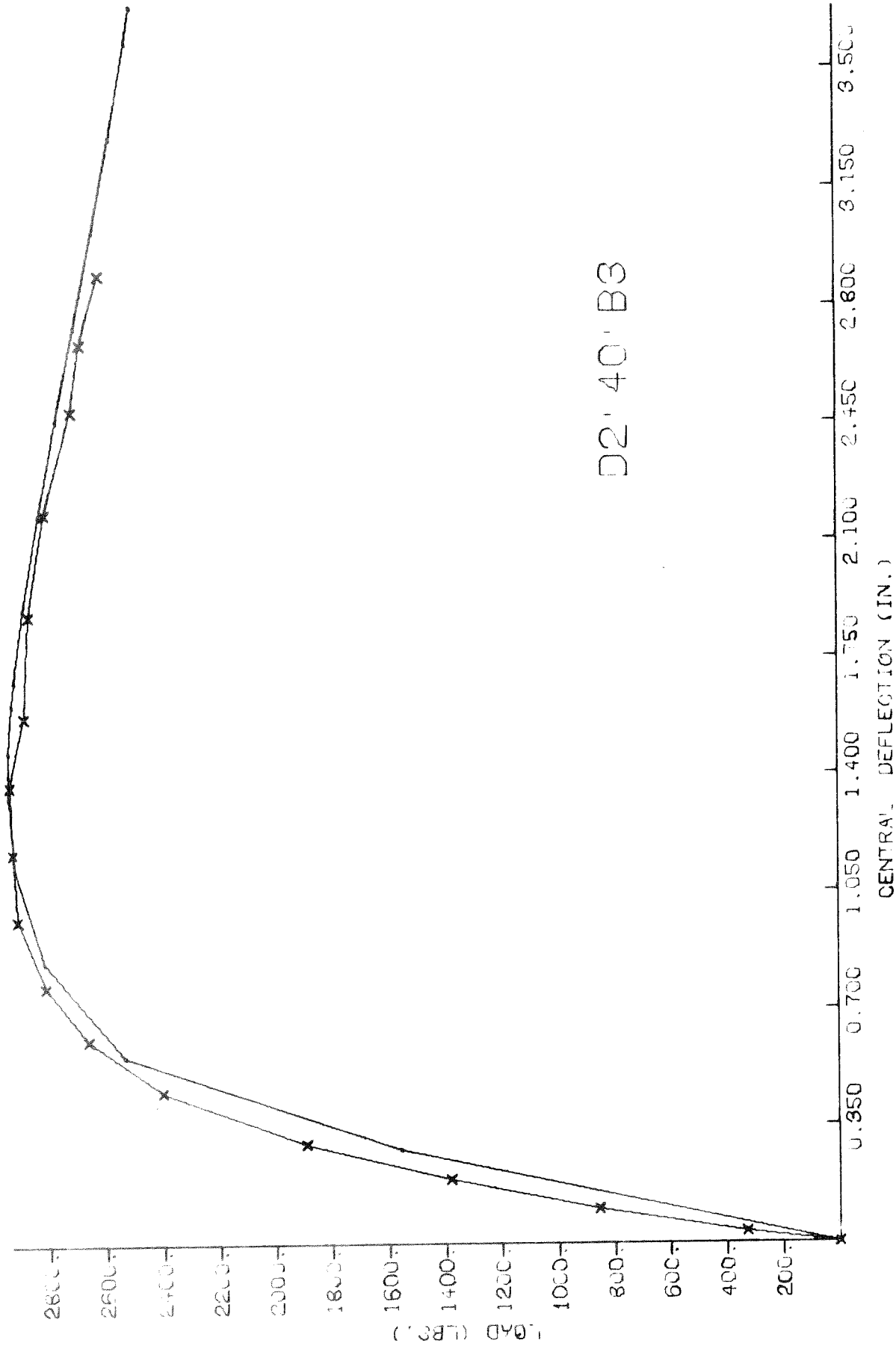


FIG A7

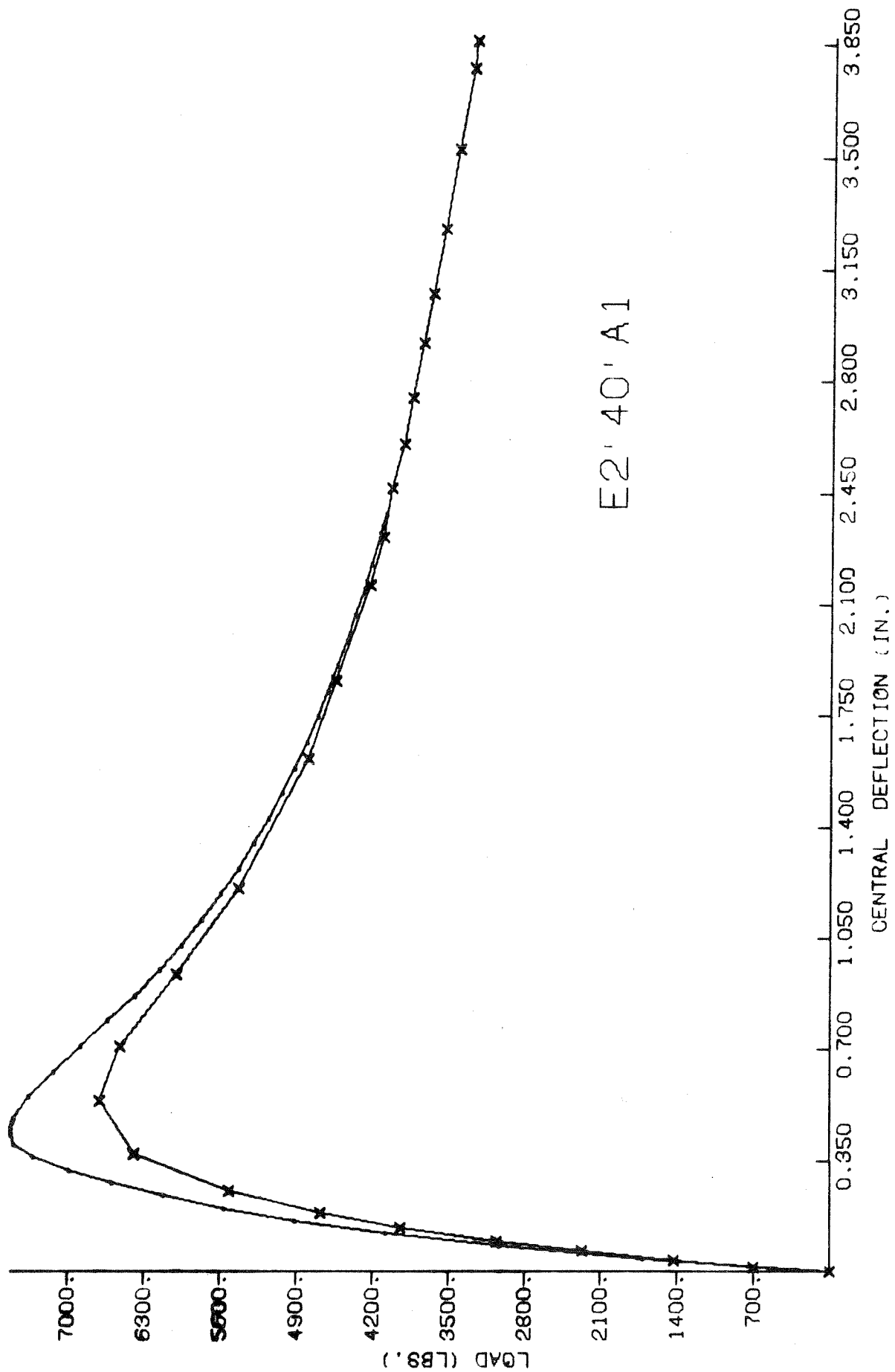


FIG. A8

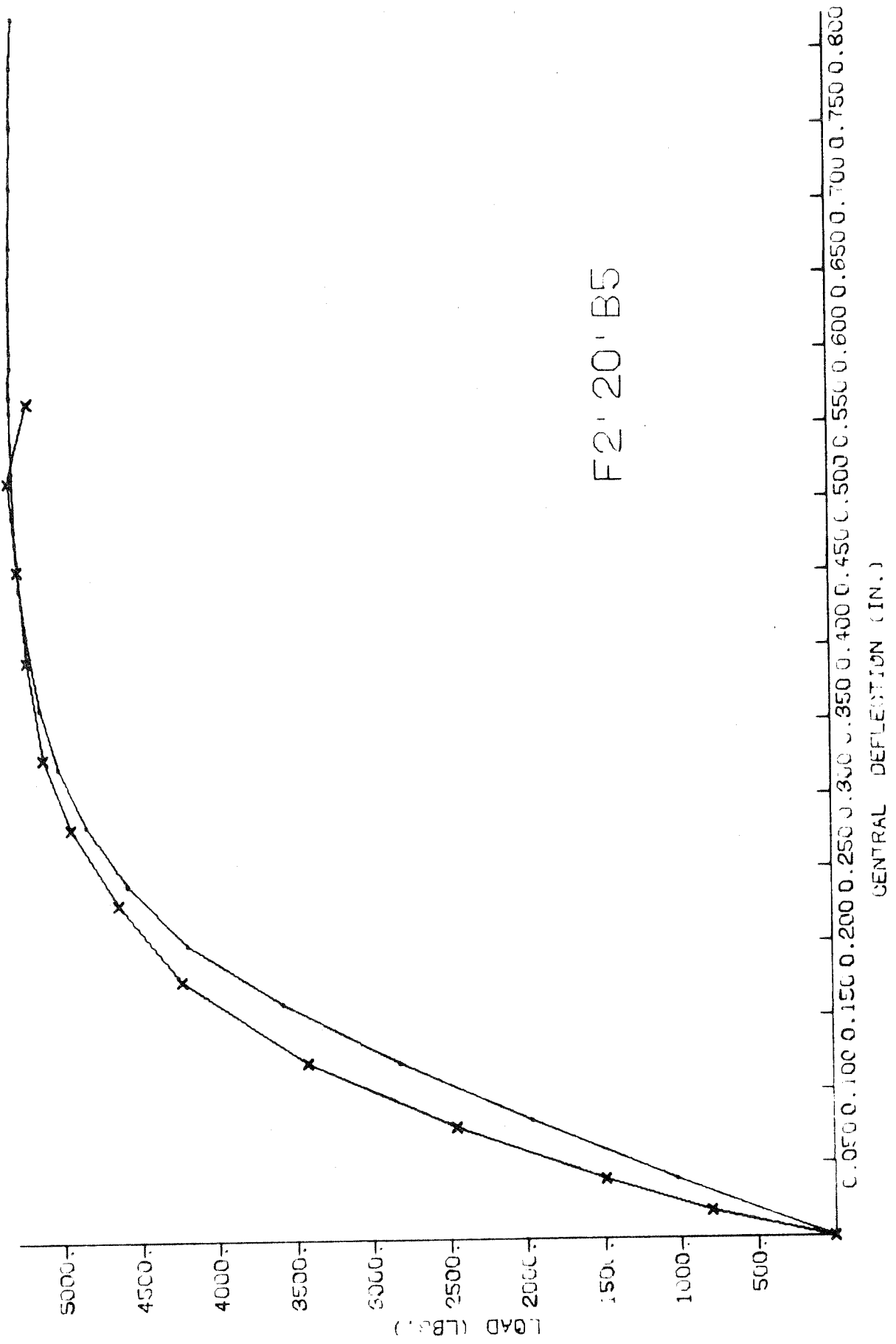


FIG. A9

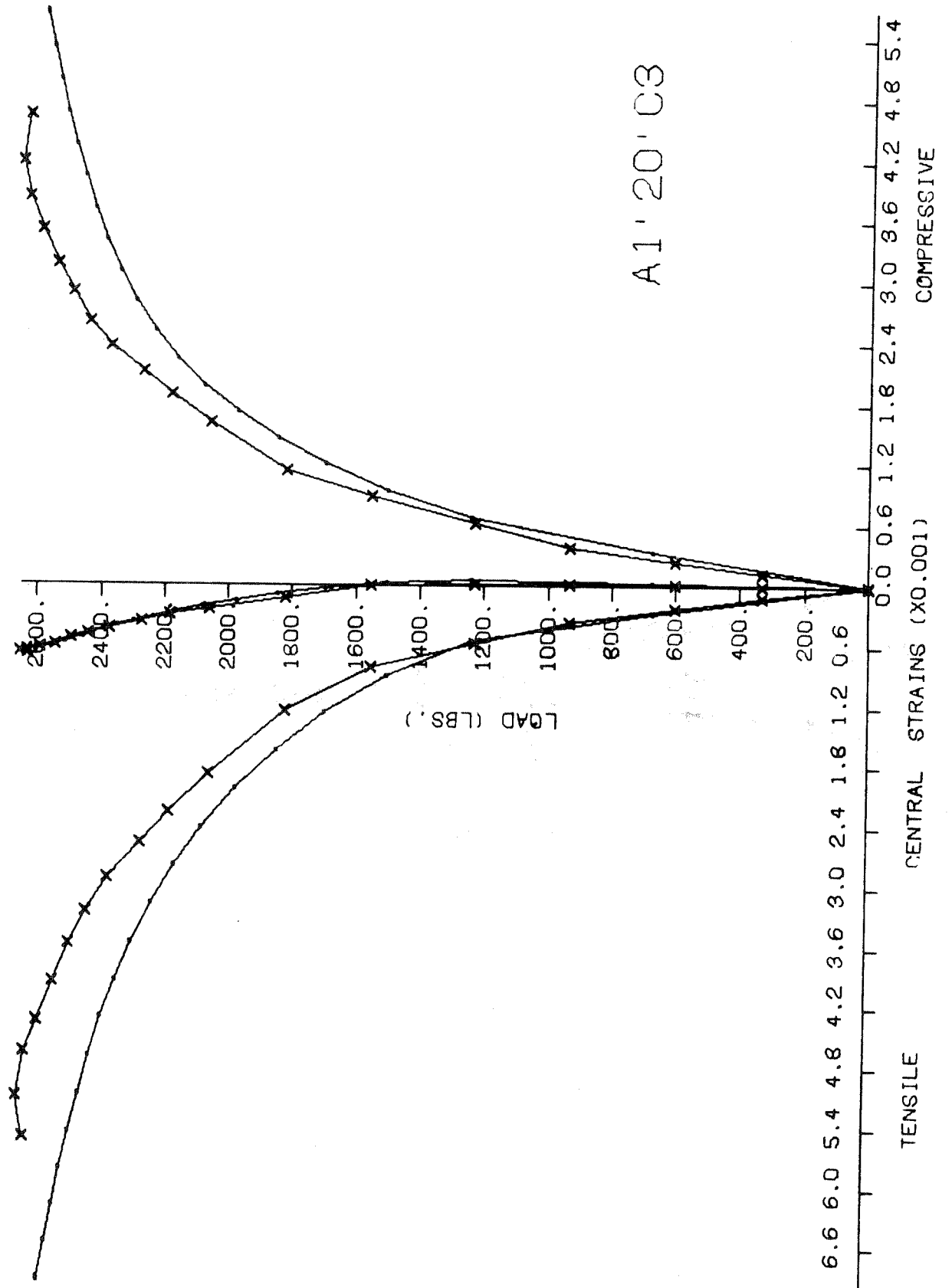


FIG. A10

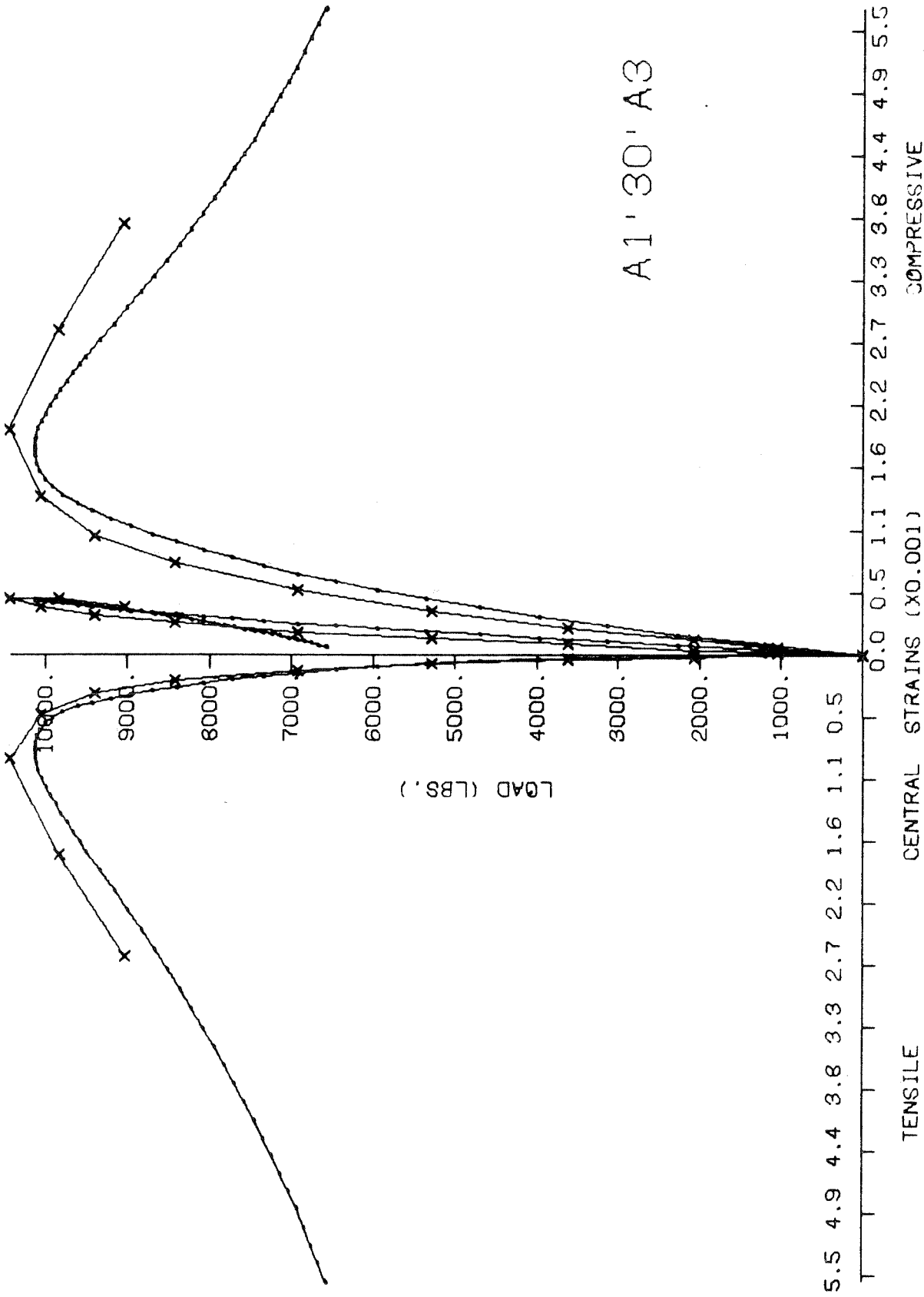


FIG. A11

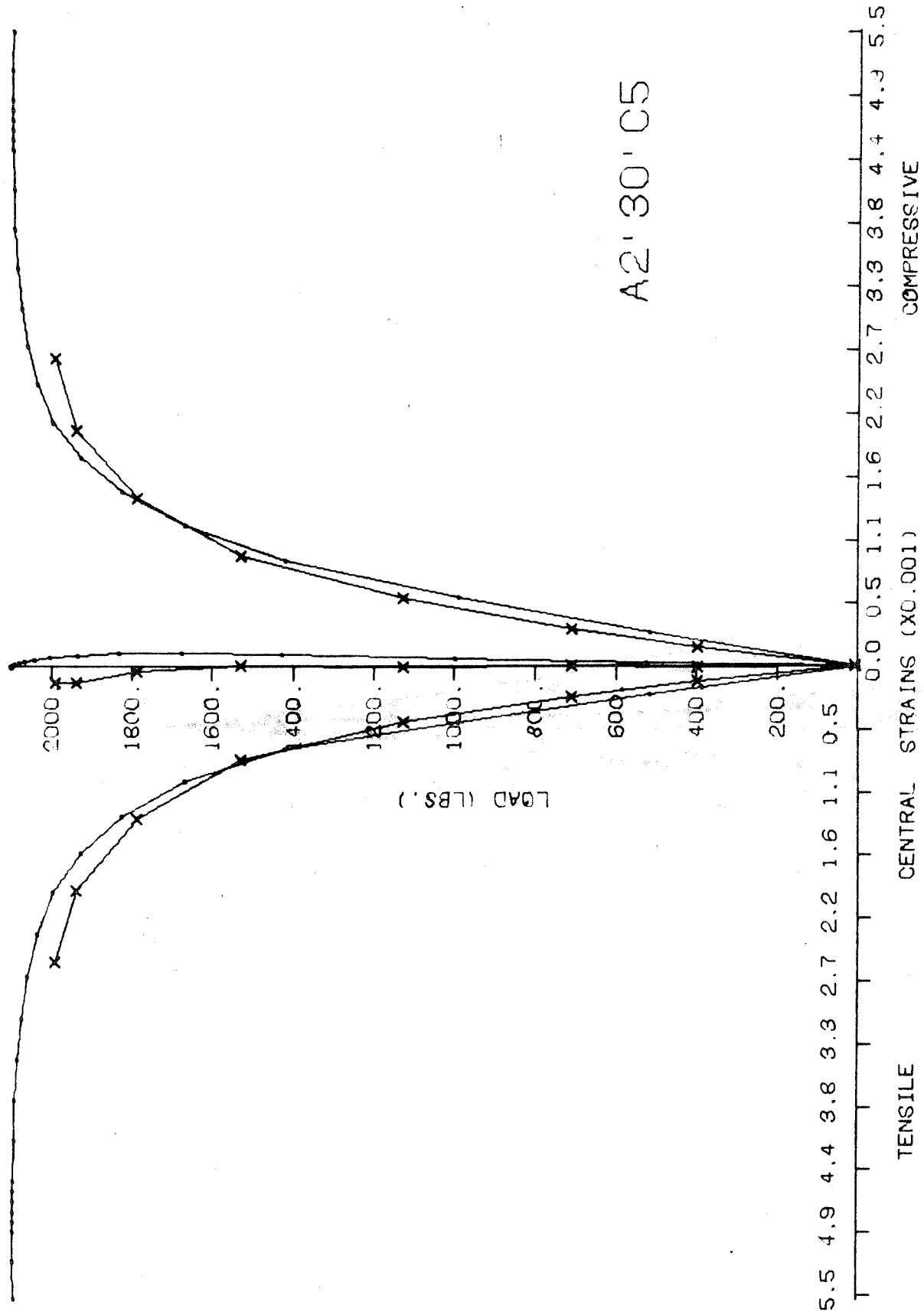


FIG. A12

A2' 40' A5

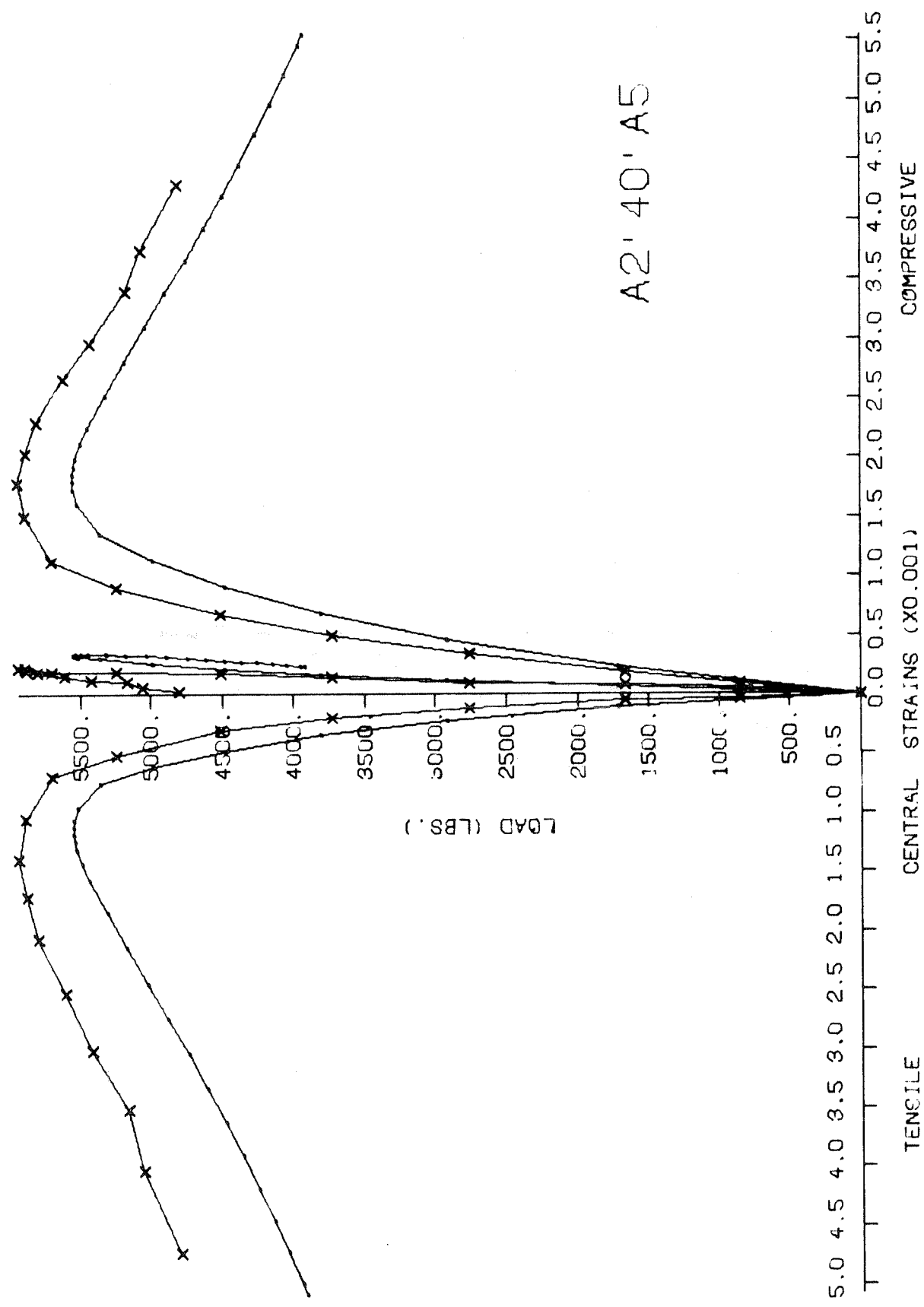


FIG. A13

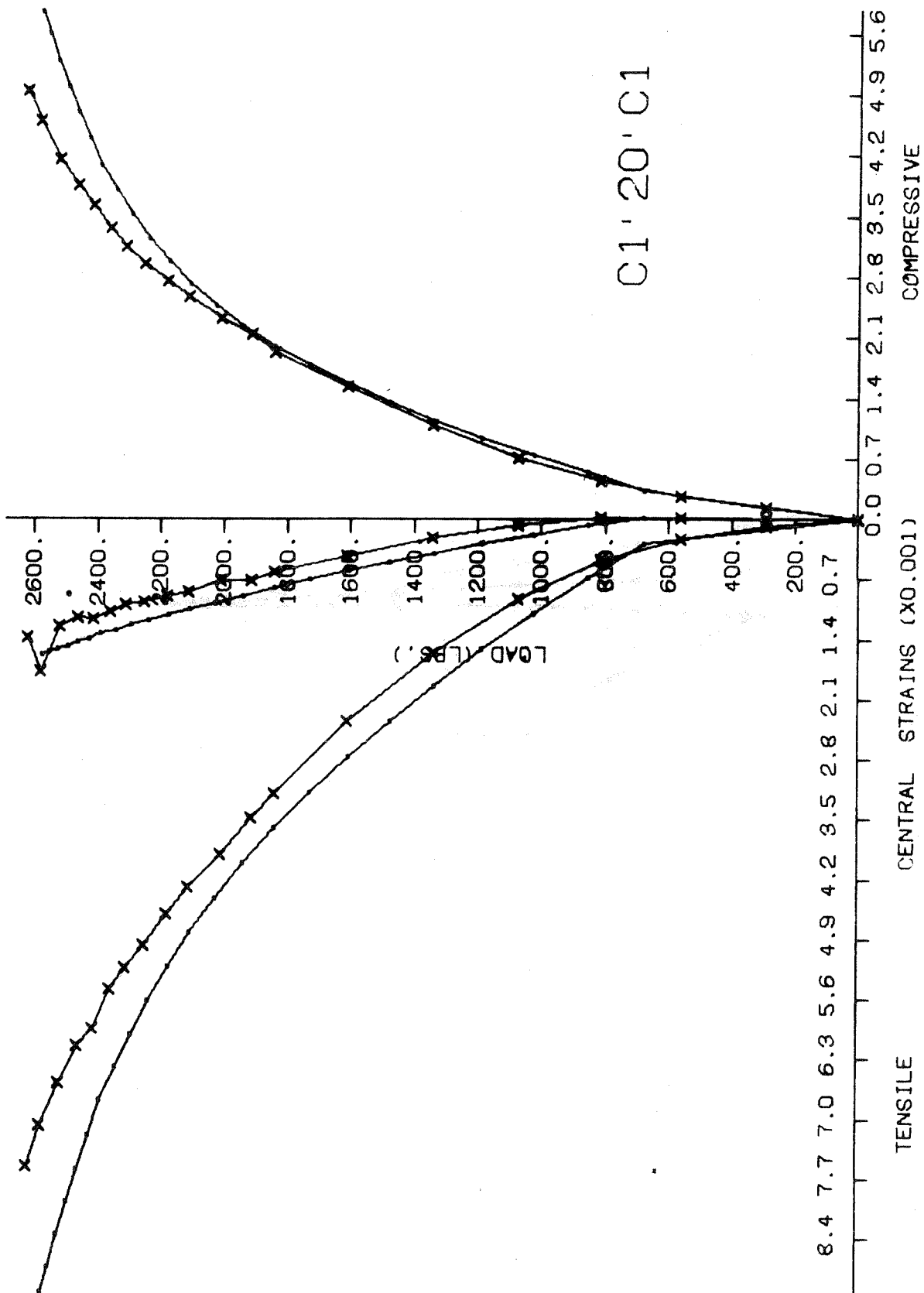


FIG. A14

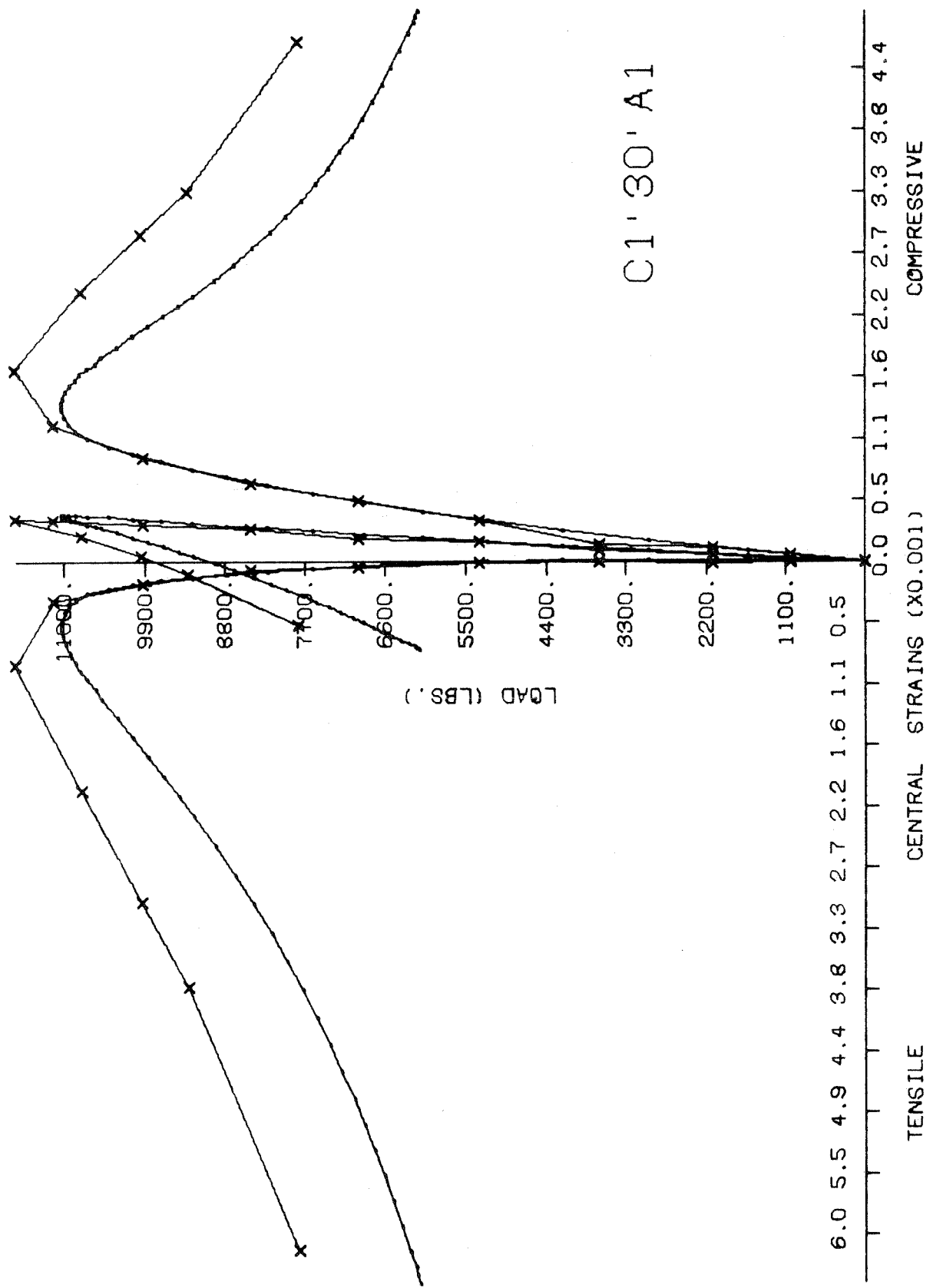


FIG. A15

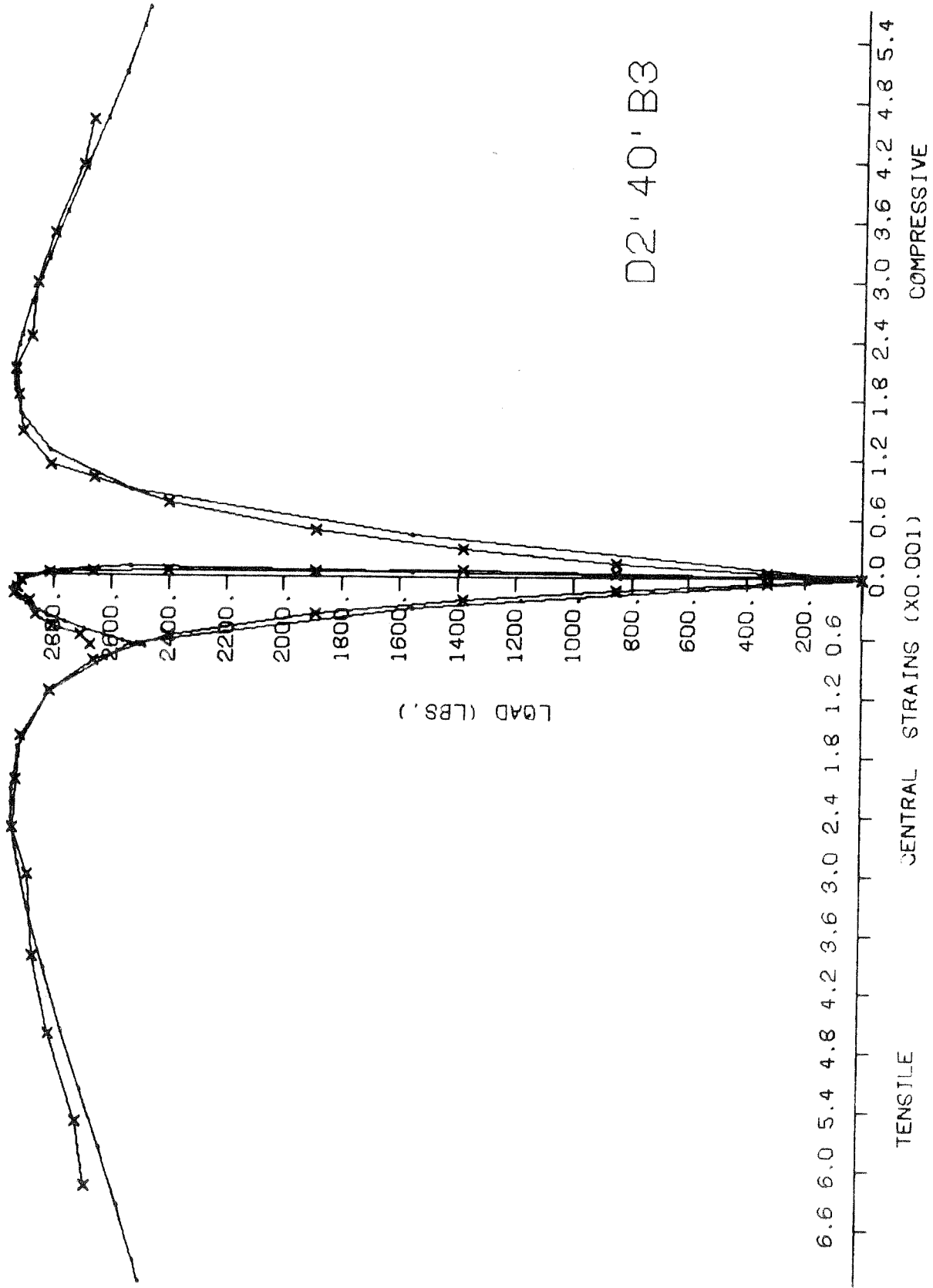
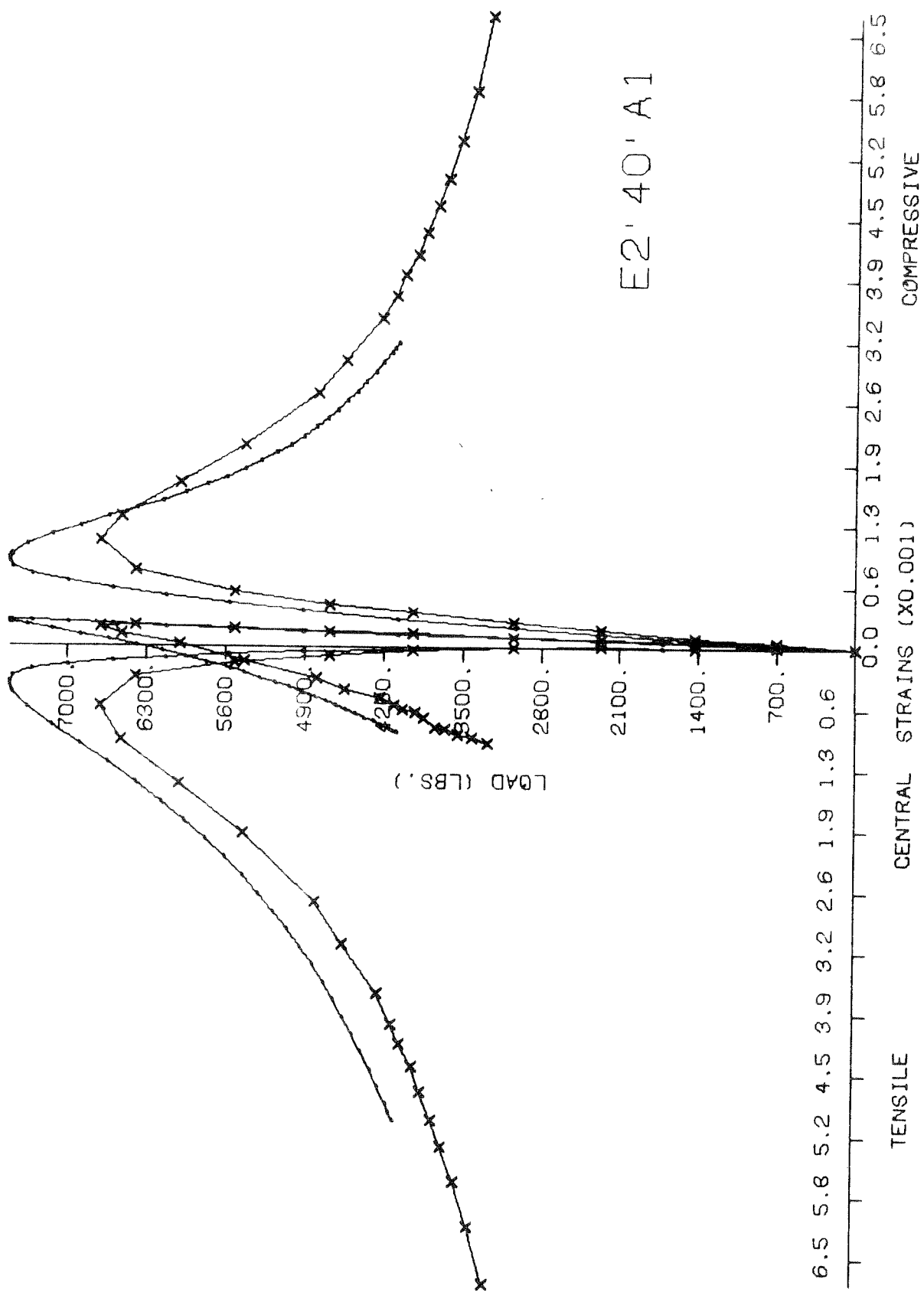


FIG. A16



E2' 40' A1

FIG. A17

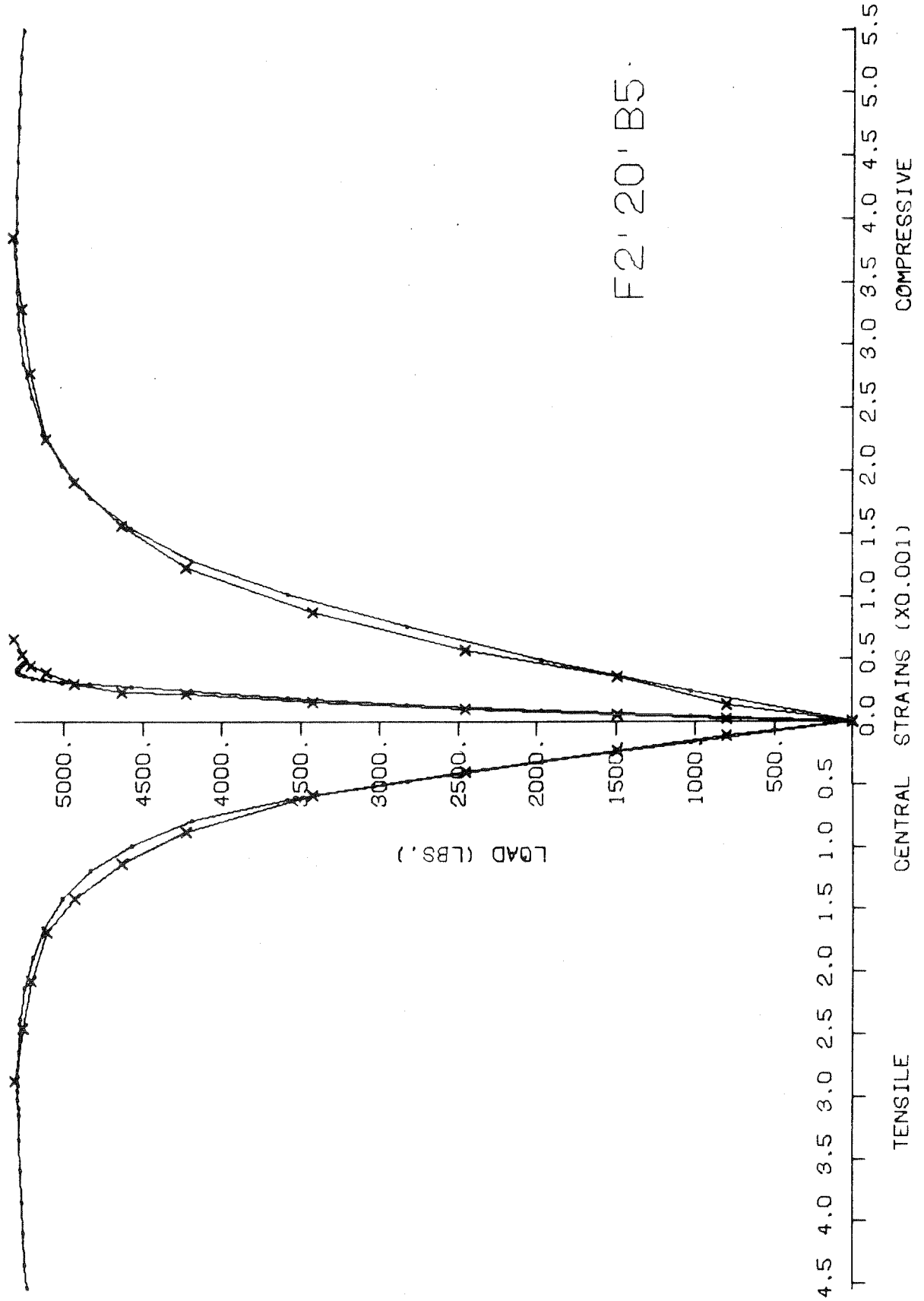


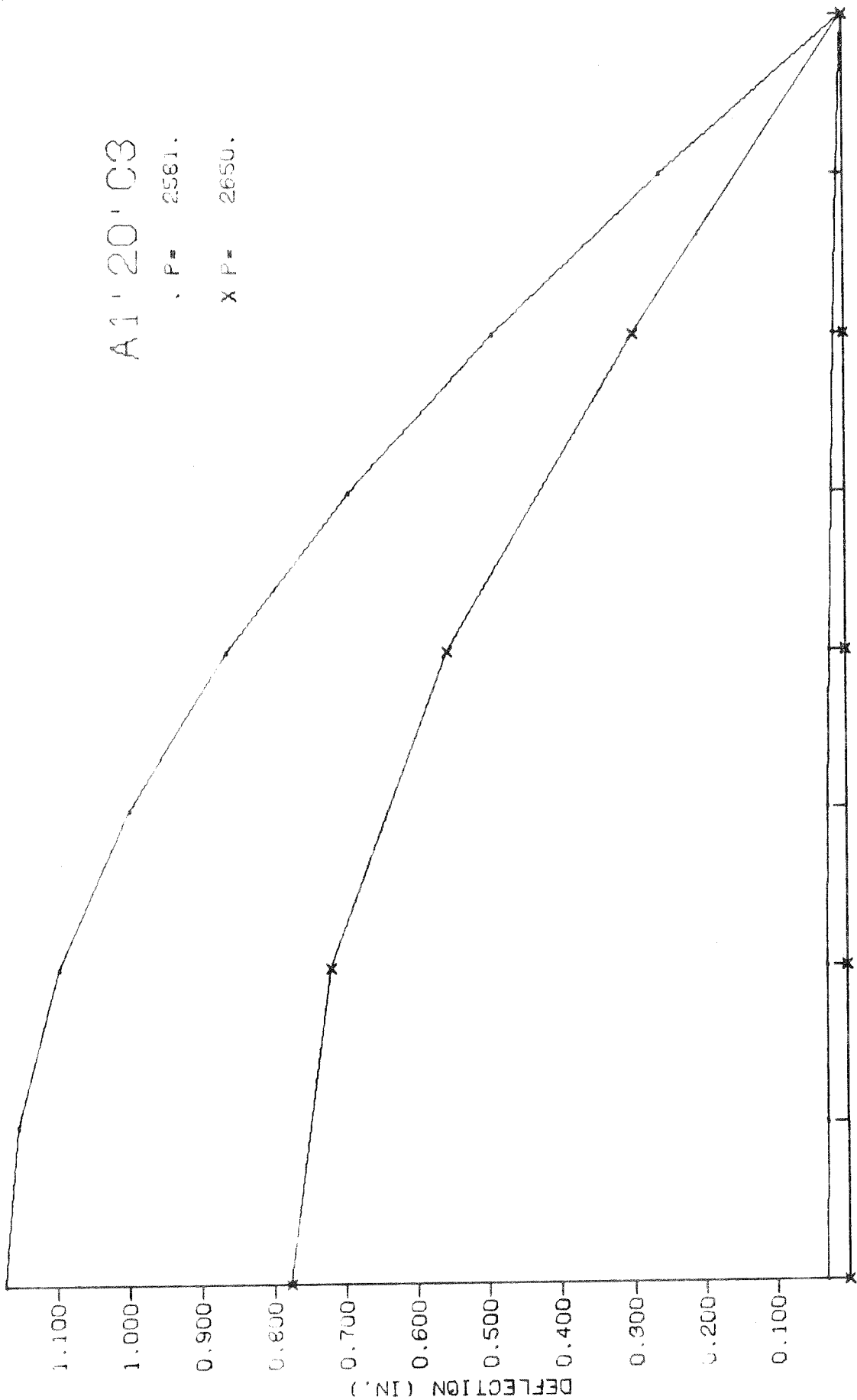
FIG. A18

A1' 20' C3

P = 2581.

X P = 2650.

180



POSITION ALONG COLUMN LENGTH

FIG A19

A1' 30' A3
P- 10123.
X P- 10430.

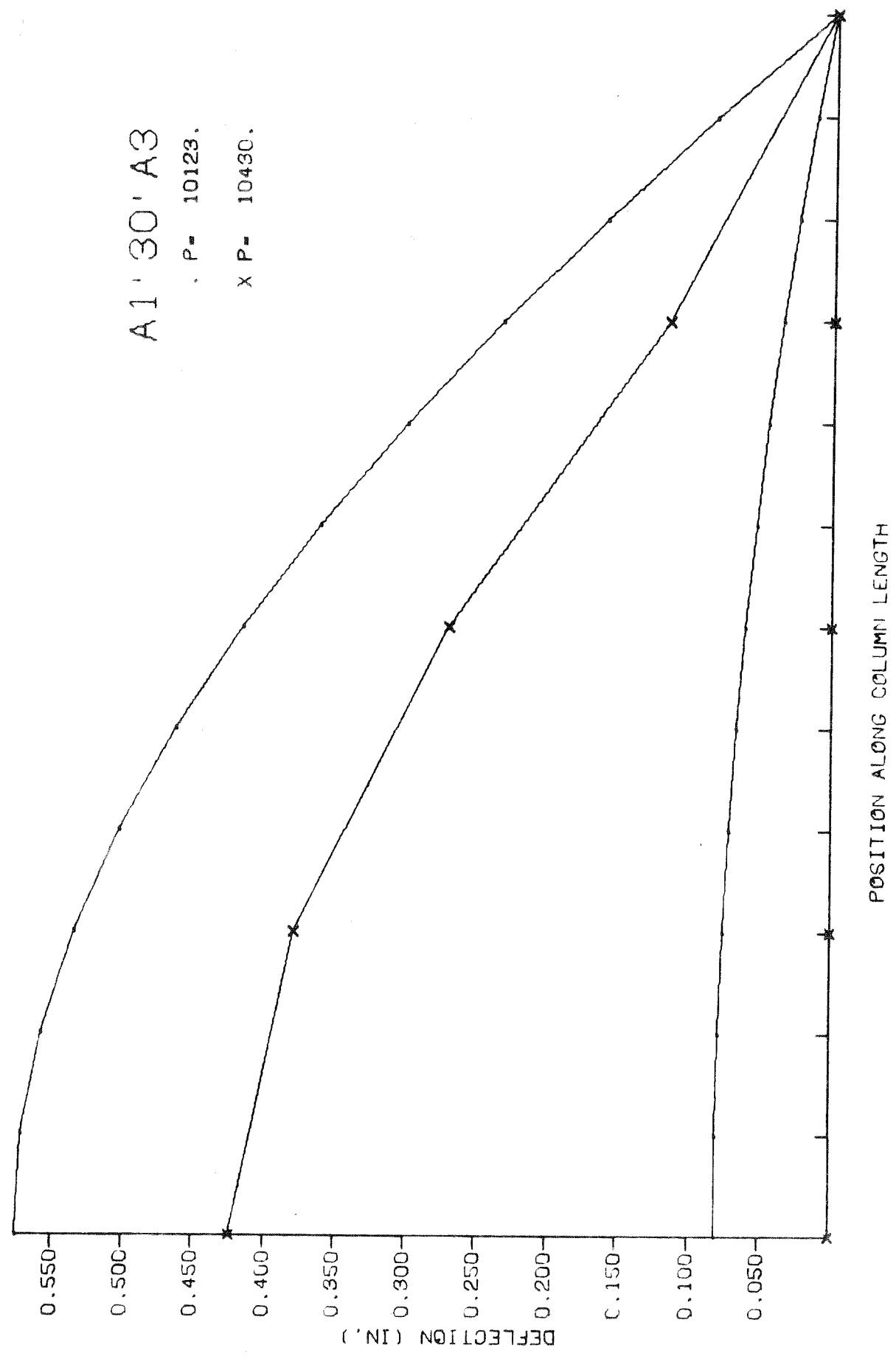
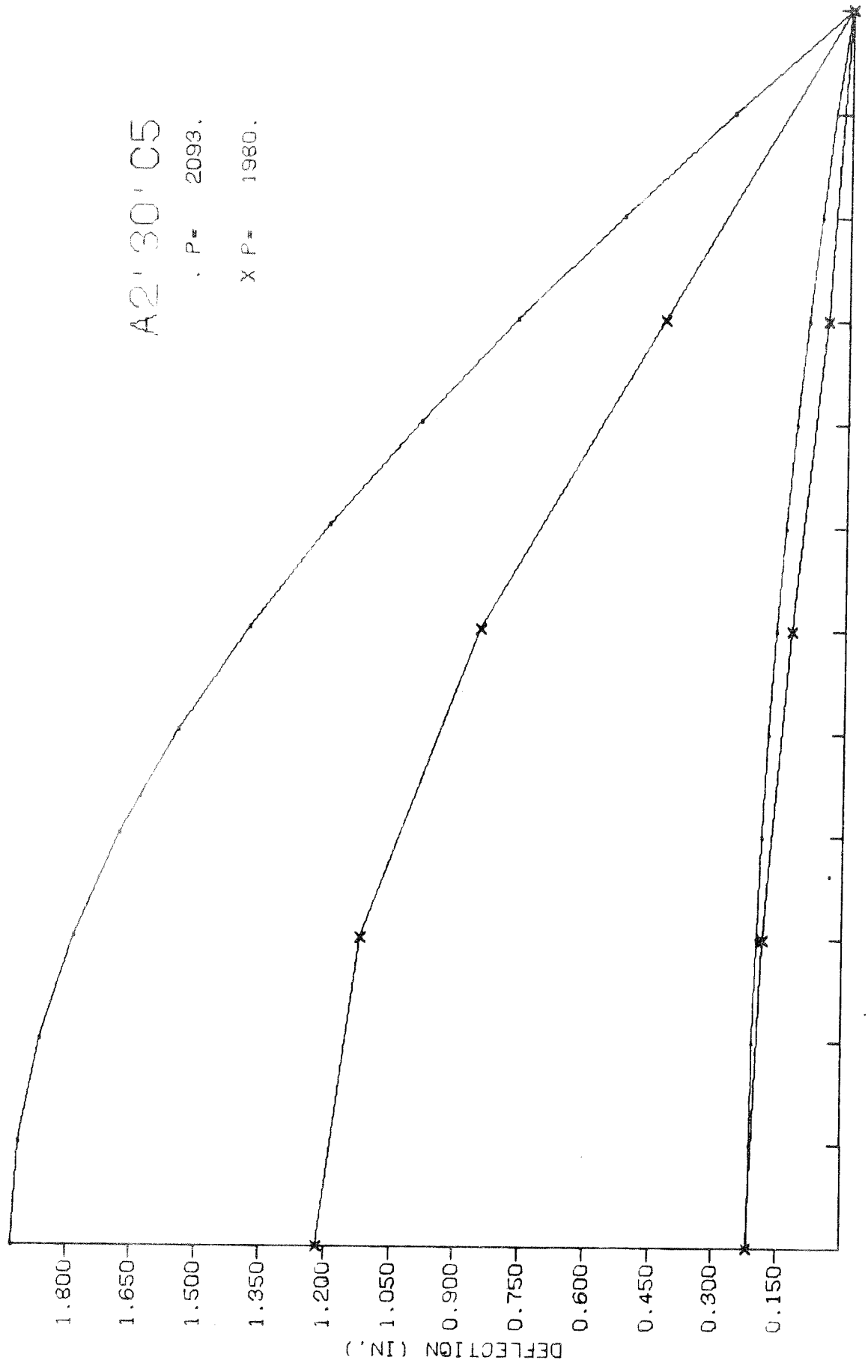


FIG A20

A2' 30" C5
P= 2093.
X P= 1980.



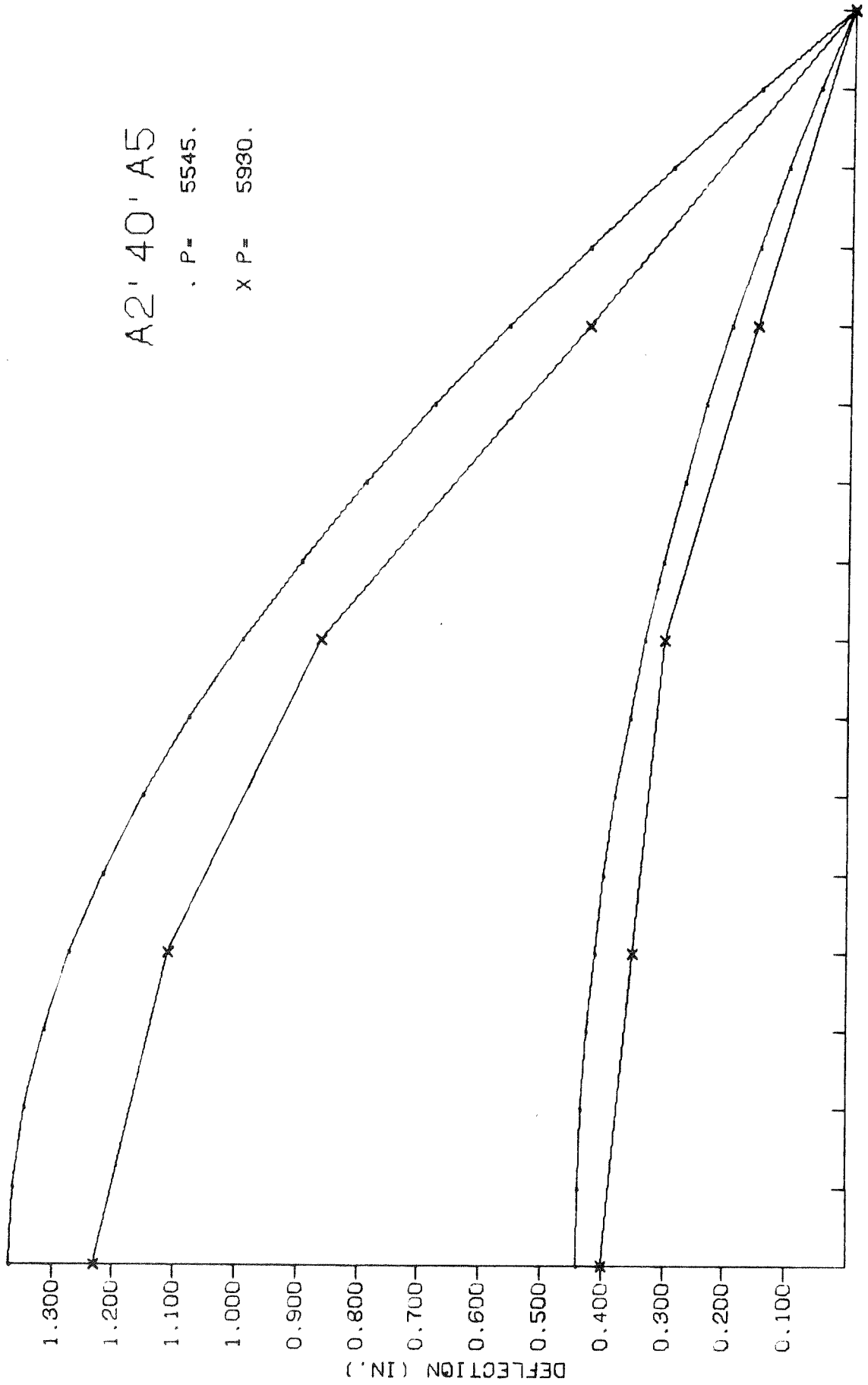
POSITION ALONG COLUMN LENGTH

FIG A2I

A2' 40' A5

P = 5545.

X P = 5930.



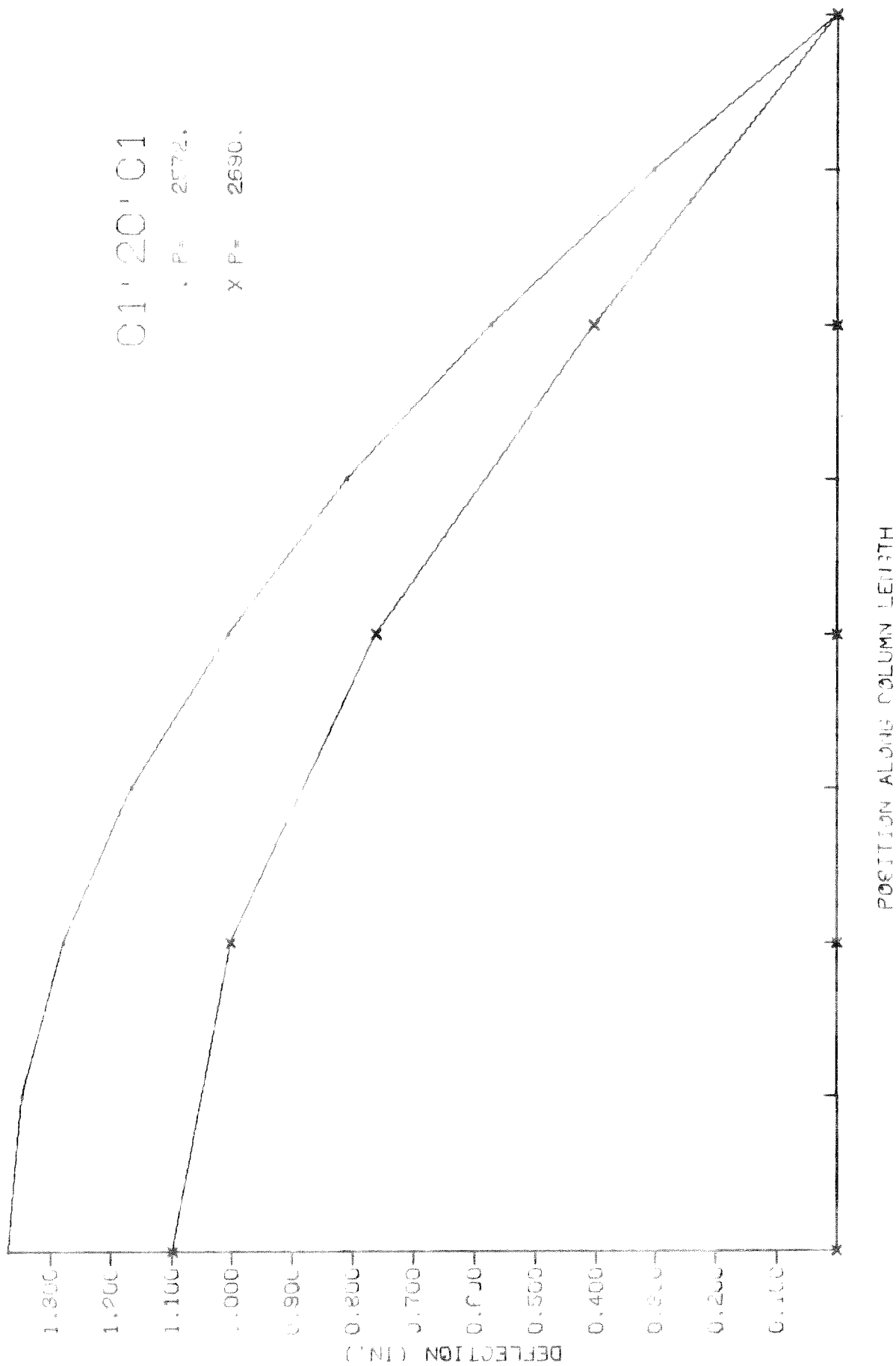
POSITION ALONG COLUMN LENGTH

FIG. A22

C1' 20' C1

. P= 2572.

X P= 2690.



POSITION ALONG COLUMN LENGTH

FIG. A23

C1' 30' A1

. P= 11022.

X P= 11660.

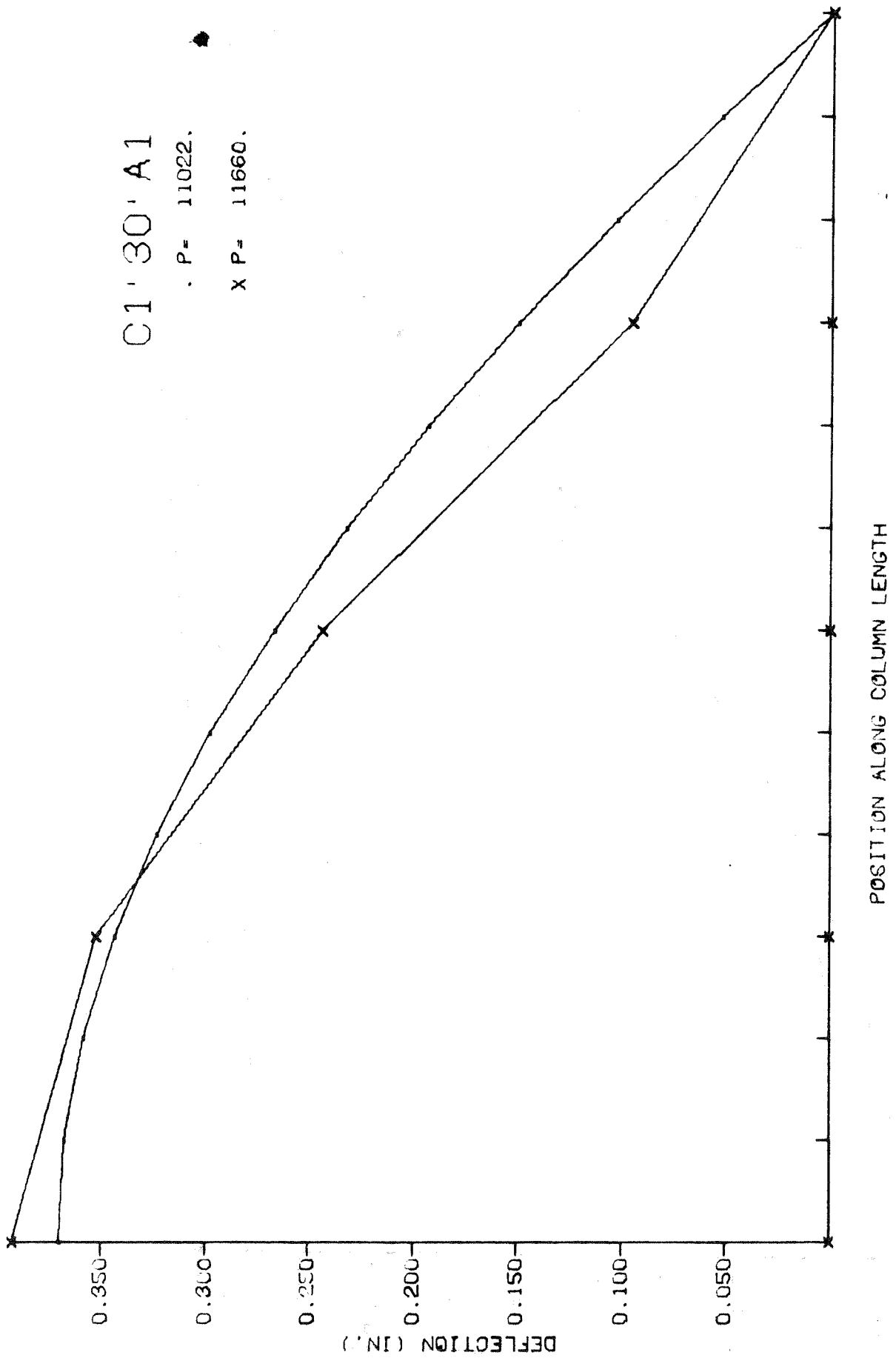
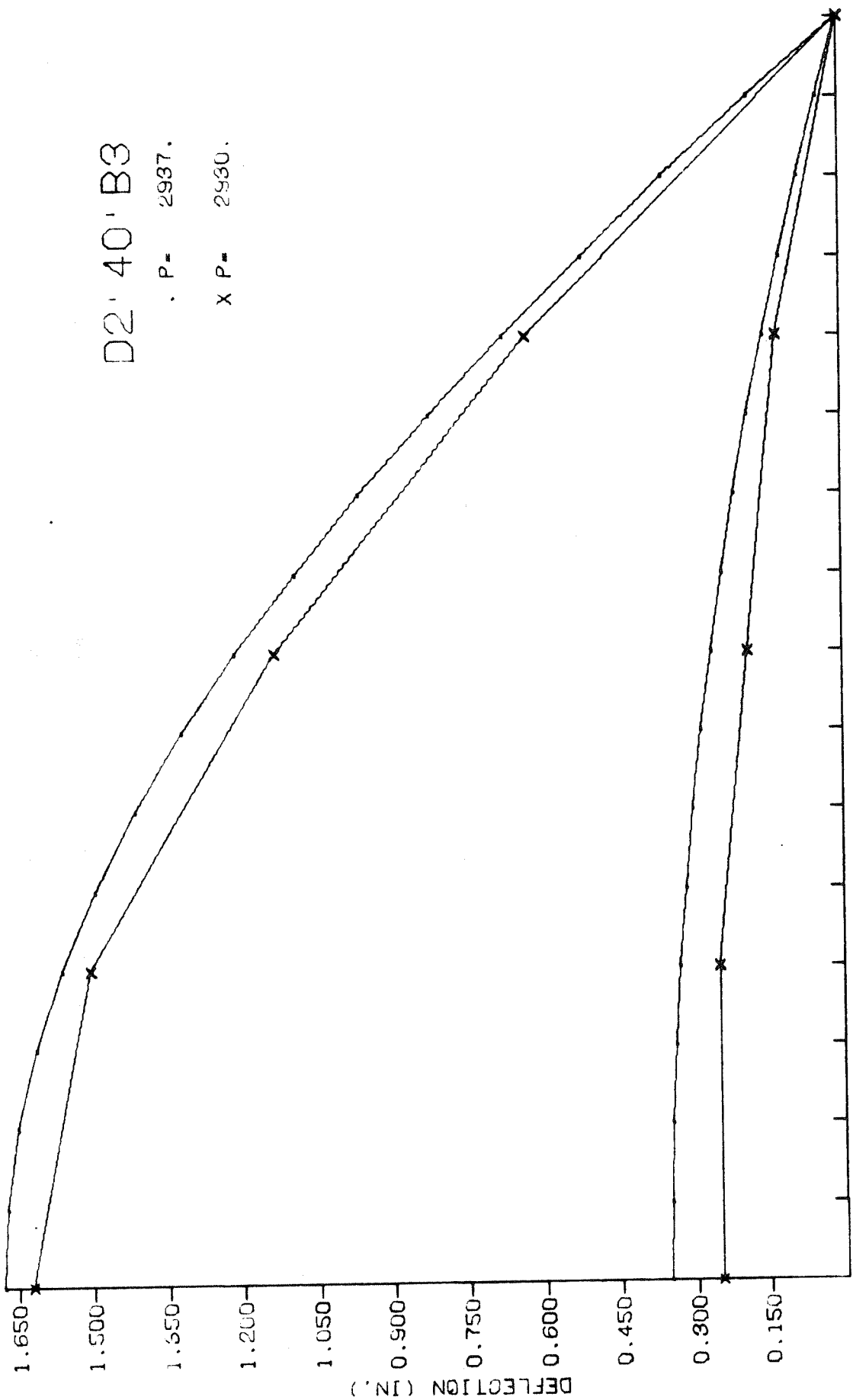


FIG. A24



D2 40 B3

P= 2937.

X P= 2930.

FIG. A25

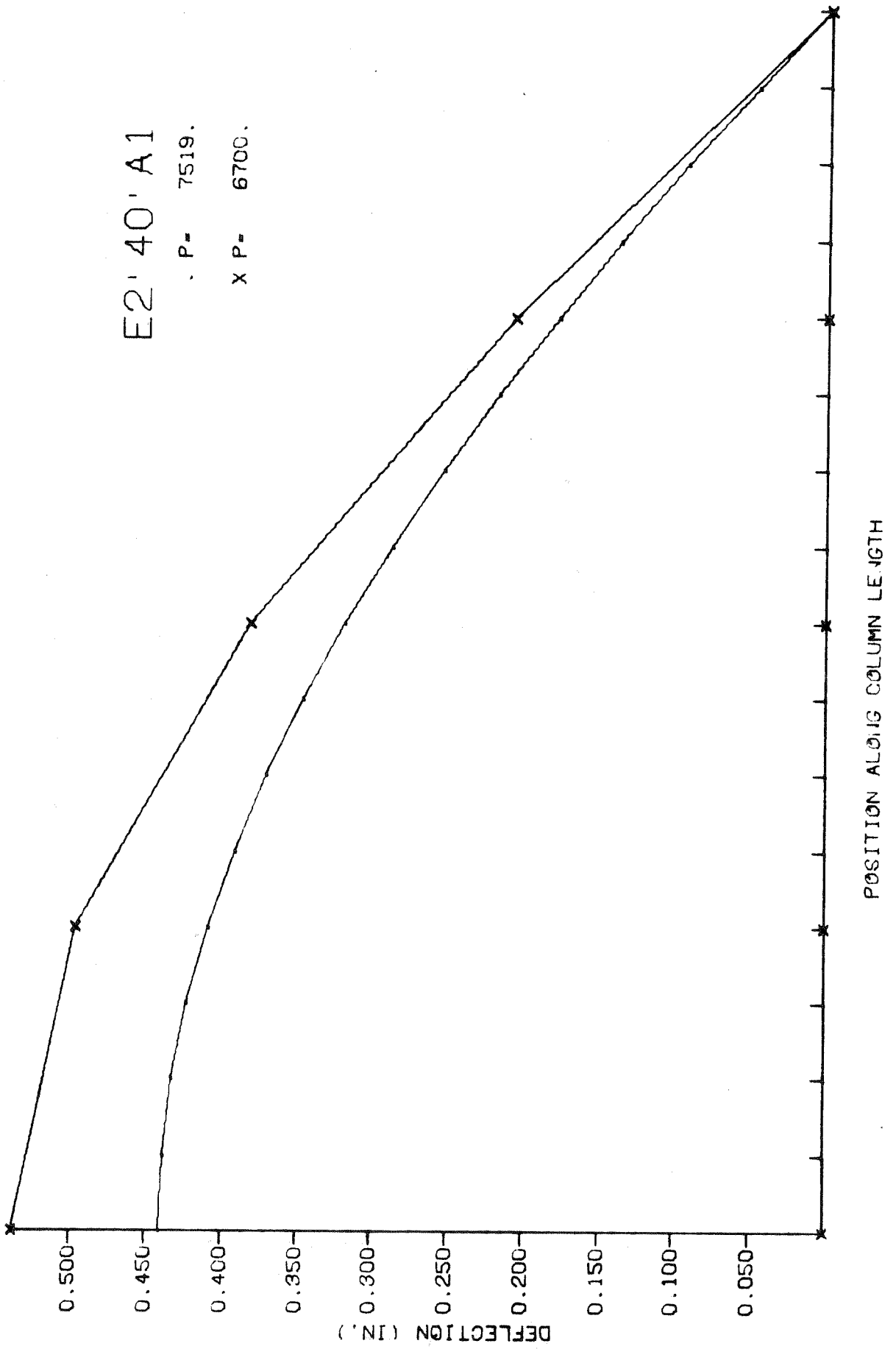


FIG. A26

F2' 20' B5

P = 5288.

X P = 5310.

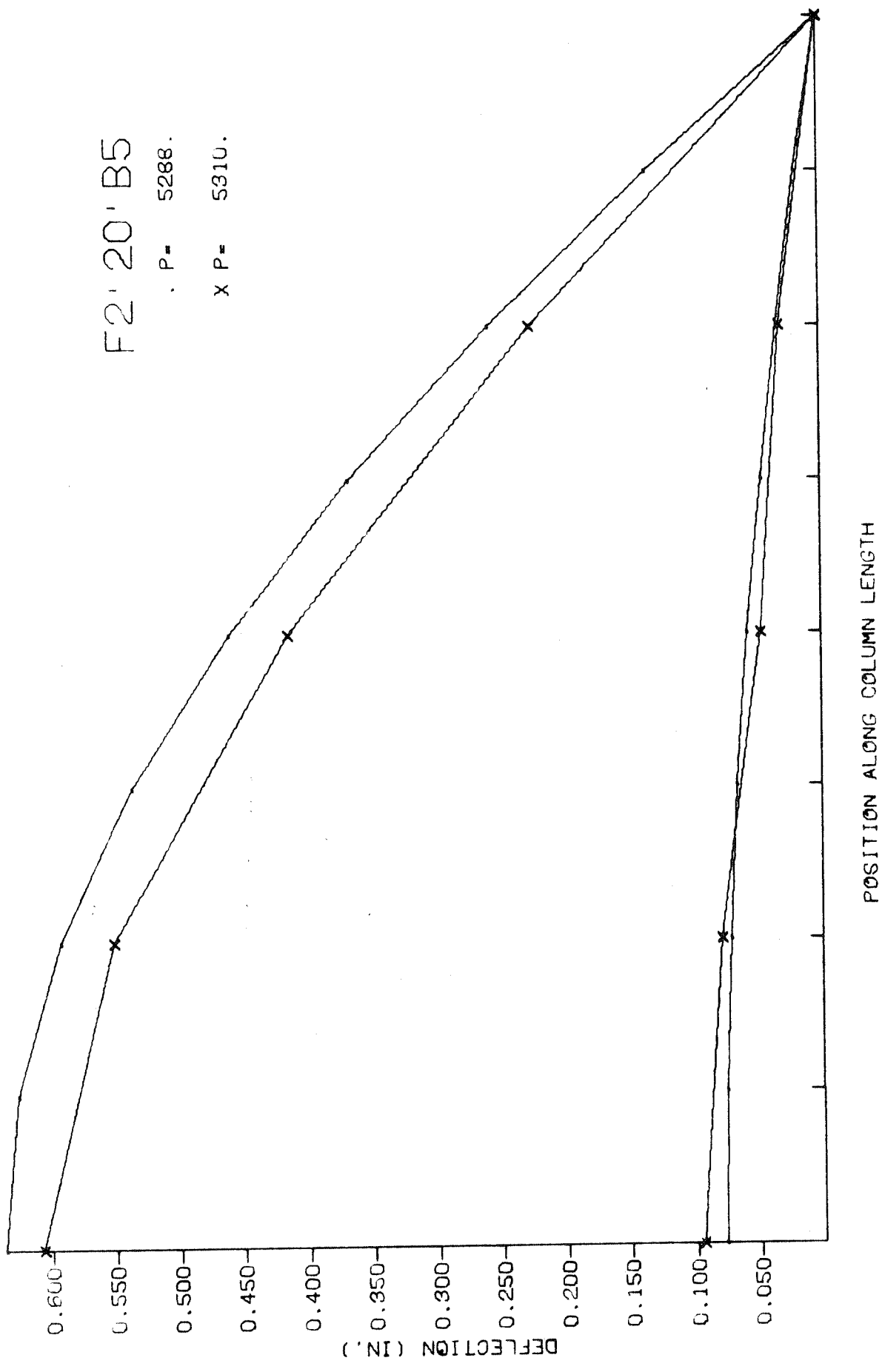


FIG. A27

APPENDIX B

Properties of Concrete Stress Block

General expressions for the magnitude and position of the resultant C of a concrete stress block are presented in this Appendix.

Fig. B1 shows the two cases considered.

Case 1

Here the concrete compressive stress block extends over a depth d_c , where $d_c \leq d$, with zero stress at one end.

From the stress-strain curve:

$$\text{Average Stress} = \frac{1}{\epsilon_4} \int_0^{\epsilon_4} f_c d\epsilon_c \quad (\text{B1})$$

The magnitude of the stress block resultant is thus

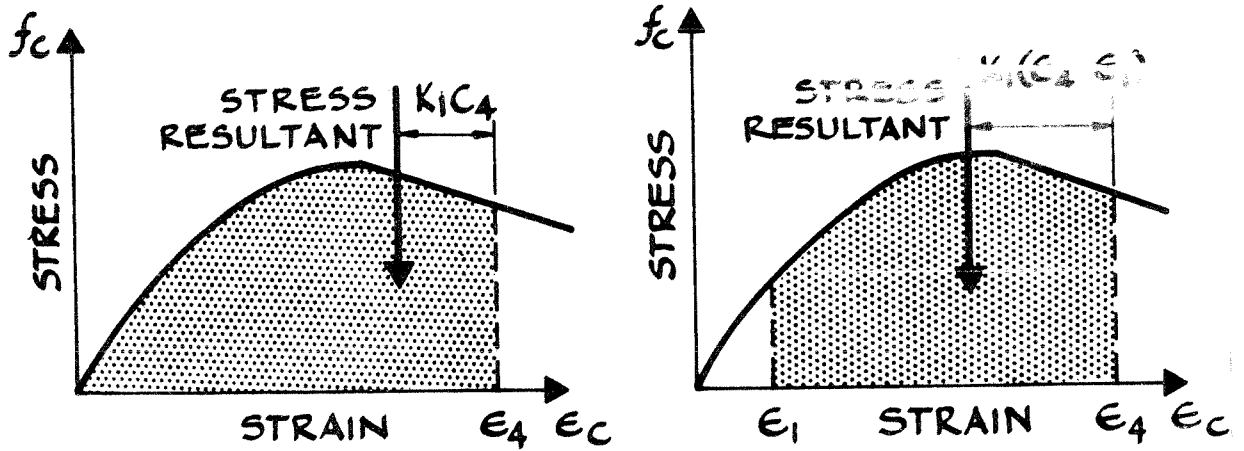
$$C = \frac{bd_c}{\epsilon_4} \int_0^{\epsilon_4} f_c d\epsilon_c \quad (\text{B2})$$

Also, from the geometry of the stress-strain curve and taking moments about the origin.

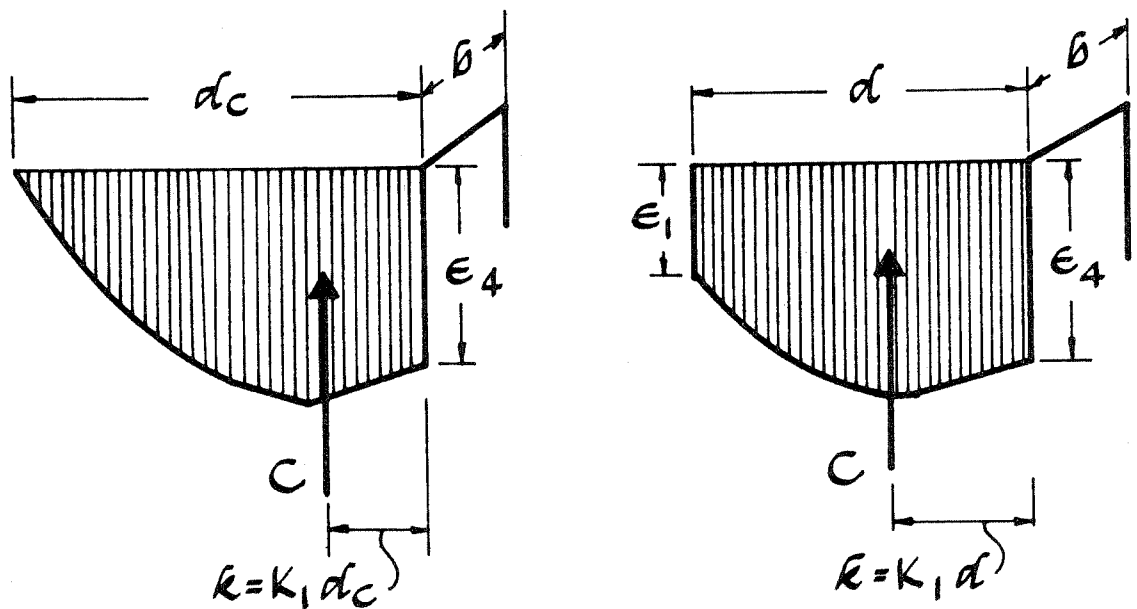
$$K_1 \epsilon_4 = \epsilon_4 - \frac{\int_0^{\epsilon_4} f_c \epsilon_c d\epsilon_c}{\int_0^{\epsilon_4} f_c d\epsilon_c} \quad (\text{B3})$$

Thus

$$k = K_1 d_c = d_c \left(1 - \frac{\int_0^{\epsilon_4} f_c \epsilon_c d\epsilon_c}{\int_0^{\epsilon_4} f_c d\epsilon_c} \right) \quad (\text{B4})$$



STRESS-STRAIN CURVES



CONCRETE STRESS BLOCKS

CASE 1

CASE 2

FIG. B1 PROPERTIES OF CONCRETE STRESS BLOCK

Case 2

Here the stress block extends over the full section depth d , with extreme strain values of ϵ_1 and ϵ_4 .

Again,

$$\text{Average Stress} = \frac{1}{\epsilon_4 - \epsilon_1} \int_{\epsilon_1}^{\epsilon_4} f_c d\epsilon_c \quad (\text{B5})$$

and

$$C = \frac{bd}{\epsilon_4 - \epsilon_1} \int_{\epsilon_1}^{\epsilon_4} f_c d\epsilon_c \quad (\text{B6})$$

Also,

$$K_1(\epsilon_4 - \epsilon_1) = \epsilon_4 - \frac{\int_{\epsilon_1}^{\epsilon_4} f_c \epsilon_c d\epsilon_c}{\int_{\epsilon_1}^{\epsilon_4} f_c d\epsilon_c} \quad (\text{B7})$$

and finally

$$k = K_1 d = d \left[\frac{\epsilon_4}{\epsilon_4 - \epsilon_1} - \frac{\int_{\epsilon_1}^{\epsilon_4} f_c \epsilon_c d\epsilon_c}{(\epsilon_4 - \epsilon_1) \int_{\epsilon_1}^{\epsilon_4} f_c d\epsilon_c} \right] \quad (\text{B8})$$

The integrals can be evaluated after substitution of $f_c = f(\epsilon_c)$.

Integration is carried out between the discontinuities of the stress-strain curve and the separate integrals added up.

APPENDIX C

Newton's Method of Tangents

The solution of simultaneous nonlinear equations can be performed by successive approximations, using Newton's method of tangents, (59) when initial values are available which are sufficiently close to the roots.

Consider two nonlinear equations

$$f(x,y) = 0 \quad \text{and} \quad h(x,y) = 0 \quad (C1)$$

and initial values x_0, y_0 for the unknowns x and y .

The first approximations are then given by

$$x_1 = x_0 + H \quad (C2)$$

$$y_1 = y_0 + G$$

where

$$H = - \frac{f_0 h_{y,0} - h_0 f_{y,0}}{f_{x,0} h_{y,0} - h_{x,0} f_{y,0}} \quad (C3)$$

and

$$G = - \frac{f_{x,0} h_0 - h_{x,0} f_0}{f_{x,0} h_{y,0} - h_{x,0} f_{y,0}} \quad (C4)$$

In Equations (C3) and (C4):

$$f_0 = f(x_0, y_0), \quad h_0 = h(x_0, y_0)$$

and

$$f_{x,o} = \left(\frac{\partial f}{\partial x} \right)_{x_o, y_o}$$

$$f_{y,o} = \left(\frac{\partial f}{\partial y} \right)_{x_o, y_o}$$

$$h_{x,o} = \left(\frac{\partial h}{\partial x} \right)_{x_o, y_o}$$

$$h_{y,o} = \left(\frac{\partial h}{\partial y} \right)_{x_o, y_o}$$

Similarly, further approximations are calculated until H and G are as small as required.

APPENDIX D

Equations of Equilibrium at a Section

This appendix presents the equations of equilibrium at a section, equations (4.37), for all seven strain distributions shown in Fig. D1.

Case 1

$$P+F_{s2}+F_{s3}-C_2(2\epsilon_4-\Delta\epsilon) - \frac{C_3}{\Delta\epsilon} [(\epsilon_4-\Delta\epsilon)^3 - \epsilon_4^3] = 0 \quad (D1)$$

and

$$\begin{aligned} \frac{\epsilon_4}{\Delta\epsilon} - \frac{F_{s2}(d'+d'') + F_{s3}d'' - P(y-0.5d)}{d(P+F_{s2}+F_{s3})} - C_7 \frac{\epsilon_4^3 - (\epsilon_4-\Delta\epsilon)^3}{(\Delta\epsilon)^2(P+F_{s2}+F_{s3})} \\ - C_8 \frac{(\epsilon_4-\Delta\epsilon)^4 - \epsilon_4^4}{(\Delta\epsilon)^2(P+F_{s2}+F_{s3})} = 0 \end{aligned} \quad (D2)$$

Case 2

$$P+F_{s2}+F_{s3} - \frac{1}{\Delta\epsilon} [C_9 - C_2(\epsilon_4-\Delta\epsilon)^2 + C_3(\epsilon_4-\Delta\epsilon)^3 + C_{13}\epsilon_4 - C_{14}\epsilon_4^2 - C_{12}] = 0 \quad (D3)$$

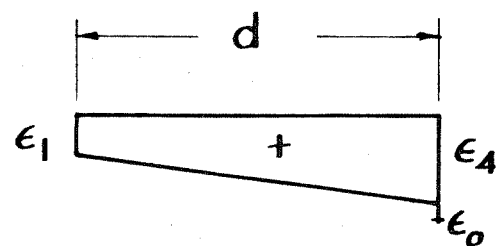
and

$$\begin{aligned} \frac{\epsilon_4}{\Delta\epsilon} - \frac{F_{s2}(d'+d'')+F_{s3}d'' - P(y-0.5d)}{d(P+F_{s2}+F_{s3})} \\ - \frac{1}{\Delta\epsilon^2(P+F_{s2}+F_{s3})} [C_{15} - C_7(\epsilon_4-\Delta\epsilon)^3 + C_8(\epsilon_4-\Delta\epsilon)^4 + C_{16}\epsilon_4^2 - C_{17}\epsilon_4^3 - C_{18}] = 0 \end{aligned} \quad (D4)$$

CASE 1

$$0 \leq \epsilon_1 < \epsilon_0$$

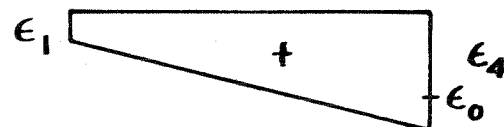
$$0 < \epsilon_4 \leq \epsilon_0$$



CASE 2

$$0 \leq \epsilon_1 < \epsilon_0$$

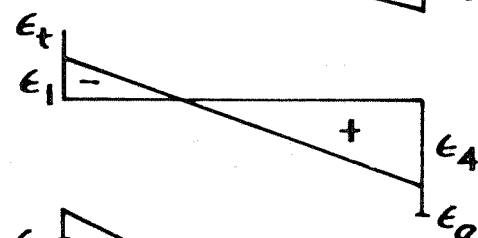
$$\epsilon_0 < \epsilon_4 \leq \epsilon_u$$



CASE 3

$$\epsilon_t \leq \epsilon_1 < 0$$

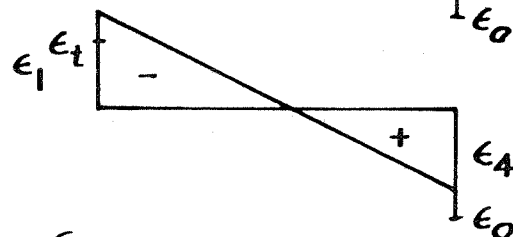
$$0 < \epsilon_4 \leq \epsilon_0$$



CASE 4

$$\epsilon_1 < \epsilon_t$$

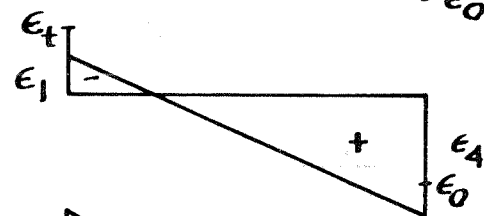
$$0 < \epsilon_4 \leq \epsilon_0$$



CASE 5

$$\epsilon_t \leq \epsilon_1 < 0$$

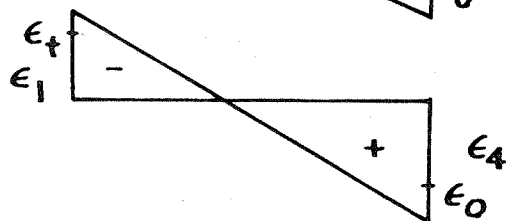
$$\epsilon_0 < \epsilon_4 \leq \epsilon_u$$



CASE 6

$$\epsilon_1 < \epsilon_t$$

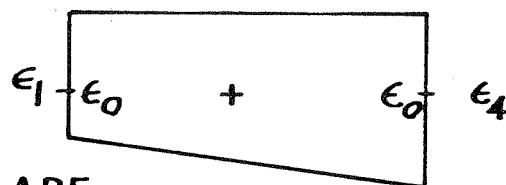
$$\epsilon_0 < \epsilon_4 \leq \epsilon_u$$



CASE 7

$$\epsilon_0 \leq \epsilon_1 < \epsilon_u$$

$$\epsilon_0 < \epsilon_4 \leq \epsilon_u$$



NOTE: COMPRESSIVE STRAINS ARE CONSIDERED POSITIVE.

FIG. D1 STRAIN DISTRIBUTION SEVEN CASES

Case 3

$$P + F_{s2} + F_{s3} - \frac{1}{\Delta\epsilon} \left[\epsilon_4^2 (C_2 - C_3 \epsilon_4) - C_{19} (\epsilon_4 - \Delta\epsilon)^2 \right] = 0 \quad (D5)$$

and

$$F_{s2} (d' + d'') + F_{s3} d''' + \frac{C_{19} d}{3\Delta\epsilon} (\epsilon_4 - \Delta\epsilon)^2 \left(2 + \frac{\epsilon_4}{\Delta\epsilon} \right) - P(y - 0.5d) - \frac{\epsilon_4^3 d}{\Delta\epsilon^2} (C_2 - C_3 \epsilon_4) \left(1 - \frac{C_7 - C_8 \epsilon_4}{C_2 - C_3 \epsilon_4} \right) = 0 \quad (D6)$$

Case 4

$$P + F_{s2} + F_{s3} + \frac{1}{\Delta\epsilon} \left[C_{20} - \epsilon_4^2 (C_2 - C_3 \epsilon_4) \right] = 0 \quad (D7)$$

and

$$F_{s2} (d' + d'') + F_{s3} d''' + \frac{C_{20} d}{\Delta\epsilon^2} (C_{21} + \epsilon_4) - P(y - 0.5d) - \frac{\epsilon_4^3 d}{\Delta\epsilon^2} (C_2 - C_3 \epsilon_4) \left(1 - \frac{C_7 - C_8 \epsilon_4}{C_2 - C_3 \epsilon_4} \right) = 0 \quad (D8)$$

Case 5

$$P + F_{s2} + F_{s3} + \frac{1}{\Delta\epsilon} \left[C_{19} (\epsilon_4 - \Delta\epsilon)^2 - C_{22} - C_{13} \epsilon_4 + C_{14} \epsilon_4^2 \right] = 0 \quad (D9)$$

and

$$F_{s2} (d' + d'') + F_{s3} d''' + \frac{C_{19} d}{3\Delta\epsilon} (\epsilon_4 - \Delta\epsilon)^2 \left(2 + \frac{\epsilon_4}{\Delta\epsilon} \right) - P(y - 0.5d) - \frac{1}{\Delta\epsilon^2} (C_{26} \epsilon_4 - C_{23} + C_{27} \epsilon_4^2 + C_{28} \epsilon_4^3) = 0 \quad (D10)$$

Case 6

$$P + F_{s2} + F_{s3} + \frac{1}{\Delta\epsilon} [C_{20} - C_{22} - C_{13} \epsilon_4 + C_{14} \epsilon_4^2] = 0 \quad (D11)$$

and

$$F_{s2} (d' + d'') + F_{s3} d'' + \frac{C_{20} d}{\Delta\epsilon} (C_{21} + \epsilon_4) - P(y - 0.5d) - \frac{1}{\Delta\epsilon} (C_{26} \epsilon_4 - C_{23} + C_{27} \epsilon_4^2 + C_{28} \epsilon_4^3) = 0 \quad (D12)$$

Case 7

$$P + F_{s2} + F_{s3} - C_{13} + 2 C_{14} \epsilon_4 - C_{14} \Delta\epsilon = 0 \quad (D13)$$

and

$$F_{s2} (d' + d'') + F_{s3} d'' - C_{24} - C_{14} d \epsilon_4 - P(y - 0.5d) + 2 C_{14} d \frac{\epsilon_4^2}{\Delta\epsilon} + \frac{C_{25}}{2} [(\epsilon_4 - \Delta\epsilon)^3 - \epsilon_4^3] = 0 \quad (D14)$$

The subscripted constants, used in the above equations, are

as follows:

$$C_2 = \frac{bd\alpha E_t}{2\beta}$$

$$C_3 = \frac{bd\alpha E_c^2}{10.2 \beta^2 f_c}$$

$$C_7 = \frac{2}{3} C_2$$

$$C_8 = \frac{3}{4} C_3$$

$$C_9 = \epsilon_o^2 (C_2 - C_3 \epsilon_o)$$

$$C_{10} = \frac{0.85 \gamma f_c' \alpha}{0.0038\beta - \epsilon_o}$$

$$C_{11} = 0.85 f_c' \alpha + C_{10} \epsilon_o$$

$$C_{12} = bd \epsilon_o (C_{11} - 0.5 C_{10} \epsilon_o)$$

$$C_{13} = bd C_{11}$$

$$C_{14} = 0.5 bd C_{10}$$

$$C_{15} = \epsilon_o^3 (C_7 - C_8 \epsilon_o)$$

$$C_{16} = 0.5 C_{13}$$

$$C_{17} = \frac{2}{3} C_{14}$$

$$C_{18} = \epsilon_o^2 (C_{16} - C_{17} \epsilon_o)$$

$$C_{19} = 0.5 bd E_t$$

$$C_{20} = C_{19} \epsilon_t^2$$

$$C_{21} = \frac{2}{3} \epsilon_t$$

$$C_{22} = C_9 - C_{12}$$

$$C_{23} = d (C_{15} - C_{18})$$

$$C_{24} = d C_{16}$$

$$C_{25} = d C_{17}$$

$$C_{26} = d C_{22}$$

$$C_{27} = d C_{13} - C_{24}$$

$$C_{28} = C_{25} - d C_{14}$$

APPENDIX E

Geometric Relations for Large Rotations

In the derivation of the geometric relations of Section 4.3.3 (Fig. 26(b) and (c)), the assumption was made that the rotations θ were small. Also the effect of axial strain on the column shape was neglected. This appendix presents the general equations, which do not include the above assumptions.

Fig. E1(a) shows the deflected shape of half the column length. For simplicity of presentation, the column is assumed to be initially straight. In general the number of nodal points is n and the number of finite elements $(n-1)$. The initial length l' includes prestress and creep shortening. Thus

$$l' = l (1 - \epsilon_{14}) \quad (E1)$$

For the initial straight shape, the creep strains

$$\epsilon_{c2} = \epsilon_{c3} = \epsilon_c \quad (E2)$$

The initial length of each element is

$$\Delta l' = \frac{l'/2}{n-1} \quad (E3)$$

Under a load P , the length of the i^{th} element becomes

$$V_i = \frac{l}{2(n-1)} \left[1 - \left(\frac{\epsilon_1 + \epsilon_4}{2} + \epsilon_c \right) \right] \quad (E4)$$

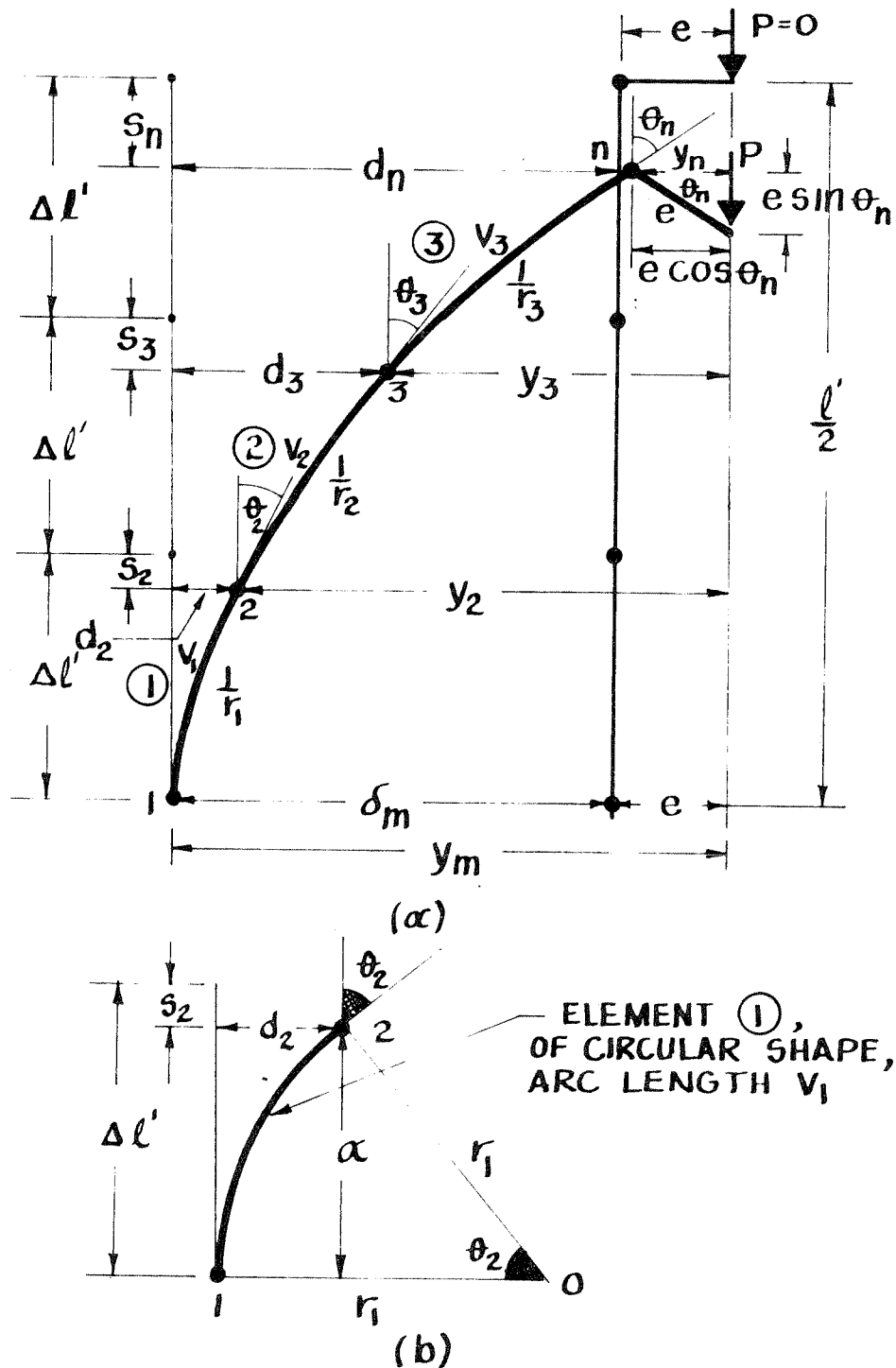


FIG. E1 GEOMETRY OF LARGE ROTATIONS

where

ϵ_1 and ϵ_4 are the extreme fiber strains in the particular i^{th} element.

The first element has boundary conditions $d_1 = 0$, $\theta_1 = 0$ and $s_1 = 0$, where s_i denotes the vertical movement of the i^{th} nodal point, due to load P.

From Fig. E1(b)

$$\theta_2 = \frac{V_1}{r_1} \quad (\text{E5})$$

$$d_2 = r_i (1 - \cos \theta_2) \quad (\text{E6})$$

and

$$S_2 = \Delta \ell' - r_1 \sin \theta_2 \quad (\text{E7})$$

It can be shown, from geometric considerations, that the recurrence relations are

$$d_i = d_{i-1} + \frac{r_{i-1}}{\cos \theta_{i-1}} \left[\sin \theta_{i-1} (\sin \theta_i - \sin \theta_{i-1}) \right] + \frac{r_{i-1}}{\cos \theta_{i-1}} \left(1 - \cos \frac{V_{i-1}}{r_{i-1}} \right) \quad (\text{E8})$$

$$\theta_i = \theta_{i-1} + \frac{V_{i-1}}{r_{i-1}} \quad (\text{E9})$$

and

$$S_i = \Delta \ell' + S_{i-1} - r_{i-1} (\sin \theta_i - \sin \theta_{i-1}) \quad (\text{E10})$$

Neglecting axial strains, i.e., assuming $V_i = \Delta\ell$, assuming small rotations, i.e., $\sin \theta = \theta$ and $\cos \theta = 1$, and using

$$\cos \frac{V_i}{r_i} = 1 - \frac{1}{2} \left(\frac{V_i}{r_i} \right)^2$$

we can convert (E6) into (4.42), (E8) into (4.46) and (E9) into (4.47).

Finally, the correct boundary condition is

$$y_n = e \cos \theta_n \tag{E11}$$

which becomes Equation (4.49) for small θ .

APPENDIX F

Upper Bound Method of Solution

This appendix describes the method of obtaining upper bound load solutions. These require the assumed constant curvature within each finite element to be equal to the curvature obtained from the solution of equilibrium equations at the top nodal point of the element. Thus, to obtain the upper bound load P , for a given total central deflection y_m , we must proceed from the top of the column towards the mid-height (see Fig. 26 (b)). There will be now two boundary conditions to be satisfied at the mid-height, namely

$$\theta_1 = 0 \quad (F1)$$

and

$$y_1 - y_m = 0 \quad (F2)$$

and two parameters at the top of the column, the top slope θ_n and the "stress curvature" $(\Delta\epsilon)_n$, to be obtained by iteration. This increases the difficulties of the iteration procedure and requires the use of some special optimization techniques. The calculation of the upper bound load, for each given value of y_m , is carried out immediately after the lower bound solution, for the given deflection, has been obtained. Thus, the lower bound values are available, where required, to serve as initial guesses in the upper bound solution.

The method of solution follows the following steps, for a given deflection y_m :

1. In the first iteration, values of load and top slope are assumed. The load is taken to be $E7xP$, when $E7$ is an assumed factor, larger than unity, and P is the lower bound solution. The assumed top slope θ_{n_1} is obtained from the lower bound slope, adjusted using the initial and final θ_n values for the upper bound solution at the previous deflection y_m . Using the above value of P and $y_n = e$, the appropriate equations of equilibrium are solved, at the top nodal point n , for the strain $(\epsilon_4)_{n_1}$ and the "stress curvature" $(\Delta\epsilon)_{n_1}$.
 2. Using the assumed θ_{n_1} , the calculated $(\Delta\epsilon)_{n_1}$, and the known value of d_n , the position of nodal point $(n-1)$, i.e., the value of d_{n-1} , and the slope θ_{n-1} are determined from equations (4.46) and (4.47).
 3. Next, the equations of equilibrium are solved at nodal point $(n-1)$, using Newton's method (App. C), for the unknown values of $(\Delta\epsilon)_{(n-1)_1}$ and $(\epsilon_4)_{(n-1)_1}$.
 4. The position of nodal point $(n-2)$ is found next and the equations of equilibrium solved as under step 3 above. This is repeated for each lower nodal point until y_1 and θ_1 are determined at nodal point 1.
 5. The required boundary conditions (F1) and (F2) can now be checked and, if these are not satisfied, further iterations are necessary.
- For this purpose, a criterion function F is defined

$$F = (y_1 - y_m)^2 + (E6x\theta_1)^2 \quad (F3)$$

where

$E6 =$ assumed numerical factor, to adjust the influence of θ_1
on F .

Since y_1 and θ_1 depend on the values θ_n and $(\Delta\epsilon)_n$, F is a positive function of these parameters (Fig. F1(a)). The boundary conditions are satisfied when $F=0$ and our aim is to determine, by iteration, the values of θ_n and $(\Delta\epsilon)_n$ which cause F to vanish, within a prescribed accuracy.

After the first iteration, the value $F(1)$, at point 1 in Fig. F1(b), can be calculated.

6. We aim next to determine the values of the F function in the vicinity of point 1, so that the direction of the maximum slope on the surface of the criterion function can be found, and we can proceed to iterate towards the required point of $F = 0$. Thus, we use in turn the θ_n and $(\Delta\epsilon)_n$ coordinates of points 2, 3, 4, and 5, and proceed to nodal point n to solve the equations of equilibrium, with the assumed $(\Delta\epsilon)_n$ and known $y_n = e$, for the unknowns P and $(\epsilon_4)_n$. Repeating steps 2, 3, and 4 above, for each point, we obtain the values of $F(2)$, $F(3)$, $F(4)$, and $F(5)$. The location of points 2,3,4, and 5 is determined in relation to the values of θ_{n_1} and $(\Delta\epsilon)_{n_1}$, by specifying the factors $FAC1$ and $FAC2$ used in

$$S1 = (\Delta\epsilon)_{n_1} (FAC1 - 1.0) \quad (F4)$$

and

$$S2 = \theta_{n_1} (FAC2 - 1.0) \quad (F5)$$

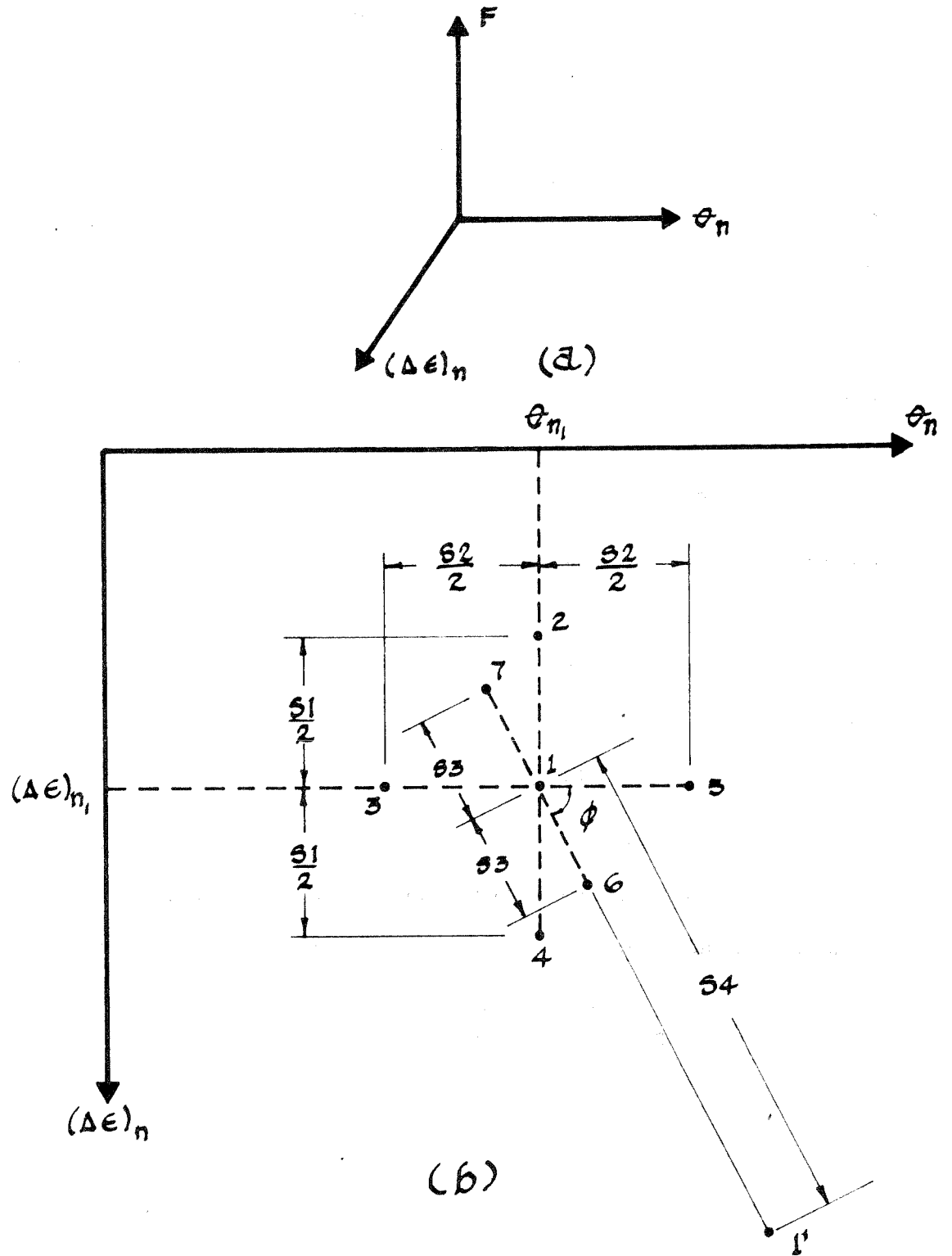


FIG. F1 UPPER BOUND
ITERATION PROCEDURE

7. The magnitude and direction of the maximum slope at point 1 can now be established, using central difference expressions. The maximum slope is given by the gradient vector. Its magnitude is

$$|\nabla F| = \sqrt{\left(\frac{\partial F}{\partial(\Delta\epsilon)_n}\right)^2 + \left(\frac{\partial F}{\partial\theta_n}\right)^2} \quad (\text{F6})$$

where

$$\frac{\partial F}{\partial(\Delta\epsilon)_n} = \frac{F(4) - F(2)}{S1}$$

and

$$\frac{\partial F}{\partial\theta_n} = \frac{F(5) - F(3)}{S2}$$

The direction ϕ is specified by

$$\cos \phi = \frac{\frac{\partial F}{\partial\theta_n}}{|\nabla F|} \quad (\text{F7})$$

and

$$\sin \phi = \frac{\frac{\partial F}{\partial(\Delta\epsilon)_n}}{|\nabla F|} \quad (\text{F8})$$

We proceed next to determine F(6) and F(7), where the coordinates of points 6 and 7 are obtained from the direction ϕ and assumed

$$S3 = \frac{1}{2} \sqrt{S1^2 + S2^2} \quad (\text{F9})$$

8. To determine the position of point 1', the central point of the next set of iterations, we first calculate an approximation to the second derivative at point 1, in the direction of the maximum slope

$$F'' = \frac{F(6) - 2F(1) + F(7)}{S_3^2} \quad (F10)$$

Finally,

$$S_4 = - \frac{|\nabla F|}{F''} \quad (F11)$$

The iterations are continued until, at any point in the procedure, the boundary conditions (F1) and (F2) are satisfied, within a prescribed accuracy.

APPENDIX GComputer Program

The listing of the computer program is presented in this appendix. The program is written in FORTRAN IV and was executed on an IBM 7094 computer, at the Computer Centre, University of California at Berkeley.

```

C          ANALYSIS OF SLENDER PRESTRESSED CONCRETE COLUMNS
C*****
  DIMENSION DEFIN(99),DEL(99),RADI(99),W(99),CURI(99),EPSI4(99),
  IYI(99),THETA(99),PDEL(99),PRADI(99),PW(99),PCURI(99),PEPSI4(99),
  2PYI(99),PTHETA(99),COLUMN(2),DELT(99),UCURI(99),URADI(99),
  3UDEL(99),UTHETA(99),UEPSI4(99),UW(99),UYI(99),F(8)
  COMMON AS
  CALL TIME (TI)

C
C INPUT AND OUTPUT OF DATA
C
101 READ 31, (COLUMN(I),I=1,2)
  31 FORMAT ( 2A5)
  READ 301,NF1,NF2,NF3,NF4,NF5,FAC1,FAC2,E5,E6,E7
301 FORMAT (5I4,5F10.0)
  READ 32,B,D,D1,D2,AS,FPRC,ALPHA,BETA,EPSPR,EPS23,EPS14
  32 FORMAT ( 7F10.0)
  READ 33,A,E1,E2,E3,EPSU,ET,NMAX,S,E,FT,DEFINC,DINC,E4,SLOPE
  33 FORMAT (6F10.0/I4/(F10.0))
  PRINT 34, (COLUMN(I),I=1,2)
  34 FORMAT (1H12A5)
  IF (NF1) 807,807,808
808 PUNCH 998
  998 FORMAT (6H -999.)
  PUNCH 997,(COLUMN(I),I=1,2),NMAX
  997 FORMAT (2A5,I10)
807 PRINT 35,S,E,B,D,D1,D2,AS
  35 FORMAT(22H0DATA- COLUMN DETAILS F10.1,5F10.2, F10.4)
  PRINT 36,FPRC,FT,ET,EPSU,ALPHA,BETA,SLOPE
  36 FORMAT (10H MATERIAL F10.0,F10.1,1PE15.2 ,0PF10.4,3F10.3)
  PRINT 37,A,E1,E2,E3,NMAX,DEFINC,DINC,E4
  37 FORMAT ( 9H PROGRAM F10.2,E15.2 , F5.0, F10.3, I5,F10.3,F10.1,
  1 F10.5)
  PRINT 887,FAC1,FAC2,E5,E6,E7
887 FORMAT (15H          2F10.4,F10.5,F10.1,F10.2)
  PRINT 38,EPSPR,EPS23,EPS14
  38 FORMAT (34H PRESTRESS AND INITIAL CONDITIONS 3F15.6)
C*****
C          CALCULATION OF CONSTANTS
C*****
  D6=D1+D2
  D4=D1/D
  D5=D2/D
  EC=1800000.0+391.0*FPRC
  EPS0=1.7*FPRC*BETA/EC
  EPST=FT/ET
  LAST=NMAX-1
  C2=B*D*ALPHA*EC/(2.0*BETA)
  C3=C2*EC/(5.1*BETA*FPRC)
  C7=2.0*C2/3.0
  C8=0.75*C3
  C9=EPS0**2*(C2-C3*EPS0)
  C10=0.85*SLOPE*FPRC*ALPHA/(0.0038*BETA-EPS0)
  C11=0.85*FPRC*ALPHA+C10*EPS0
  C12=B*D*EPS0*(C11-C10*0.5*EPS0)
  C13=B*D*C11

```

```

C14=0.5*D*B*C10
C15=EPS0**3*(C7-C8*EPS0)
C16=0.5*C13
C17=2.0*C14/3.0
C18=EPS0**2*(C16-C17*EPS0)
C19=0.5*B*D*ET
C20=EPST**2*C19
C21=2.0*EPST/3.0
C22=C9-C12
C23=D*(C15-C18)
C24=D*C16
C25=D*C17
C26=D*C22
C27=D*C13-C24
C28=C25-D*C14
C29=C15-C18
D3=D6/D
E8=(E6*E5)**2+E3**2
C*****
C   MAIN CONTROL
C*****
C
C   SET FLAGS, COUNTS AND SOME VARIABLES TO ZERO
C
C       NU=0
C       NEU=0
C       KL=0
C       KLM=0
C       M=0
C       MM=0
C       K=0
C       KK=0
C       THETA(1)=0.0
C       W(1)=0.0
C       PP=0.0
C       P=0.0
C       NE=0
C       ME=0
C       NF6=1
C
C   CHECK IF INITIAL CONDITIONS, AFTER CREEP, CORRESPOND TO AXIAL OR
C   ECCENTRIC PRESTRESS AND GO TO APPROPRIATE INITIAL CASE A OR B
C
C       IF(EPS23-EPS14) 2,1,2
C
C   RETURN AFTER CALCULATING INITIAL CONDITIONS
C   SET AND CALCULATE SOME STRAINS RELATED TO INITIAL CONDITIONS
C
102 EPS4I=EPS4
    EPS1I=EPS1
    EPSCLI=EPSCL
    EPSD2=EPSPR-EPSC2
    EPSD3=EPSPR-EPSC3
C
C   OUTPUT INITIAL CONDITION RESULTS
C

```

```

PRINT 39
39 FORMAT(18HOANALYSIS RESULTS )
PRINT 40
40 FORMAT (92H   LOAD   EPS1   EPSCL   EPS4   D(1)   D(2)   D(
13)   D(4)   D(5)   D(6)   D(7)   D(8)/95H
2           D(9)   D(10)  D(11)  D(12)  D(13)  D(14)  D(15)  D(1
36) )
PRINT 41,P, EPS1, EPSCL, EPS4, (DEFIN(N), N=1, 8)
41 FORMAT (F7.0, 3F10.5, 8F7.3)
IF(LAST-8) 43, 43, 42
42 IF(LAST-17) 626, 627, 627
627 PRINT 44, (DEFIN(N), N=9, 16)
GO TO 43
626 PRINT 44, (DEFIN(N), N=9, LAST)
44 FORMAT(37H                                     8F7.3)
C
C   SET *A* VARIABLES TO ZERO
C
43 A1=0
A2=0
A3=0
C
C   PUNCH RESULTS IF NF1=1
C
IF (NF1) 630, 630, 302
302 IF(LAST-17) 628, 629, 629
628 PUNCH 991, P, A1, A3, A2, (DEFIN(N), N=1, LAST)
GO TO 630
629 PUNCH 991, P, A1, A3, A2, (DEFIN(N), N=1, 16)
C
C   SET INITIAL STRAINS AND CURVATURES FOR ALL ELEMENTS.
C   WILL SERVE AS INITIAL VALUES FOR FIRST DEFLECTION INCREMENT
C
630 DO 26 N=1, LAST
EPSI4(N)=EPS4
26 CUR1(N)=CUR
C
C   INITIAL VALUES OF LOAD, CURVATURE AND STRAIN
C   FOR FIRST DEFLECTION INCREMENT
C
P=(3.14**2*EC*B*D**3*DEFINC)/((DEFINC+E)*12.0*S**2)
DEL(1)=DEFINC
CUR=(DEL(1)+DEFIN(1))*D*(3.1416/S)**2-CURCOR
EPS4=EPS4+CUR/2.0+P/(B*D*EC)
C
C   BEGINNING OF CALCULATIONS FOR PARTICULAR DEFLECTION DEL(1)
C   SET CURRENT Y=PARTICULAR YI(1) AND CURRENT CUR=SINE APPROXIMATION
C   GO TO CASE A TO CALCULATE LOAD P AND STRAIN EPS4 AT MID-HEIGHT
C
500 YI(1)=E+DEFIN(1)+DEL(1)
CUR=(DEL(1)+DEFIN(1))*D*(3.1416/S)**2-CURCOR
Y=YI(1)
GO TO 5
C
C   RETURN FROM CASE A
C   STORE VALUES OF EPS4, EPS1 AND CUR FOR FIRST ELEMENT (LOWER END)

```

```

C CALCULATE RADIUS OF CURVATURE
C
108 EPSI4(1)=EPS4
    IF (NF3) 809,809,810
810 PRINT 192 ,CUR,Y,P,EPS4,EPS1
192 FORMAT (8H 108 5E20.5)
809 EPS11=EPS1
    CURI(1)=CUR
    RADI(1)=D/(CURI(1)+CURCOR)
C
C START DO LOOP FOR THE REMAINING ELEMENTS
C CALCULATE DEFLECTION AND ROTATION
C
    DO 109 N=2,NMAX
    W(N)=W(N-1)+A*THETA(N-1)+A**2/(2.0*RADI(N-1))
    YI(N)=YI(1)-W(N)
    IF(N-NMAX) 110,111,111
110 THETA(N)=THETA(N-1)+A/RADI(N-1)
    DEL(N)=YI(N)-DEFIN(N)-E
    Y=YI(N)
C
C AS INITIAL GUESSES SET CURRENT CUR AND EPS4 EQUAL TO
C VALUES OF LOWER ELEMENT
C GO TO CASE B TO CALCULATE CURVATURE CUR AND
C STRAIN EPS4 FOR GIVEN P AND Y
C
    CUR=CURI(N-1)
    EPS4=EPSI4(N-1)
    IF(CUR) 13,799,13
799 CUR=0.00001
    GO TO 13
C
C RETURN FROM CASE B
C STORE VALUES OF EPS4 AND CUR, CALCULATE RADIUS OF CURVATURE
C
99 EPSI4(N)=EPS4
    IF (NF3) 811,811,812
812 PRINT 182 ,CUR,Y,P,EPS4,EPS1
182 FORMAT (8H 99 5E20.5)
811 CURI(N)=CUR
109 RADI(N)=D/(CURI(N)+CURCOR)
C
C CHECK ERROR IN BOUNDARY CONDITIONS
C IF ERROR SMALL ENOUGH WE HAVE FINISHED FOR THIS DEL(1).
C GO TO 200
C IF ERROR TOO LARGE PROCEED TO CHECK COUNT
C
111 ERROR=YI(NMAX)-E
    IF (NF3) 813,813,814
814 PRINT 180,ERROR
180 FORMAT (10H ERROR E20.5)
813 IF(ABS (ERROR)-E3) 200,200,100
100 IF (NE) 170,170,169
C
C FIRST COLUMNWISE ITERATION (NE=0), STORE ERROR AND CURI(1),
C RESET FOR NEW APPROXIMATION OF CUR, SET COUNT AND

```

```

C   START NEW ITERATION BY GOING TO 52
C
170 CUR=CURI(1)+ERROR*9.0*D/S**2
    PERROR=ERROR
    CURP=CURI(1)
    NE=1
    GO TO 52

C
C   SUBSEQUENT COLUMNWISE ITERATIONS.
C   IF COUNT EXCEEDED TERMINATE BY GOING TO 117
C   OTHERWISE CORRECT CUR, SET Y AND EPS4 FOR MID-HEIGHT AND
C   START NEW ITERATION BY GOING TO 5 (SELECTION OF APPROPRIATE CASE A)
C
169 IF (NE-50) 168,601,601
601 PRINT 602
602 FORMAT ( 25H COLUMN DOES NOT CONVERGE)
    GO TO 117
168 NE=NE+1
    CUR=CURI(1)+ERROR*(CURP-CURI(1))/(ERROR-PERROR)
    CURP=CURI(1)
    PERROR=ERROR
52 Y=YI(1)
    IF (NF3) 815,815,816
816 PRINT 179 ,CUR,Y,P,EPS4,EPS1
179 FORMAT (8H 52 5E20.5)
815 EPS4=EPSI4(1)
    GO TO 5

C
C   PROCEED TO NEW SET OF CALCULATIONS (NEW P-Y POINT)
C   CHECK FIRST IF WE ARE IN THE PROCESS OF FINDING MATERIAL FAILURE POINT
C   EPS4=EPSU (I.E. IF KL IS GREATER THAN ZERO)
C   IF KL=0, CHECK MAGNITUDE OF EPS4 AT MID-HEIGHT
C       1. IF SMALL, CONTINUE TO 201
C       3. IF GREATER THAN EPSU, GO TO 203
C       2. IF EQUAL TO EPSU, SET KLM=1, PRINT AND TERMINATE
C   IF KL IS GREATER THAN ZERO, CHECK IF WITHIN LIMIT E4
C       1. IF YES, PROCEED AS UNDER 2. ABOVE
C       2. IF NO, PROCEED AS UNDER 3. ABOVE
C
200 IF(KL) 53,53,54
54 IF(ABS (EPSU-EPSI4(1))-E4) 202,202,203
53 IF(EPSI4(1)-EPSU) 201,202,203

C
C   SET KLM=1 IF READY TO PRINT MATERIAL FAILURE AND TERMINATE
C
202 KLM=1

C
C   BEFORE PROCEEDING TO NEW SET OF CALCULATIONS, OUTPUT RESULTS
C
201 A1=EPSI1-EPS11
    A2=EPSI4(1)-EPS41
    A3=(A1+A2)/2.0
    PRINT 58,P,A1,A3,A2,(DEL(N),N=1,8) ,NE
58 FORMAT ( F7.0,3F10.5,8F 7.3,I10)
    IF(LAST-8) 61,61,59
59 IF (LAST-17) 631,632,632

```



```

632 PRINT 60,(DEL(N),N=9,16)
      GO TO 61
631 PRINT 60,(DEL(N),N=9,LAST)
      60 FORMAT(37H
C
C   RESET COLUMNWISE COUNT
C
      61 NE=0
C
C   PUNCH RESULTS IF NF1=1
C
      IF (NF1) 639,639,303
303 DO 992 N=1, LAST
992 DELT(N)=DEL(N)+DEFIN(N)
      IF (LAST-17) 993,634,634
993 PUNCH 991,P,A1,A3,A2,(DELT(N),N=1, LAST)
991 FORMAT(F10.0,3F10.6/16F5.3)
      GO TO 639
634 PUNCH 991,P,A1,A3,A2,(DELT(N),N=1,16)
C
C   IF NF2=1 GO TO CALCULATE UPPER BOUND
C
      639 IF (NF2) 633,633,640
C
C   BACK FROM UPPER BOUND CALCULATIONS
C   CHECK FLAGS CONCERNED WITH DETERMINING MAXIMUM LOAD
C   WITH SMALLER DEFLECTION INCREMENTS
C
      633 IF(MM) 62,62,400
      62 IF(M) 63,63,1200
      63 IF(K) 64,64,600
      64 IF(P-PP) 300,300,700
C
C   HERE THE LOAD IS STILL INCREASING AND WE SHALL STORE PRESENT VALUES
C   TO BE ABLE TO RETURN AFTER THE MAXIMUM LOAD IS PASSED
C
      700 PP=P
          PEPSI1=EPSI1
          DO 65 N=1,NMAX
          PDEL(N)=DEL(N)
          PRADI(N)=RADI(N)
          PW(N)=W(N)
          PCURI(N)=CURI(N)
          PEPSI4(N)=EPSI4(N)
          PYI(N)=YI(N)
          65 PTHETA(N)=THETA(N)
C
C   COME HERE FROM 633 (OR 73) IF MM=1, WHICH IS AFTER
C   THE MAXIMUM LOAD HAS BEEN INVESTIGATED AND PRINTED OUT.
C   HERE WE NEED STORE ONLY DEL AND EPSI4(1)
C
      400 PDEL(1)=DEL(1)
          PEPSI4(1)=EPSI4(1)
C
C   WHEN KLM=1, THE MATERIAL FAILURE POINT HAS BEEN PRINTED OUT AND
C   WE ARE READY TO TERMINATE

```

8F7.3)

```

C
      IF(KLM) 66,66,117
C
C   INCREASE THE DEFLECTION BY THE REQUIRED INCREMENT
C   RESET EPS4 TO MID-HEIGHT
C AND FINALLY RETURN TO 500 FOR A NEW SET OF CALCULATIONS
C
      66 DEL(1)=DEL(1)+DEFINC
        EPS4=EPSI4(1)
        GO TO 500
C *****
C
C HERE THE LOAD HAS JUST DECREASED FOR THE FIRST TIME
C   THEREFORE SET K=1
C
      300 K=1
C
C RETURN TO PREVIOUS VALUES
C
      1000 P=PP
        EPSI1=PEPSI1
        DO 67 N=1,NMAX
          DEL(N)=PDEL(N)
          RADI(N)=PRADI(N)
          W(N)=PW(N)
          CURI(N)=PCURI(N)
          EPSI4(N)=PEPSI4(N)
          YI(N)=PYI(N)
        67 THETA(N)=PTHETA(N)
C
C CHECK IF THE LOAD HAS DECREASED FOR THE FIRST TIME (M=0) OR
C   AFTER A PREVIOUS RETURN (M=1)
C IF M=0, WILL INCREASE THE DEFLECTION BY GOING TO 1400
C IF M=1, WILL DECREASE THE DEFLECTION BY GOING TO 1100
C
      IF(M) 1400,1400,1100
C
C INCREASE THE DEFLECTION BY REDUCED INCREMENT, RESET EPS4 AND
C   RETURN TO 500 FOR A NEW SET OF CALCULATIONS
C
      1400 DEL(1)=DEL(1)+DEFINC/DINC
        EPS4=EPSI4(1)
        GO TO 500
C *****
C
C WE HAVE PREVIOUSLY RETURNED (K=1) AND ARE INVESTIGATING THE LOAD FOR
C THE REDUCED FORWARD DEFLECTION INCREMENTS
C   (IF KK=1, I.E. THE LOAD KEPT INCREASING, GOTO 1500)
C IF THE LOAD INCREASED, GO TO 800
C IF THE LOAD IS THE SAME IT IS THE MAXIMUM, GO TO 1300
C IF THE LOAD DECREASED, GO TO 900
C
      600 IF(KK) 68,68,1500
        68 IF(P-PP) 900,1300,800
C
C WE HAVE NOT RETURNED SUFFICIENTLY FAR. SET M=1, GO TO 1000 TO RESET

```

```

C          PREVIOUS VALUES AND PROCEED TO 1100
C
C    900 M=1
C        GO TO 1000
C
C    DECREASE THE DEFLECTION BY THE REDUCED INCREMENT
C    RESET EPS4 AND RETURN TO 500
C    FOR A NEW SET OF CALCULATIONS
C
C    1100 DEL(1)=DEL(1)-DEFINC/DINC
C        EPS4=EPSI4(1)
C        GO TO 500
C *****
C
C WE HAVE COME HERE FROM 62, AFTER HAVING RETURNED AT LEAST TWICE (M=1)
C IF NEW LOAD STILL HIGHER, GO TO 1100 AND RETURN FURTHER
C IF NEW LOAD EQUAL OR LOWER, THE MAXIMUM HAS BEEN REACHED,GO TO 1300
C
C    1200 IF(P-PP) 1300,1300,1100
C
C        THE MAXIMUM LOAD HAS BEEN REACHED
C        OUTPUT IT A SECOND TIME AND CONTINUE TO 400
C
C    1300 A1=EPSI1-EPSI1
C        A2=EPSI4(1)-EPS4I
C        A3=(A1+A2)/2.0
C        PRINT 69,P,A1,A3,A2,(DEL(N),N=1,8) ,NE
C    69  FORMAT (F7.0,3F10.5 ,8F 7.3,I10)
C        IF(LAST-8) 72,72,70
C    70  IF (LAST-17) 635,636,636
C    636 PRINT 71,(DEL(N),N=9,16)
C        GO TO 72
C    635 PRINT 71,(DEL(N),N=9,LAST)
C        71  FORMAT(37H                                8F7.3)
C        72  NE=0
C
C    PUNCH RESULTS IF NF1=1
C
C        IF (NF1) 638,638,304
C    304 DO 892 N=1, LAST
C    892 DELT(N)=DEL(N)+DEFIN(N)
C        IF (LAST-17) 893,637,637
C    893 PUNCH 991,P,A1,A3,A2,(DELT(N),N=1, LAST)
C        GO TO 638
C    637 PUNCH 991,P,A1,A3,A2,(DELT(N),N=1,15)
C
C    WHEN KLM=1, THE MATERIAL FAILURE POINT HAS BEEN PRINTED OUT AND
C    WE ARE READY TO TERMINATE
C
C    638 IF(KLM) 73,73,117
C
C    AT THIS POINT WE HAVE FINISHED INVESTIGATING MAXIMUM LOAD
C    SET MM=1 AND GO TO 400 TO PROCEED WITH THE USUAL DEFLECTION INCREMENT
C
C    73  MM=1
C        GO TO 400

```

```

C
C THE LOAD HAS INCREASED AFTER RETURNING AND
C CONTINUING WITH REDUCED INCREMENT
C SET KK=1 AND GO TO 1400 FOR ADDITIONAL FORWARD REDUCED INCREMENT
C
      800 KK=1
          GO TO 1400
C
C HERE KK=1 (I.E. THE LOAD HAS PREVIOUSLY INCREASED AFTER RETURNING)
C IF THE LOAD KEEPS INCREASING,
C GO TO 1400 FOR A FURTHER FORWARD REDUCED INCREMENT
C IF THE LOAD IS SAME OR DECREASES, THE MAXIMUM HAS BEEN REACHED
C
          GO TO 1300
C
      1500 IF(P-PP) 1300,1300,1400
C *****
C INITIAL CONDITIONS CASE B
C *****
C
C CASE OF AXIAL PRESTRESS AFTER CREEP, DIRECT SOLUTION POSSIBLE
C
      1 EPSS2=EPSPR-EPS14
        EPSS3=EPSS2
        C1=FORS(EPSS2)+FORS(EPSS3)
        EPS4=(2.0*C2-SQRT ((2.0*C2)**2-12.0*C3*C1))/(6.0*C3)
        EPS1=EPS4
        EPSCL=EPS4
        EPSC2=EPS14-EPS4
        EPSC3=EPSC2
        CURIN=0.0
        CURCOR=0.0
        CUR=0.0
        DO 74 N=1, LAST
      74 DEFIN(N)=0.0
          GO TO 102
C *****
C INITIAL CONDITIONS CASE A- SOLUTION BY NEWTONS METHOD
C *****
C
C CASE OF ECCENTRIC PRESTRESS AFTER CREEP,
C ITERATION SOLUTION FOR EPS4 AND EPS1
C PRELIMINARY CALCULATIONS
C
      2 EPSS3=EPSPR-(EPS14+(EPS23-EPS14)*D4)
        EPSS2=EPSPR-(EPS14-(EPS23-EPS14)*D4)
        C1=FORS(EPSS2)+FORS(EPSS3)
        C4=(FORS(EPSS2)*D6+FORS(EPSS3)*D2)/(D*C1)
        C5=(2.0*C2)/(3.0*C1)
        C6=0.75*C3/C1
C
C INITIAL VALUES
C
        EPS4=0.3*EPS23
        EPS1=(2.0*EPS14-EPS23)*0.75
C
C ITERATION BEGINS

```

```

C
21 CUR=EPS4-EPS1
   B1=EPS4**3-EPS1**3
   B2=EPS4**4-EPS1**4
   FN1=C2*(EPS4+EPS1)-C3*B1/CUR-C1
   FN2=EPS4/CUR-C4-(C5*B1-C6*B2)/CUR**2
   B3=3.0*C3/CUR
   B4=C3/CUR**2
   DEXFN1=C2-B3*EPS4**2+B4*B1
   DEYFN1=C2+B3*EPS1**2-B4*B1
   B5=2.0*(C5*B1-C6*B2)/CUR**3
   DEXFN2=-EPS1/CUR**2-(3.0*C5*EPS4**2-4.0*C6*EPS4**3)/CUR**2+B5
   DEYFN2=EPS4/CUR**2-(4.0*C6*EPS1**3-3.0*C5*EPS1**2)/CUR**2-B5
   B6=DEXFN1*DEYFN2-DEXFN2*DEYFN1
   H=(FN2*DEYFN1-FN1*DEYFN2)/B6
   G=(FN1*DEXFN2-FN2*DEXFN1)/B6
   EPS1=EPS1+G
   EPS4=EPS4+H
   IF (ABS (H)-E1) 22,22,21
22 IF (ABS (G)-F1) 24,24,21
C
C VALUES WITHIN PRESCRIBED BOUNDS. CALCULATE CREEP CURVATURE CURCOR
C
24 CUR=EPS4-EPS1
   EPSC1=0.5*(EPS4+EPS1)
   EPSC2=EPSPR-EPSS2-EPS4+D3*CUR
   EPSC3=EPSPR-EPSS3-EPS4+D5*CUR
   CURIN=CUR
   CURCOR=(EPSC3-EPSC2)/D4
C
C CALCULATE INITIAL DEFLECTIONS
C
   RADI(1)=D/(CURIN+CURCOR)
   DEFIN(1)=S**2/(8.0*RADI(1))
   B7=A/RADI(1)
   B8=B7*A/2.0
   DO 25 N=2, LAST
   W(N)=W(N-1)+A*THETA(N-1)+B8
   THETA(N)=THETA(N-1)+B7
25 DEFIN(N)=DEFIN(1)-W(N)
   GO TO 102
C *****
C SELECTION OF APPROPRIATE CASE A
C *****
5 EPS1=EPS4-CUR
  IF (EPS1) 27,28,28
27 IF (EPST+EPS1) 29,30,30
28 IF (EPS4) 617,616,616
616 IF (EPS1-EPS0) 612,612,613
617 IF (EPST+EPS4) 618,619,619
618 IF (EPS1-EPS0) 9,9,11
619 IF (EPS1-EPS0) 8,8,10
612 IF (EPS4-EPS0) 6,6,7
613 IF (EPS4-EPS0) 7,7,610
29 IF (EPS4-EPS0) 9,9,11
30 IF (EPS4-EPS0) 8,8,10

```

C CASE 1A

C-----
 6 EPSS2=EPD2-EP4+D3*CUR
 IF (NF3) 817,817,818
 818 PRINT 199 ,CUR,Y,P,EP4,EP1
 199 FORMAT (8H 1A 5E20.5)
 817 EPSS3=EPD3-EP4+D5*CUR
 B1=P+FOR(EPSS2)+FOR(EPSS3)
 B7=DEFOR(EPSS2)+DEFOR(EPSS3)
 B8=EP4**3-EP1**3
 FN1=B1-C2*(2.0*EP4-CUR)+C3*B8/CUR
 DEXFN1=1.0
 DEYFN1=-2.0*C2+3.0*C3*(EP4**2-EP1**2)/CUR-B7
 B2=CUR**2*B1
 B3=B2*B1
 B4=D*B1
 B5=B4*B1
 B6=FOR(EPSS2)*D6+FOR(EPSS3)*D2-P*(Y-0.5*D)
 B9=EP1**4-EP4**4
 FN2=EP4/CUR-B6/B4-(C7*B8+C8*B9)/B2
 DEXFN2=(B6-B1*(0.5*D-Y))/B5+(C7*B8+C8*B9)/B3
 DEYFN2=1.0/CUR+(B1*(D6*DEFOR(EPSS2)+D2*DEFOR(EPSS3))-
 1B6*B7)/B5-(B1*3.0*C7*(EP4**2-EP1**2)+C7*B8*B7-B1*4.0*C8*
 2B8+C8*B9*B7)/B3
 GO TO 12

C CASE 2A

C-----
 7 EPSS2=EPD2-EP4+D3*CUR
 IF (NF3) 819,819,820
 820 PRINT 198 ,CUR,Y,P,EP4,EP1
 198 FORMAT (8H 2A 5E20.5)
 819 EPSS3=EPD3-EP4+D5*CUR
 B1=P+FOR(EPSS2)+FOR(EPSS3)
 B2=CUR**2*B1
 B3=B2*B1
 B4=D*B1
 B5=B4*B1
 B6=FOR(EPSS2)*D6+FOR(EPSS3)*D2-P*(Y-0.5*D)
 B7=DEFOR(EPSS2)+DEFOR(EPSS3)
 B8=EP1**2
 B9=B8*EP1
 B10=C7-C8*EP1
 B11=-C16+C17*EP4
 B12=C29-B11*EP4**2-B10*B9
 FN1=B1-(C22-B8*(C2-C3*EP1)-EP4*(C14*EP4-C13))/CUR
 DEXFN1=1.0
 DEYFN1=-B7+(EP1*(2.0*C2-3.0*C3*EP1)-C13+2.0*C14*EP4)/CUR
 FN2=EP4/CUR-B6/B4-B12/B2
 DEXFN2=(B6-B1*(0.5*D-Y))/B5+B12/B3
 DEYFN2=1.0/CUR+(B1*(D6*DEFOR(EPSS2)+D2*DEFOR(EPSS3))-
 1B6*B7)/B5-(B1*(-EP4*(-2.0*C16+3.0*C17*EP4)+B8*(C8*EP1-
 23.0*B10))+B12*B7)/B3
 GO TO 12

C CASE 3A

C-----
 8 EPSS2=EPD2-EP4+D3*CUR

```

      IF (NF3) 821,821,822
822 PRINT 197 ,CUR,Y,P,EPS4,EPSS1
197 FORMAT (8H 3A 5E20.5)
821 EPSS3=EPSS2-EPSS4+D5*CUR
      B1=P+FORSS(EPSS2)+FORSS(EPSS3)
      B2=C2-C3*EPS4
      B3=EPS4**2
      B4=C19*EPSS1**2
      B5=C7-C8*EPS4
      B6=B5/B2
      B7=2.0+EPS4/CUR
      B8=D*C19*EPSS1/(3.0*CUR)
      B9=B2*B3
      B10=EPSS1/CUR
      B11=(D*EPS4)/CUR**2
      FN1=B1-(B9-B4)/CUR
      DEXFN1=1.0
      DEYFN1=-DEFORS(EPSS2)-DEFORS(EPSS3)-EPS4*(2.0*B2-C3*EPS4)/CUR+
12.0*C19*B10
      FN2=FORSS(EPSS2)*D6+FORSS(EPSS3)*D2-P*(Y-0.5*D)+
188*EPSS1*B7-(1.0-B6)*B11*B9
      DEXFN2=D/2.0-Y
      DEYFN2=-D6*DEFORS(EPSS2)-D2*DEFORS(EPSS2)+B8*(2.0*B7+B10)-
1811*(EPS4*(3.0*C2-4.0*C3*EPS4)*(1.0-B6)+B3*B2*(1.0+(B2*C8-
2B5*C3)/B2**2))
      GO TO 12
C     CASE 4A
C-----
9 EPSS2=EPSS2-EPSS4+D3*CUR
      IF (NF3) 823,823,824
824 PRINT 196 ,CUR,Y,P,EPS4,EPSS1
196 FORMAT (8H 4A 5E20.5)
823 EPSS3=EPSS2-EPSS4+D5*CUR
      B1=C2-C3*EPS4
      B2=EPS4/CUR
      B3=B2*EPS4
      B4=C7-C8*EPS4
      B5=B4/B1
      B6=D/CUR
      B7=C20/CUR
      B8=B7*B6
      B9=Y-D/2.0
      B10=B6*B3
      B11=B10*EPS4
      B12=FORSS(EPSS2)
      B13=FORSS(EPSS3)
      B14=DEFORS(EPSS2)
      B15=DEFORS(EPSS3)
      FN1=P+B12+B13+B7-B3*B1
      DEXFN1=1.0
      DEYFN1=-B14-B15-2.0*B2*B1+B3*C3
      FN2=B12*D6+B13*D2+B8*(C21+EPS4)-P*B9-B11*B1*(1.0-B5)
      DEXFN2=-B9
      DEYFN2=-D6*B14-D2*B15+B8-B10*(3.0*C2-4.0*EPS4*C3)*(1.0-B5)-
1811*B1*(1.0-(C3*B5-C8)/B1)
      GO TO 12

```

C CASE 5A

C-----
 10 EPSS2=EPSD2-EPS4+D3*CUR
 IF (NF3) 825,825,826
 826 PRINT 195 ,CUR,Y,P, EPS4, EPS1
 195 FORMAT (8H 5A 5E20.5)
 825 EPSS3=EPSD3-EPS4+D5*CUR
 B1=FORs(EPSS2)
 B2=FORs(EPSS3)
 B3=DEFORs(EPSS2)
 B4=DEFORs(EPSS3)
 B5=2.0+EPS4/CUR
 B6=C19*EPS1/CUR
 B7=B6*EPS1
 B8=D*B6*B5/3.0
 B9=Y-D/2.0
 B10=C13/CUR
 B11=C14*EPS4/CUR
 B12=1.0/CUR**2
 B13=EPS4**2
 B14=B13*EPS4
 FN1=P+B1+B2+B7-C22/CUR-EPS4*(B10-B11)
 DEXFN1=1.0
 DEYFN1=-B3-B4+2.0*(B6+B11)-B10
 FN2=B1*D6+B2*D2+B8*EPS1-P*B9-B12*(C26*EPS4-C23+C27*B13+C28*
 B14)
 DEXFN2=-B9
 DEYFN2=-D6*B3-D2*B4+2.0*B8+D*B7/(3.0*CUR)-B12*(C26+2.0*C27*
 EPS4+3.0*C28*B13)
 GO TO 12

C CASE 6A

C-----
 11 EPSS2=EPSD2-EPS4+D3*CUR
 IF (NF3) 827,827,828
 828 PRINT 194 ,CUR,Y,P, EPS4, EPS1
 194 FORMAT (8H 6A 5E20.5)
 827 EPSS3=EPSD3-EPS4+D5*CUR
 B1=FORs(EPSS2)
 B2=FORs(EPSS3)
 B3=DEFORs(EPSS2)
 B4=DEFORs(EPSS3)
 B5=1.0/CUR**2
 B6=B5*C20*D
 B7=C13/CUR
 B8=C14*EPS4/CUR
 B9=Y-D/2.0
 B10=EPS4**2
 B11=B10*EPS4
 FN1=P+B1+B2+(C20-C22)/CUR+EPS4*(B8-B7)
 DEXFN1=1.0
 DEYFN1=-B3-B4-B7+2.0*B8
 FN2=B1*D6+B2*D2+B6*(C21+EPS4)-P*B9-B5*(C26*EPS4-C23+C27*B10+
 C28*B11)
 DEXFN2=-B9
 DEYFN2=-D6*B3-D2*B4+B6-B5*(C26+2.0*C27*EPS4+3.0*C28*B10)
 GO TO 12


```

C      CASE 7A
C-----
610 EPSS2=EPSD2-EPS4+D3*CUR
    IF (NF3) 829,829,830
830 PRINT 624 ,CUR,Y,P,EPS4,EPS1
624 FORMAT (8H 7A 5E20.5)
829 EPSS3=EPSD3-EPS4+D5*CUR
    B1=FORS(EPSS2)
    B2=FORS(EPSS3)
    B3=DEFORS(EPSS2)
    B4=DEFORS(EPSS3)
    B5=P+B1+B2
    B6=Y-0.5*D
    B7=P*B6-B1*D6-B2*D2
    B8=EPS4/CUR
    B9=B8*B8
    B10=B9*B8
    B11=(EPS4-CUR)/CUR
    B12=B11*B11
    B13=312*B11
    FN1=B5-C13+2.0*C14*EPS4-C14*CUR
    DEXFN1=1.0
    DEYFN1=-B3-B4+2.0*C14
    FN2=B7+C24+D*C14*EPS4-2.0*D*C14*B9*CUR+C25*B10*CUR-C25*B13*CUR
    DEXFN2=B6
    DEYFN2=D*C14-4.0*D*C14*B8+3.0*C25*B9-3.0*C25*B12+D6*B3+D2*B4
    GO TO 12
C*****
C      SOLUTION BY NEWTON'S METHOD
C*****
12 B1=DEXFN1*DEYFN2-DEXFN2*DEYFN1
    ME=ME+1
    H=(FN2*DEYFN1-FN1*DEYFN2)/B1
    G=(FN1*DEXFN2-FN2*DEXFN1)/B1
    IF (NF3) 831,831,832
832 PRINT 193,H,G,FN1,FN2,DEXFN1,DEYFN1,DEXFN2,DEYFN2
193 FORMAT (7H A H G 8E12.4)
831 P=P+H
    EPS4=EPS4+G
    IF (ME-500) 603,604,604
C
C IF H EXCEEDS LIMIT START ANOTHER ITERATION BY GOING TO 5
C
603 IF(ABS (H)-E2) 45,45,5
C
C COUNT EXCEEDED, TERMINATE BY GOING TO 117
C
604 PRINT 605 ,NU
605 FORMAT ( 25H CASE A DOES NOT CONVERGE I10)
    GO TO 117
C
C IF G EXCEEDS LIMIT START ANOTHER ITERATION BY GOING TO 5
C OTHERWISE HAVE REQUIRED P AND EPS4. CALCULATE EPS1, RESET COUNT
C AND PROCEED TO HIGHER ELEMENTS BY GOING TO 108
C OR 305 (IF CALCULATING UPPER BOUND)
C

```

```

45 IF(ABS (G)-E1) 105,105,5
105 EPS1=EPS4-CUR
    ME=0
    IF(NU) 108,108,305
C *****
C   SELECTION OF APPROPRIATE CASE B
C *****
  13 EPS1=EPS4-CUR
    IF(EPS1) 46,47,47
  46 IF(EPST+EPS1) 48,49,49
  47 IF (EPS4) 621,620,620
 620 IF (EPS1-EPS0) 614,614,615
 621 IF (EPST+EPS4) 622,623,623
 622 IF (EPS1-EPS0) 17,17,19
 623 IF (EPS1-EPS0) 16,16,18
 614 IF(EPS4-EPS0) 14,14,15
 615 IF (EPS4-EPS0) 15,15,611
  48 IF(EPS4-EPS0) 17,17,19
  49 IF(EPS4-EPS0) 16,16,18
C   CASE 1B
C-----
  14 EPSS2=EPSSD2-EPS4+D3*CUR
    IF (NF3) 833,833,834
 834 PRINT 189 ,CUR,Y,P,EPSS2,EPSS3
 189 FORMAT (8H 1B 5E20.5)
 833 EPSS3=EPSSD3-EPS4+D5*CUR
    B1=FORSS(EPSS2)
    B2=FORSS(EPSS3)
    B3=DEFORS(EPSS2)
    B4=DEFORS(EPSS3)
    B5=P+B1+B2
    B22=EPS1**2
    B23=EPS4**2
    B6=B23*EPS4
    B7=B22*EPS1
    B8=B6-B7
    B9=B7*EPS1-B6*EPS4
    B10=C3*B8/CUR
    B11=Y-0.5*D
    B12=B1*D6+B2*D2-P*B11
    B13=B3+B4
    B14=CUR**2
    B15=B14**2
    B16=B3*D6+B4*D2
    B17=B5**2
    B18=B14*B5
    B19=C8*B9
    B20=C7*B8
    B21=B19+B20
    FN1=B5-C2*(2.0*EPS4-CUR)+B10
    DEXFN1=B16/D+C2-C3*(B8-3.0*B22*CUR)/CUR**2
    DEYFN1=-2.0*C2+3.0*C3*(EPS4**2-EPS1**2)/CUR-B13
    FN2=EPS4/CUR-B12/(D*B5)-B21/B18
    DEXFN2=-EPS4/B14-(B5*(D6**2*B3+D2**2*B4)-B12*B16)/(D**2*B17)-
    1(B14*B5*(3.0*C7*B22-4.0*C8*B7)-B21*(2.0*CUR*B5+B14*B16/D))/(B15*
    2B17)

```

DEYFN2=1.0/CUR+(B5*B16-B12*B13)/(D*B17)-(B5*3.0*C7*(B23-B22)+
1B13*B21-B5*4.0*C8*B8)/(B14*B17)

GO TO 20

C CASE 2B

C
15 EPSS2=EPSSD2-EPSS4+D3*CUR
IF (NF3) 835,835,836
836 PRINT 188 ,CUR,Y,P,EPSS4,EPSS1
188 FORMAT (8H 2B 5E20.5)
835 EPSS3=EPSSD3-EPSS4+D5*CUR
B14=FORS(EPSS2)
B15=FORS(EPSS3)
B1=P+B14+B15
B13=CUR**2
B2=B13*B1
B3=B2*B1
B4=D*B1
B5=B4*B1
B6=B14*D6+B15*D2-P*(Y-0.5*D)
B16=DEFORS(EPSS2)
B17=DEFORS(EPSS3)
B7=B16+B17
B8=EPSS1**2
B9=B8*EPSS1
B10=C7-C8*EPSS1
B11=-C16+C17*EPSS4
B21=EPSS4**2
B12=C29-B21*B11-B9*B10
B22=B16*D6+B17*D2
B18=B22/D
B19=C22+C3*B9-C2*B8+EPSS4*(C13-C14*EPSS4)
B20=(2.0*C2*EPSS1-3.0*C3*B8)/CUR
FN1=B1-B19/CUR
DEXFN1=B18-B20+B19/B13
DEYFN1=-B7+B20-(C13-2.0*C14*EPSS4)/CUR
FN2=EPSS4/CUR-B6/B4-B12/B2
DEXFN2=-EPSS4/B13-(B1*(D6**2*B16+D2**2*B17)-B6*B22)/(D*B5)-
1(B13*B1*(3.0*B8*B10-C8*B9)-(C29-B21*B11-B9*B10)*(2.0*CUR*B1+
2B13*B18))/(B3*B13)
DEYFN2=1.0/CUR+(B1*B22-B6*B7)/B5-(B1*(-EPSS4*(-2.0*C16+3.0*C17*EPSS4
1)+B8*(C8*EPSS1-3.0*B10))+B12*B7)/B3
GO TO 20
C CASE 3B

C
16 EPSS2=EPSSD2-EPSS4+D3*CUR
IF (NF3) 837,837,838
838 PRINT 187 ,CUR,Y,P,EPSS4,EPSS1
187 FORMAT (8H 3B 5E20.5)
837 EPSS3=EPSSD3-EPSS4+D5*CUR
B22=FORS(EPSS2)
B23=FORS(EPSS3)
B1=P+B22+B23
B2=C2-C3*EPSS4
B3=EPSS4**2
B5=C7-C8*EPSS4
B6=B5/B2

```

B7=2.0+EPS4/CUR
B10=EPS1/CUR
B8=D*C19*B10/3.0
B9=B2*B3
B16=CUR**2
B11=D*EPS4/B16
B12=DEFORS(EPSS2)
B13=DEFORS(EPSS3)
B14=B12+B13
B15=D6*B12+D2*B13
B17=C19*B10*EPS1
B18=B3/CUR
B19=B3/B16
B20=B19*EPS4/CUR
FN1=B1-B18*B2+B17
DEXFN1=B15/D+B19*B2-C19*B10*(2.0+B10)
DEYFN1=-B14-2.0*EPS4*B2/CUR+C3*B18+2.0*C19*B10
FN2=B22*D6+B23*D2-P*(Y-0.5*D)+B17*B7*D/3.0-B9*B11*(1.0-B6)
DEXFN2=D6*D3*B12+D2*D5*B13+B8*(-B10*(B7+EPS4/CUR)-2.0*B7)+
12.0*D*B20*B2*(1.0-B6)
DEYFN2=-B15+B8*(2.0*B7+B10)-B11*(EPS4*(3.0*C2-4.0*C3*EPS4)*
1(1.0-B6)+B3*B2*(1.0+(B2*C8-B5*C3)/B2**2))
GO TO 20
C
CASE 4B

```

C

C

```

-----
17 EPSS2=EPSS2-EPS4+D3*CUR
   IF (NF3) 839,839,840
840 PRINT 186 ,CUR,Y,P,EPS4,EPS1
186 FORMAT (8H 4B 5E20.5)
839 EPSS3=EPSS3-EPS4+D5*CUR
   B1=C2-C3*EPS4
   B2=EPS4/CUR
   B3=B2*EPS4
   B4=C7-C8*EPS4
   B5=B4/B1
   B6=D/CUR
   B7=C20/CUR
   B8=B7*B6
   B20=B2**2
   B10=B20*D
   B11=B10*EPS4
   B12=FORSS(EPSS2)
   B13=FORSS(EPSS3)
   B14=DEFORS(EPSS2)
   B15=DEFORS(EPSS3)
   B16=D3*B14
   B17=D5*B15
   B19=B11/CUR
   FN1=P+B12+B13+B7-B3*B1
   DEXFN1=B16+B17-B7/CUR+B20*B1
   DEYFN1=-B14-B15-2.0*B2*B1+C3*B3
   FN2=B12*D6+B13*D2+B8*(C21+EPS4)-P*(Y-D*0.5)-B11*B1*(1.0-B5)
   DEXFN2=B16*D6+B17*D2-2.0*B8*(C21+EPS4)/CUR+2.0*B19*B1*(1.0-B5)
   DEYFN2=-D*(B16+B17)+B8-B10*(3.0*C2-4.0*EPS4*C3)*(1.0-B5)-
1B11*B1*(1.0-(C3*B5-C8)/B1)
GO TO 20

```

C CASE 5B

C-----

```

18 EPSS2=EPSS2-EPSS4+D3*CUR
   IF (NF3) 841,841,842
842 PRINT 185 ,CUR,Y,P,EPSS4,EPSS1
185 FORMAT (8H 5B 5E20.5)
841 EPSS3=EPSS3-EPSS4+D5*CUR
   B1=FORSS(EPSS2)
   B2=FORSS(EPSS3)
   B3=DEFORSS(EPSS2)
   B4=DEFORSS(EPSS3)
   B5=2.0+EPSS4/CUR
   B6=C19*EPSS1/CUR
   B7=B6*EPSS1
   B21=B6*D/3.0
   B8=B21*B5
   B12=1.0/CUR**2
   B13=EPSS4**2
   B14=B13*EPSS4
   B15=D3*B3
   B16=D5*B4
   B17=B15+B16
   B18=B12*(C26*EPSS4-C23+C27*B13+C28*B14)
   B19=C22+C13*EPSS4-C14*B13
   B20=EPSS4/CUR
   FN1=P+B1+B2+B7-C22/CUR-C13*B20+C14*B13/CUR
   DEXFN1=B15+B16-B7/CUR-2.0*B6+B12*B19
   DEYFN1=-B3-B4+2.0*B6-C13/CUR+2.0*C14*B20
   FN2=B1*D6+B2*D2+B8*EPSS1-P*(Y-D/2.0)-B18
   DEXFN2=D6*B15+D2*B16+2.0*B18/CUR+B21*(-2.0*EPSS1/CUR*(1.0-B20)-
12.0*B5)
   DEYFN2=-D*(B15+B16)+2.0*B8+B7*D/(3.0*CUR)-B12*(C26+2.0*C27*EPSS4+
13.0*C28*B13)
   GO TO 20

```

C CASE 6B

C-----

```

19 EPSS2=EPSS2-EPSS4+D3*CUR
   IF (NF3) 843,843,844
844 PRINT 184 ,CUR,Y,P,EPSS4,EPSS1
184 FORMAT (8H 6B 5E20.5)
843 EPSS3=EPSS3-EPSS4+D5*CUR
   B1=FORSS(EPSS2)
   B2=FORSS(EPSS3)
   B3=DEFORSS(EPSS2)
   B4=DEFORSS(EPSS3)
   B12=1.0/CUR
   B5=B12**2
   B6=B5*C20*D
   B10=EPSS4**2
   B11=B10*EPSS4
   B13=D3*B3+D5*B4
   B14=B5*(C26*EPSS4-C23+C27*B10+C28*B11)
   B15=C20-C22-C13*EPSS4+C14*B10
   FN1=P+B1+B2+B15*B12
   DEXFN1=B13-B5*B15
   DEYFN1=-B3-B4+(2.0*C14*EPSS4-C13)/CUR

```

```

FN2=B1*D6+B2*D2+B6*(C21+EPS4)-P*(Y-0.5*D)-B14
DEXFN2=(D6**2*B3+D2**2*B4)/D-2.0*B6*B12*(C21+EPS4)+2.0*B14*B12
DEYFN2=-B13*D+B6-B5*(C26+2.0*C27*EPS4+3.0*C28*B10)
GO TO 20

```

```
C CASE 7B
```

```

-----
611 EPSS2=EPSD2-EPS4+D3*CUR
    IF (NF3) 845,845,846
846 PRINT 625 ,CUR,Y,P,EPS4,EPS1
625 FORMAT (8H 7B 5E20.5)
845 EPSS3=EPSD3-EPS4+D5*CUR
    B1=FORSS(EPSS2)
    B2=FORSS(EPSS3)
    B3=DEFORS(EPSS2)
    B4=DEFORS(EPSS3)
    B5=P+B1+B2
    B6=Y-0.5*D
    B7=P*B6-B1*D6-B2*D2
    B8=EPS4/CUR
    B9=B8*B8
    B10=B9*B8
    B11=(EPS4-CUR)/CUR
    B12=B11*B11
    B13=B12*B11
    FN1=B5-C13+2.0*C14*EPS4-C14*CUR
    DEXFN1=D3*B3+D5*B4-C14
    DEYFN1=-B3-B4+2.0*C14
    FN2=B7+C24+D*C14*EPS4-2.0*D*C14*B9*CUR+C25*B10*CUR-C25*B13*CUR
    DEXFN2=2.0*C25*(B13-B10+3.0*B12/2.0)+2.0*D*C14*B9-D6*D3*B3-D2*D5*
1B4
    DEYFN2=D*C14-4.0*D*C14*B8+3.0*C25*B9-3.0*C25*B12+D6*B3+D2*B4
GO TO 20

```

```
C *****
```

```
C SOLUTION BY NEWTONS METHOD
```

```
C *****
```

```

20 B1=DEXFN1*DEYFN2-DEXFN2*DEYFN1
    ME=ME+1
    H=(FN2*DEYFN1-FN1*DEYFN2)/B1
    G=(FN1*DEXFN2-FN2*DEXFN1)/B1
    IF (NF3) 847,847,848
848 PRINT 183,H,G,FN1,FN2,DEXFN1,DEYFN1,DEXFN2,DEYFN2 /
183 FORMAT (7H B H G 8E12.4)
847 CUR=CUR+H
    EPS4=EPS4+G
    IF (ME-500) 606,607,607

```

```
C
C COUNT EXCEEDED, TERMINATE BY GOING TO 117
```

```

C
607 PRINT 608 ,NU,N
608 FORMAT ( 25H CASE B DOES NOT CONVERGE 2I10)
GO TO 117

```

```

C
C IF H AND G EXCEED LIMITS START ANOTHER ITERATION BY GOING TO 13
C OTHERWISE HAVE REQUIRED CUR AND EPS4.
C RESET COUNT AND PROCEED TO THE NEXT HIGHER ELEMENT BY GOING TO 99
C OR 308 (IF CALCULATING UPPER BOUND)

```

```

C
606 IF (ABS (H)-E1) 50,50,13
50 IF (ABS (G)-E1) 609,609,13
609 ME=0
      IF (NU0) 889,889,888
889 IF (NU) 99,99,308
C*****
C      CALCULATIONS FOR EPS4=EPSU
C*****
C
C      CALCULATIONS BY ITERATION. ADJUST VALUE OF DEFLECTION AND
C      PROCEED TO RECALCULATE (GO TO 500)
C      TERMINATE AFTER 5 ITERATIONS (GO TO 202)
C
203 KL=KL+1
      IF (KL-5) 51,51,202
51 A1=DEL(1)
      DEL(1)=A1+(PDEL(1)-A1)*(EPSU-EPSI4(1))/(PEPSI4(1)-EPSI4(1))
      EPS4=EPSI4(1)
      PEPSI4(1)=EPSI4(1)
      PDEL(1)=A1
      NE=0
      GO TO 500
C*****
C      CALCULATION OF UPPER BOUND
C*****
640 NU=1
C      STORE
      PS=P
      EPSI1S=EPSI1
C
C      COPY LOWER BOUND SOLUTION
C
      DO 340 N=1,NMAX
      UCURI(N)=CURI(N)
      URADI(N)=RADI(N)
      UDEL(N)=DEL(N)
      UTHETA(N)=THETA(N)
      UEPSI4(N)=EPSI4(N)
      UW(N)=W(N)
340 UYI(N)=YI(N)
C      CENTRAL DEFLECTION FOR WHICH P IS BEING SOUGHT
      EE=YI(1)
C      CALCULATE TOP SLOPE, CONSIDER AS INITIAL VALUE FOR SLOPE ITERATION
      UTHETA(NMAX)=UTHETA(LAST)+A/URADI(LAST)
      IF (NF6) 890,890,891
890 THETAT=(UTHETA(NMAX)*UTHPRE)/UTHGES
      UTHGES=UTHETA(NMAX)
      GO TO 894
891 THETAT=UTHETA(NMAX)
      UTHGES=UTHETA(NMAX)
      NF6=0
C
C      INITIAL VALUES FOR TOP CURVATURE ITERATION
C
894 Y=E

```

```

      P=P*E7
      I=1
      NUO=1
      IF (NF5) 849,849,850
850 PRINT 851, THETAT,P
851 FORMAT (12H UB START 2E20.5)
C
C SET INITIAL GUESSES FOR CUR AND EPS4 BEFORE GOING TO CASE B
C
849 EPS4=UEPSI4(LAST)
      CUR=UCURI(LAST)
      GO TO 13
C
C FIRST ITERATION
C RETURN FROM CASE B, PREPARE FOR CALCULATIONS OF LOWER ELEMENTS
C
888 NUO=0
C
C SUBSEQUENT ITERATIONS
C RETURN FROM CASE A, PREPARE FOR CALCULATIONS OF LOWER ELEMENTS
C
305 UEPSI4(NMAX)=EPS4
      IF (NF3) 852,852,853
853 PRINT 801,CUR,Y,P,EPS4,EPS1
801 FORMAT (10H 801 5E20.5)
852 UCURI(LAST)=CUR
      UTHETA(NMAX)=THETAT
      UW(NMAX)=EE-E
      URADI(LAST)=D/(UCURI(LAST)+CURCOR)
C
C START DO LOOP FOR THE REMAINING ELEMENTS
C
      DO 309 N=1, LAST
      NN=NMAX-N
      UTHETA(NN)=UTHETA(NN+1)-A/URADI(NN)
      UW(NN)=UW(NN+1)-A*UTHETA(NN)-A**2/(2.0*URADI(NN))
      UYI(NN)=EE-UW(NN)
      UDEL(NN)=UYI(NN)-DEFIN(NN)-E
      IF (N-LAST) 306,310,310
306 Y=UYI(NN)
C
C SET INITIAL GUESSES, BEFORE GOING TO CASE B TO SOLVE FOR
C CUR AND EPS4 FOR GIVEN P AND Y
C
      CUR=UCURI(NN)
      EPS4=UEPSI4(NN+1)
      IF (CUR) 13,307,13
307 CUR=0.00001
      GO TO 13
C
C RETURN FROM CASE B, STORE VALUES
C
308 UEPSI4(NN)=EPS4
      IF (NF3) 854,854,855
855 PRINT 802,CUR,Y,P,EPS4,EPS1
802 FORMAT (10H 802 5E20.5)

```



```

854 UCURI(NN-1)=CUR
809 URADI(NN-1)=D/(UCURI(NN-1)+CURCOR)
C
C CHECK ERRORS IN BOUNDARY CONDITIONS
C IF ERRORS SMALL ENOUGH WE HAVE FINISHED UPPER BOUND, GO TO 319
C IF ERRORS TOO LARGE CONTINUE ITERATIONS
C
310 UEPSI4(1)=UEPSI4(2)
    UERROR=UYI(1)-EE
    IF (NF5) 856,856,857
857 PRINT 803, UTHETA(1),P,UERROR
803 FORMAT (25H UTHETA(1) , P ,UERROR 3E20.5)
856 IF(NEU-10) 895,895,896
896 F(I)=UERROR**2+(UTHETA(1)*E6)**2
    B1=F(I)
    IF(B1-E8) 897,897,312
897 IF(NF5) 319,319,898
898 PRINT 899,I,F(I),E8
899 FORMAT (13H I,F(I),E8 I10,2E20.5)
    GO TO 319
895 IF (ABS(UERROR)-E3) 311,311,312
311 IF (ABS(UTHETA(1))-E5) 319,319,312
312 GO TO (859,860,861,862,313,877,881),I
C
C I=1
C
859 F(I)=UERROR**2+(UTHETA(1)*E6)**2
    THETAP=THETAT
    UCURP=UCURI(LAST)
    S1=UCURP*(FAC1-1.0)
    S2=THETAP*(FAC2-1.0)
    CUR=UCURI(LAST)-S1/2.0
    THETAT=THETAP
    IF(NF5) 864,864,865
865 PRINT 866,NEU,THETAT,CUR,F(I),I
866 FORMAT (10H F(1) I10,3E20.5,I10)
864 I=2
    GO TO 315
C
C I=2
C
860 F(I)=UERROR**2+(UTHETA(1)*E6)**2
    CUR=UCURP
    THETAT=THETAP-S2/2.0
    IF (NF5) 863,863,868
868 PRINT 869,NEU,THETAT,CUR,F(I),I
869 FORMAT (10H F(2) I10,3E20.5,I10)
863 I=3
    GO TO 315
C
C I=3
C
861 F(I)=UERROR**2+(UTHETA(1)*E6)**2
    CUR=UCURP+S1/2.0
    THETAT=THETAP
    IF(NF5) 870,870,871

```

```

871 PRINT 872,NEU,THETAT,CUR,F(I),I
872 FORMAT (10H  F(3)  I10,3E20.5,I10)
870 I=4
GO TO 315

```

C
C
C

```

I=4
862 F(I)=UERROR**2+(UTHETA(1)*E6)**2
CUR=UCURP
THETAT=THETAP+S2/2.0
IF (NF5) 314,314,873
873 PRINT 874,NEU,THETAT,CUR,F(I),I
874 FORMAT (10H  F(4)  I10,3E20.5,I10)
314 I=5
GO TO 315

```

C
C
C

```

I=5
313 F(I)=UERROR**2+(UTHETA(1)*E6)**2

```

C
C
C

CALCULATION OF DERIVATIVES AT POINT 1. PROCEED TO POINT 6

```

DF1CUR=(F(4)-F(2))/S1
DF1SLP=(F(5)-F(3))/S2
DF1MX=SQRT(DF1SLP**2+DF1CUR**2)
CAS=DF1SLP/DF1MX
SEN=DF1CUR/DF1MX
S3=SQRT(S1**2+S2**2)*0.5
CUR=UCURP+S3*SEN
THETAT=THETAP+S3*CAS
IF (NF5) 858,858,875
875 PRINT 876,NEU,THETAT,CUR,F(I),I
876 FORMAT (10H  F(5)  I10,3E20.5,I10)
PRINT 885
885 FORMAT (54H  DF1CUR  DF1SLP  DF1MX  CAS  SEN  S3)
PRINT 886,DF1CUR,DF1SLP,DF1MX,CAS,SEN,S3
886 FORMAT (6E15.5)
858 I=6
GO TO 315

```

C
C
C

```

I=6
877 F(I)=UERROR**2+(UTHETA(1)*E6)**2
CUR=UCURP-S3*SEN
THETAT=THETAP-S3*CAS
IF (NF5) 878,878,879
879 PRINT 880,NEU,THETAT,CUR,F(I),I
880 FORMAT (10H  F(6)  I10,3E20.5,I10)
878 I=7
GO TO 315

```

C
C
C

```

I=7  NEXT SET UP NEW INCREMENT

```

```

881 F(I)=UERROR**2+(UTHETA(1)*E6)**2
DD1MX=(F(6)-2.0*F(1)+F(7))/S3**2
S4=-DF1MX/DD1MX

```

```

CUR=UCURP+S4*SEN
THETAT=THETAP+S4*CAS
IF (NF5) 882,882,883
883 PRINT 884,NEU,THETAT,CUR,F(1),I
884 FORMAT (10H F(7) I10,3E20.5,I10)
PRINT 901,DD1MX
901 FORMAT (15H DD1MX E20.5)
882 I=1
IF (NEU-20) 316,317,317
317 PRINT 318
318 FORMAT(30H COLUMN UB DOES NOT CONVERGE )
IF (NF4) 117,117,867
667 NF2=0
GO TO 327
316 NEU=NEU+1
315 Y=E
EPS4=UEPSI4(NMAX)
GO TO 5
C
C OUTPUT UPPER BOUND RESULTS
C
319 A1=UEPSI4(1)-UCURI(1)-EPS1I
A2=UEPSI4(1)-EPS4I
A3=(A1+A2)/2.0
PRINT 321,P,A1,A3,A2,(UDEL(N),N=1,8)
321 FORMAT (F8.0,3F10.5,8F7.3)
IF (LAST-8) 322,322,323
323 IF (LAST-17) 324,325,325
325 PRINT 326, (UDEL(N),N=9,16)
GO TO 322
324 PRINT 326, (UDEL(N),N=9,LAST)
326 FORMAT(38H 8F7.3)
322 NEU=0
C
C PUNCH RESULTS IF NF=1
C
IF (NF1) 327,327,328
328 DO 329 N=1, LAST
329 DELT(N)=UDEL(N)+DEFIN(N)
IF (LAST-17) 330,331,331
330 PUNCH 332,P,A1,A3,A2,(DELT(N),N=1, LAST)
332 FORMAT (F10.0,3F10.6/16F5.3)
GO TO 327
331 PUNCH 332,P,A1,A3,A2,(DELT(N),N=1,16)
C
C EXIT FROM UPPER BOUND CALCULATIONS, GO TO 633
C
327 NU=0
UTHPRE=THETAT
P=PS
EPS11=EPS11S
GO TO 633
C *****
C TERMINATE CALCULATIONS. PROCEED TO NEXT COLUMN (GO TO 101)
C
117 CALL TIME(T)

```

```
TU=T-TI  
PRINT 999,TU  
999 FORMAT(7H TIME= F10.2)  
TI=T  
GO TO 101  
END
```

```
C    STEEL FORCE*STRAIN RELATIONSHIP
      FUNCTION FORS(EPS)
      COMMON  AS
      IF(EPS)2,3,3
3     IF(EPS-0.0049575)4,4,5
4     FORS=AS*EPS*29340000.0
      RETURN
5     IF(EPS-0.0069)6,6,7
6     FORS=AS*(145454.0+26208000.0*(EPS-0.004975))
      RETURN
7     IF(EPS-0.00863)8,8,9
8     FORS=AS*(196363.0+12610000.0*(EPS-0.0069))
      RETURN
9     FORS=AS*(218181.0+4630000.0*(EPS-0.00863))
      RETURN
2     IF(EPS+0.0049575)10,4,4
10    IF(EPS+0.0069)11,12,12
11    IF(EPS+0.00863)13,14,14
12    FORS=AS*(-145454.0+26208000.0*(EPS+0.004975))
      RETURN
13    FORS=AS*(-218181.0+4630000.0*(EPS+0.00863))
      RETURN
14    FORS=AS*(-196363.0+12610000.0*(EPS+0.0069))
      RETURN
      END
```

```
C      CALCULATION OF PARTIAL DERIVATIVES
      FUNCTION DEFORS(EPS)
      COMMON AS
      IF(ABS (EPS)-0.0049575) 1,1,2
1     DEFORS=AS*29340000.0
      RETURN
2     IF(ABS (EPS)-0.0069) 3,3,4
3     DEFORS=AS*26208000.0
      RETURN
4     IF(ABS (EPS)-0.00863) 5,5,6
5     DEFORS=AS*12610000.0
      RETURN
6     DEFORS=AS*4630000.0
      RETURN
      END
```